CONTRACTOR REPORT

SAND95–2939
Unlimited Release
UC–1301

Heat Loss from an Open Cavity

Christopher G. McDonald
College of Engineering
California State Polytechnic University
Pomona, CA 91768

Prepared by Sandia National Laboratories Albuquerque, New Mexico 87185
and Livermore, California 94550 for the United States Department of Energy
under Contract DE-AC04-94AL85000

Printed December 1995

Issued by Sandia National Laboratories, operated for the United States Department of Energy by Sandia Corporation.

Printed in the United States of America. This report has been reproduced directly from the best available copy.

Available to DOE and DOE contractors from
Office of Scientific and Technical Information
PO Box 62
Oak Ridge, TN 37831

Prices available from (615) 576-8401, FTS 626-8401

Available to the public from
National Technical Information Service
US Department of Commerce
5285 Port Royal Rd
Springfield, VA 22161

NTIS price codes
Printed copy: A10
Microfiche copy: A01

This report was printed as submitted to Sandia National Laboratories by the author and California State Polytechnic University.

Distribution
Category UC-1301

SAND95-2939
Unlimited Release
Printed December 1995

HEAT LOSS FROM AN OPEN CAVITY

Christopher G. McDonald
College of Engineering
California State Polytechnic University
Pomona, CA 91768

Sandia Contract 02-5759

ABSTRACT

This report presents the results of an investigation into the heat-loss characteristics of a cavity-type receiver for a parabolic dish concentrating solar collector. The receiver is similar to the type used in the Solar Total Energy Project in Shenandoah, Georgia. This investigation examines the effects of aperture size, orientation, and operating temperature on the heat loss of the receiver. The total receiver heat loss is quantitatively separated into its three modes: radiative, conduction, and convection. The testing was performed in a controlled environment, thereby eliminating any potential wind contribution. It was executed off flux, i.e., with no incident insulation. The receiver was operated in reverse of its typical operating configuration, whereby the heat-transfer fluid was heated externally. Previous heat-loss models or correlations with similar cavity receivers are compared with the experimental results from this study. A convective heat-loss correlation is presented from these experimental results. A theoretical model for the radiative heat loss is developed and compared with two methods used to quantitatively determine the radiative component of total heat loss.

ACKNOWLEDGMENTS

I would like to thank Dr. William Stine for his unending support and guidance. Dr. Stine provided overall project management. He has extended enormous patience and understanding through all the delays.

I would also like to thank Dr. Carl Rathmann for his advice regarding the analytical radiative heat loss, and the general assumptions used in experimentally determining convective heat loss.

Technical assistance was provided by Jack Kovar, Mechanical Engineering Department Technician, and Jim Rounds, Chemical Engineering Department Technician. Their knowledge and experience provided most valuable advice.

Special thanks go to all the undergraduate students who worked long, hard hours bringing the test phase of the project to conclusion. Working with so many students on this project, established quite a few lasting friendships. These students provided support in the design and fabrication of test apparatus. They also extended valuable assistance during testing, wherein, shifts would often run more than 15 hours. They continuosly exhibitied dedication and determination.

Finally, I would like to extend my gratitude to Sandia National Laboratories for their financial and technical support. This project could never have taken place without the strong support of this company.

CONTENTS

LIST OF ILLUSTRATIONS

LIST OF TABLES

Table | Page

LIST OF ABBREVIATIONS

ADC	analog to digital converter
AC	alternating current
HTF	heat transfer fluid
N	number of sectioned elements of the receiver cavity internal surface area
STEP	Solar Total Energy Project
TC	thermocouple

I. INTRODUCTION

Cavity type receivers are used extensively in concentrating solar thermal energy collecting systems. The Solar Total Energy Project (STEP) in Shenandoah, Georgia is a large scale field test for the collection of solar thermal energy.(1) The STEP experiment consists of a large field array of solar collectors used to supplement the process steam, cooling and other electrical power requirements of an adjacent knitwear manufacturing facility.

The main components of each collector are the concentrator, the tracking mechanism, and the receiver (Fig. 1). The concentrator is a 7 meter diameter parabolic dish with a highly reflective coating on the inside surface. Each collector has two axes of rotation for tracking the sun all throughout the days of the year. The collectors are subjected to continuous changes in ambient conditions such as wind, solar insulation, and ambient temperature.

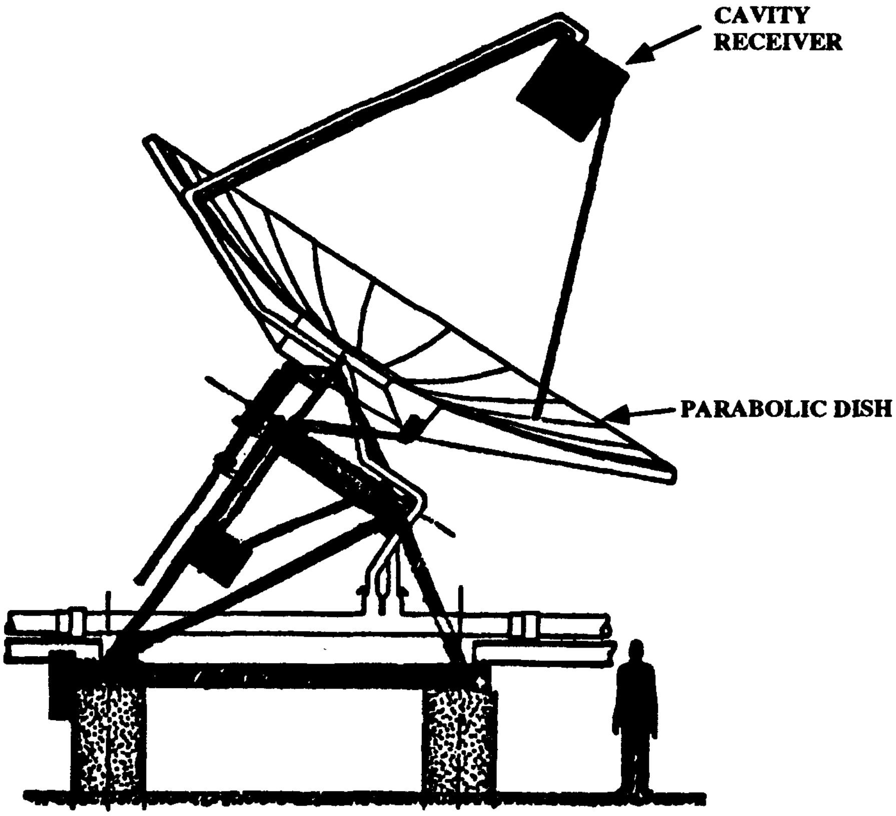

Figure 1. Solar Collector(1)

These environmental variations, as well as changes in receiver tilt, affect the overall receiver performance. The receiver used in this study is a parabolic collector.

A thorough understanding of receiver heat loss characteristics is essential for future development of solar receivers, and optimization of the STEP system presently in use. The system boundary of the receiver is defined as the outer skin of the receiver and the aperture opening (Fig. 2). The portion of the boundary formed by solid walls are only subject to conductive heat transfer. The aperture, however; is subject to convective, conductive and radiative heat transfer. Mass transfer occurs across the aperture and through the heat transfer fluid lines crossing the system boundary.

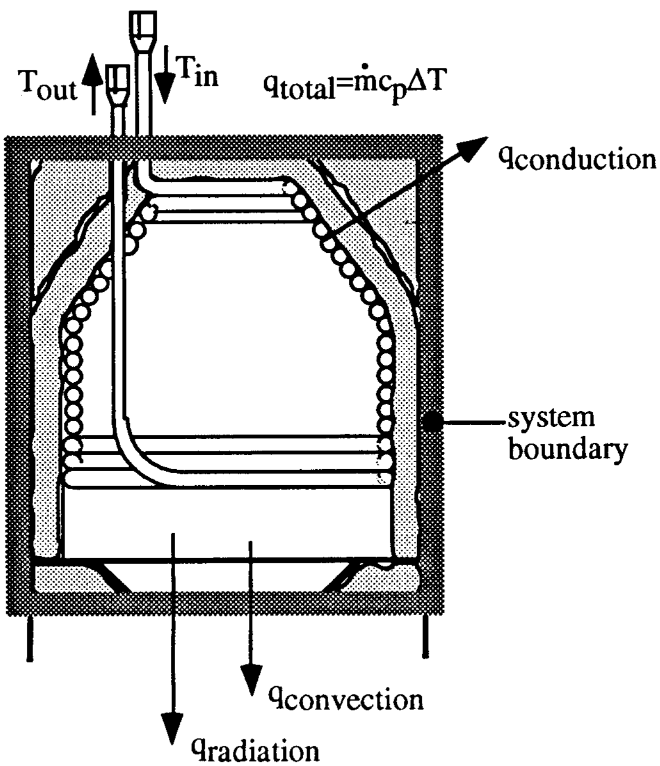

Figure 2. Heat transfer system boundary

Analytical methods for predicting the conductive and radiative heat losses from a cavity receiver are fairly straight forward. This, however; is not the case for convective heat loss analysis. The complex geometry of the cavity makes it difficult to use existing analytical models for predicting convective heat loss. Few convective heat loss correlations, for cavity receivers, exist due to the lack of significant empirical data. Correlations for receivers with simple geometry are not considered valid for this receiver.

An extensive search of current literature produced only a few studies on heat loss from cavities. A study was performed by LeQuere, Penot, and Mirenayat in which heat loss characteristics of two different sized cubical cavities were examined.(2) They considered variations in receiver operating temperature and angle, in their study. A study performed by Koenig and Marvin, presented by Harris and Lenz, gave an empirically derived correlation for convective heat loss from cylindrical cavity type receivers, including the effects of variation in operating temperature and angle.(3) An analytical model for convective heat loss for an open cubical cavity receiver was presented by A. M. Clausing.(4) The Clausing model was developed for a central receiver operating at much higher temperatures than the receiver studied here. Siebers and Kraabel presented a model for the convective heat loss from a central cylindrical cavity receiver.(5)

There is some experimental data available for this type of receiver from previous tests on off-flux field measurements conducted with limited instrumentation at STEP.(6) Field measurement experiments, such as the one conducted at STEP, provide no control over environmental conditions such as wind, and ambient temperature. In order to control the environmental conditions, receiver testing for this study, took place indoors.

The purpose of the tests, conducted for this study, was to isolate and quantify the radiative, conductive, and convective components of total heat loss, and to determine the effects of operating temperature, receiver angle, and aperture size on cavity heat loss. An analytical model for radiative heat loss was developed and compared with two other methods used to determine radiative heat loss. A proposed convective heat loss correlation, including effects of aperture size, receiver operating temperature, and receiver angle is presented. The resulting data is a source to evaluate the STEP measurements.

II. APPARATUS

A. Receiver

A drawing of the receiver studied in this work is shown in cross section in Figure 3. The cavity of the receiver is composed of a single tube wound in a conical frustum-cylinder shape with the aperture at the cylindrical end of the tube bundle. The tube bundle is wrapped in a thick blanket of Kaowool® insulation. The outer skin of the receiver is formed by a single cylindrical wrap of sheet metal. The outer skin extends beyond the aperture face to serve as a wind break. The flow lines to and from the receiver are heavily insulated. The inlet and outlet lines for these tests, as shown in Figure 3, are the reverse of those for an on-flux receiver in field operation.

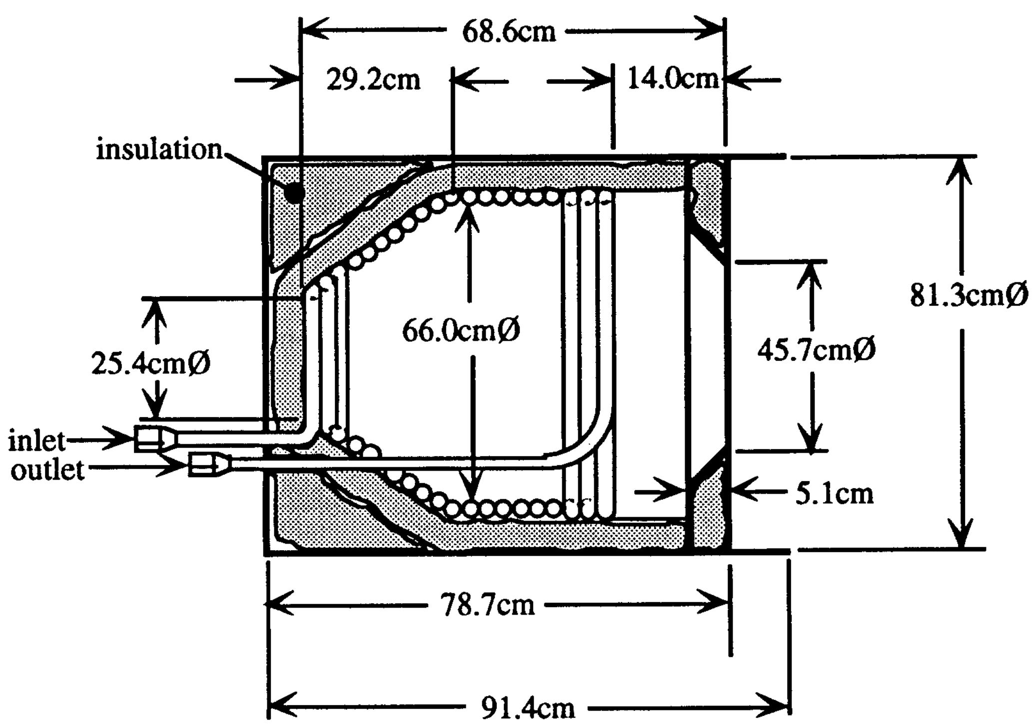

Figure 3. Cavity receiver cross section.

The receiver is cradled in a frame that allows it to rotate 180° (Fig. 4). The receiver can be fixed at 15° increments from -90°, where the aperture is upward, to +90°, where the aperture is downward (Fig. 5). The high pressure flexible lines on the sides of the receiver test stand allow the receiver to rotate freely for each test position.

Thermocouples were used to measure the receiver inlet and outlet temperatures. Two in-house calibrated K-type thermocouples were immersed in each of the heat transfer fluid (HTF) inlet and outlet lines of the receiver. One of the thermocouples from the inlet and outlet lines measured absolute temperature. The remaining two thermocouples were connected in series to yield a direct measure of the temperature difference between the inlet and the outlet. The receiver was further instrumented with seventeen surface thermocouples and thirteen internal air thermocouples (Figure 6). The surface thermocouples were spot welded in place with the lead ends spaced approximately one-eighth inch apart.

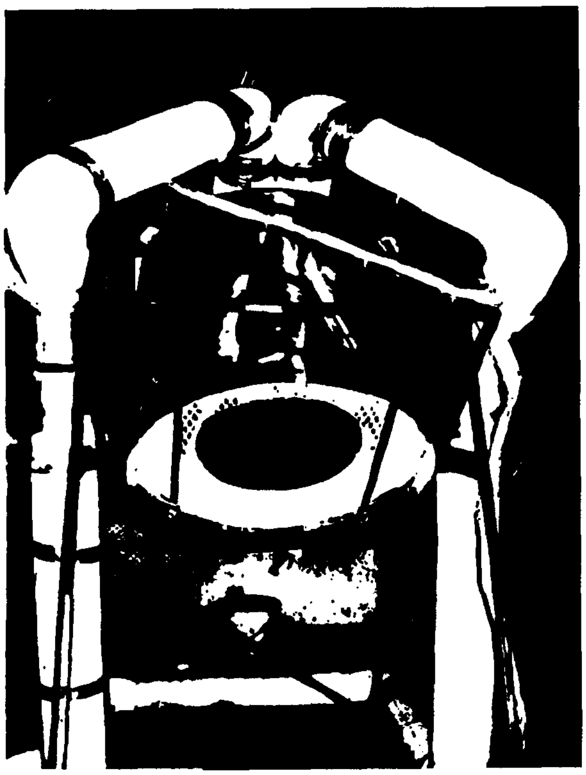

Figure 4. Receiver test stand

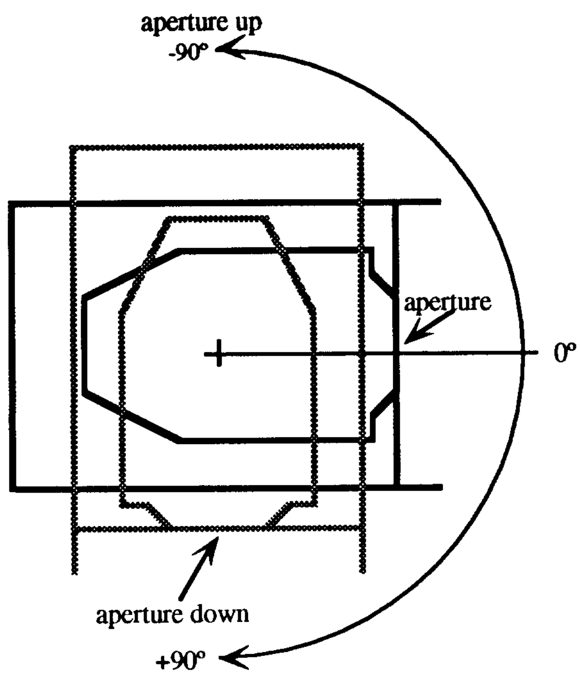

Figure 5. Receiver angles

Thermocouple Identification

A: air TC
T: tube surface TC
S: outer skin surface TC
C: back cover surface TC

TC/Switch Correlation

TC ID	SW #	TC ID	SW #	TC ID	SW #	TC ID	SW #
1A	1	3A	8	5S	15	8A	22
1T	2	3S	9	6A	16	8T	23
1S	3	4A	10	6T	17	8S	24
2A	4	4T	11	6S	18	9A	25
2T	5	4S	12	7A	19	9S	26
2S	6	5A	13	7T	20	10A	27
3T	7	5T	14	7S	21	11A	28
						12A	29
						13A	30

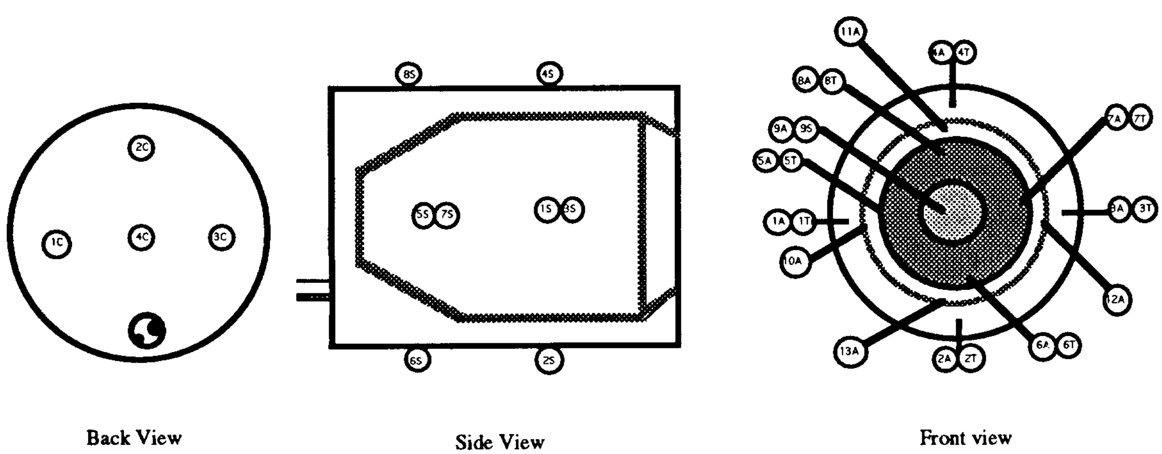

Figure 6. Receiver thermocouples locations

An insulating annulus with a corresponding center plug were fabricated for each of the aperture sizes tested (Fig. 7). The aperture sizes tested were 6 inch diameter, 12 inch diameter, 18 inch diameter, and 26 inch diameter. The 18 inch diameter aperture is the size presently being used for this model of receiver. The 26 inch diameter, the internal diameter of the cavity, aperture leaves no lip to the cavity. The aperture plug and annulus were fabricated of 1 inch thick solid insulation boards. The plug was tapered inward to fit snugly in the respective aperture annulus. The plugs were held in place by two wooden straps extending across the aperture end of the receiver.

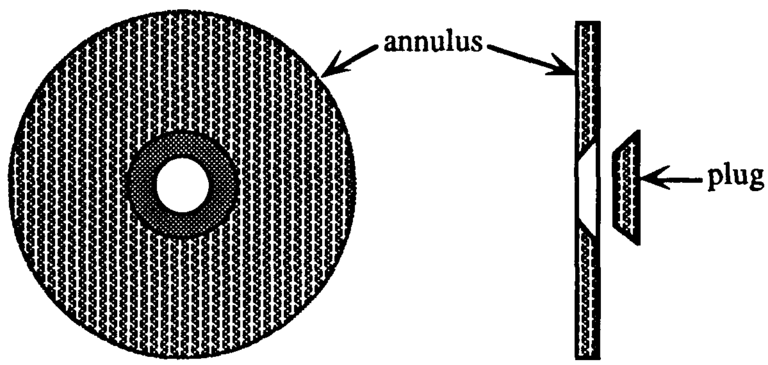

Figure 7. Annulus and plug

B. Flow Loop

The heat transfer fluid was heated by a heating and pumping station adjacent to the receiver (Fig 8). The flow system consists of two parallel flow loops- the primary heating loop and the receiver feed loop. The primary heating loop has available two in-line 12 kW electric heaters. A minimum flow rate of 5 gpm was maintained in the heating loop to prevent excessive film temperatures of the HTF in the heaters. The receiver feed loop was throttled for a flow rate through the receiver of 1 gpm. The HTF flow rate through the receiver was measured using three turbine flow meters connected in a series on the inlet line to the receiver. The flow meters are located in a straight section of piping allowing ample upstream and downstream damping lengths. Three flow meters are used for measurement redundancy. One flow meter was factory calibrated. The remaining two flow meters were calibrated against the factory calibrated flow meter.

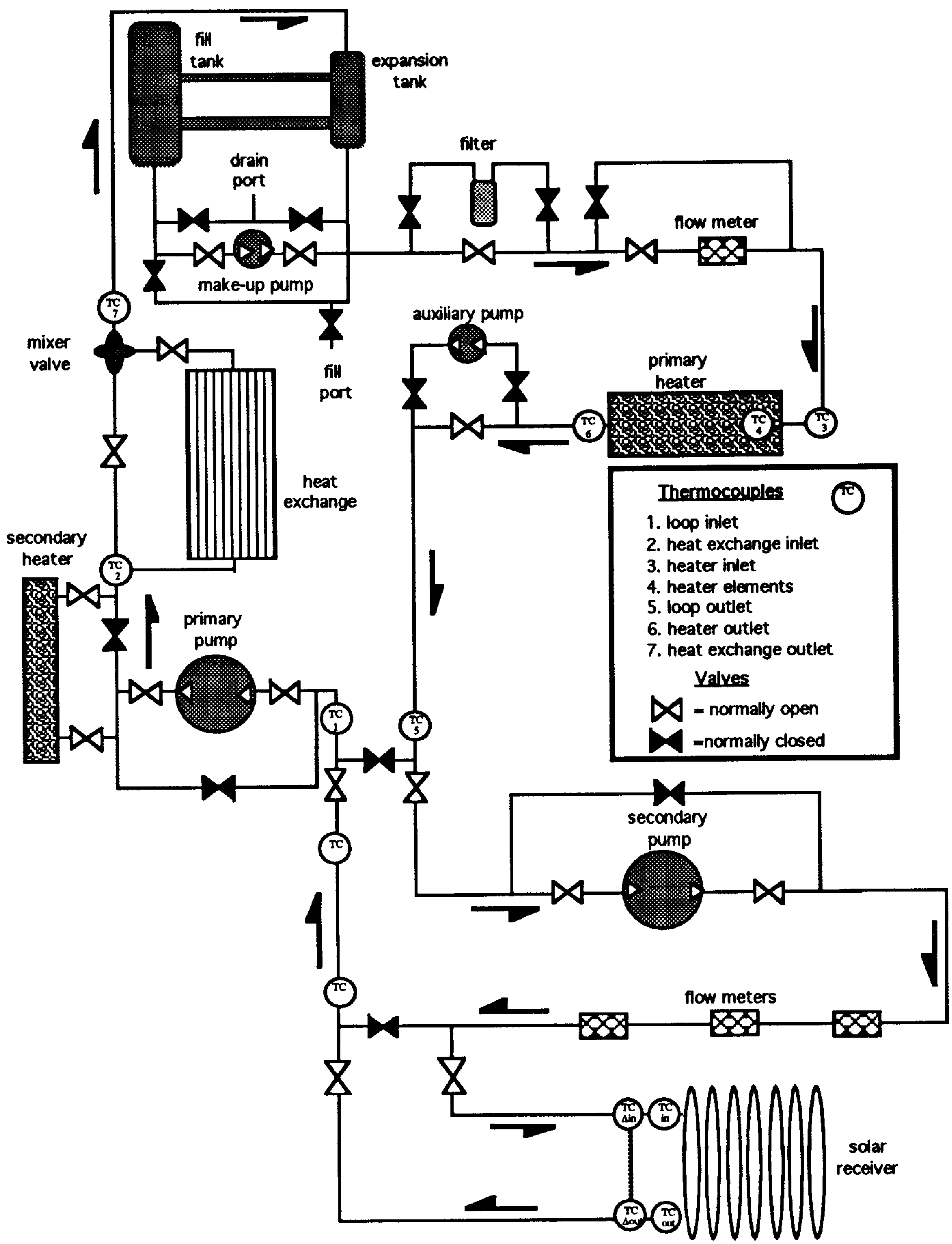

Figure 8. Heat transfer fluid heating system

C. Radiometer Setup

One method used to determine the thermal radiative heat loss from the aperture was with a radiometer. The radiometer was mounted on a tripod and placed directly below and centered on the receiver. The radiometer was water cooled and the return water temperature was monitored. The radiometer signal output leads were connected to the computer data acquisition system. A Saran Wrap window assembly was positioned over the radiometer in place of the quartz window bezel. The radiometer window serves to isolate the temperature sensitive thermopile surface from localized convective currents. This is discussed further in radiometer calibration section.

D. Data Acquisition

A computer was used for data acquisition and display. This consisted of an Apple IIe computer with two 16-channel data acquisition cards each connected to a thermocouple cold junction terminal box. The following transducers were connected to the data acquisition system; receiver inlet and outlet thermocouples, two ambient thermocouples, three receiver flow meters; radiometer; radiometer water thermocouple; loop inlet and outlet thermocouples; and the main flow loop flow meter . The surface and air thermocouples on the receiver were connected to a digital display unit via a multi-channel thermocouple switch. The surface and air receiver temperature readings were recorded manually when steady state conditions were obtained for each test point.

III. TEST METHOD

The testing was conducted in two phases. Phase One of the testing examined the effects of receiver operating temperature and receiver angle on the receiver heat loss. Phase Two looked at the effects of receiver aperture size on the receiver heat loss. After Phase One, and before Phase Two, the receiver was overhauled. The overhaul of the receiver included replacing the insulation in the walls, repainting the tube surfaces, and resealing the seams and ports through the outer skin of the receiver.

A. Temperature and Receiver Angle Effects

The model of the effects of temperature and receiver angle on heat loss developed in this study utilizes results from both Phase One and Phase Two tests. The overlap portion of the Phase One and Phase Two tests were compared for ease of repetition. The four nominal operating temperatures in Phase One testing were 300°F, 400°F, 500°F, and 600°F with the standard 18 inch aperture. The Phase Two study was conducted at operating temperatures of 400°F and 600°F and incorporated 6, 12, 18, and 26 inch apertures. The nominal operating temperature was based on the average of the inlet and outlet temperatures. For each operating temperature the receiver was tested at ten angles from -90° to +90° in Phase One. The receiver angles tested were from 0 to +90°, every 15° and from 0 to -90°, every 30°. Phase Two included receiver angles from 0° to +90°, every 15°. More angles were tested in the positive range, since most cavity receivers operate in this range. The negative angles were tested to provide a clearer understanding of heat loss characteristics, as a function of receiver angle. However, some concentrating solar collector designs operate with inverted cavity receivers.

At the beginning of each test, the receiver was placed in the +90° position with the aperture facing down. The flow system was started and the fluid was heated as close to the operating temperature as possible. Obtaining the nominal HTF temperature at the receiver inlet usually meant setting the heater temperature 25°F to 50°F higher, accounting for heat loss from the connecting line. The flow rate through the receiver was adjusted to approximately one gallon per minute. The one gallon per minute flow rate is typical for these type of receivers at STEP. Thermal stabilization is attained when there is less than 0.1 degree change in the inlet and outlet temperatures over the two minute data sampling interval. Reaching thermal stabilization often takes several hours depending upon the nominal operating temperature and the ambient laboratory conditions. When thermal stabilization was reached, temperature and flow measurements were recorded.

The convective heat loss from the cavity of the receiver is assumed to be negligible when the receiver is in the +90° position. This assumption is supported in two ways. First, smoke flow visualization techniques revealed negligible air flow across the aperture with the receiver in the +90° position. The second is the minimal variance between experimentally determined radiative heat loss at +90° and the calculated values and radiometer measurements.

Therefore, the total heat loss from the receiver in the +90° position is composed of radiative losses from the aperture and conductive losses through the side, back, and annulus walls of the receiver. The aperture of the receiver was then fitted with an insulated plug to eliminate the radiative component from the total heat loss. With the plug in place, the system was again allowed to reach steady state and again the temperature and flow measurements were recorded. In this manner, the radiative and conductive components of the total heat loss from the receiver for a particular operating temperature were isolated. The radiative and conductive heat losses are assumed constant with receiver angle.

The receiver was then positioned in the +75° attitude and the system allowed to stabilize. The temperature and flow measurements were again recorded. The total heat loss measurements were normalized linearly to the nominal test temperature for comparison purposes. This accounted for the variation in the operating temperature from one test setup to the next. The thermal stabilization procedure was repeated for each receiver angle tested. The entire procedure was repeated for each nominal operating temperature test point.

The total heat loss from the receiver can be expressed as a mathematical relation. The preceding appears as:

$$q_{total} = \dot{m}\, Cp\, (T_{in} - T_{out}) \qquad (1)$$

where:

T_{in} = temperature of fluid at the inlet to the receiver [K]

T_{out} = temperature of fluid at outlet to receiver [K]

$\dot{m}$ = mass flow rate of the fluid [g/m]

Cp = specific heat of the fluid [K]

The mass flow rate is given by:

$$\dot{m} = \dot{v}\rho \qquad (2)$$

where:

$\dot{v}$ = volumetric flow rate

ρ = heat transfer fluid density at the inlet temperature

The conductive heat loss is given by:

$$q_{conductive} = q_{plugged\ @+90°\angle} \qquad (3)$$

The radiative heat loss is given by:

$$q_{radiative} = q_{unplugged\ @+90°\angle} - q_{plugged\ @+90°\angle} \qquad (4)$$

The convective heat loss at any angle, α, is then given by:

$$q_{convective\ @\ \alpha\angle} = q_{total\ @\ \alpha\angle} - q_{conduction} - q_{radiative} \qquad (5)$$

The HTF volumetric flow rate, inlet temperature, outlet temperature, and temperature difference were all measured with transducers. The density and heat capacity were both calculated as functions of temperature.

B. Aperture Size Effects

The second Phase of the testing examined the effects of receiver aperture size on the receiver heat loss. This Phase of the testing was performed at two operating temperatures of 400°F and 600°F, and seven receiver angles from 0 to +90° at 15° increments. The four aperture sizes tested were 6 inches, 12 inches, 18 inches, and 26 inches. The 18 inch diameter aperture is the standard size for this receiver. The Phase Two testing followed the same procedure used in Phase One testing with the additional step of changing aperture size. Heat loss values from Phase One were compared with Phase Two.

V RESULTS

A. Temperature and Angle Effects on Total and Convective Heat Losses

The data summary of the receiver operating temperature and receiver angle effects from the Phase One tests are tabulated in Appendix 1. These results were first presented by Stine and McDonald[8]. Total receiver heat loss varies, approximately, linearly with operating temperature (Fig. 9).

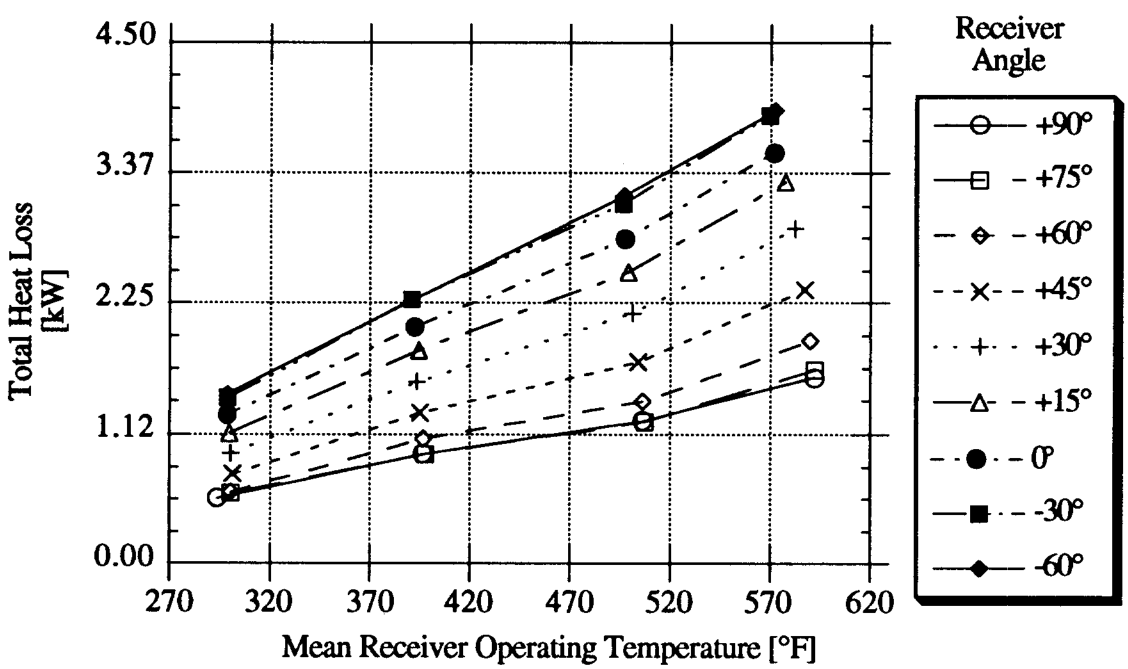

Figure 9. Total receiver heat loss versus operating temperature

The total receiver heat loss varies non-linearly with receiver angle (Fig. 10). The total heat loss is at a minimum when the receiver aperture orientation is downward. This supports the assumption of negligible convective heat loss with the receiver in this position. The maximum heat loss occurs when the receiver aperture is oriented at approximately +45° above horizontal. This particular receiver would not normally operate at angles above horizontal as these are negative angles.

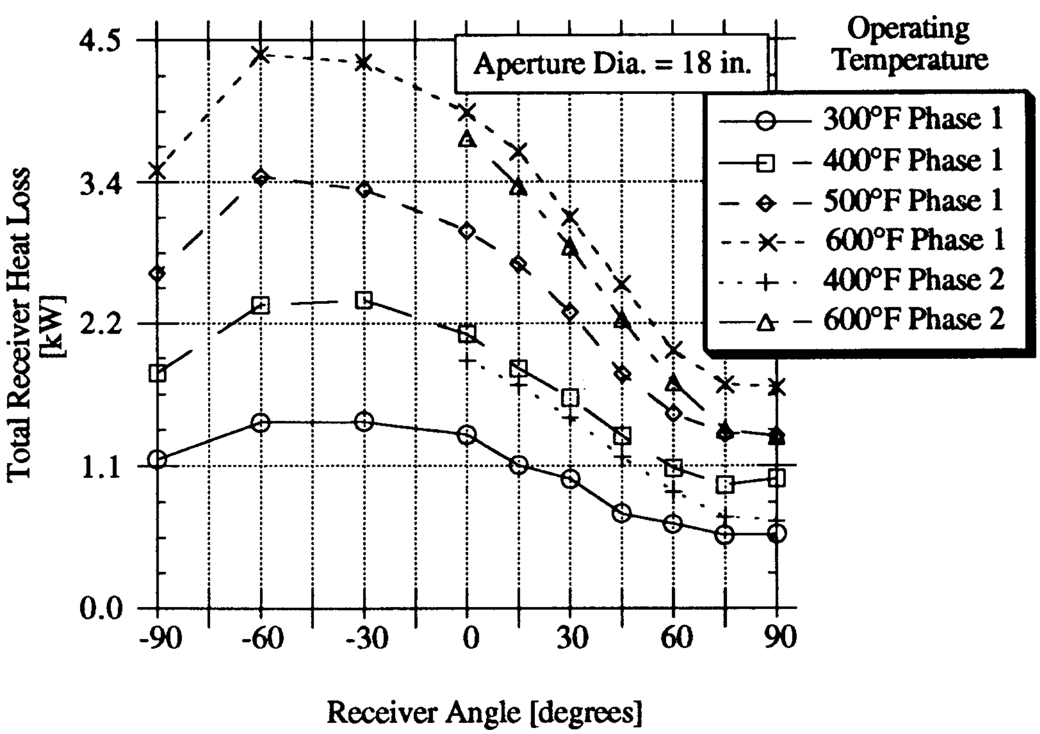

Figure 10. Total heat loss versus receiver angle for 18 inch aperture

Results from duplicate test conditions from Phase Two are also presented in Figure 10. As discussed previously, the convective heat loss through the aperture is determined by the difference between the total heat loss at any angle and the total heat loss for the +90° angle (Fig. 11). This requires that the convective heat loss be zero when the receiver is positioned at +90°, with the aperture down. The maximum convective heat loss occurred with the receiver in the -45° position. The reduction in total heat loss from Phase One to Phase Two testing, for receiver angles less than +60°, was assumed to be primarily due to the improved insulating properties of the cavity walls. The larger difference in the total receiver heat loss from Phase One to Phase Two for receiver angles greater than +60° resulted from the combined effects of improved insulation in the cavity walls and better sealing of the outer receiver skin. Apparently, sealing of the skin had little effect on heat loss from the receiver for angles less than +60°.

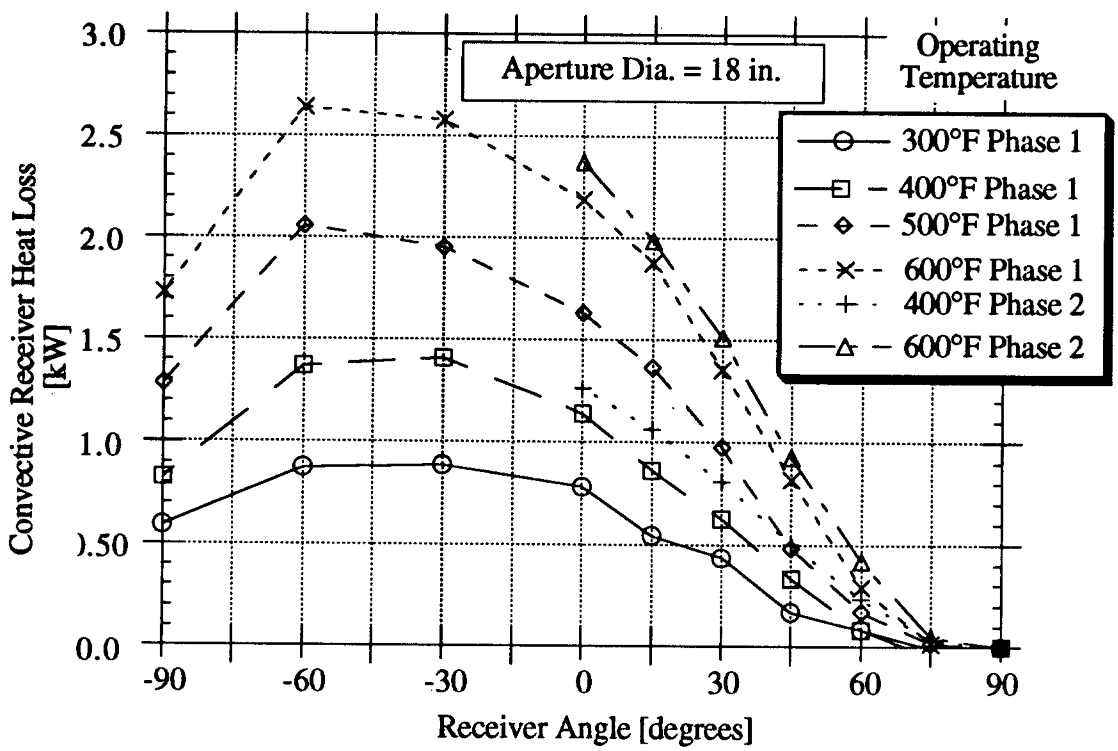

Figure 11. Convective heat loss for 18 inch aperture versus receiver angle

B. Aperture Size Effects on Total and Convective Heat Losses

The data summary of the Phase Two aperture size testing are tabulated in Appendix 2. These results were first presented by Stine and McDonald [8]. The effect of aperture size on the receiver total heat loss is shown (Fig. 12) for an operating temperature of 600°F. At a receiver angle of 0°, the total receiver heat loss increases by a factor of three as the aperture diameter increases from 6 inches to 26 inches. The total heat loss at the +75° and +90°

receiver angles are approximately equal. This agrees with a previous study (Stein and McDonald) on the effects of receiver angle(6). At these positions the total receiver heat loss increases by a factor of two when the aperture diameter increases from 6 inches to 26 inches for a 600°F operating temperature. At +45° the total heat loss increases approximately linearly with increase in aperture size. The receiver angle has less effect on the total heat loss for small apertures. The maximum variation due to receiver angle in the total heat loss is 0.4 kW for the 6 inch diameter aperture as compared to 1.2 kW loss with no aperture (26 inch aperture).

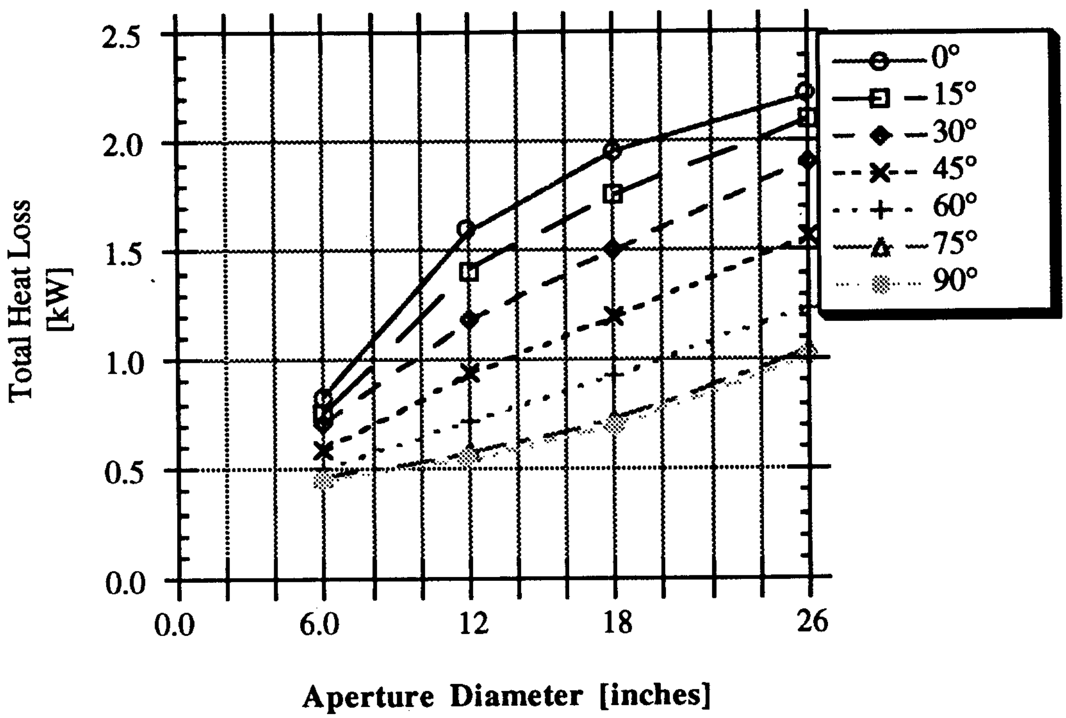

Figure 12. Total Receiver Heat Loss versus Aperture Size for 600°F

The effect of aperture size on the convective component of the total heat loss is shown in Figures 13 and 14. Aperture size has a much greater effect for low receiver angles than high receiver angles. The results also showed the convective loss increased dramatically when the aperture increased from 6 inches to 18 inches. There was little change in the convective loss as the aperture increased beyond 18 inches.

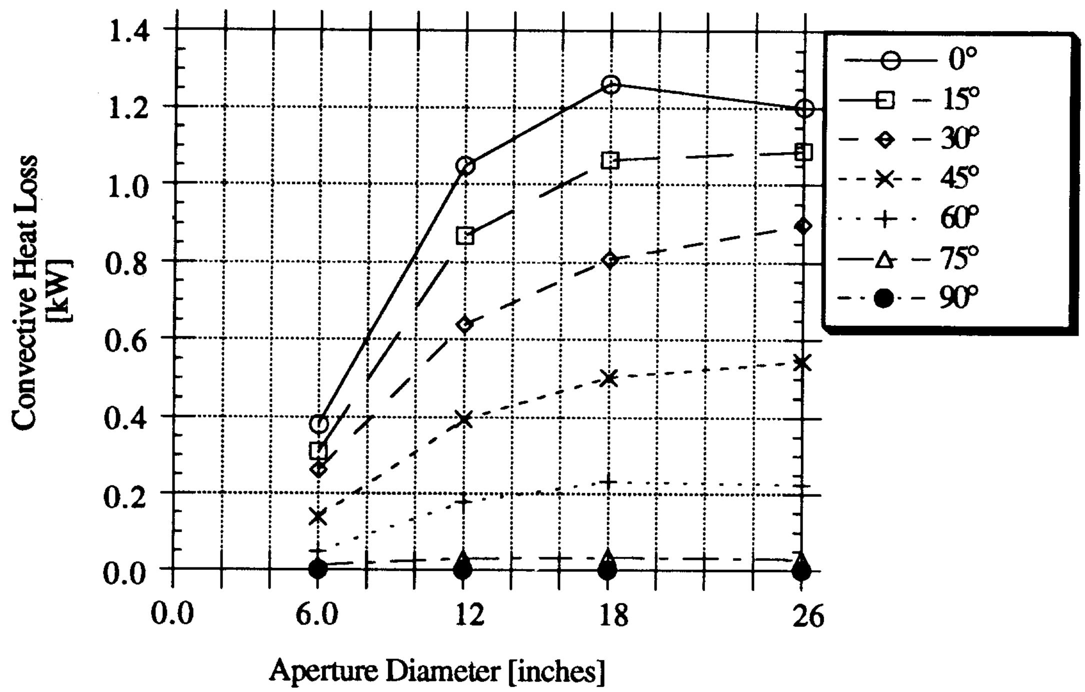

Figure 13. Convective Heat Loss versus Aperture Size for 400°F

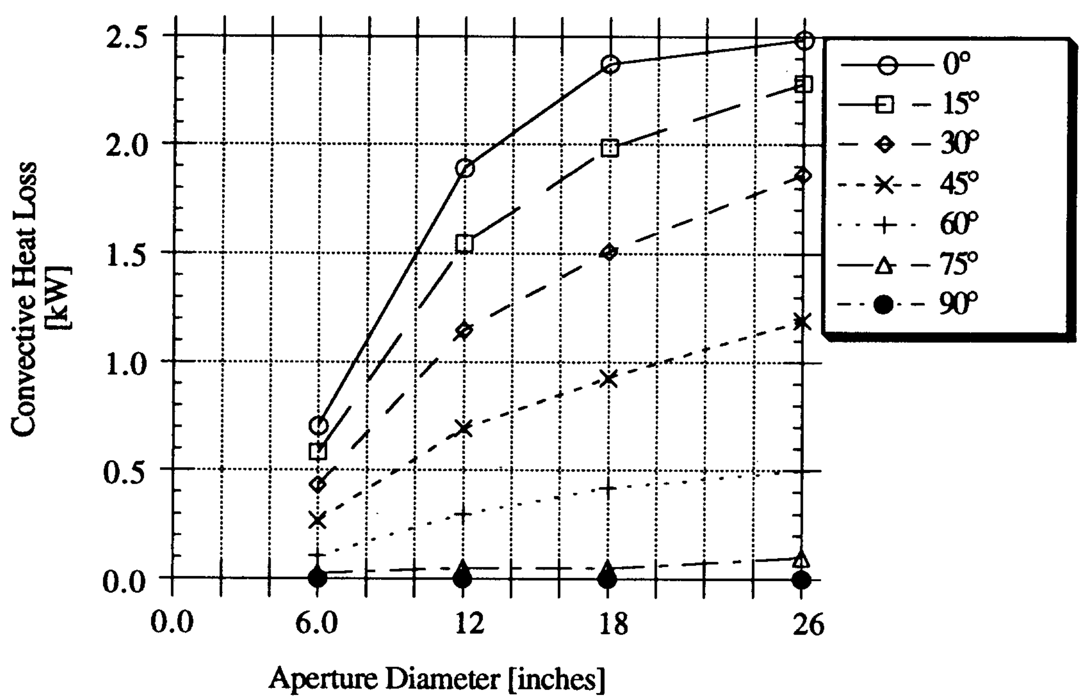

Figure 14. Convective Heat Loss versus Aperture Size for 600°F

C. Radiative and Conductive Heat Losses

In these tests, the radiative heat loss was determined from the difference between the plugged and unplugged values of the total heat when the receiver is in the +90° position. The radiative heat loss was assumed constant for all receiver angles. The conductive heat loss, through the receiver walls, was given by the total receiver heat loss when the receiver was in the +90° position with the aperture plugged. The conductive heat loss was also assumed constant for all receiver angles. The radiative and conductive heat losses from Phase One and Two of the testing were compared for repeatability (Fig. 15). Some differences were expected as a result of overhauling the receiver after the Phase One tests.

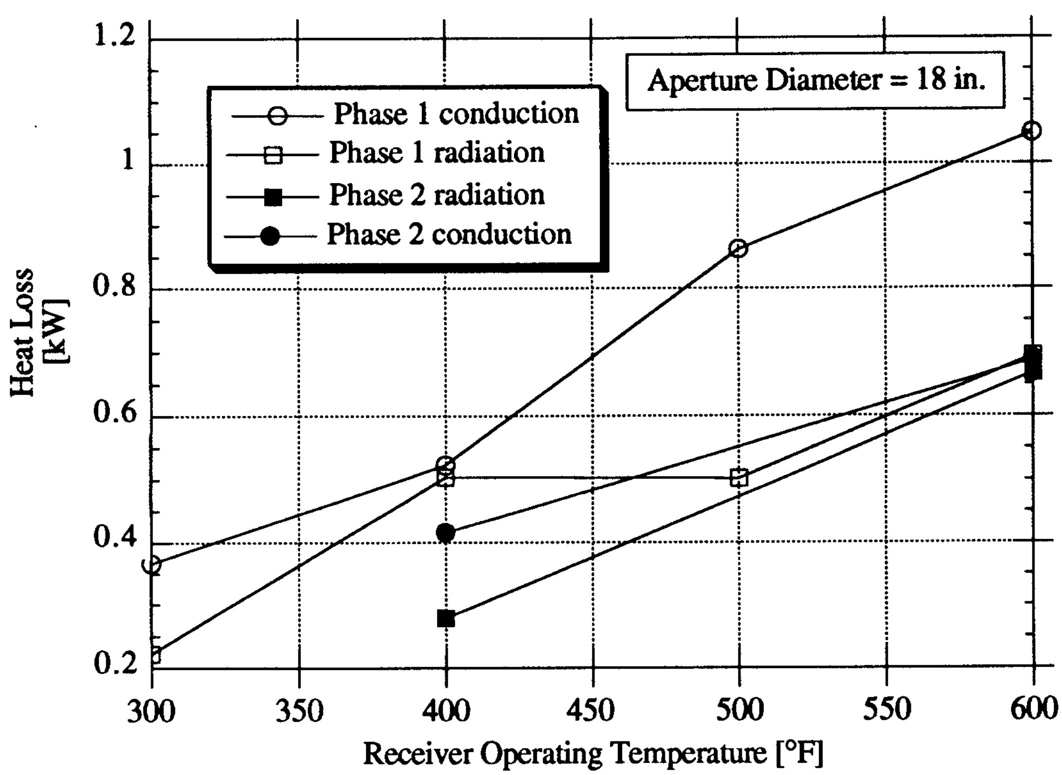

Figure 15. Radiative and Conductive Heat Losses versus Receiver Temperature

An infrared radiometer was another method used to determine radiative heat loss. The difference between radiometer readings taken with the receiver plugged and unplugged measured the radiative heat loss through the aperture. The two methods for determining the radiative heat loss are compared for operating temperatures of 600°F and 400°F (Figs. 16 and 17). The radiative heat loss increased approximately with the square of the aperture area. For each of the two nominal operating temperatures, the analytical heat loss was slightly higher. The difference between the analytical and experimental data, radiative heat loss, increased positively with aperture size. The disparity was accounted for via the estimated parameters used in analysis. These parameters include surface emissivity, temperature distribution, refractory and non-refractory. For small aperture diameters to cavity volume ratios, the cavity will radiate through the aperture essentially as a black body regardless of the emittances of the internal surfaces. However, as the ratio increases the cavity becomes less of a black body emitter. For large aperture diameter to cavity volume ratios, the emittances of the internal surfaces become critical in determining the cavity emittance. Also, for larger apertures the temperature difference between the inlet and outlet becomes significant. The fixed difference used in the analysis for all aperture sizes could affect the results. Further investigation is required to provide more accurate temperature distributions.

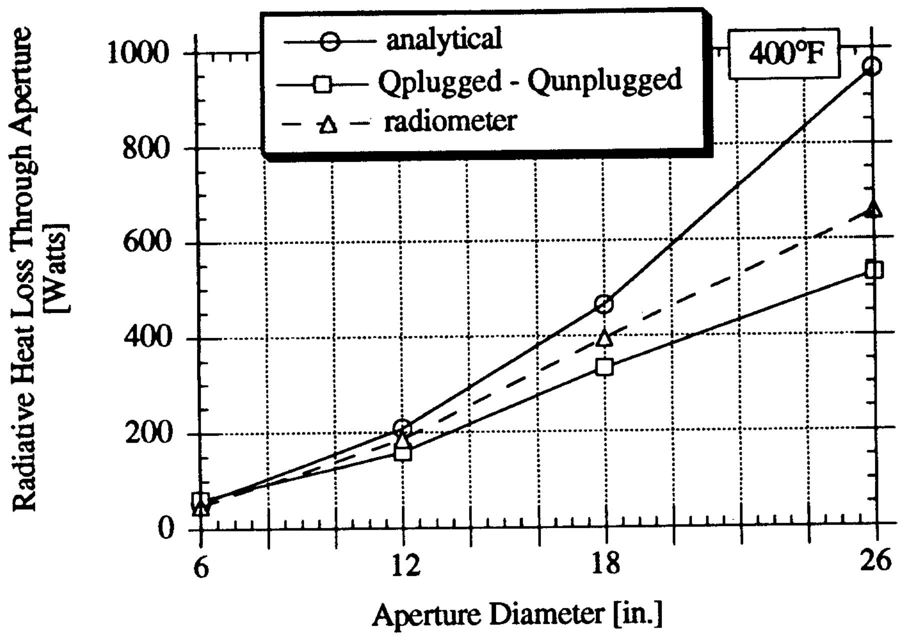

Figure 16 Radiative Heat Loss versus Aperture Size at 400°F

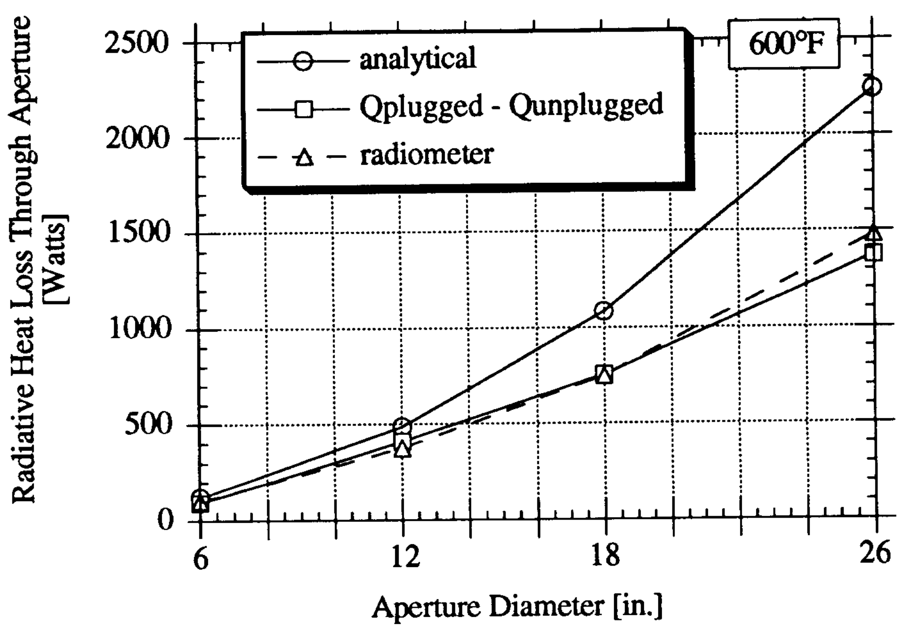

Figure 17 Radiative Heat Loss versus Aperture Size at 600°F

The total heat loss make-up, in terms of the radiative, conductive, and convective components, changes with aperture size. With a 6 inch aperture and the receiver at 45° the conduction loss forms about 65% of the total heat loss. With the receiver at a typical operating angle of 45° and an operating temperature of 600°F, radiative and convective percentages of total heat loss are approximately equal to an aperture of 26 inches (Fig. 18).

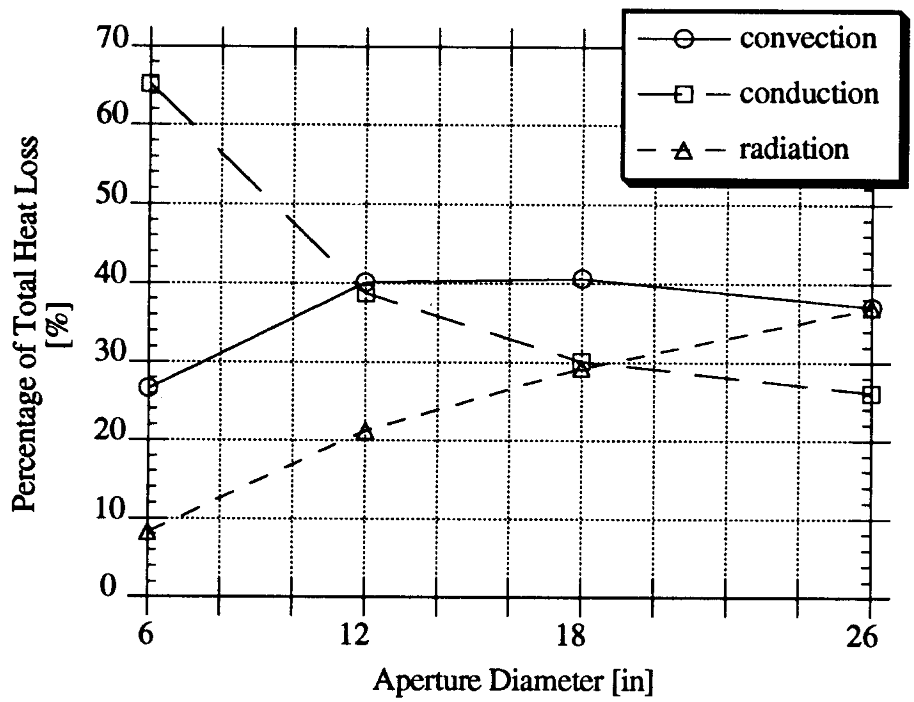

Figure 18. Percent Heat Loss Modes versus Aperture Size for 600°F at 45° angle

VI. PREVIOUS CAVITY CONVECTION LOSS MODELS

A. LeQuere, Penot, and Mirenayat Model

LeQuere, Penot and Mirenayat presented an experimental correlation for Nusselt number as a function of Grashof number.(9) Their study used a cubical cavity typical of those used in central receiver systems. The study investigated varying receiver temperatures and angles. The model was developed for a maximum temperature difference between cavity walls and the ambient, 230°F. Variation in receiver angles used in the model were from 0°, where the aperture is upward, to 180°, where the aperture is downward.

The cavity used in their testing was modular in design so that each panel could be heated independently. The panels were electrically heated. The electrical power and temperature of each panel were measured. Modular design allowed for local as well as global heat loss analysis. The total heat loss of the cavity was determined from the total electrical power used by all the panels. They determined the radiative component for total heat loss by summing the radiative heat loss of each panel to the cavity aperture.

$$q_{radiative} = \sum_{i}^{Nm} \varepsilon \, \sigma \, S \, (T^4_{panel} - T^4_{ambient}) \, F_{i\text{-}o} \tag{6}$$

where:

$\bar{\sigma}$ = Stefan-Boltzmann constant [W/m^2-K^4]

ε = emissivity of each panel

S = panel surface area [m^2]

T_{panel} = individual panel temperature [K]

$T_{ambient}$ = ambient temperature [K] opening

$F_{i\text{-}o}$ = view factor for a panel to cavity opening

N_m = total number of panels that compose the cavity

The conduction heat loss component is determined by the total heat loss of a plugged cavity. By plugging the aperture of the receiver, the radiative and convective components of the total heat loss are eliminated.

The convective heat loss is determined by subtracting the conductive and radiative components from the total heat loss.

$$q_{convection} = q_{total} - q_{conductive} - q_{radiative} \tag{7}$$

Their Nusselt number is given by:

$$Nu = \frac{q_{convection}\, L}{S\, k\, (T_{panel} - T_{ambient})} \tag{8}$$

where:

L = dimension of cavity aperture [m]

k = thermal conductivity of air [W/m•K]

S= total interior cavity surface area [m^2]

The Grashof number is given by:

$$Gr = \frac{g\, \beta\, (T_{panel} - T_{ambient})\, L^3}{\nu^2} \tag{9}$$

where:

g = local gravitational acceleration [m/s^2]

β = thermal expansion coefficient of air [K^{-1}]

ν = kinematic viscosity of air [m^2/s]

All fluid properties were evaluated at the ambient temperature. The experimental correlation for Nusselt number as a function of the Grashof number is given by:

$$Nu = a\, Gr^b \tag{10}$$

The coefficient 'a' and the exponent 'b' are empirically derived and are both a function of receiver angle. The values of 'a' and 'b' are presented in Table 1 for receiver angles of interest in this study. Equation 10 is valid for a Grashof number between 10^7 and 5×10^9.

Table 1.
Empirical correlation coefficients and exponents

Receiver Angle ø	Coefficient a	Exponent b
-90	0.0570	0.353
-75	0.0470	0.360
-60	0.0545	0.360
-45	0.0465	0.370
-30	0.0480	0.369
-15	0.0465	0.368
0	0.0925	0.330
15	0.0810	0.331
30	0.0640	0.332
45	0.0605	0.316
60	0.0685	0.292
75	0.0330	0.302
90	NA	NA

Consideration must be given to the difference in the cavity geometry from receiver used by LeQuere, Penot and Mirenayat and that used in this study. The receiver used by LeQuere, Penot and Mirenayat was cubical whereas the receiver used in this test was cylindrical and conical. The LeQuere, Penot and Mirenayat receiver aperture is the same as the characteristic interior dimension. They did not study the effect of varying aperture sizes.

LeQuere, Penot and Mirenayat modeled convective heat loss through the aperture is given by:

$$q_{convective} = h\,A\,(T_{cav} - T_{ambient}) \tag{11}$$

where:

h = convective heat transfer coefficient [w/m^{2}k]

A = total interior cavity surface area [m^2]

T_{cav} = area average cavity surface temperature [K]

$T_{ambient}$ = ambient air temperature [K]

The convective heat transfer coefficient is given by:

$$h = \frac{k\,Nu}{L} \tag{12}$$

where:

L = dimension of cavity aperture [m]

k = thermal conductivity of air [W/m-K]

Nu = Nusselt number

A BASIC computer language program was written to solve for the convective heat loss from the receiver used in this study applying the LeQuere, Penot, and Mirenayat model. For a listing of the computer program see Appendix 3. The results are presented in Appendix 4. The variations in the convective heat loss with receiver angles for operating temperatures from 300°F to 600°F and aperture sizes from 6 inches to 26 inches are presented (Fig. 19).

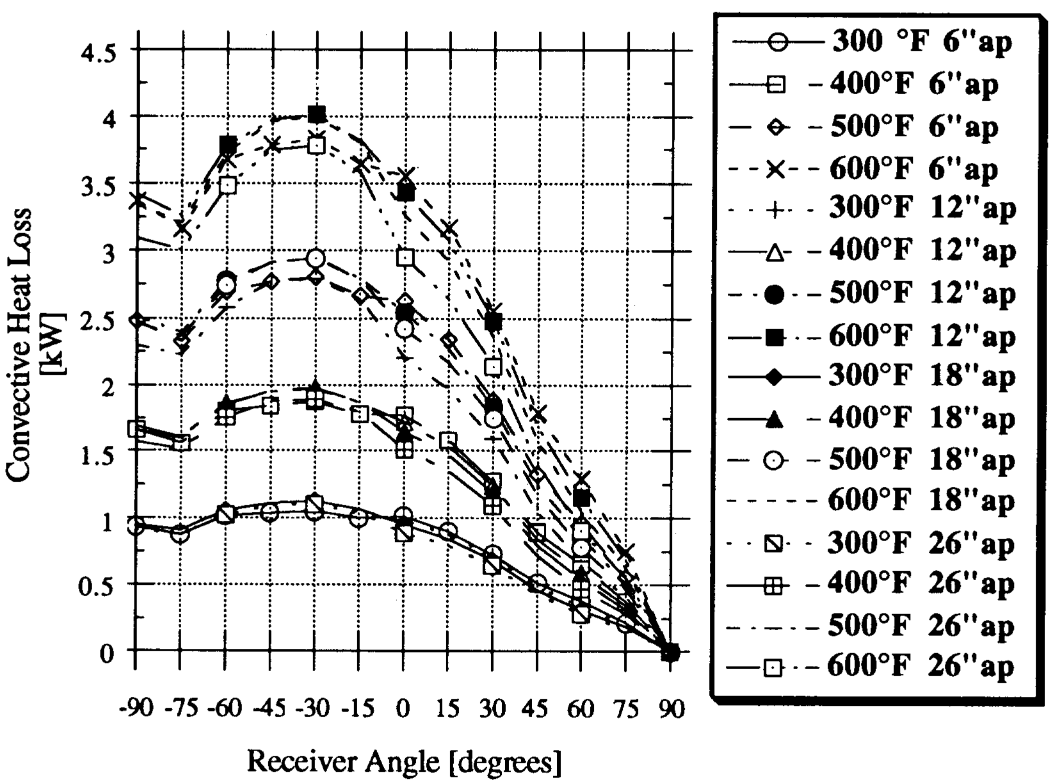

Figure 19. Convective heat loss for LeQuere, Penot, and Mirenayat model

B. Koenig and Marvin Model

The Koenig and Marvin model for predicting convective heat loss from a cavity receiver is presented by Harris and Lenz.[10] Their model is based on operating temperatures between 550°C(1022°F) and 900°C(1652°F) for an on-flux analysis. The operating temperature range used by Koenig and Marvin is considerably higher than any receiver temperature tested in this study. The Koenig and Marvin receiver was designed to operate at higher temperatures.

For the Koenig and Marvin model the convective heat loss through the cavity aperture is given by:

$$\dot{q}_{cav} = h\, A_T(T_{cav} - T_{amb}) \tag{13}$$

where:

A_T = area of heat transfer tubing facing inside cavity [m^2]

T_{cav} = inside cavity temperature or mean operating temperature [K]

T_{amb} = ambient air temperature [K]

h = cavity convective heat transfer coefficient [W/m^2k]

The heat transfer coefficient is given by:

$$h = \frac{k\, Nu_{cav}}{L} \tag{14}$$

where:

k = thermal conductivity of air [W/m-K]

Nu_{cav} = Nusselt number of the cavity

L = characteristic length of the cavity [m]

The characteristic length of the cavity used by Koenig and Marvin is given by:

$$L = \sqrt{2}\, R_{cav,i} \tag{15}$$

where:

$R_{cav,i}$ = mean inner cavity radius [m]

The Nusselt number is given by:

$$Nu_{cav} = 0.52\ P(\phi)\ \ell_c^{1.75}(Gr_L Pr)^{1/4} \tag{16}$$

where:

$P(\phi)$ = is an expression that accounts for the effects of receiver angle

ℓ_c = is an expression that corrects for aperture size

Gr_L = Grashof number

Pr = Prandtl number

The receiver angle function is given by:

$$P(\phi) = \cos^{3.2}\phi \qquad \text{for } 0° \le \phi \le 45° \tag{17}$$

$$P(\phi) = 0.707\ \cos^{2.2}\phi \qquad \text{for } 45° \le \phi \le 90° \tag{18}$$

where:

ϕ = angle of cavity axis with the horizontal [degrees]

The aperture size function is given by:

$$\ell_c = \frac{R_{ap}}{R_{cav,i}} \tag{19}$$

where:

R_{ap} = cavity aperture radius [m]

The Grashof number is given by:

$$Gr_L = \frac{L^3 g\beta(T_{cav} - T_{amb})}{\nu^2} \tag{20}$$

where:

g = gravitational acceleration [m/sec^2]

β = coefficient of volumetric expansion [K-1]

ν = kinematic viscosity [m^2/sec]

The volumetric expansion coefficient for air is calculated as:

$$\beta = \frac{1}{T_{prop}} \tag{21}$$

where:

T_{prop} = temperature at which the air properties are evaluated [K]

The Koenig and Marvin air properties temperature is given by:

$$T_{prop} = \frac{11}{16} T_{cav} + \frac{3}{16} T_{amb} \tag{22}$$

The thermal radiative losses through the cavity aperture from the hot interior surface is given by:

$$\dot{q}_{rad} = \pi R_{ap}^2 \varepsilon_a \overline{\sigma} \, (T_{cav}^4 - T_{amb}^4) \tag{23}$$

where:

ε_a = emissivity of the aperture

$\bar{\sigma}$ = Stefan-Boltzmann constant [W/m^2-K^4]

$\varepsilon_a \approx 0.9$ for these studies

The conduction heat loss through the walls of the cavity is given by:

$$\dot{q}_{cond} = \frac{k_i A_c (T_{cav} - T_{amb})}{t} \tag{24}$$

where:

A_c = area for conduction through the cavity [m^2]

k_i = thermal conductivity of the cavity insulation [W/(m - K)]

t = thickness of cavity insulation [m]

The conduction area of the cavity for the receiver considered in this study is given by:

$$A_c = \pi \left(\frac{R_{cav,i} + R_{cav,o}}{2}\right)^2 + 2\,\pi \left(\frac{R_{cav,i} + R_{cav,o}}{2}\right) + \pi \left(R^2_{cav,i} - R^2_{ap}\right) \tag{25}$$

where:

$R_{cav,o}$ = cavity outside radius [m]

Application of the Koenig and Marvin model to the receiver under study here was accomplished using a BASIC computer language program. The program is listed in Appendix 5. The results of the Koenig and Marvin modeling are found in Appendix 6. Figure 20 summarizes the values in Appendix 6.

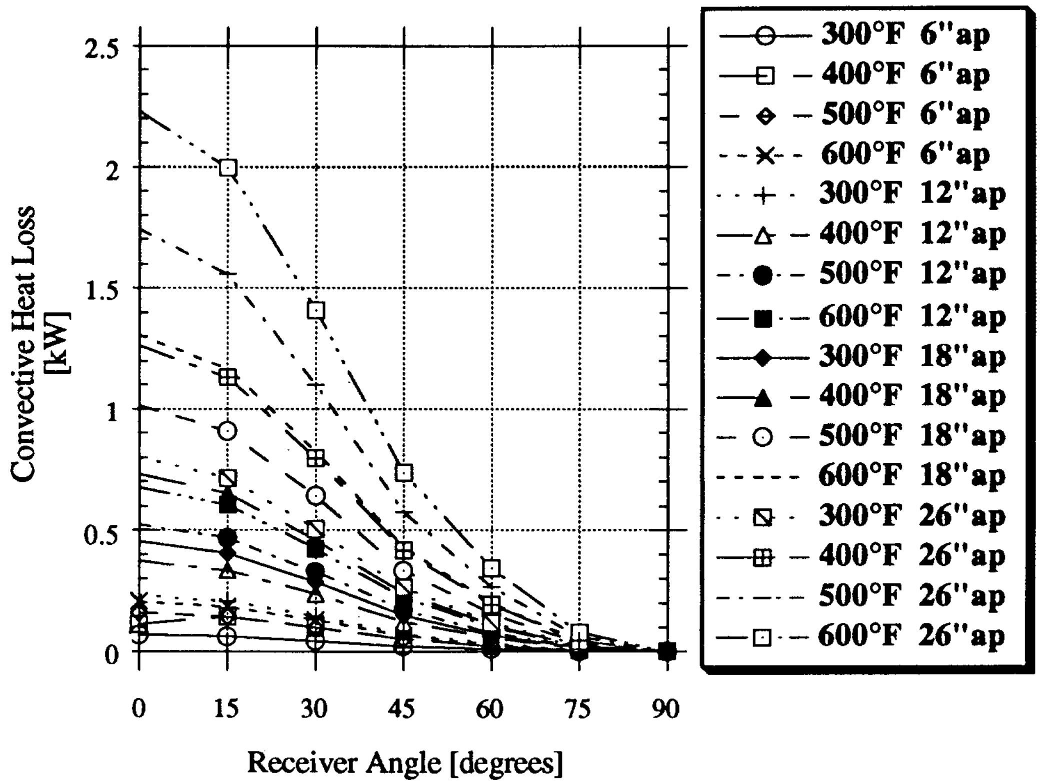

Figure 20. Convective heat loss for Koenig and Marvin model

C. CLAUSING MODEL

The Clausing model of convective heat loss from cavities was developed for large central receivers as opposed to the small receiver, used in this study.[11] The receivers utilized for the development of the Clausing model were simple in geometry with no curved surfaces. The Clausing model has been modified for application to the receiver provided in this study. The model was developed for on-flux mode of operation. For on-flux analysis the refractory surfaces are assumed to have a higher temperature than the active surfaces, whereas, for off-flux analysis the temperature conditions are reversed. Many of the temperature terms used in the Clausing model required modification to work for an off-flux situation.

Clausing's convective heat loss is based on an energy balance between the convective energy loss within the cavity, q_c, and the energy transported through the aperture of the cavity, q_a (i.e. $q_a = q_c$) (Fig 21).

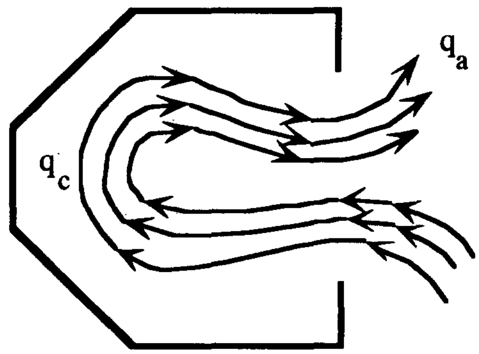

receiver cavity

Figure 21. Convective heat loss balance

The cavity is divided into two zones: a convective zone and a stagnation zone (Fig. 22). The horizontal plane cutting through the upper lip of the cavity aperture divides the convective zone from the stagnation zone. The convective current in the cavity flow over the heated surfaces, the refractory surfaces, and the area of the horizontal plane dividing the stagnation zone from the convective zone. The heated and refractory walls in the stagnation zone do not participate in any convective heat transfer.

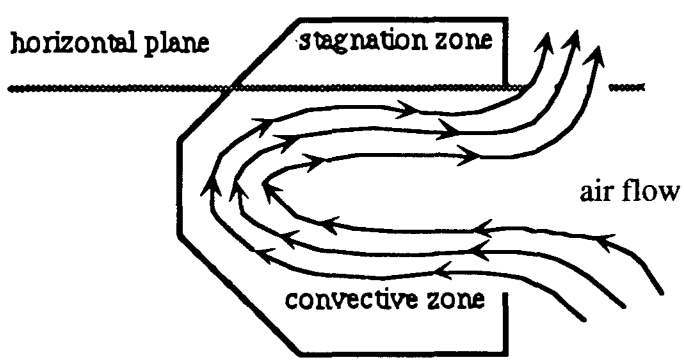

receiver cavity

Figure 22. Receiver internal cavity zones

1. Convective Energy Loss Through the Aperture

According to Clausing, the convective energy loss through the aperture is given by:

$$q_a = c_p(\rho_\infty V_a A_a)(T_c - T_\infty) \tag{26}$$

where:

ρ_∞ = ambient air density [kg/m^3]

V_a = average air flow velocity into the aperture [m/s]

A_a = area of the aperture through which air flows into the aperture [m^2]

c_p = specific heat of ambient air [J/kg-K]

T_c = temperature of the exiting air [K]

T_∞ = ambient air temperature [K]

The average exiting velocity is given by[11]:

$$V_a = \frac{1}{2}\sqrt{[(C_3 V_b)^2 + (C_4 V)^2]} \tag{27}$$

where:

$C_3 = 1$

$C_4 = 1/2$

V = wind speed [m/s]

V_b = buoyancy induced velocity [m/s]

For the no-wind condition, the interest of study, the equation reduces to:

$$V_a = \frac{1}{2}V_b \tag{28}$$

The buoyancy induced velocity is given by:

$$V_b = \sqrt{g\beta(T_c + T_\infty)L_a} \tag{29}$$

where:

g = local gravitational acceleration [m/s^2]

β = coefficient of volume expansion [k^{-1}]

L_a = projected vertical height of the aperture [m]

For air the temperature coefficient of volume expansion is given by:

$$\beta = \frac{1}{T_b} \tag{30}$$

where:

T_b = bulk air temperature in the convective zone of the cavity [K]

The bulk air temperature is given by:

$$T_b = \frac{T_c + T_\infty}{2} \tag{31}$$

The projected vertical height of the cavity is given by:

$$L_a = D_a \cos\theta \tag{32}$$

where:

D_a = the cavity aperture diameter [m]

θ = receiver angle [degrees]

2. Convective Energy Loss Within the Receiver

The Clausing model for convective heat loss within the cavity is given by:

$$q_c = hA_t(T_t - T_b) + hA_w(T_w - T_b) + hA_s(T_s - T_b) \qquad (33)$$

where:

h = average heat transfer coefficient [W/m^2-K]

A_t = tube surface area in convective zone [m^2]

T_t = average tube surface temperature [K]

A_w = refractory surface area of cavity in convective zone [m^2]

T_w = average refractory surface temperature [K]

A_s = area of interface plane between convective zone and stagnation zone [m^2]

T_s = average temperature of interface plane [K]

The average heat transfer coefficient is determined from the Nusselt number and is given by:

$$h = \frac{Nu\,k}{L_a} \qquad (34)$$

where:

Nu = Nusselt number

k = kinematic viscosity of air at the bulk fluid temperature [W/m-K]

For small receivers with a Grashof number of around 2.6 x 10^9 the Nusselt number is given by:

$$Nu = 0.10\,(Gr\,Pr)^{1/3} \qquad (35)$$

where:

Pr = Prandtl number = 0.7 (air)

Gr = Grashof number

The Grashof number is given by:

$$Gr = \frac{g\beta}{\nu^2}(T_w - T_\infty)L_a^3 \tag{36}$$

where:

ν = kinematic viscosity of air at the film temperature [m^2/s]

The film temperature is given by:

$$T_f = \frac{T_w + T_b}{2} \tag{37}$$

For the Grashof number expression the coefficient of expansion is given by:

$$\beta = \frac{1}{T_f} \tag{38}$$

Clausing assumes the temperature of the shear plane to be equal to the tube surface temperature in the convective zone (i.e. $T_s = T_t$). The cavity convective heat loss is then given by:

$$q_c = hA_t(T_t - T_b) + hA_w(T_w - T_b) + hA_s(T_t - T_b) \tag{39}$$

In this work, the refractory surface temperature is assumed to be 100°F cooler than the tube surface temperature. This temperature difference is typical for measured values at the end plate refractory surface and a heated tube surface near the end plate.

The convective heat transfer areas within the convective zone will vary in size with changes in receiver angle. The expressions for the convective heat transfer areas as a function of receiver angle area are developed in the Zone Area Formulas section.

3. Radiative Energy Loss Through the Aperture

An approximation for the radiative energy loss from the cavity through the aperture, as presented by Clausing, is given by:

$$q_r = A_a \, \varepsilon \, \sigma \left[\frac{A_c}{A_c + A_h} (T_w^4 - T_a^4) + \frac{A_h}{A_c + A_h} (T_m^4 - T_a^4) \right] \tag{40}$$

where:

ε = emittance of the cavity

σ = Stefan-Boltzmann constant [W/m^2-K^4]

If the aperture is assumed to radiate as a black body then the emissivity of the cavity is equal to one; especially when the ratio of aperture size to cavity volume is small.

4. Conductive Energy Loss From the Receiver

The Clausing model for the conductive heat loss through the cavity walls is given by:

$$q_k = \frac{k}{t} \left[A_h \, (T_m - T_a) + A_w \, (T_w - T_a) \right] \tag{41}$$

where:

k = thermal conductivity of the cavity walls [W/mK]

t = thickness of the cavity walls [m]

For this study:

k = .04756 [W/mK]

t = .0889 [m]=(3.5 [in.])

5. Zone Area Formulas

The receiver cavity is divided into two zones (Fig. 23). The boundary between the zones is formed by a horizontal plane cutting through the cavity at the upper lip of the aperture. The upper zone is assumed stagnant while the lower zone has active convective currents. The area in zone 1 is represented by the internal surface area of the receiver above the horizontal plane. The area in zone 2 is represented by the internal surface area of the receiver below the horizontal plane. The areas of zone 1 and zone 2 vary with receiver angle for a given receiver geometry.

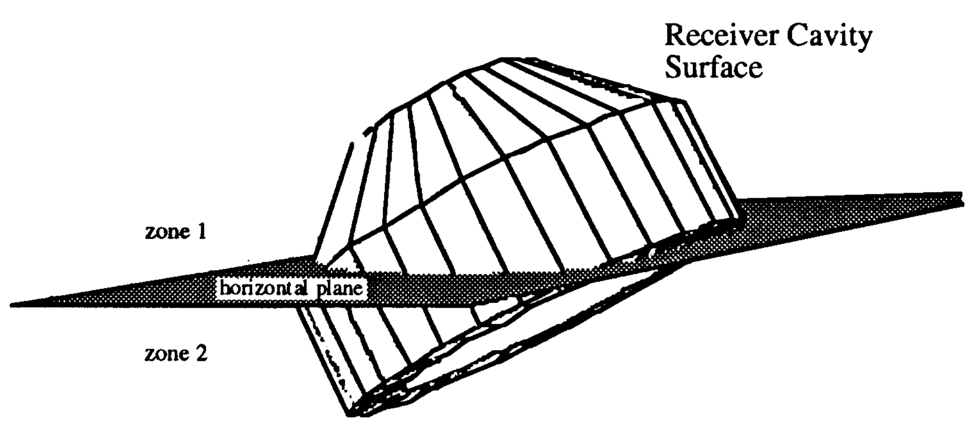

Figure 23. Cavity zones areas

The receiver internal geometry is divided into five sections representing the hot and cold surfaces in the receiver (Fig. 24). The hot surfaces are actively heated. The cold surfaces represent the refractory surfaces . Section 1 is the circular plate at the end of the frustum. Section 2 is the frustum portion of the tube bundle. Section 3 is the cylindrical portion of the tube bundle. Section 4 is the short refractory portion of the cylindrical section. Section 5 is the refractory ring that forms the aperture.

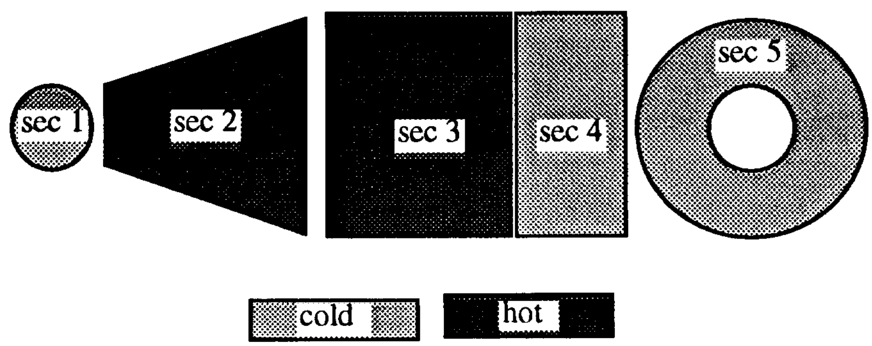

Figure 24. Cavity sections

As the receiver is rotated through various angles, each section of the internal receiver geometry may be divided by the horizontal plane that cuts through the upper inside edge of section 5. The formulas defining the portion of the area of each section that is in zone 1 for a given receiver angle range are derived in Appendix 7.

6. Shear Plane Area

The shear plane area is the area of the horizontal plane within the cavity (Fig. 25). The shear plane area is divided into two sections. The first section is formed by the horizontal plane cutting through the cylindrical portion of the receiver cavity. Not all of the horizontal plane in the cylindrical portion participates in the convective heat loss. The sides of the aperture reduce the effective shear plane area by restricting flow along the horizontal plane at the sides of the cavity near the aperture. The shear plane expands from the upper lip of the aperture in the horizontal plane. The second section is formed where the horizontal plane cuts the frustum portion of the receiver cavity. The formulas that describe the shear plane area in the specified portion of the cavity for a given receiver angle are derived in Appendix 7.

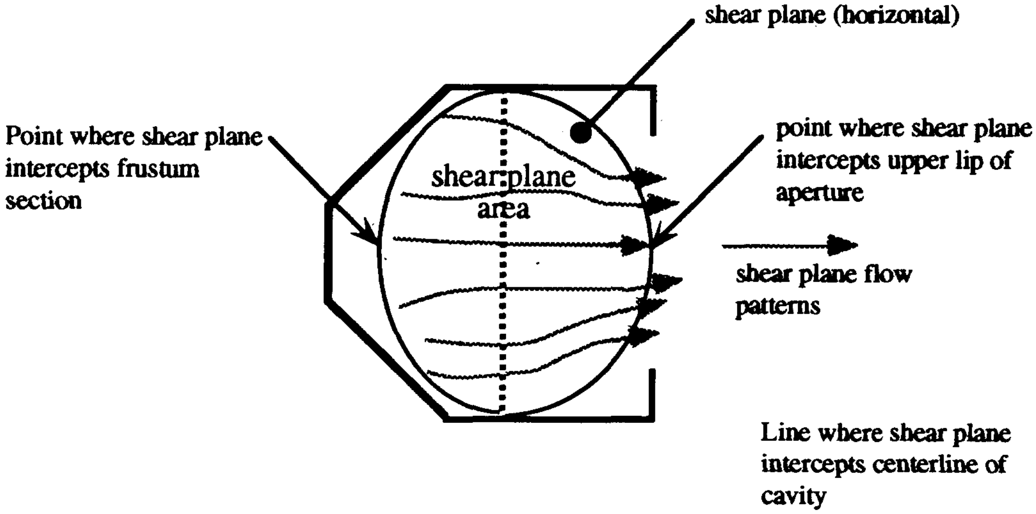

Figure 25. View looking down showing the effective shear plane area

7. Clausing Model Analysis

A BASIC computer language program was written to solve the convective heat transfer equations (Appendix 8). The mean operating temperature in the program is taken as the tube surface temperature in the convective zone of the receiver. The program calculates the convective energy loss from the receiver cavity for receivers at operating temperatures of 300°F, 400°F, 500°F, and 600°F, receiver angles from 0 to 90° at 15° increments, and aperture diameters of 6 inches, 12 inches, 18 inches, and 26 inches. The results of the Clausing heat loss analysis are presented in Appendix 9. The results of the Clausing model analysis are shown in Figure 26.

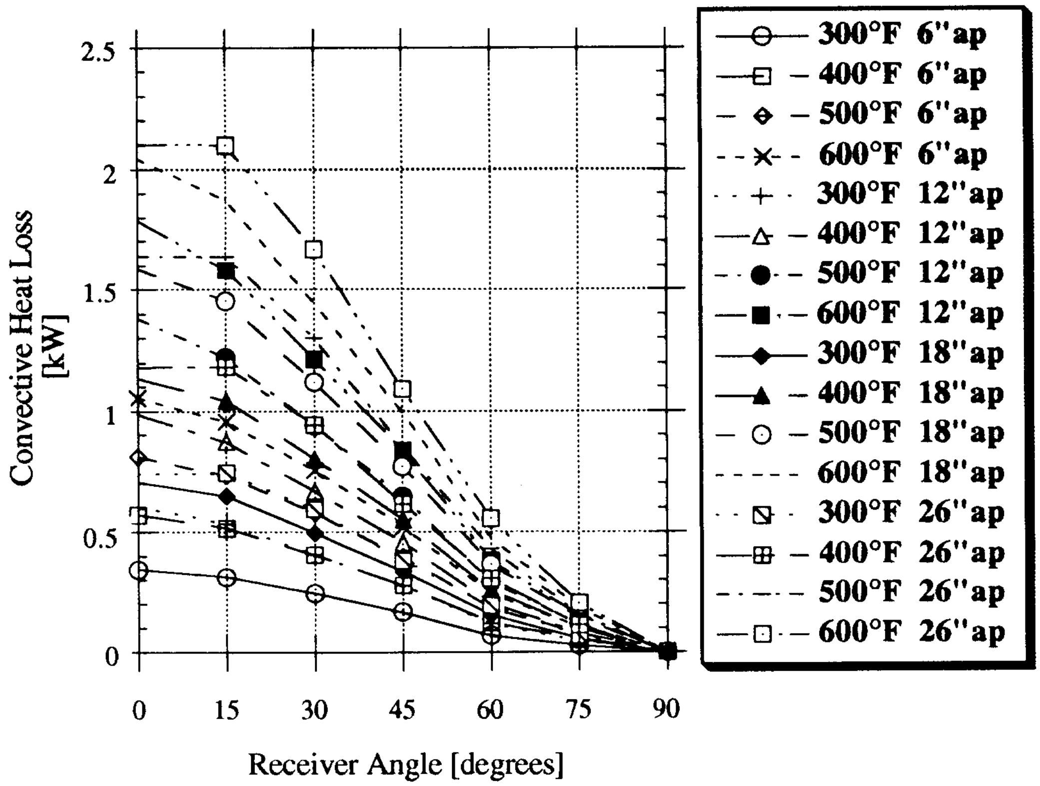

Figure 26. Convective heat loss for Clausing model

D. Siebers and Kraabel Model

Siebers and Kraabel present a simple model for the convective heat transfer from a solar cavity receiver.[12] They emphasize that the model has a large degree of uncertainty due to the lack of sufficient data on cavity receivers. The model was developed for a large central receiver cavity operations on-flux. This model is based primarily on the results of experimental studies from cubical cavities.

The following are the equations used to determine the convective loss from a solar cavity receiver. For natural convection the Nusselt number is given by:

$$Nu_L = 0.088 Gr_L^{1/3} \left[\frac{T_w}{T_\infty}\right]^{0.18} \quad (42)$$

for $10^5 \leq Gr_L \leq 10^2$

where:

Gr_L = Grashoff number

T_w = average interior cavity wall temperature [K]

T_∞ = ambient temperature [K]

$[\ ]_L$ = the projected vertical height of the receiver aperture [m]

An approximation for the average interior surface area of the cavity is given by:

$$\overline{T}_w = \frac{T_h A_h + T_c A_c}{A_{total}} \qquad (43)$$

where:

T_h = average operating temperature of the system [°C]

T_c = average refractory surface temperature in the cavity [°C]

$T_c = T_h - 56°C$

A_h = heated surface area in the cavity [m^2]

A_c = refractory surface area in the cavity [m^2]

The 1/3 exponent on the Grashof number results in a heat transfer coefficient that is independent of cavity dimensions. All fluid properties are evaluated at T_∞. The natural convective heat transfer coefficient is given by:

$$h_{nc,o} = 0.81\,(\overline{T}_w - T_\infty)^{0.426} \qquad (44)$$

where:

$[\ ]_{nc}$ = natural convection

$[\ ]_o$ = no lip heat transfer coefficient

The convective heat loss energy is given by:

$$Q_{conv} = \overline{h}_{nc,o}\, A\, (\overline{T}_w - T_\infty) \qquad (45)$$

where:

A = the total interior surface area of the cavity receiver [m^2]

$\overline{T}_w$ = the average receiver heated surface temperature [°C]

Siebers and Kraabel account for aperture effects by multiplying the natural convective heat transfer coefficient by an area ratio factor. The natural convective heat transfer coefficient including the effects of the aperture lip is given by:

$$\overline{h}_{nc} = h_{nc,o} \left[\frac{A_1}{A_2}\right]\left[\frac{A_3}{A_1}\right]^n \qquad (46)$$

where:

n = 0.63 for 0° ≤ ø ≤ 30°

n = 0.8 for 30° ≤ ø ≤ 90°

A_1 = total interior cavity surface area [m^2](Fig. 27)

A_3 = interior cavity surface area below the horizontal plane [m^2] (Fig. 27)

A_2 = A_1 minus the area of the lower lip [m^2] (Fig. 27)

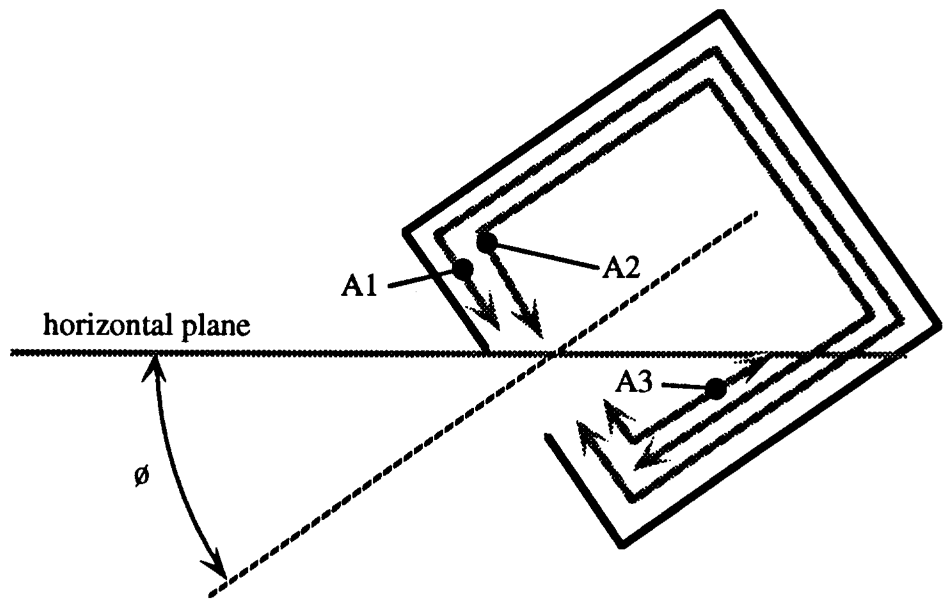

Figure 27. Siebers and Kraabel cavity areas

The refractory surfaces are assumed to be 56°C cooler than the mean operating temperature of the receiver. The formulas for areas A1 and A2 are given as follows:

$$A_1 = \pi(R_e + R_c)\sqrt{L_f^2 + (R_c - R_e)^2} + 2\pi R_c L_h + \pi R_e^2 + \pi\left(R_c^2 - R_a^2\right) + 2\pi R_c L_c \tag{47}$$

$$A_2 = A_1 - R_c^2 \cos^{-1}\frac{R_a}{R_c} + R_a\sqrt{\left(R_c^2 - R_a^2\right)} \tag{48}$$

The formula for A_3 depends on the particular receiver angle. The expressions developed for the variation of the cavity internal zone areas as a function of receiver angle can be found in Appendix 7.

The Grashof number is given by:

$$Gr_L = g\,\beta\,(\overline{T}_w - T_\infty)\,\frac{L^3}{\upsilon^2} \tag{49}$$

where:

g = gravitational constant, 9.81 m/s^2

L = cavity diameter [m]

υ = kinematic viscosity [m^2/s]

β = coefficeint of volumetric expansion [K^{-1}]

The uncertainty analysis provided by Siebers and Kraabel is presented in Table 2.

Table 2
Siebers and Kraabel Uncertainty Analysis

Parameters	Uncertainty
A_1	± 10%
A_2	± 10%
A_3	± 10%
A_{ap}	± 5%
T_w	± 10%
T_∞	± 2%
natural convection correlation	± 20%

A computer program was used to solve for the Siebers and Kraabel convective heat loss for various aperture diameters, receiver operating temperatures, and receiver angle. A listing of the computer program is in Appendix 10. The results of the convective heat loss analysis using the Siebers and Kraabel model are presented in Appendix 11. The Siebers and Kraabel predictions for the receiver convective heat loss variation with receiver angle are presented in Figure 28.

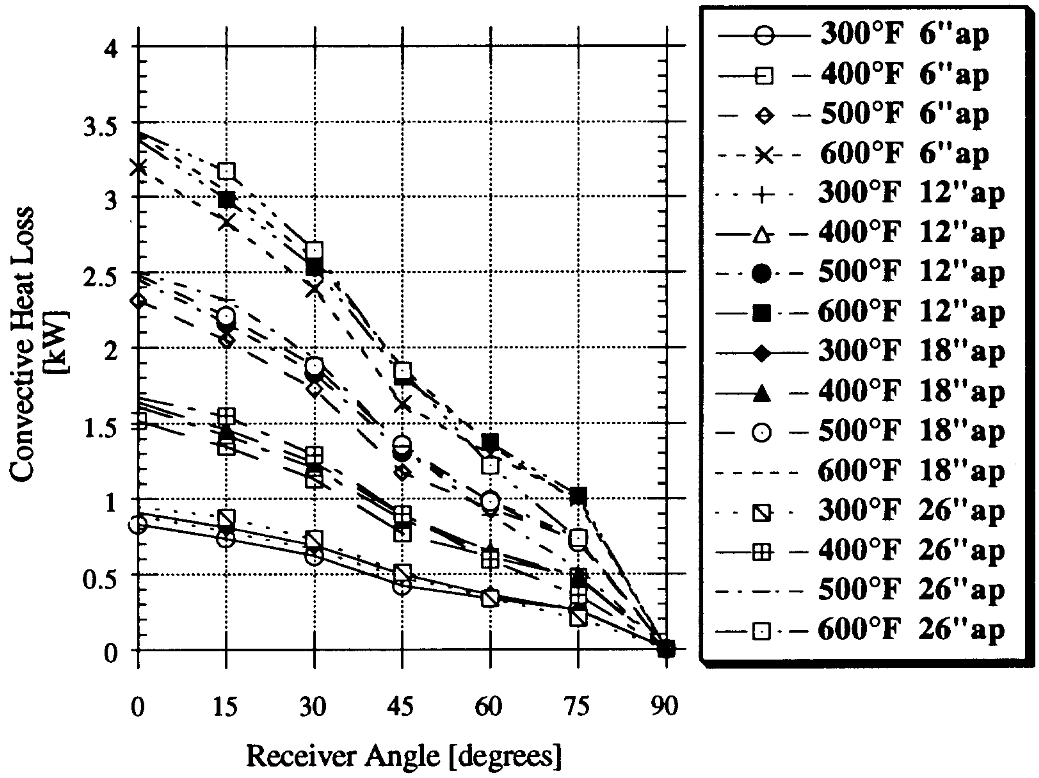

Figure 28. Convective heat loss for the Siebers and Kraabel model

VII COMPARISON OF CAVITY HEAT LOSS MODELS

With increasing aperture diameter there is a decrease in convective heat loss (Fig. 13 & 14). The effect of receiver angle on the convective heat loss is more pronounced on larger aperture diameters.

The conduction heat loss forms approximately 65% of the total heat loss for all operating temperatures when the aperture diameter is small and the receiver is placed at a typical operating angle of 45° (Fig. 21).

The percent conduction is reduced and the percent radiative increased with increases in the aperture . With an aperture greater than 12 inches, the percent conduction of the total heat loss is constant at about 38%. With the 6 inch diameter the percent conduction of the total heat loss is reduced to 25%.

Of primary interest is how well the various models compare with the experimental results. Of the six models examined, only the LeQuere, Penot and Mirenayat model provides for negative receiver angles.

A. Comparison of Previous Models with Experimental Data

The convective heat loss values predicted by the LeQuere, Penot and Mirenayat model are compared with the experimental results of Phase One and Phase Two(Fig. 29). For an ideal correlation, all the data points would fall on the equal value line. An ideal correlation occurs when the predicted results equal the experimental results. All the convective heat loss values predicted by the LeQuere, Penot and Mirenayat model are lower than the experimental results. The large degree of data scattering for higher heat loss values makes it difficult to apply a simple correction factor to the model.

The Koenig and Marvin model for convective heat loss demonstrates more agreement with experimental result than the LeQuere, Penot and Mirenayat model (Fig. 30). The Koenig and Marvin model yields higher convective heat loss values, as compared to the experimental results. The data shows increasing scatter for higher heat loss values. The model only works for positive receiver angles.

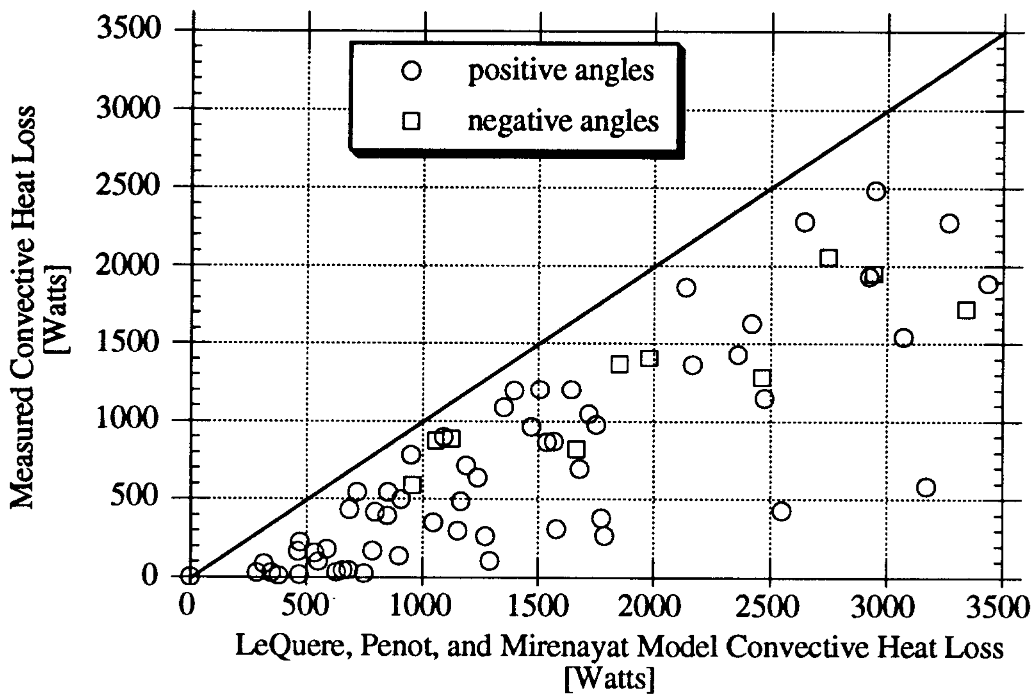

Figure 29. LeQuere, Penot, Mirenayat Convective Heat Loss Model Correlation

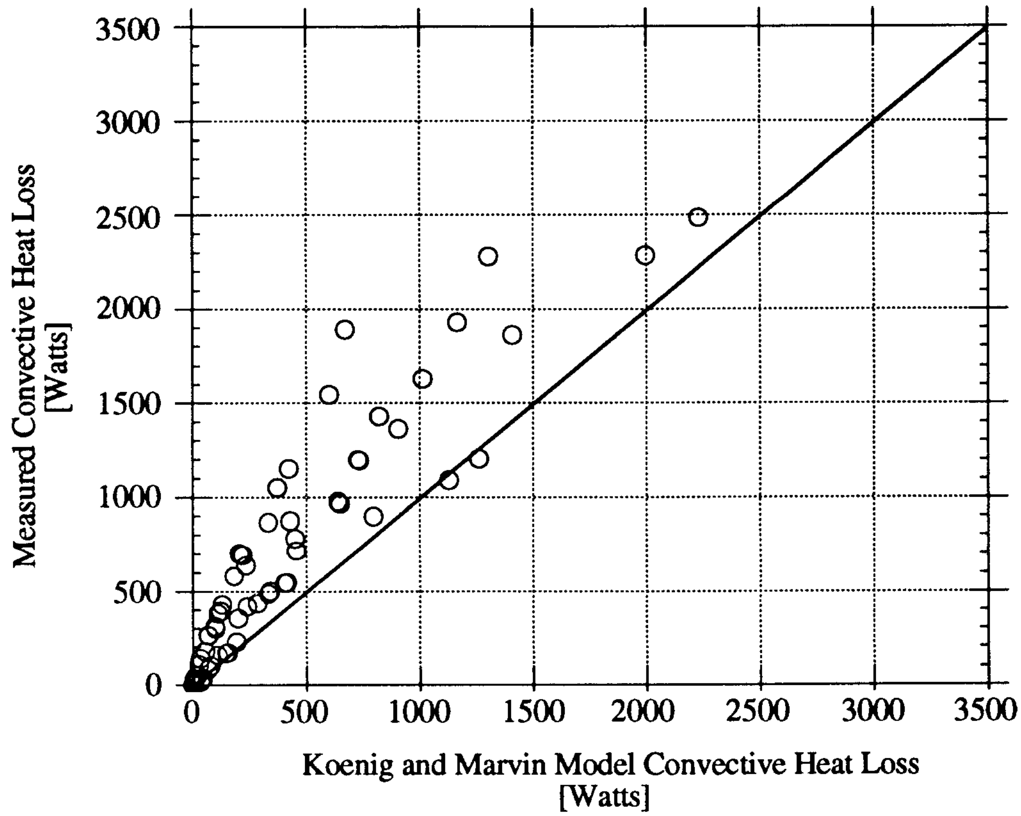

Figure 30. Koenig and Marvin Convective Heat Loss Model Correlation

The Clausing model provides the best fit of all the previous models examined (Fig. 31). This model predicts only heat loss values for positive receiver angles. The Clausing model is considerably more complicated than any of the other models. The Clausing model overestimates the convective heat loss for lower heat loss conditions and underestimates the convective heat loss for higher heat loss conditions.

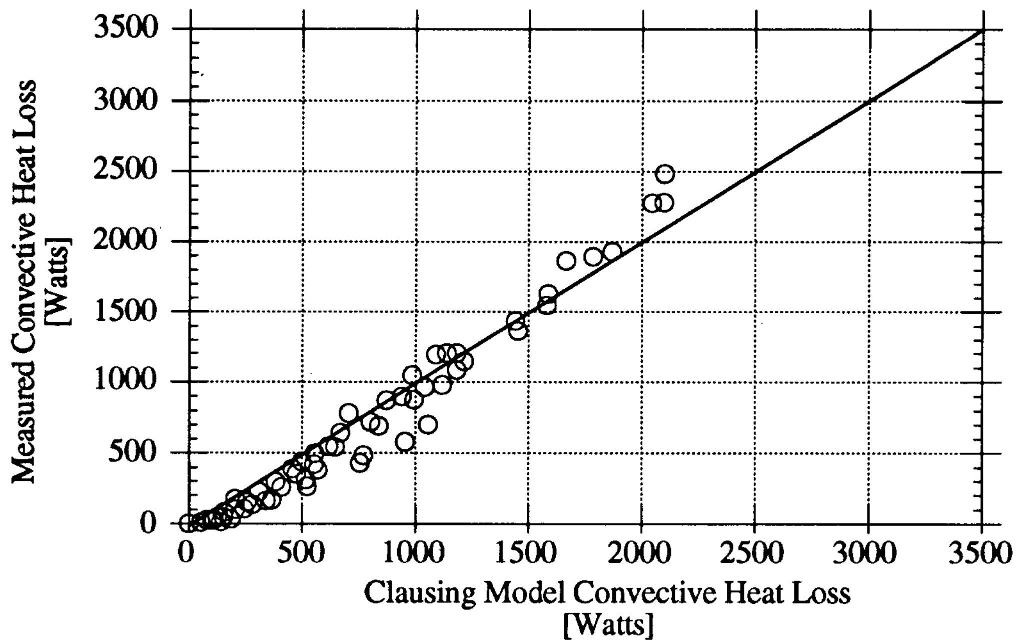

Figure 31. Clausing Convective Heat Loss Model Correlation

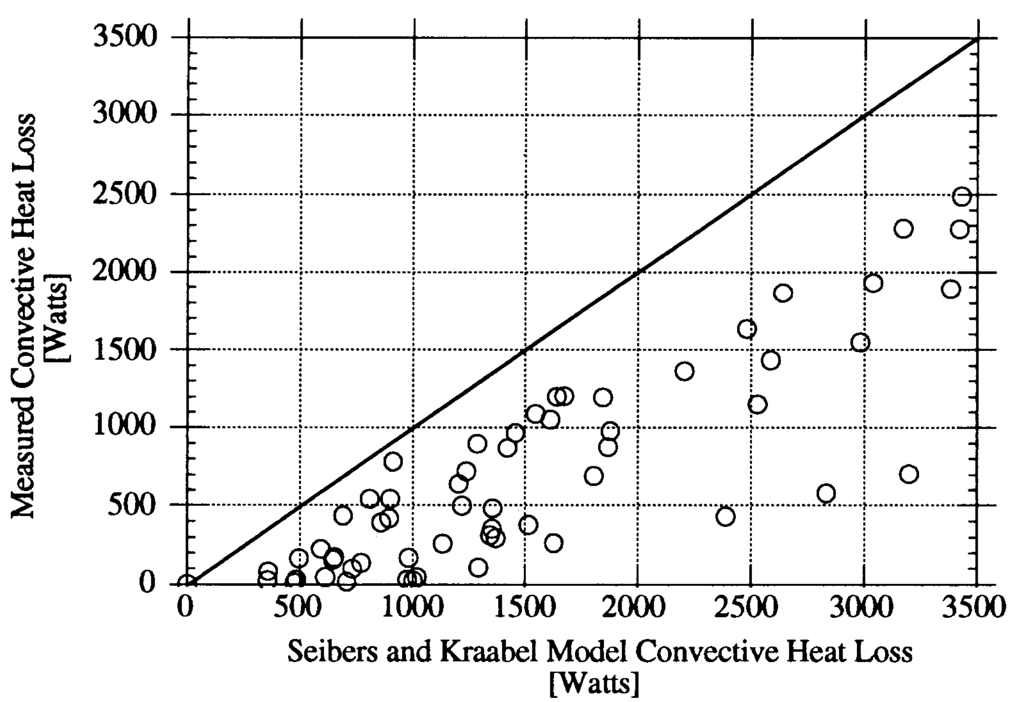

Figure 32. Siebers and Kraabel Convective Heat Loss Model Correlation

The Siebers and Kraabel model over estimates the convective heat loss as compared with the experimental results (Fig. 32). This model also shows considerable scatter for all heat loss conditions.

B. Stine and McDonald Correlation

The Stine and McDonald model is an extension of the Siebers and Kraabel model to include the effects of varying receiver aperture size and receiver angle (8). The complex set of area determinations are not used in the Stine and McDonald model. The Stine and McDonald correlation for the Nusselt number is given as follows:

$$Nu_L = 0.088\, Gr_L^{\frac{1}{3}} \left(\frac{T_w}{T_\infty}\right)^{0.18} (\cos\phi)^{2.47} \left(\frac{d}{L}\right)^{s} \tag{50}$$

and

$$s = 1.12 - 0.98 \left(\frac{d}{L}\right) \tag{51}$$

where:

- d = aperture diameter [m]
- Gr_L = Grashof number based on length L
- L = average internal dimension of cavity [m]
- Nu_L = Nusselt number based on length L
- T_∞ = ambient temperature [K]
- T_w = average internal wall temperature [K]
- f = tilt angle of cavity
- ($f = 90°$ is aperture-down, $f = 0°$ is aperture-sideways)

The aspect ratio term, d/L, accounts for the combined effects of internal surface area and aperture flow area. The effect of the receiver aspect diminishes with increase in aperture size, with the exponent 's'. The Stine and McDonald model predictions compare well with experimental results (Fig. 33). This model can only be applied for positive receiver angles.

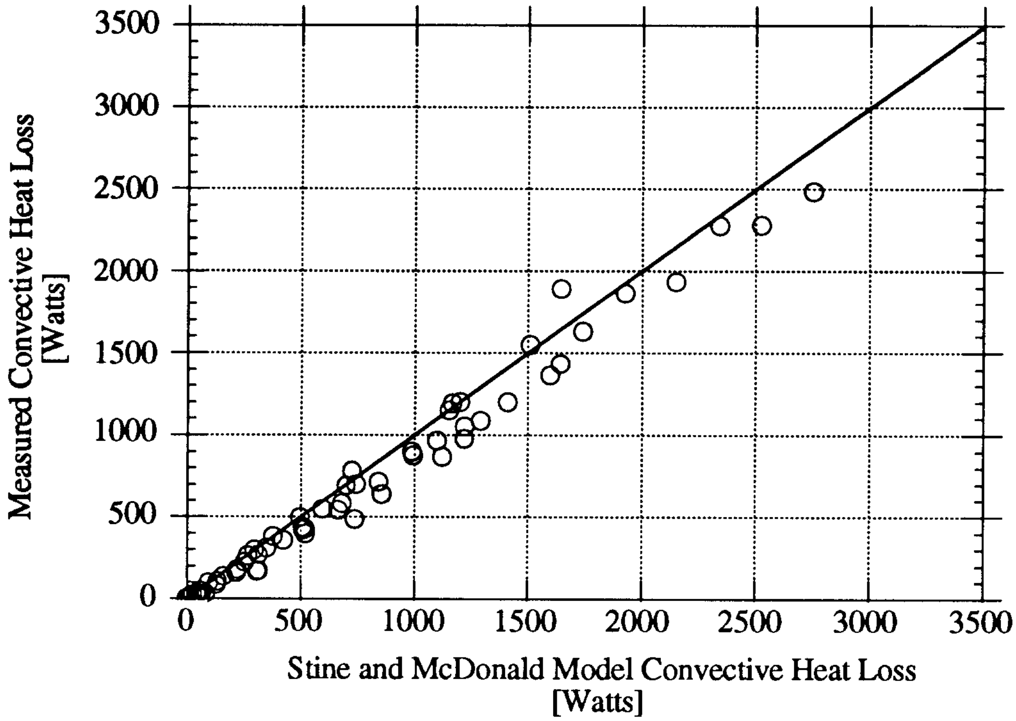

Figure 33. Stine and McDonald Convective Heat Loss Model Correlation

The computer program used to generate the Stine and McDonald convective heat loss values is provided in Appendix 12. The data output from the program is presented in Appendix 13.

VIII. ANALYTICAL RADIATIVE HEAT LOSS

In this section the equations used to predict the thermal radiative heat loss through the aperture of the cavity solar receiver are developed. The receiver cavity surfaces are assumed to radiate as gray bodies. The internal geometry is simplified to aid in the formulation of the shape factor expressions.

A. Internal Geometry

The internal receiver surfaces were divided into five main sections (Fig. 34). The sections are defined as either hot or cold. The hot sections were those whose walls were formed by the heat transfer tubing. The hot sections were divided into an integer number of flat, concentric, isothermal bands. The number of bands in each section was determined by the number of turns the heat transfer tubing made in that section. The frustum section has 23 bands and the hot cylindrical section has 15 bands. The width of each band is equal to the surface length of each section divided by the number of bands in each section. The actual spacing between adjacent tubes was not considered significant.

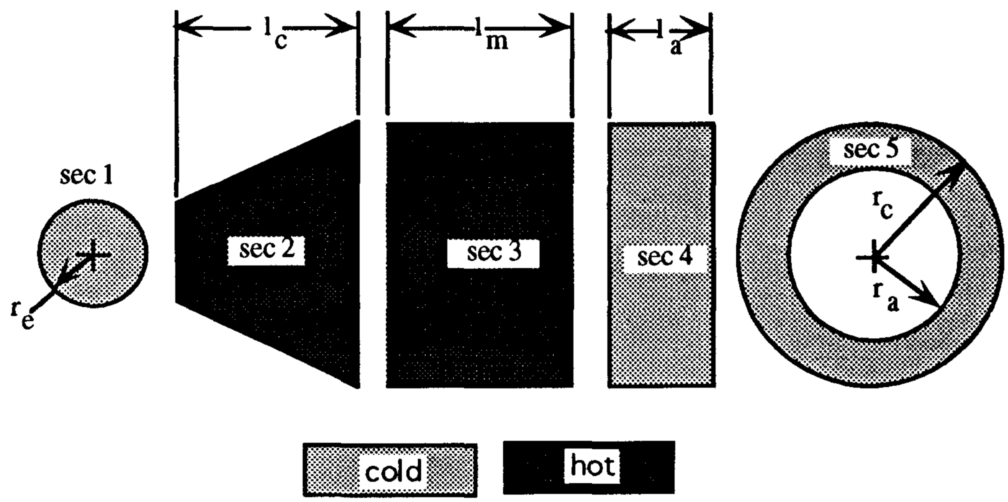

Figure 34. Receiver internal surface sections.

1. Nomenclature

The following list defines the nomenclature used in the thermal radiative heat loss formulas.

- r_e= end plate radius [12.7 cm]
- r_c= cavity radius [33.0 cm]
- r_a= aperture radius [7.6, 15.2, 22.9, 33.0 cm]
- l_c= length of frustum section [29.2 cm]
- l_m= length of hot cylindrical section [25.4 cm]
- l_a= length of cold cylindrical section [14.0 cm]
- l_b= width of hot isothermal bands [1.7 cm]

N_c= number of bands in frustum section (23)

N_m= number of bands in hot cylindrical section (15)

$$l_c \equiv [(l_b \; N_c)^2 - (r_c - r_e)^2]^{1/2} \tag{54}$$

B. Assumptions

A number of assumptions are necessary to simplify the thermal radiative heat loss calculations. The assumptions made for this analysis are listed as follows:

1. Each band is isothermal based on a linear interpolation between the inlet temperature at the narrow end of the frustum section to the outlet temperature at the bottom end of the hot cylindrical section.
2. Each band is considered as a flat surface.
3. Each tube band is diffuse and gray with emissivity, $\varepsilon = 0.85$.
4. The incident and reflected energy flux is uniform over each area.
5. Each band is adjacent to the next (i.e., no gaps between bands).
6. Each refractory surface has an emissivity of 0.70.

C. Shape Factors

All formulas are developed from the basic disc-to-disc shape factor formula.[20] The N by N coefficient matrix of the surface energy balance equation (Eqn. 64) requires N^2 shape factors . The equations are solved using a digital computer. Equation 64 is conservation of energy from all the surfaces. Shape factors describe the geometric relationship between surfaces. The derivation of the shape factor formulas used in the coefficient matrix are presented in Appendix 14.

D. Thermal Radiative Heat Loss Equations

The general equation for thermal radiative heat loss from the receiver through the aperture for internal black body surfaces is given by:

$$Q_a = -\sigma T_e^4 A_e F_{A_e - A_a} - \sigma T_s^4 A_s F_{A_s - A_a} - \sigma A_{n_m} \sum_{n_m=1}^{N_m} T_{n_m}^4 F_{n_m - A_a} - \sigma \sum_{n_c=1}^{N_c} T_{n_c}^4 A_{n_c} F_{n_c - A_a}$$

where:

$[\ ]_s$ = annuls

$[\ ]_e$ = end plate

$[\ ]_a$ = aperture

$[\ ]_{nm}$ cylindrical section

$[\ ]_{nc}$ = frustum section

As the aperture size to cavity volume ratio decreases, the radiative characteristics of the receiver cavity approach those of a black body emitter. To account for the various aperture sizes studied, the diffuse gray surface formulas were used. Using the net radiative method, the radiative heat loss for a cavity with diffuse gray surfaces is given by:

$$Q_k = q_k A_k = (q_{o,k} - q_{i,k}) A_k \tag{56}$$

$$q_{o,k} = \varepsilon_k \sigma T_k^4 + \rho_k q_{i,k} \tag{57}$$

$$q_{o,k} = \varepsilon_k \sigma T_k^4 + (1 - \varepsilon_k) q_{i,k} \tag{58}$$

where:

q_o is the outgoing radiant energy flux (radiosity) [W/m^2]

q_i is the incoming radiant energy flux [W/m^2]

For the aperture:

$$q_{o,opening} = 0$$

$$T_{opening} = 0$$

$$\varepsilon_{opening} = 1$$

For the cavity:

$$\sum_{j=1}^{N} [\delta_{kj} - (1 - \varepsilon_k)F_{k-j}]q_{o,j} = \varepsilon_k \sigma T_k^4 \tag{59}$$

where

N = total number of surfaces

F_{k-j} = shape factor for surface k to surface j

∂_{kj} = Kronecker delta

$$\delta_{kj} = \begin{cases} 1 \text{ when } k = j \\ 0 \text{ when } k \neq j \end{cases}$$

therefore:

$$Q_k = A_k \frac{\varepsilon_k}{(1 - \varepsilon_k)} (\sigma T_k^4 - q_{o,k}) \tag{60}$$

and

$$q_{i,k} = \sum_{j=1}^{N} F_{k-j}\, q_{o,j} \tag{61}$$

letting

$$a_{kj} = \delta_{kj} - (1 - \varepsilon_k)F_{k-j} \tag{62}$$

and

$$C_k = \varepsilon_k \sigma T_k^4 \tag{63}$$

then

$$\begin{bmatrix} a_{11} \cdots\cdots & a_{1j} \cdots\cdots & a_{1N} \\ a_{k1} \cdots\cdots & a_{kj} \cdots\cdots & a_{kN} \\ a_{N1} \cdots\cdots & a_{Nj} \cdots\cdots & a_{NN} \end{bmatrix} \begin{bmatrix} q_{o,1} \\ q_{o,k} \\ q_{o,N} \end{bmatrix} = \begin{bmatrix} C_1 \\ C_k \\ C_N \end{bmatrix} \tag{64}$$

The solutions for $q_{o,k}$ are accomplished using a BASIC computer language program (Appendix 15). The heated surfaces are assumed to have an emissivity of 0.85 based on the paint coating specifications. The refractory surfaces are assumed to have a emissivity of 0.70.

E. Assumed Cavity Temperature Distribution

The axial temperature distribution along the heating surface sections is assumed to vary linearly from the top of the frustum section to the bottom of the cylindrical section. The temperature of the top band of the frustum section is equal to the receiver inlet temperature. The temperature of the bottom band of the cylindrical section is equal to the receiver outlet temperature. The inlet and outlet temperature values used in the computer program are assumed to be plus and minus 7.5°F of the operating temperature, respectively.

Table 3
Inlet and Outlet temperatures

Test Phase	Aperture Diameter [in]	Inlet [°F]	Outlet [°F]
1	18	297.7	289.0
1	18	402.4	389.6
1	18	515.6	497.1
1	18	603.9	581.3
2	6	395.2	389.9
2	6	609.3	595.9
2	12	429.4	419.1
2	12	611.3	592.9
2	18	429.3	415.7
2	18	600.3	576.2
2	26*	414.3	399.5
2	26*	602.6	570.4

* There is no annulus therefore the aperture diameter is equal to the cavity diameter.

F. Comparison with Measurements

The radiometer and the analytical methods are compared with the experimental method, $Q_{unplugged}$ minus $Q_{plugged}$, for determining the radiative heat loss from the cavity through the aperture. The experimentally determined radiative heat loss was the difference between the open and plugged total receiver heat loss when the receiver aperture was down. A correction was made to account for the heat loss through the aperture plug. The heat loss through the plug must be added to the experimentally determined radiative heat loss data to get the total radiative heat loss from the receiver. The conductive heat loss through the plug is given by:

$$Q_{plug} = \frac{k_{plug} \Delta T A_{plug}}{\Delta x} \tag{65}$$

where:

k_{plug} = thermal conductivity of the plug[W/m-K]

ΔT= temperature difference between the inner and outer surface[K]

A_{plug} = mean surface area of the plug[m]

Δx= distance over which ΔT occurs (the thickness of the plug)[m]

The plugs were fabricated from one inch thick Cera Form® boards. The boards have a mean thermal conductivity of 0.32 Btu-in/hr-sq. ft.-Δ°F (0.0462 W/m-K).

Log-log scales are used to provide linear constant percent difference lines.

1. Radiometer Method

The radiometer determined heat loss values compared well with the experimentally determined radiative heat loss, $Q_{unplugged}$ minus $Q_{plugged}$, with differences within ±20% (Fig. 35).

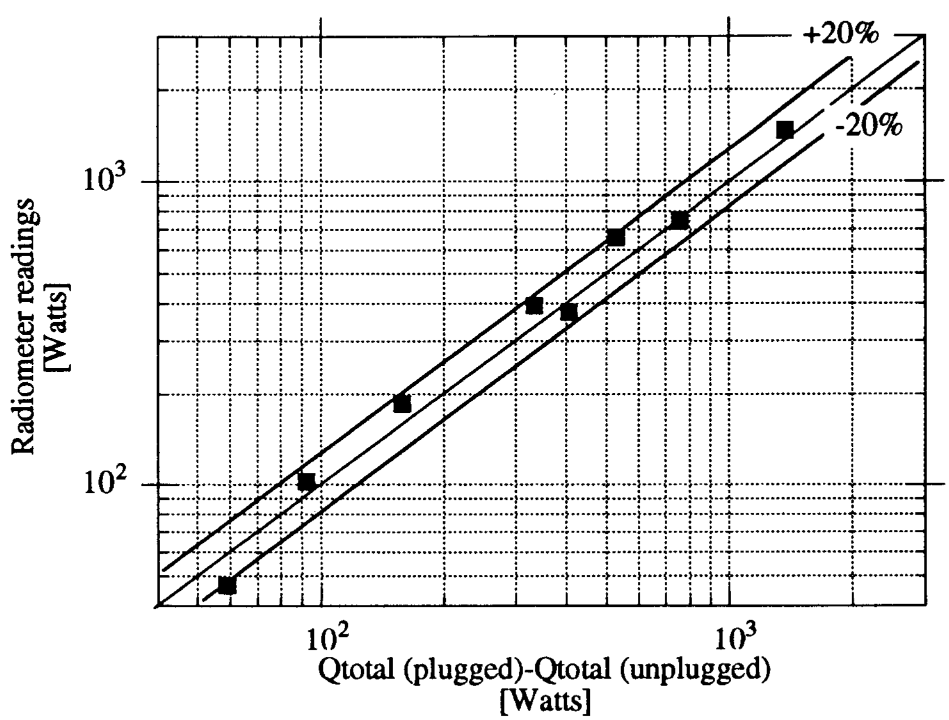

Figure 35. Experimentally determined radiometer method correlation

2. Analytical Method

The analytical method (Fig. 36) did not compare well with the experimental method for determining the radiative heat loss from the receiver. A number of possible reasons for the discrepancies have been discussed previously.

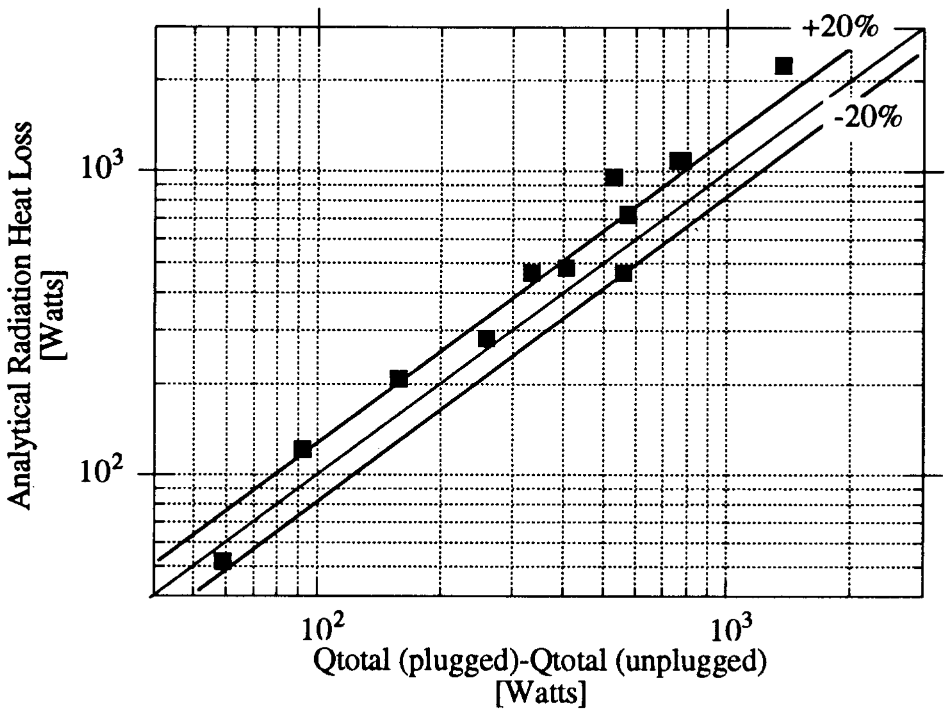

Figure 36. Analytically determined radiative correlation

IX. INSTRUMENTATION CALIBRATION

A. Flow Meter Calibration

The flow measurement apparatus consists of three basic parts: the turbine flow meter, the inductive pick-off, and the pulse rate counter (Fig. 37). The turbine flow meter rotates at a specific rate for a given fluid type and volumetric fluid flow rate. The rate of rotation is linearly proportional to the fluid flow rate within the specified range. The flow meter must be calibrated for a specific fluid viscosity, temperature, and flow rate range for accurate measurement.

The inductive pick-off is positioned above the turbine flow meter. When a turbine blade passes the inductive pick-off, an electromagnetically induced pulse signal is sent to the pulse rate converter (PRC). The PRC changes the pulse rate signal to voltage or current outputs. The current or voltage signal is then read by the data acquisition computer. The voltage signal should be used when the distance from the PRC to the computer input terminal is less than ten feet. For distances greater than ten feet the current signal should be used, as long leads result in substantial voltage drops. Voltage drops may significantly skew the voltage signal. The current signal is not affected by the voltage drop. The current signal requires a precision resistor across the computer input terminals. The resistor effectively converts the current signal to a voltage input at the computer terminals. Since precision resistors are expensive, economy requires the voltage signal should be used whenever possible.

Voltage signal output was used during testing for the reasons stated above. The computer displays the equivalent fluid volumetric flow rate based on the voltage input. The slope and offset values of the flow rate versus voltage linear function were inputted into the computer.

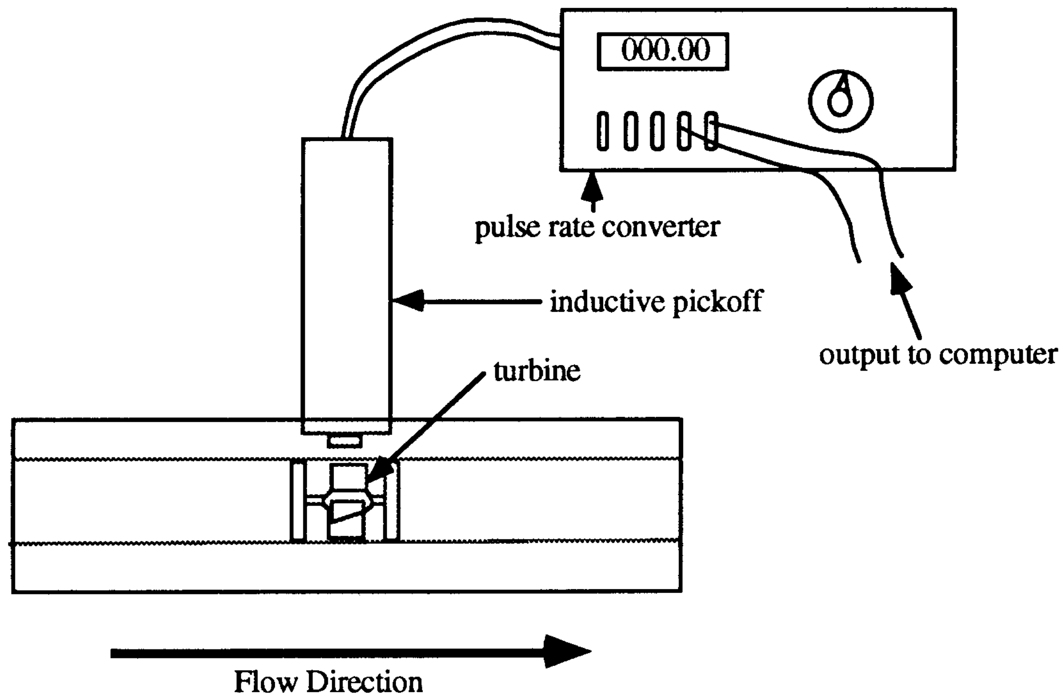

Figure 37. Flow measurement system

The heat transfer fluid flow rate is measured with three turbine type flow meters in series. Three flow meters are used for measurement redundancy. One of these flow meters was factory calibrated. The factory calibration specifications sheet is Appendix 16. The calibration curve for the factory calibrated flow meter is presented in Figure 38. The equation of the volumetric flow rate as a function of flow meter output frequency for the factory calibrated flow meter is:

$$\dot{v} = 0.0039578 + 0.001489f \tag{65}$$

where:

f = is the flow meter output frequency [Hz]

$\dot{v}$ = volumetric flow rate [gpm]

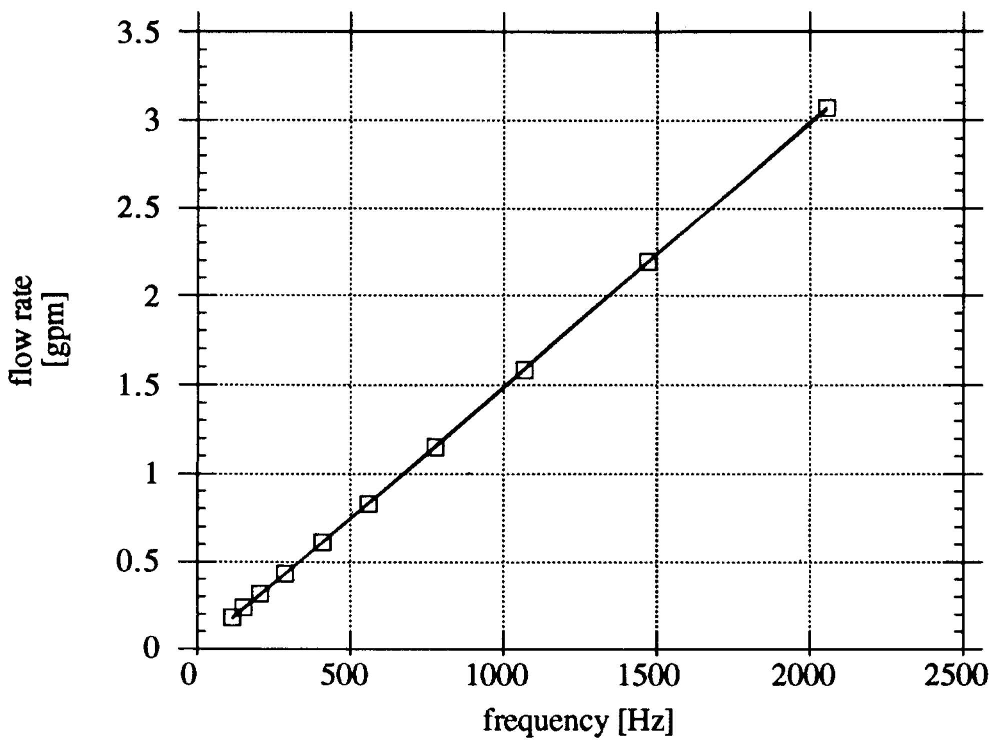

Figure 38. Factory calibrated flow meter flow rate versus frequency output

The pulse rate converters (PRCs) were calibrated in-house according to the manufacturer's procedure [13]. The calibration points for the PRC used with the factory calibrated flow meter are presented in Table 4.

Table 4
Pulse Rate Converter Calibration Points

frequency [Hz]	output voltage [volts]
1600	8.0
2000	10.0

The linear relationship for the frequency as a function of output voltage, as determined by the calibration points, is given as:

$$f = 200\ \mathrm{E} \tag{66}$$

where:

f = is the frequency input to the PRC [Hz]

E = is the output signal from the PRC [volts]

Substituting the frequency equation of the PRC calibration into the flow rate equation of the factory calibrated flow meter yields an expression for the volumetric flow rate as a function of voltage as follows:

$$\dot{v} = 0.0039578 + 0.001489(200\ \mathrm{E}) \tag{67}$$

which reduces to:

$$\dot{v} = 0.0039578 + 0.2978\mathrm{E} \tag{68}$$

which can be approximated as:

$$\dot{v} = 0.2978\mathrm{E} \tag{69}$$

Because E> 3.36 volts at typical flow rates the error due to this approximation is less than:

$$\frac{0.0039578}{(0.2978)(3.36)}$$

The remaining two flow meters were calibrated against the factory calibrated flow meter. Three meters were used for redundancy in the event one meter fails during testing.

1. Flow Meters Calibration

The outputs from the three flow meters were compared for various flow rates. The voltage outputs of the three flow meters were recorded (Appendix 17) (Fig. 39). The heat transfer fluid temperature was maintained at 300°F. Corrective slope and offset values were determined for each of the two uncalibrated flow meters. Applying the linear corrections will bring the two uncalibrated flow meter voltage outputs into agreement with the factory calibrated flow meter output.

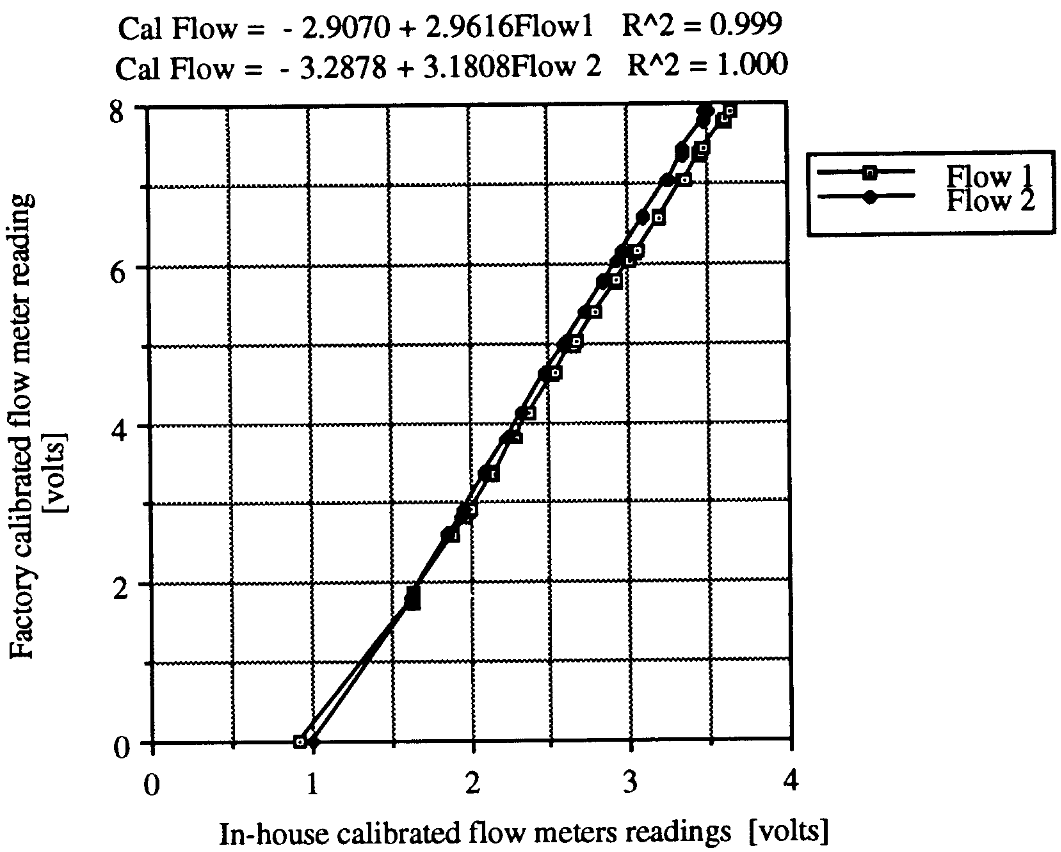

Figure 39. In-house calibrated flow meters correlation curves

The difference between the corrected readings and the factory calibrated readings are compared (Fig. 40). The minimum flow rate for all testing never went below one gallon per minute or 3.36 volts. This flow rate is well within the manufacture specified flow range. The maximum difference between the backup flow meters and the factory calibrated flow meter is ± 0.15 volts or ±0.045 gallons per minute. Temperature effects are negligible [(14)].

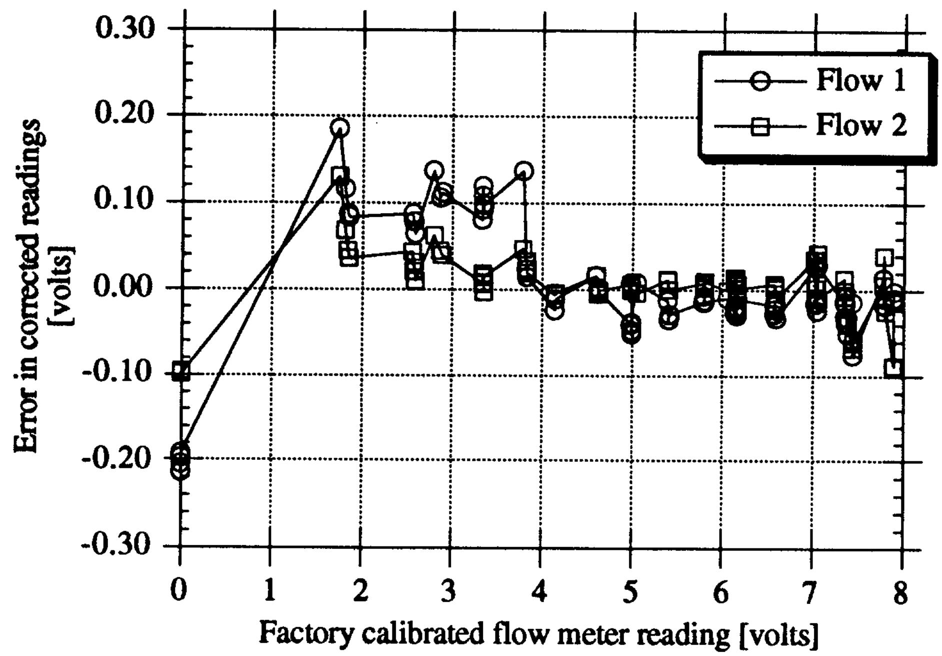

Figure 40. In-house calibrated flow meters errors.

Substituting the linear correction expression for the in-house calibrated flow meters into the volumetric flow rate expression of the factory calibrated flow meter yields expressions for the volumetric flow rates as a function of voltage inputs to the computer. The resulting expressions are given as follows:

$$\dot{v}_{flow\ 1} = 0.2978(-2.9070 + 2.9616E_{flow\ 1}) \quad (70)$$

$$\dot{v}_{flow\ 2} = 0.2978(-3.2878 + 3.1808E_{flow\ 2}) \quad (71)$$

which reduce to:

$$\dot{v}_{flow\ 1} = -0.8657 + 0.88196E_{flow\ 1} \quad (72)$$

$$\dot{v}_{flow\ 2} = -0.9791 + 0.94724E_{flow\ 2} \quad (73)$$

The scale and offset values from these expressions were inputted into the computer. The computer then displays the flow rate for each flow meter in gallons per minute (gpm).

B. Thermocouple Calibration

The total receiver heat loss, Q_T, was given by the product of the mass flow rate, the specific heat of the heat transfer fluid and the temperature difference between the fluid inlet and outlet temperatures (ΔT). Of the three variables, the largest error in the heat loss was due to the measurement of ΔT. Two redundant methods were used to measure ΔT for these experiments. One method of determining ΔT was by subtracting the fluid outlet temperature from the fluid inlet temperature. The other method utilized a direct temperature difference measurement from two thermocouples, one in each of the fluid inlet and outlet lines. This differential thermocouple connection avoids inaccuracies due to reference junction compensation but still requires knowledge of the absolute temperature values. To reduce the error introduced to the total heat loss calculation by the thermocouple readings it was necessary to calibrate the inlet, outlet, and delta temperature thermocouples used in the receiver. Standard thermocouple probes have a maximum error of ±2.2°C or 0.75%, whichever is greater [15]. Using two absolute temperature measurements from standard thermocouple probes would result in a ΔT error of ±3.11 °C (±5.60°F) or 1.06% whichever is greater. With temperature differences as low as 2.78°C (5°F) recorded, the standard thermocouples did not yield values within an acceptable error.

A single factory calibrated K-type thermocouple probe was purchased and all other probes were calibrated against it. Only one calibrated probe could be purchased due to budget constraints. The calibrated probe has an accuracy of ±0.2°F after linear correction is applied (Fig. 41). The three point calibration data for the factory calibrated thermocouple is provided in Table 7. The calibration is certified traceable to the U.S. National Bureau of Standards (Appendix 18).

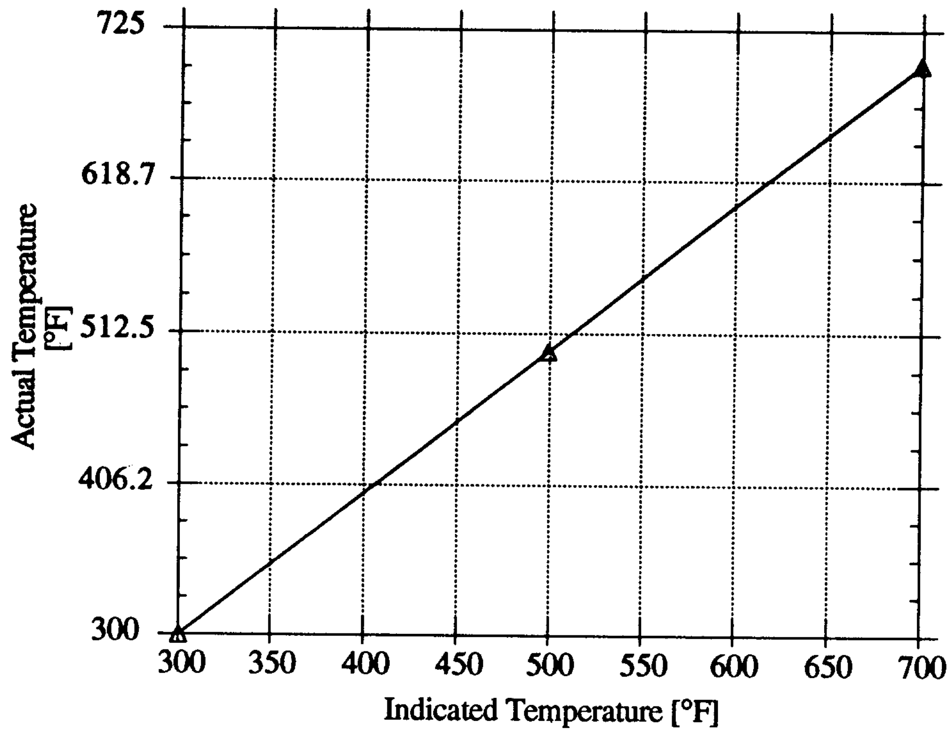

Figure 41 Calibrated thermocouple probe curve

A linear variation of the actual temperature as a function of the indicated temperature is given by:

$$T_{actual} = -2.4256 + 1.006T_{indicated} \tag{74}$$

with a correlation coefficient, R=1.00

Table 5 shows the error in the calibrated probe after linear correction is applied.

Table 5
Factory Calibrated thermocouple probe error

Indicated Temperature [°F]	Actual Temperature [°F]	Corrected Temperature [°F]	Absolute Error [°F]
300.56	300.06	299.94	0.12
499.39	499.77	499.96	0.19
699.09	701.00	700.86	0.14

1. Thermocouple Calibration Apparatus

A thermocouple calibrating device was fabricated (Fig. 42). The calibrator consisted of a heat source, a heat sink, and an insulated cover. The heat sink was formed from a solid brass cylinder with three holes drilled in one end to accommodate thermocouple probes and a single hole in the other end to accommodate the heat source (Fig. 43). The soldering iron used was an Ungar CI-45, 0.38 A 120 V AC/DC. The soldering iron tip was modified for a snug fit in the heat sink (Fig. 44). The soldering iron was connected to a variable AC power supply. The brass block was insulated to control the rate of heat loss. The thermocouple leads were connected to a data acquisition system.

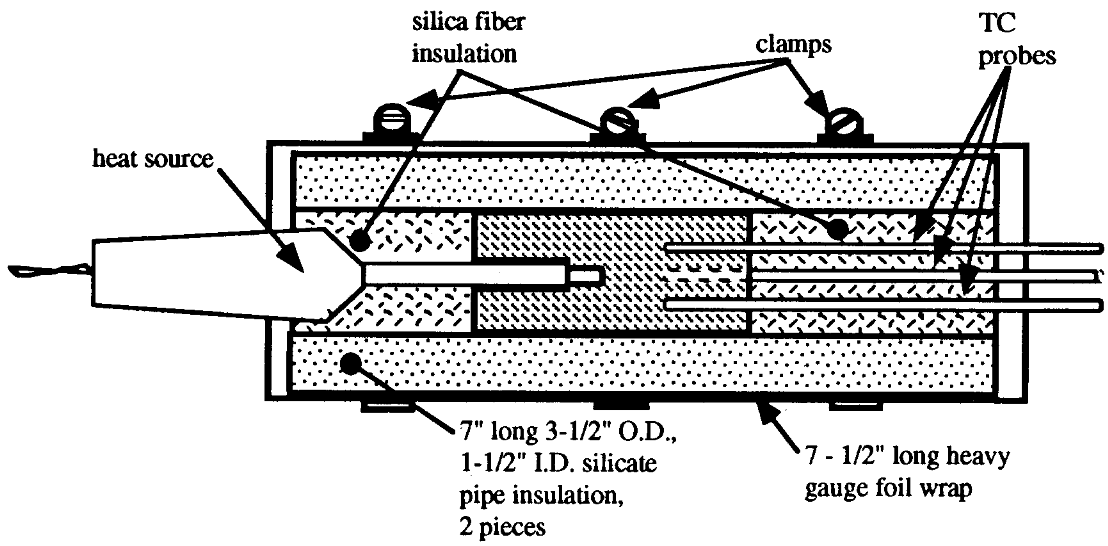

Figure 42. Thermocouple calibrator

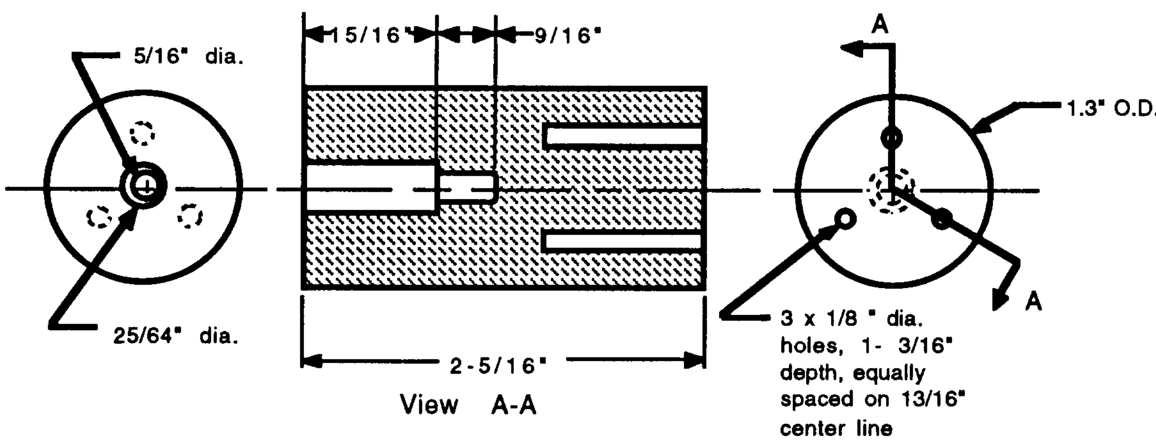

Figure 43. Thermocouple calibrator heat sink

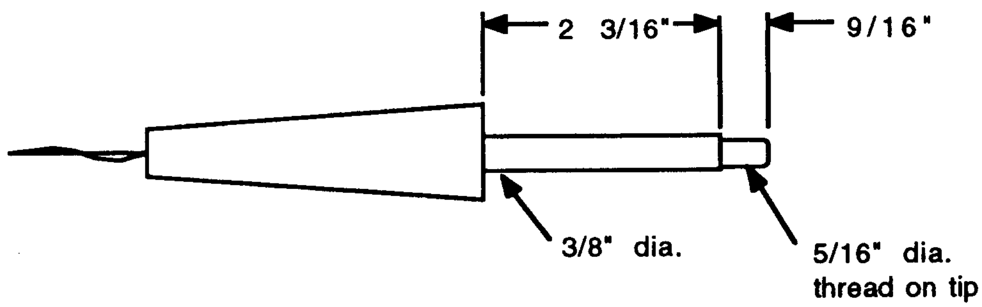

Figure 44. Modified soldering iron heat source

2. Thermocouple Calibration Procedure

Three separate tests were required to accomplish calibration of the two absolute and the two differential thermocouples. In the first test, the absolute inlet and outlet TC probes were inserted in the heat sink along with the calibrated TC probe. The heat source was plugged into a variable AC power supply. The variable AC supply was adjusted until a maximum temperature of approximately 700°F was indicated for the calibrated TC. The power supply was then removed and the system allowed to cool slowly. The temperature time histories for the absolute temperature inlet and outlet thermocouples were recorded. The heat sink was assumed to be isothermal at all TC junctions for any time. Correction factors for the TC's were obtained by comparing the TC outputs to that of the calibrated TC output.

3. Thermocouple Calibration Results

The temperature time history curves for the absolute temperature inlet and outlet thermocouples are presented in Figure 45. The relationship for the inlet thermocouple is quite linear as indicated in Fig. 46. The linear relationship between the inlet TC reading and the calibrated TC reading is given by;

$$T_{cal} = -.2217 + 1.0027\ Tin \qquad (75)$$

The relationship for the outlet thermocouple is quite linear as indicated in Fig. 47. The linear relationship between the outlet TC reading and the calibrated TC reading is given by;

$$T_{cal} = -.1850 + 1.0047 \text{ Tout} \qquad (76)$$

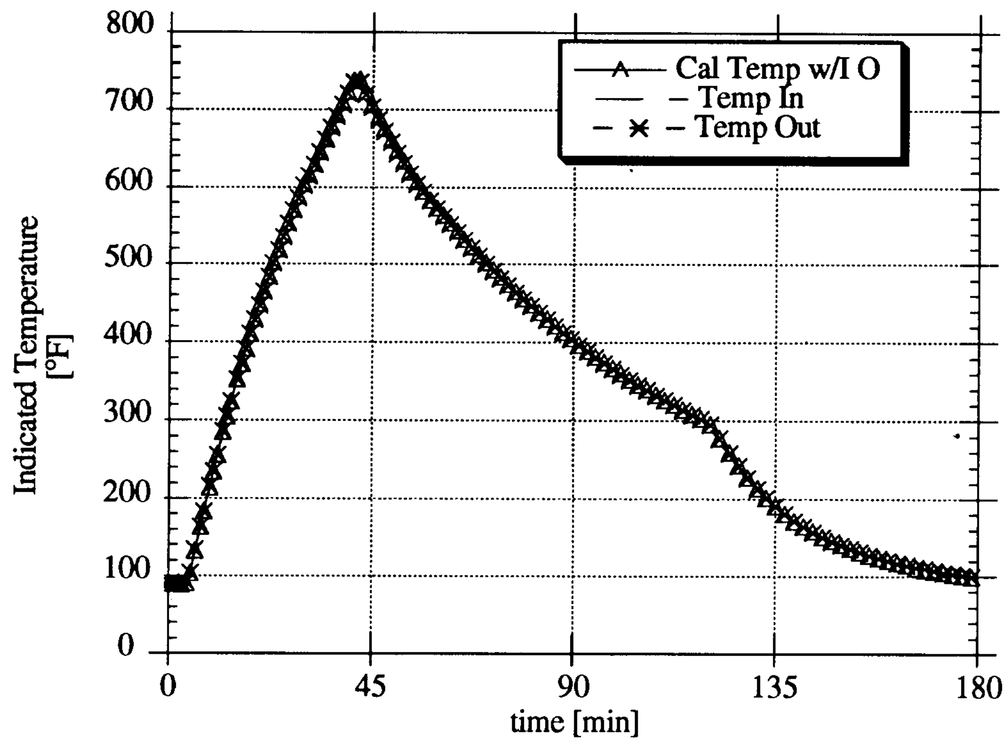

Figure 45. Inlet and Outlet thermocouples calibration histories

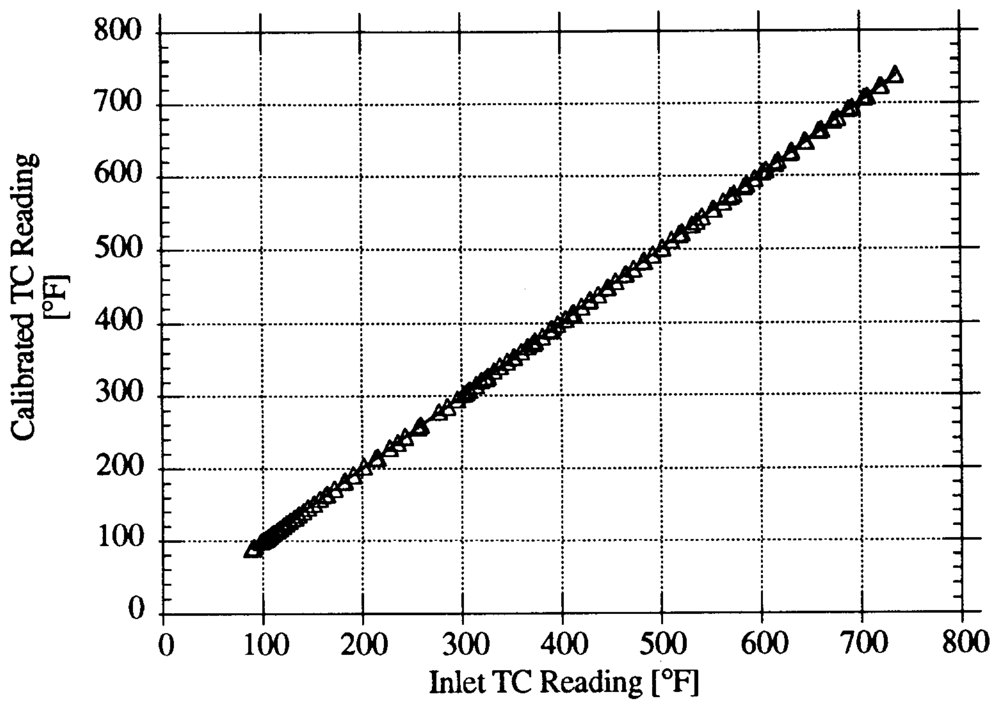

Figure 46. Factory Calibrated versus inlet thermocouple readings

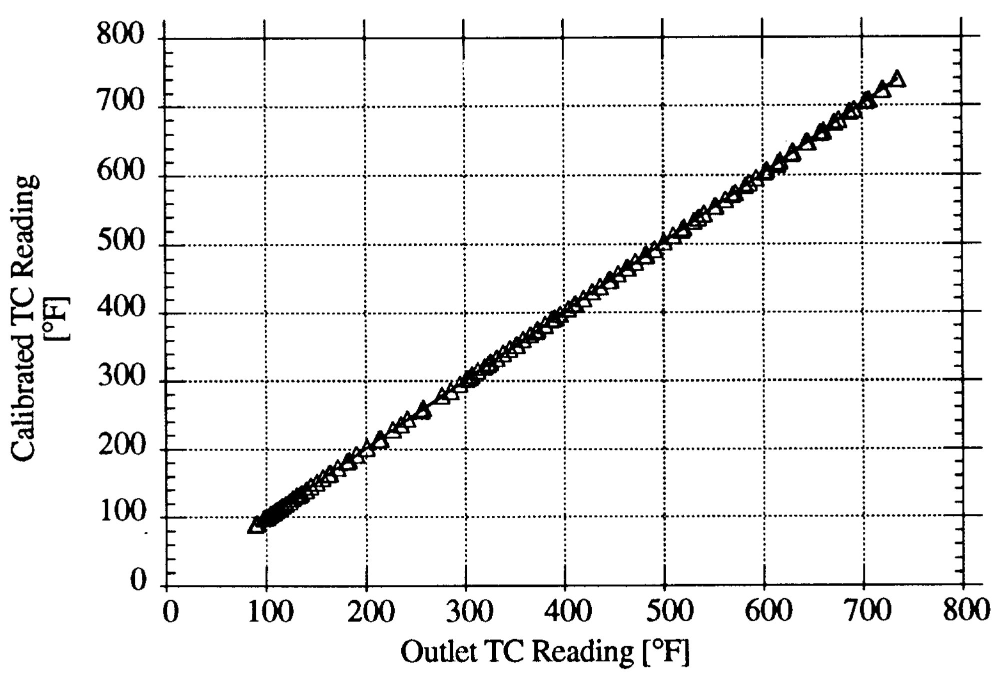

Figure 47. Factory Calibrated versus outlet thermocouple readings

These equations are used to correct the outlet TC readings to the calibrated TC readings. The difference between the calibrated and inlet TC readings are compared before and after the linearized correction factors were applied (Fig. 48). The maximum difference between the calibrated TC reading and the inlet TC reading before the correction is applied is 2.6°F. After application of the correction factors the maximum difference is 1.02°F. The maximum difference between the calibrated TC readings and the outlet TC readings before the linear correction is applied is 4.2 °F. After the linear correction is applied the maximum difference is 1.44°F (Fig. 49).

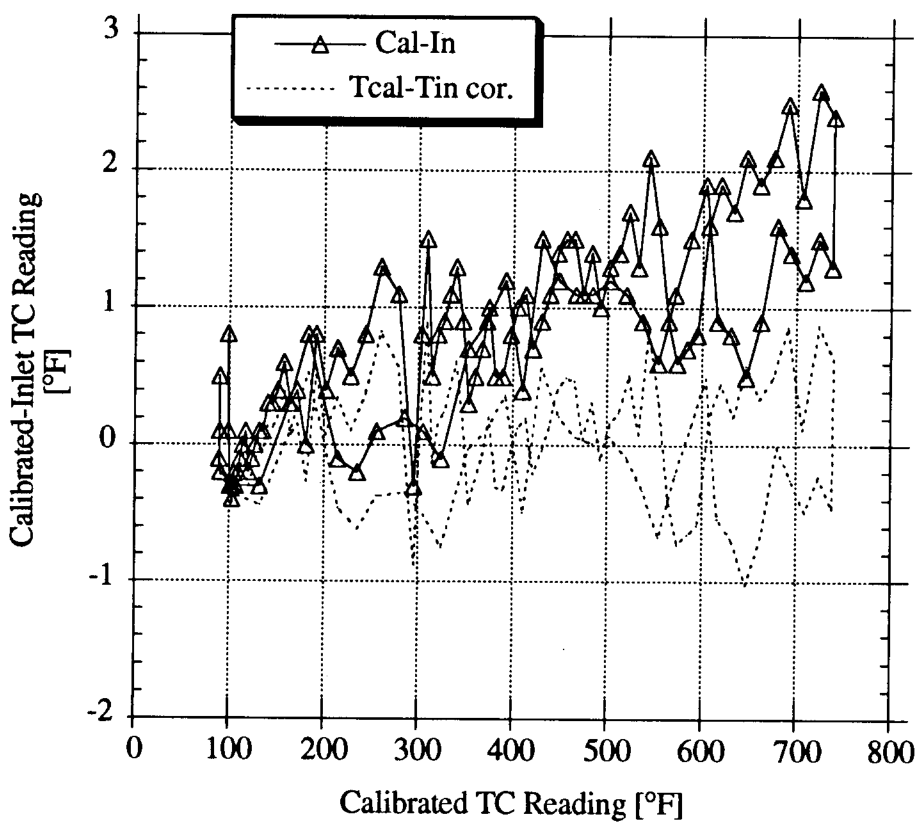

Figure 48. Inlet thermocouple errors

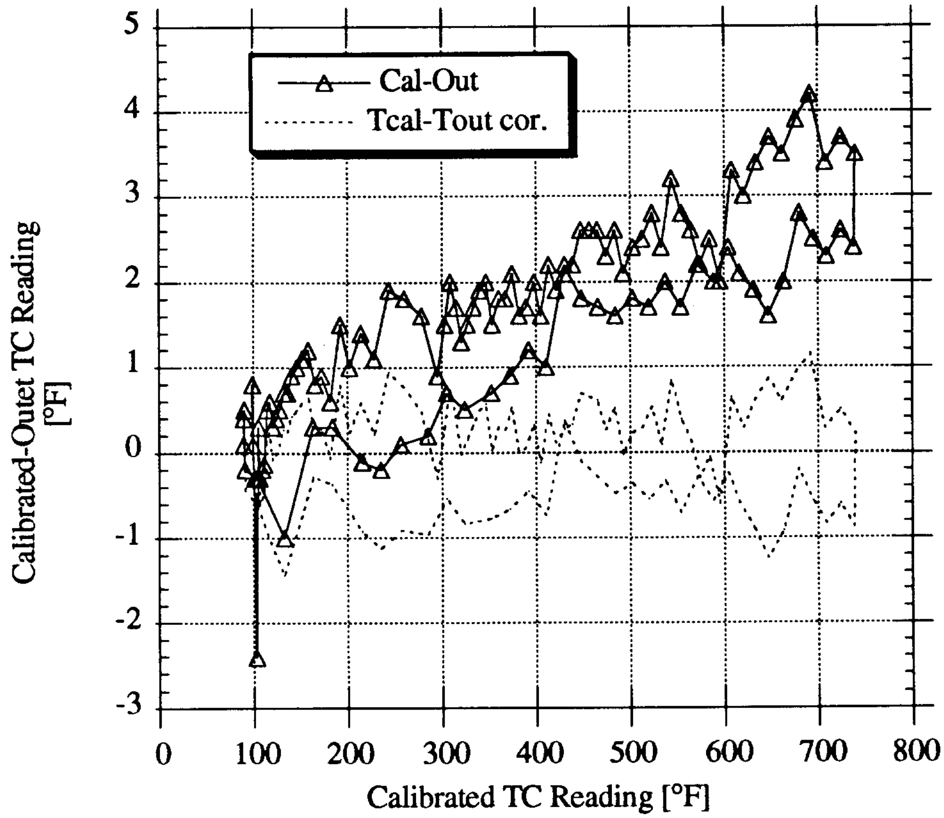

Figure 49. Outlet thermocouple errors

Two thermocouples can be arranged to provide a voltage output proportional to the temperature difference of the two junctions (Fig. 50). When both thermocouple junctions are at the same temperature the voltage output is zero.

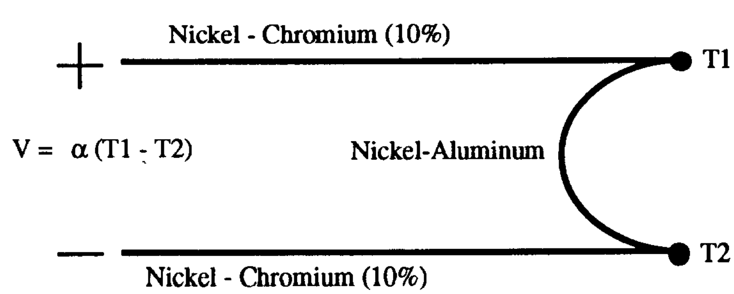

Figure 50. Differential thermocouple connection

The two thermocouple probes used for the direct temperature difference measurement were inserted in the thermocouple calibrator along with the calibrated thermocouple. The unit was then heated and cooled as per the procedure used for calibrating the inlet and outlet absolute temperature thermocouple probes. Ideally, the net voltage output from the temperature differential connection should be zero regardless of the calibrator temperature. The temperature and micro volt output histories for the calibration procedure are presented in Figure 51. Comparing the differential thermocouple's output with the calibrated thermocouple reading indicates no linear correlation (Fig. 52). The step function of the voltage output is an indication of the minimum computer analog to digital converter (ADC) resolution.

The maximum error in the differential voltage output is 25.45 μV which corresponds to a temperature difference error of 1.147 °F.

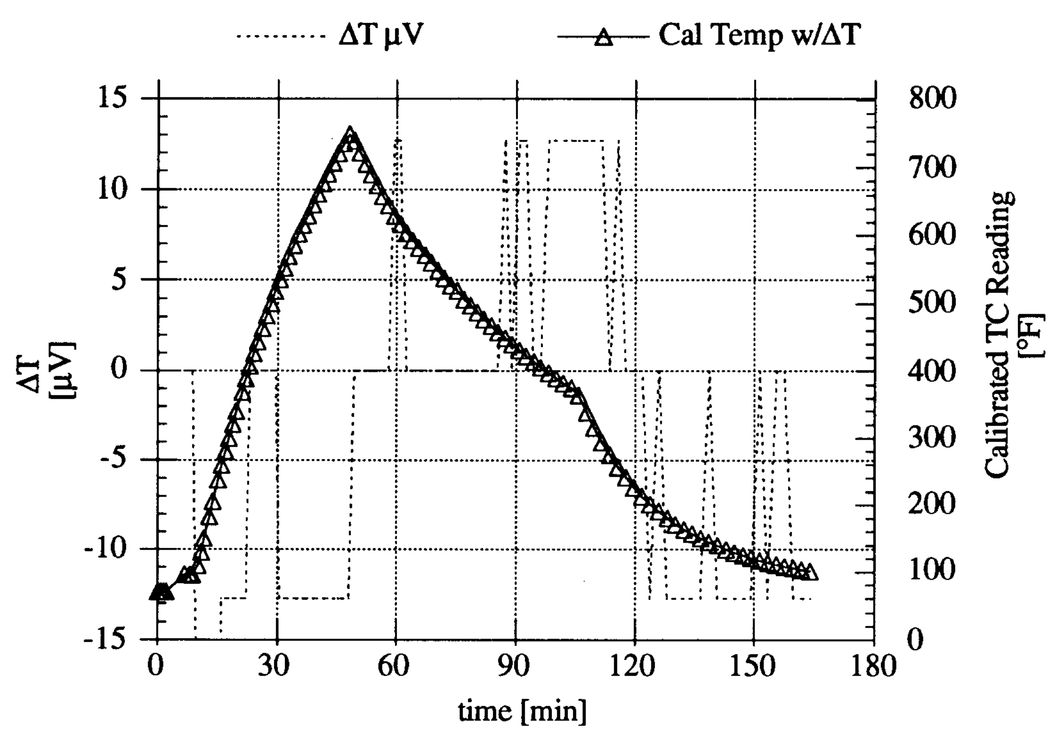

Figure 51. Differential thermocouple readings history

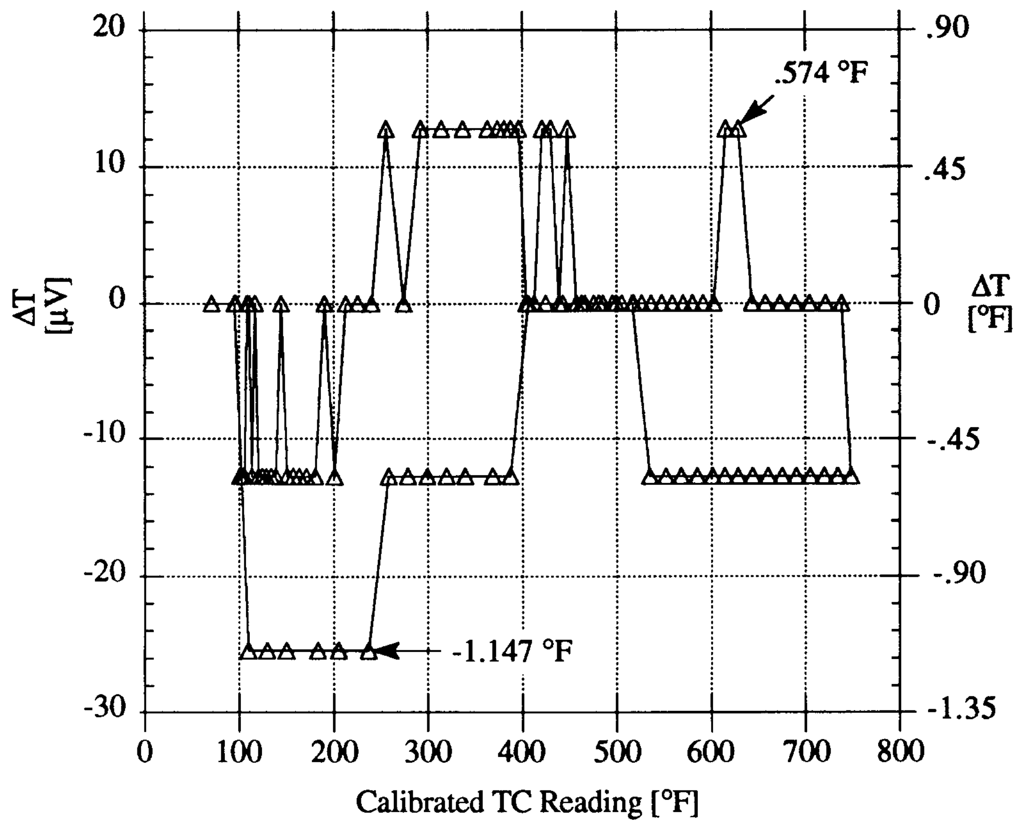

Figure 52. Differential thermocouple errors history

The absolute mean temperature must also be known to convert the millivolt output of the differential thermocouples into an equivalent temperature difference. The voltage to temperature difference conversion factor is determined from a polynomial function of the mean temperature (Fig. 53). The conversion factor polynomial was derived from the voltage-temperature tables for K-type thermocouples.[14]

No calibration of the differential thermocouples was performed with a difference in temperature at the junctions.

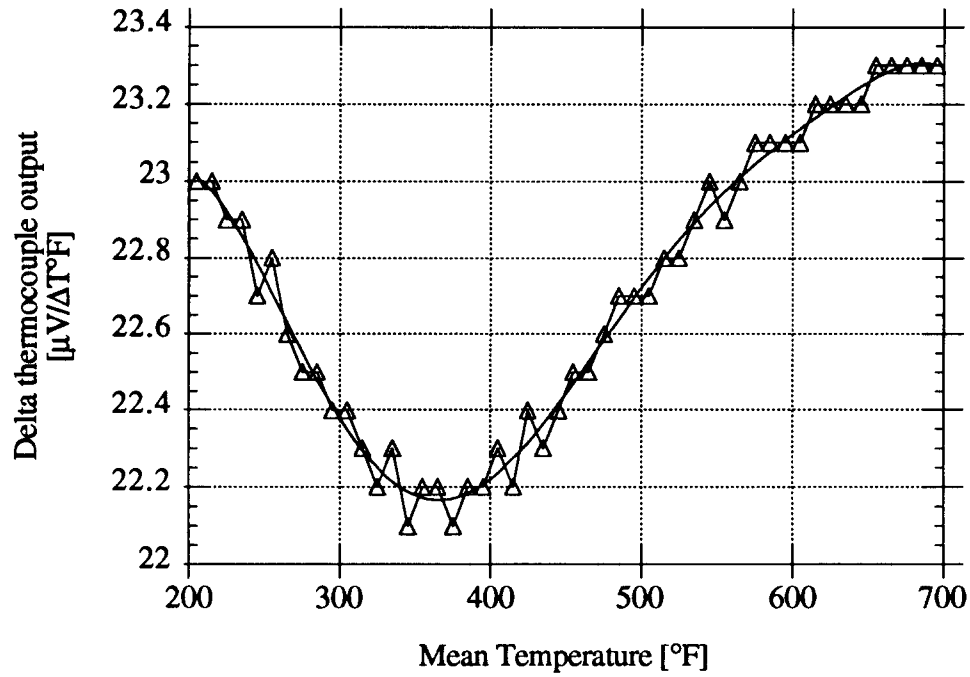

Figure 53. Differential thermocouple output versus mean temperature

C. Radiometer Calibration

The Hy-Cal® Hy-Therm® Pyrheliometer P-8400-B was used to measure the thermal radiative heat loss from the receiver cavity (Fig. 54). The spectral range of the radiometer without its quartz window is from 0.2 to 30 microns. The radiometer consists of a thermopile on top of a heat sink. The thermopile converts the temperature gradient across the pile to a proportional current signal. The heat sink is water cooled aluminum base. The exposed end of the thermopile is coated with fused colloidal graphite providing a minimum absorptivity of 0.9. The radiometer outputs 5 mV per solar constant (0.13980 Watts/cm^2). The calibration specifications are provided in Appendix 19.

The radiometer was supplied with a bezel mounted quartz window. Because the radiative being measured is in the infra-red wave length region, preliminary testing showed that the quartz window excessively attenuated the heat flux to the radiometer resulting in an insufficient signal output. When the window was removed, the radiometer became overly sensitive to localized convective heating and cooling which resulted in a fluctuating output signal. For low heat flux level measurements, a window that is virtually transparent to the infrared radiative is desirable. Various widow materials were considered and tested for replacement of the quartz window.

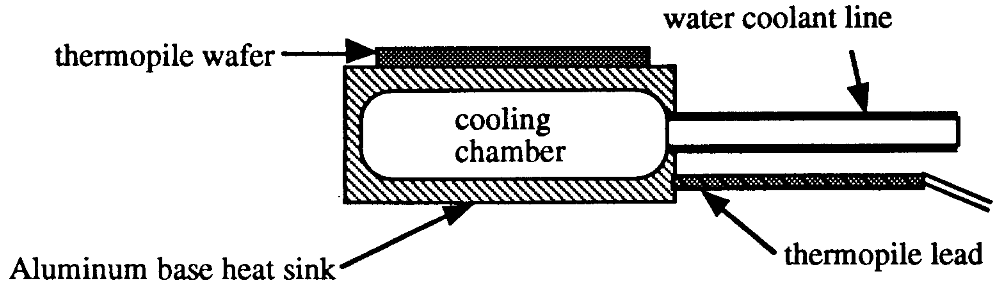

Figure 54. Radiometer section view

1. Radiometer Window Evaluations

A bezel was fabricated to accommodate various film windows for testing (Fig. 55). The film was pulled snugly over the bezel. The film was secured in place with a rubber band. The bezel fits over the radiometer. The film window is close enough to the thermopile wafer providing the thermopile with almost 180° of view.

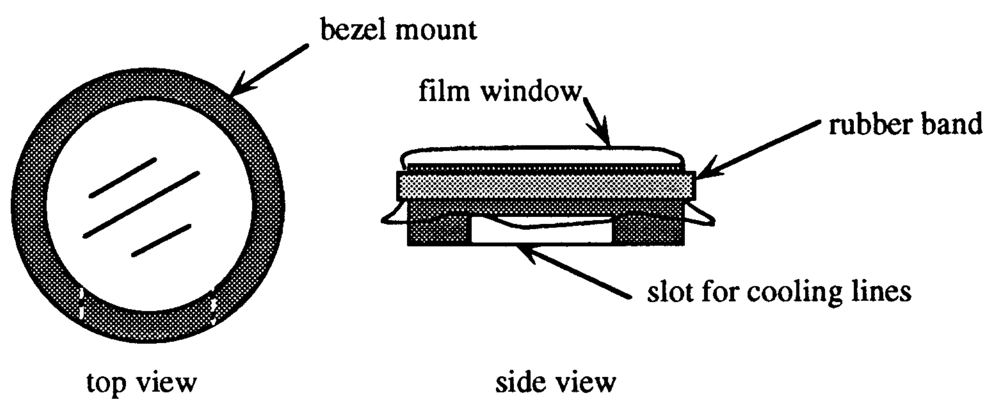

Figure 55. Film window bezel

The test stand consisted of an inverted hot plate positioned concentrically above and facing the radiometer (Fig. 56). A K-type thermocouple probe is immersed in the coolant return catch basin for the radiometer. The base of the radiometer is assumed to be at the same temperature as the water in the catch basin. The hot plate is inverted and positioned above the radiometer to prevent convective heating of the radiometer. The hot plate temperature is controlled using a variable AC power supply. The radiometer can be positioned at various vertical distances from the hot plate. The surface of the hot plate has nine K-type thermocouples welded to it.

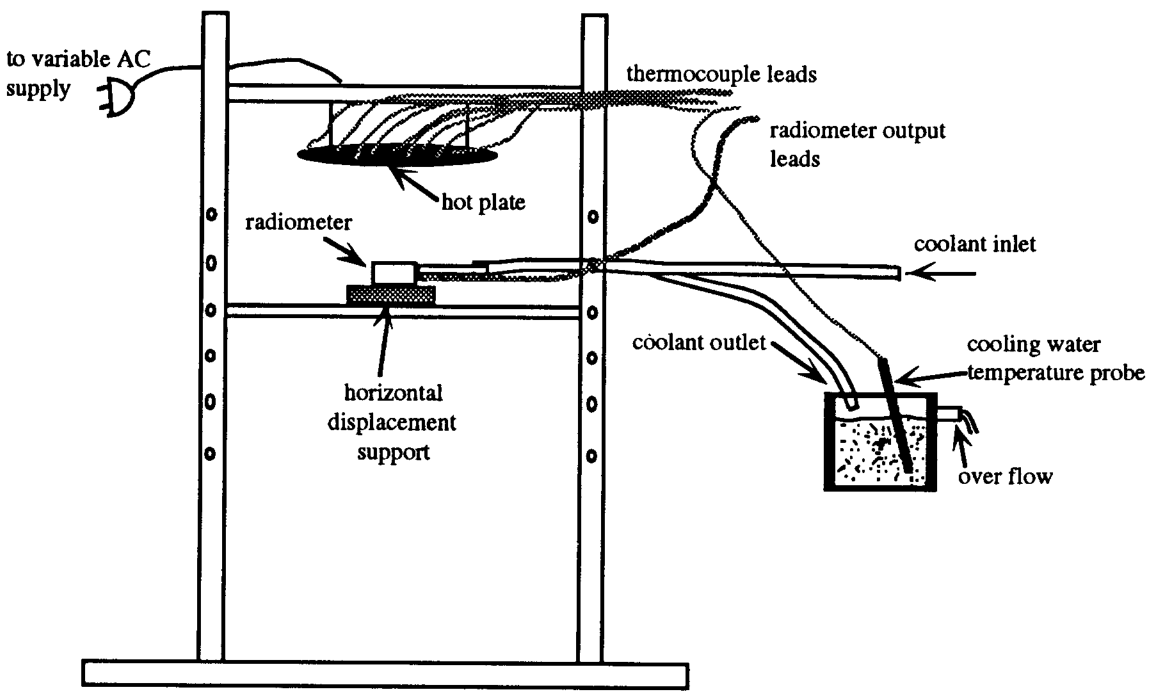

Figure 56. Radiometer calibration test stand

The hot plate surface was coated with high emissivity Pyromark® paint. The manufacturer's specifications for the Pyromark® paint are provided in Appendix 20. The average black-body normal emittance of the painted surface is a function of the surface temperature and can be as low as 0.867 at 600K (Fig. 57). A fifth order polynomial curve fit provides an equation for paint surface emittance as a function of surface temperature.

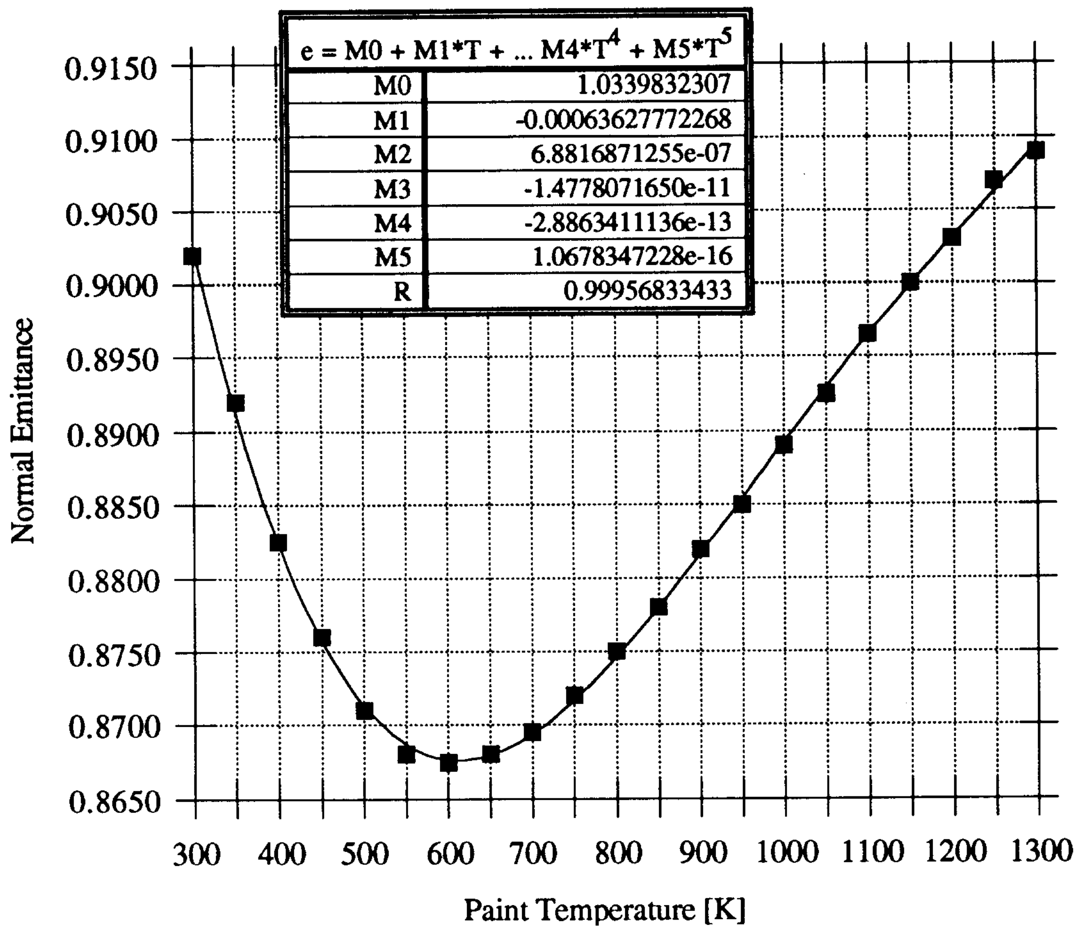

Figure 57. Pyromark paint emittance

The parameters for the window evaluation test plan are shown in Table 6. At the beginning and end of each test, background measurements were recorded by removing the radiometer from the test stand and placing it above the hot plate on an insulated pad. For each of the plate and background thermal radiative measurements the readings were recorded after a two minute stabilization period. The variable AC power supply was adjusted until the average plate temperature was close to the target temperature. The thermocouples were distributed over the plate surface (Fig. 58).

Table 6
Radiometer window test parameters

Test Window	Target Temperature	Vertical Displacement
Saran Wrap	300°F	0.32r
quartz	"	"
Glad Wrap	"	"
none	"	"
Saran Wrap	400°F	0.75r
quartz	"	"
Glad Wrap	"	"
none	"	"
Saran Wrap	500°F	1.23r
quartz	"	"
Glad Wrap	"	"
none	"	"
Saran Wrap	600°F	1.80r
quartz	"	"
Glad Wrap	"	"
none	"	"
Saran Wrap	700°F	2.5r
quartz	"	"
Glad Wrap	"	"
none	"	"

where r = radius of the hot plate

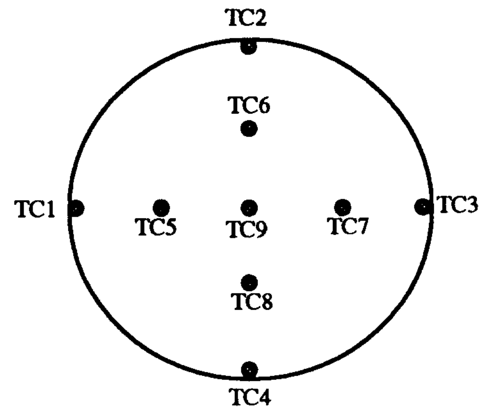

Figure 58. Hot plate thermocouple distribution

For an average area temperature only thermocouples five through nine were considered. The average area temperature is given by:

$$T_{average} = \frac{T_5 + T_6 + T_7 + T_8 + T_9}{5} \tag{77}$$

The window transmittance, τ_{window}, is given by:

$$\tau_{window} = \frac{q_{radio}}{q_{radio/plate}} \tag{78}$$

where

q_{radio} = the thermal radiative heat flux read by the radiometer

$q_{plate/radio}$ = the thermal radiative heat flux incident on the radiometer from the hot plate

The radiative leaving the hot plate and incident on the radiometer is given by:

$$q_{radio/plate} = q_{plate}F_{plate\text{-}radio} \tag{79}$$

where

q_{plate} = the thermal radiative heat flux leaving the hot plate

$F_{plate\text{ -}radio}$ = the shape factor from the hot plate to the radiometer

The radiative heat flux leaving the hot plate is given by:

$$q_{plate} = \sigma\varepsilon\,(\overline{T}^4_{plate} - T^4_{ambient})\,\pi\, r^2_{plate} \qquad (80)$$

where

ß = 5.729 X 10-8 [W/(m^2•K^4)] Stefan-Boltzmann constant

r_{plate} = 8.9 [cm] the radius of the hot plate

ε = emissivity of the plate surface.

The shape factor from the hot plate to the radiometer is given by:

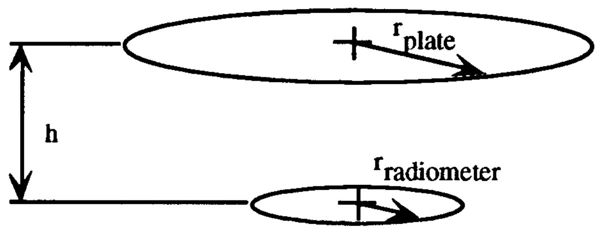

$$F_{plate\text{-}radio} = \frac{1}{2}\left\{1+\frac{h^2 + r^2_{radio}}{r^2_{plate}} - \sqrt{\left[1+\frac{h^2 + r^2_{radio}}{r^2_{plate}}\right]^2 - 4\left[\frac{r_{radio}}{r_{plate}}\right]^2}\right\} \qquad (81)$$

where

h = vertical displacement of the hot plate and radiometer.

r_{radio} = radius of the radiometer = 0.5625 [in.]

When the diameter of the radiometer approaches one inch, as is the case here, a simplified formula may be used. The simplified shape factor formula is given as follows:

$$F_{plate\text{-}radio} = \frac{r^2_{radio}}{h^2 + r^2_{plate}} \qquad (82)$$

All real gas effects have been ignored (absorption, scattering etc.).

The results of the test are in Appendix 21. The quartz window transmittance varies linearly with source temperature (Fig. 59). The transmittance for the Grad Wrap and Saran Wrap windows are nearly constant over the testing temperature range. The average transmittance for the no window condition is 0.99. Ideally, the transmittance for the no window condition should be unity. The error in the no window transmittance is well within the instrument's error. Real gas effects may also account for a small loss in the incident flux on the radiometer from the hot plate.

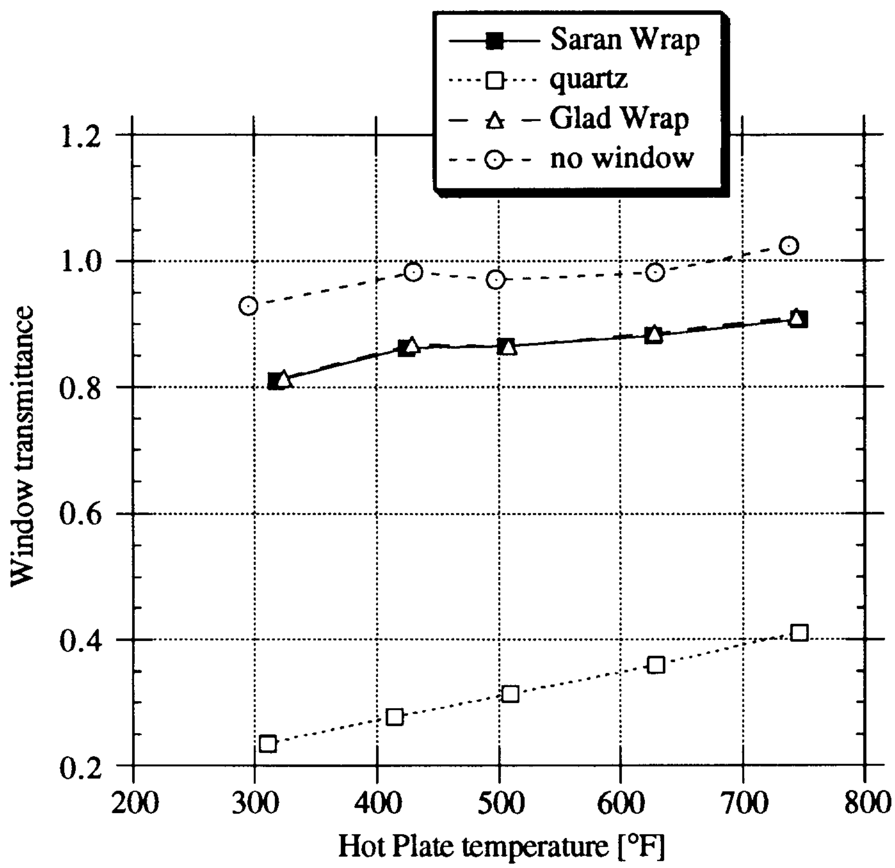

Figure 59. Radiometer windows transmittance

The average transmittance for the Saran Wrap window was determined to be 0.87. The manufacturer specifies a transmittance of 0.88 for the infrared portion of the spectrum. Technical information for Saran Wrap® films is provided in Appendix 22. Although the Glad Wrap had similar transmission characteristics, the Saran Wrap was selected as the radiometer window, since no manufacturer specifications were available for the Glad Wrap. In addition to selecting a radiometer window, it was also necessary to determine effects of radiometer positioning relative to the heat source.

2. Radiometer Positioning

The radiometer positioning sensitivity must be considered for accurate heat flux measurements. The parameters for the radiometer positioning sensitivity test plan are presented in Table 7. At the end of each test the background measurements were taken by removing the radiometer from the test stand and placing it above the hot plate on an insulated pad. For each of the plate and background thermal radiative measurements the radiometer readings were recorded after a two minute stabilization period.

Table 7
Radiometer position sensitivity test parameters

Hot Plate Temp	Offset Distance	Vertical Displacement
400°F	0 to 2r step 0.5r	0.75r
700°F	0 to 6r step 1r	2.5r
400°F	0	1 to 6r step 1r
700°F	0	2 to 12r step 2r

where r = radius of the hot plate

The shape factor from the hot plate to the radiometer is given by:

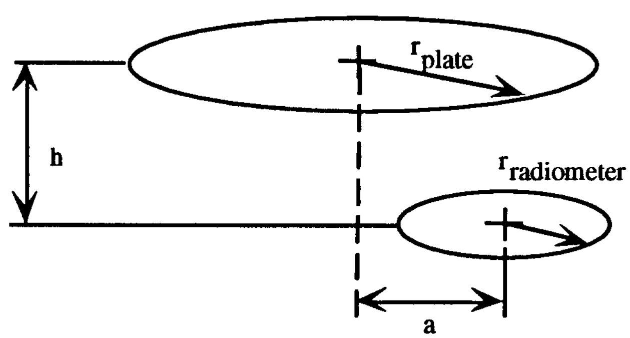

$$F_{plate\text{-}radio} = \frac{1}{2}\left\{1 - \frac{1 + \left(\frac{h}{a}\right)^2 - \left(\frac{r_{plate}}{a}\right)^2}{\sqrt{\left[1 + \left(\frac{h}{a}\right)^2 - \left(\frac{r_{plate}}{a}\right)^2\right]^2 - 4\left[\frac{r_{plate}}{a}\right]^2}}\right\}\left(\frac{r_{radio}}{r_{plate}}\right)^2 \qquad (83)$$

where

h = vertical displacement of the hot plate and radiometer.

r_{radio} = radius of the radiometer = 1.43 cm

r_{plate} = radius of the hot plate = 8.9 cm

h = vertical displacement [in.]

a = horizontal displacement [in.]

The results of the displacement sensitivity test are tabled in Appendix 23. The effects of vertical and horizontal displacement of the radiometer from the heat source are presented in Figure 60. Ideally, all values should be equal to one. The radiometer is especially sensitive to horizontal displacement (i.e. off axis readings).

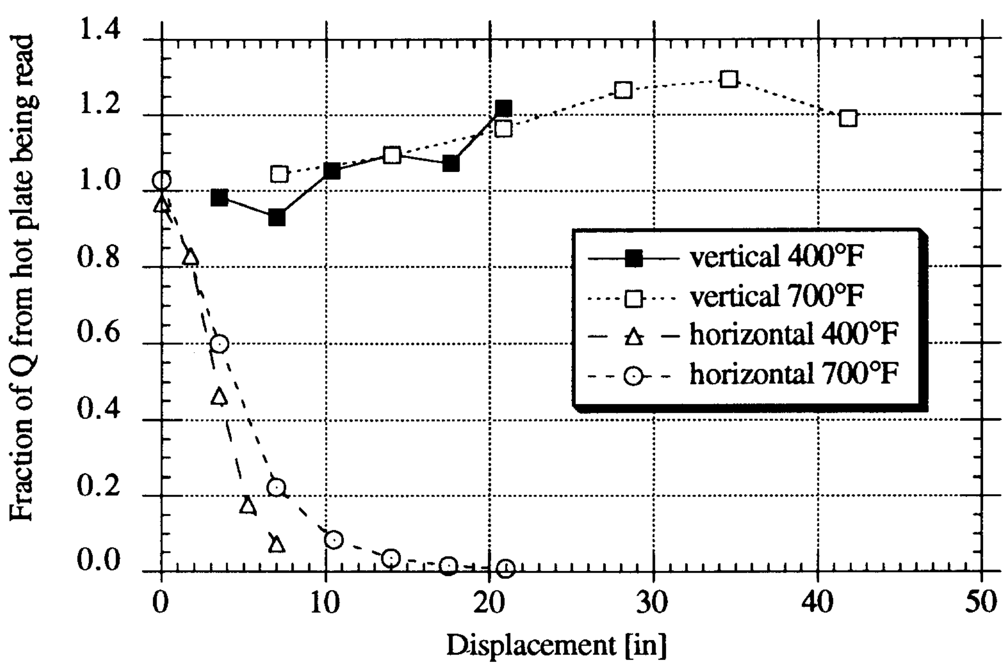

Figure 60. Radiometer displacement effects

The results indicate that the radiometer should be placed as close as possible and in line with the heat source. Extreme care was taken to assure the radiometer was centered on the receiver axis during the test phase. An elaborate string and plumb bob arrangement was used to center the radiometer.

X. ERROR ANALYSIS

This error analysis determines error in the results based on test method and instruments used. The error analysis also serves as one form of evaluating the test method. The error analysis does not account for human errors or systematic errors. The general form for the error analysis of a given function, z, where $z=z(x_i)$ is given as follows[16]:

$$\sigma_z = \sqrt{\sum_i \left[\left(\frac{\partial z}{\partial x_i}\right)\sigma_{x_i}\right]^2} \tag{84}$$

The general formula for the total heat lost from the cavity is given by:

$$Q_{total} = \rho \dot{v} c_p \Delta T \tag{85}$$

The percent error in the total heat loss is given by:

$$\frac{\sigma_{Q_{total}}}{Q_{total}} = \sqrt{\left(\frac{\sigma_\rho}{\rho}\right)^2 + \left(\frac{\sigma_{\dot{v}}}{\dot{v}}\right)^2 + \left(\frac{\sigma_{c_p}}{c_p}\right)^2 + \left(\frac{\sigma_{\Delta T}}{\Delta T}\right)^2} \tag{86}$$

The density of the heat transfer fluid is a function of the temperature and is approximated by[17]:

$$\rho = 60.6 - 0.0324\ T_{inlet} + 9.84e\text{-}6\ T_{inlet}^2 - 1.79e\text{-}8\ T_{inlet}^3\ \ [lb/ft^3] \tag{87}$$

The error in the heat transfer fluid density is approximated by:

$$\sigma_\rho = \sqrt{\left(-0.0324 + 1.968e\text{-}5T_{inlet} - 5.37e\text{-}8\ T_{inlet}^2\right)^2 \sigma_{T_{inlet}}^2} \tag{88}$$

The inlet temperature is used for density calculation. The inlet thermocouple used is the one closest to the flow meters.

The heat capacity of the heat transfer fluid is a function of the temperature and is approximated by[17]:

$$c_p = 0.3690 + 2.267e\text{-}4\ T_{mean}\ [\text{Btu/lb °F}] \tag{89}$$

The error in the heat transfer fluid heat capacity is approximated by:

$$\sigma_{c_p} = 2.267e\text{-}4\sigma_{T_{mean}} \tag{90}$$

A. Flow Measurement Error Analysis

The HTF flow rate is given by:

$$\dot{v} = 0.2978E \tag{91}$$

where:

E = is the output signal from the pulse rate converter (PRC) [volts]

$\dot{v}$ = volumetric flow rate [gpm]

The manufacturer's specified linearity of the PRC is ±0.4% of full scale. The calibrated flow meter is accurate to within ±0.5% of the reading in the flow rate range of 0.8 to 2.5 gallons per minute and with a fluid viscosity in the range of 0.4 to 2.0 centistokes.[18]

The output of the PRC to the computer is from 0 to 10 volts. The accuracy of the computer for the 10 volt input range is the larger of ±1% of the reading or ±0.2% of the range (the range is 11 volts for the -1 to 10 volt input).[19] The combined error for the factory calibrated flow meter reading is given by:

$$\sigma_{flow} = \sqrt{b^2\sigma_E^2} \tag{92}$$

$$\sigma_E = \sqrt{(\sigma_{PRC})^2 + (\sigma_{flow\ meter})^2 + (\sigma_{computer})^2} \tag{93}$$

where:

b = the slope of the flow rate versus voltage output for the PRC-flow meter combination

b = 0.2978 [gpm/volt]

β_{PRC} = the error in the pulse rate converter

$$\frac{\sigma_{PRC}}{E_{scale\ PRC}} = \pm 0.4\% \text{ of full scale}$$

$E_{scale\ PRC}$ = 10 volts

$\beta_{flow\ meter}$ = the error in the flow meter

$$\frac{\sigma_{flow\ meter}}{E_{reading}} = 0.5\% \text{ of reading}$$

$\beta_{computer}$ = the error in the voltage signal ADC

$$\frac{\sigma_{computer}}{E_{reading} \text{ or } E_{scale\ computer}} = \pm 1.\% \text{ of reading or } \pm 0.2\% \text{ of the range}$$

$E_{scale\ computer}$ = 11 volts (from -1 to + 10 volts)

The maximum error on flow rate measurement is 1.6 % or 0.0208 gpm.

B. Temperature Measurement Error Analysis

The accuracy of the computer must also be taken into consideration. The specified accuracy of the data acquisition system is given as ± 1.44°F (±0.8 °C) with a resolution of 0.18 °F (0.1°C) for K-type thermocouples. The accuracy of the differential thermocouple connection is specified as ±20μV for the ±25mV range setting. This corresponds to a temperature difference accuracy of ±0.90°F (±0.5°C). Calibration tests indicates an error of ±25.45 μV which corresponds to a temperature difference error of ±1.147 °F.

The error of the temperature readings must include the combined effects of the error of the computer, calibrated probe, the absolute temperature probes, and the computer micro volt readings. The error of the absolute temperature thermocouples is given by:

$$\sigma_{Tin} = \sqrt{\sigma^2_{Tin/cal}+\sigma^2_{cal}+\sigma^2_{computer\ TC}} \qquad (94)$$

and

$$\sigma_{Tout} = \sqrt{\sigma^2_{Tout/cal}+\sigma^2_{cal}+\sigma^2_{computer\ TC}} \qquad (95)$$

where

$\sigma_{Tin/cal}$ = error of the inlet probe as compared with the calibrated probe.

$\sigma_{Tin/cal} = \pm 1.02$ °F

$\sigma_{Tout/cal}$ = error of the outlet probe as compared with the calibrated probe.

$\sigma_{Tout/cal} = \pm 1.44$ °F

$\sigma_{computer\ TC}$ = error of the computer ADC thermocouple channels.

$\sigma_{computer\ TC} = \pm 1.0$ °F

The mean temperature is required in converting the micro volt signal from the differential thermocouple connection to an equivalent temperature difference. The mean temperature is calculated from the absolute temperature readings of the inlet and outlet thermocouples as follows:

$$T_{mean} = \frac{T_{in} + T_{out}}{2} \qquad (96)$$

The error in the mean temperature is given by:

$$\sigma_{Tmean} = \sqrt{\sigma^2_{Tin}+\sigma^2_{Tout}} \qquad (97)$$

The temperature difference from the differential thermocouple reading is given by:

$$\Delta T = \frac{\mu V}{k} \qquad (98)$$

where k is the micro volt to temperature difference conversion factor.

The conversion factor, k, is a function of the mean temperature (Fig. 49). The error in the measured temperature difference is given by:

$$\sigma_{\Delta T} = \sqrt{\left(\frac{\partial \Delta T}{\partial \mu V}\sigma_{\mu V}\right)^2 + \left(\frac{\partial \Delta T}{\partial k}\sigma_k\right)^2} \tag{99}$$

which reduces to:

$$\sigma_{\Delta T} = \sqrt{\left(\frac{\sigma_{\mu V}}{k}\right)^2 + \left(\frac{\mu V}{k^2}\sigma_k\right)^2} \tag{100}$$

The error in the micro volt reading is dependent on the error in the differential thermocouple output as well as the error in the computer ADC. The error in the micro volt reading is given by:

$$\sigma_{\mu V} = \sqrt{\sigma_{\Delta T \mu V\text{-cal}} + \sigma_{\text{computer}\ \mu V}} \tag{101}$$

where

$\sigma_{\Delta T \mu V\text{-cal}}$ = error in differential thermocouple as compared with the calibrated thermocouple.

$\sigma_{\Delta T \mu V\text{-cal}} = \pm\ 25.45\ \mu V$

$\sigma_{\text{computer}\ \mu V}$ = error in the computer microvolt reading.

$\sigma_{\text{computer}\ \mu V} = \pm 20\ \mu V$

The micro volt to temperature difference conversion factor, k , is determined from a ninth order polynomial of the mean temperature at the inlet and outlet junctions. The function for k is given as follows:

$$\begin{aligned} k = (m0)+(m1)T_{mean} + (m2)T^2_{mean} + (m3)T^3_{mean} + (m4)T^4_{mean} + (m5)T^5_{mean} \\ + (m6)T^6_{mean} + (m7)T^7_{mean} + (m8)T^8_{mean} + (m9)T^9_{mean} \end{aligned} \tag{102}$$

where

m0 = -5.9996574248

m1 = 0.57623140669

m2 = -0.0050328211032

m3 = 2.6366840630e-5

$m4 = -9.2911149803e^{-8}$

$m5 = 2.2361762393e^{-10}$

$m6 = -3.5624990721e^{-13}$

$m7 = 3.5424764505e^{-16}$

$m8 = -1.9716587450e^{-19}$

$m9 = 4.6528339298e^{-23}$

The error in k is given by:

$$\sigma_k = \sqrt{\left(\frac{\partial k}{\partial T_{mean}}\sigma_{T_{mean}}\right)^2} \qquad (103)$$

where:

$$\frac{\partial k}{\partial T_{mean}} = (m1) + 2(m2)T_{mean} + 3(m3)T_{mean}^2 + 4(m4)T_{mean}^3 + 5(m5)T_{mean}^4 + 6(m6)T_{mean}^5 + 7(m7)T_{mean}^6 + 8(m8)T_{mean}^7 + 9(m9)T_{mean}^8 \qquad (104)$$

C. Normalization Error Analysis

The heat loss is normalized using the following formula:

$$Q_{normalized} = Q_{measured}\left(\frac{T_{target} - T_{ambient\ standard}}{T_{measured} - T_{ambient\ measured}}\right) \qquad (105)$$

The percent error in the normalized heat loss is given by:

$$\frac{\sigma_{Q_{normalized}}}{Q_{normalized}} = \sqrt{\left(\frac{\sigma_{Q_{measured}}}{Q_{measured}}\right)^2 + \left(\frac{\sigma_N}{N}\right)^2} \qquad (106)$$

where

$$N = \frac{T_{target} - T_{ambient\ standart}}{T_{measured} - T_{ambient\ measured}} \qquad (107)$$

and

$$\frac{\sigma_N}{N} = \sqrt{\frac{\sigma_{T_{mean}}^2 + \sigma_{T_{ambient\ measured}}^2}{(T_{mean} - T_{ambient\ measured})^2}} \qquad (108)$$

The convective heat loss is given by:

$$\frac{\sigma_N}{N} = \sqrt{\frac{\sigma^2_{T_{mean}} + \sigma^2_{T_{ambient\ measured}}}{(T_{mean} - T_{ambient\ measured})^2}} \tag{109}$$

The error in the convective heat loss is given by:

$$Q_{convective} = Q_{total} - Q_{total_{90^\circ}} \tag{110}$$

The conductive heat loss is given by:

$$Q_{conductive} = Q_{total_{90^\circ plugged}} \tag{111}$$

The error in the conductive heat loss is given by:

$$\sigma_{Q_{conductive}} = \sigma_{Q_{total_{90^\circ plugged}}} \tag{112}$$

The radiative heat loss is given by:

$$Q_{radiative} = Q_{total_{90^\circ unplugged}} - Q_{conductive} \tag{113}$$

The error in the radiative heat loss is given by:

$$\sigma_{Q_{radiative}} = \sqrt{\sigma^2_{Q_{total_{90^\circ unplugged}}} + \sigma^2_{Q_{conductive}}} \tag{114}$$

The maximum error in the normalized total heat loss is 30.63%. This error occurs with the aperture plugged and the receiver in the +90° position (Fig. 61). The total heat loss with the aperture plugged is equivalent to the conductive heat loss.

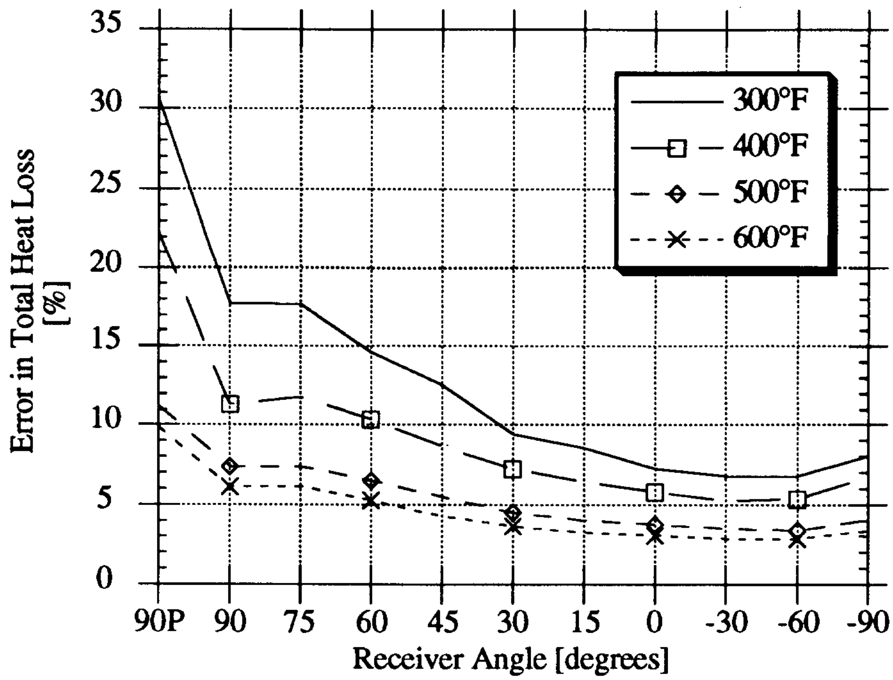

Figure 61. Error in total heat loss for various operating temperatures

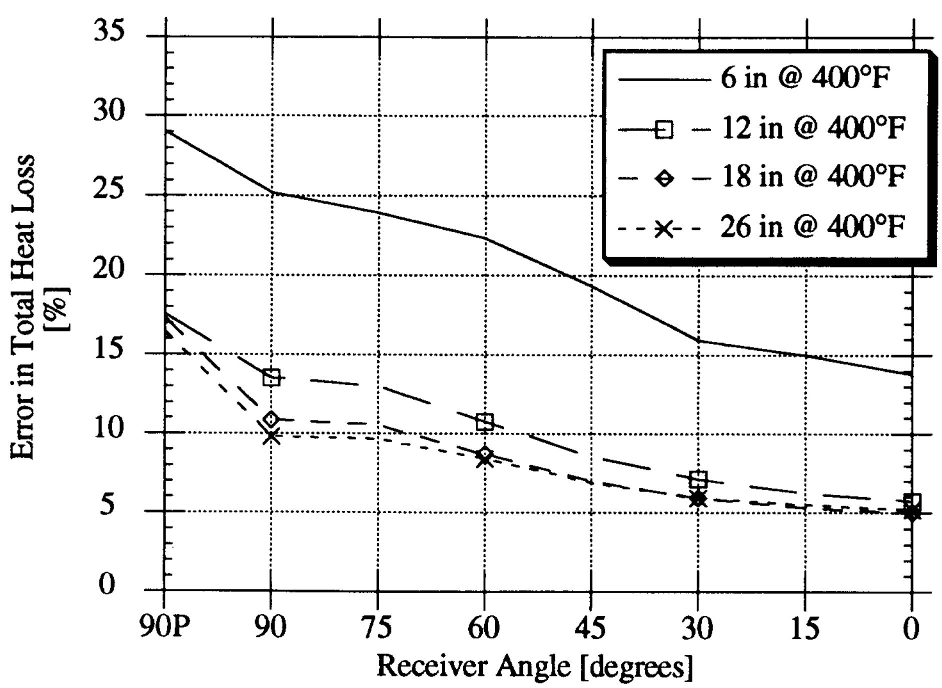

Figure 62. Error in total heat loss for various aperture diameter operating at 400°F

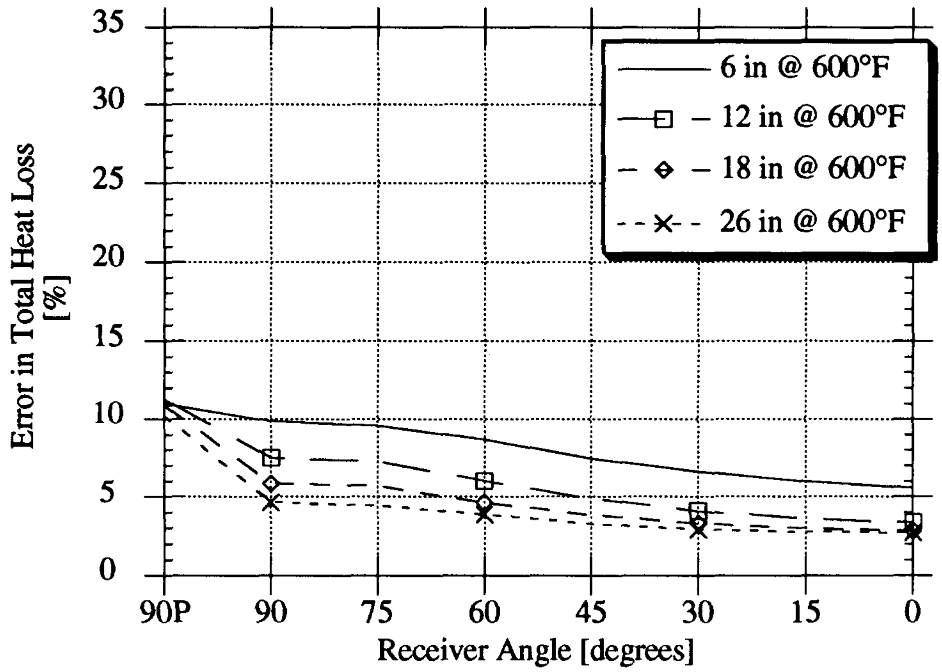

Figure 63. Error in total heat loss for various aperture diameter operating at 600°F

The errors in the convective and radiative heat losses are higher due to summation variables, each of which contains an error (Equations 110, 111, 113). The maximum error in the convective heat loss is 35.70%. The maximum convective heat loss error occurs at a receiver operating temperature of 400°F with a 6 inch aperture and the receiver in the +90° position (Fig. 64).

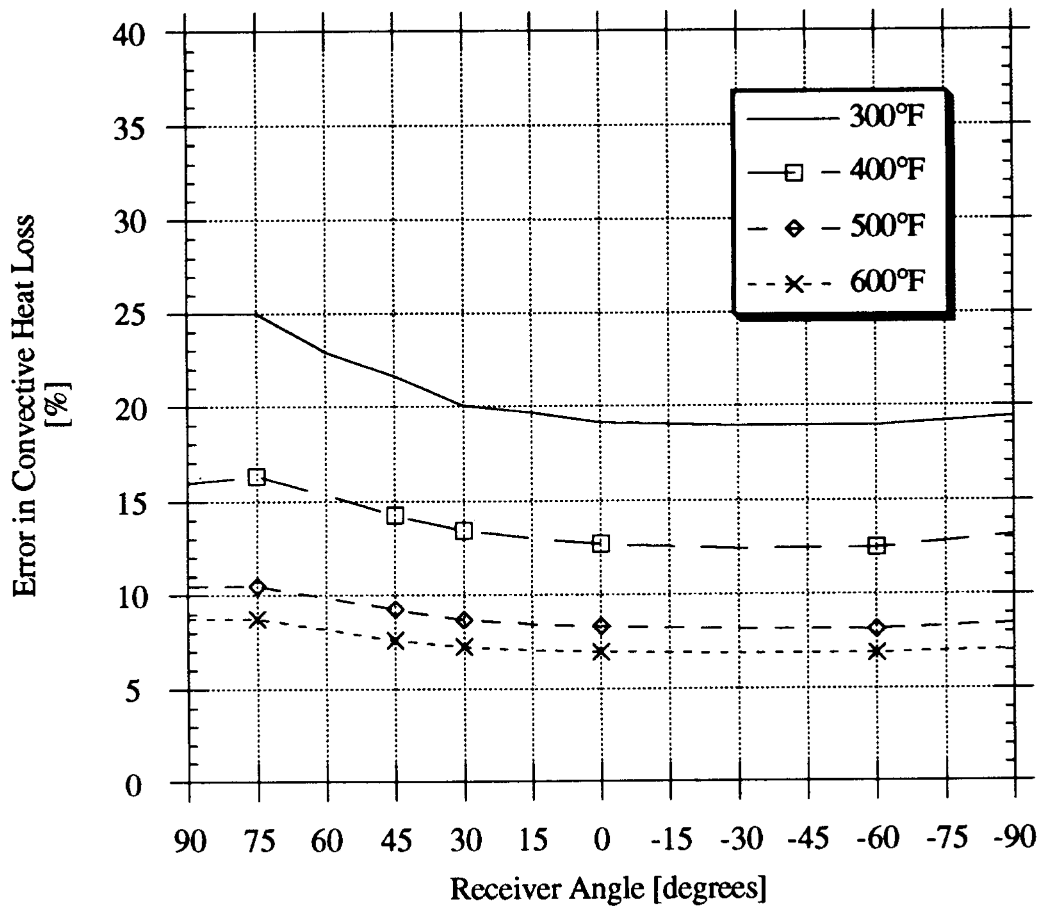

Figure 64. Error in convective heat loss for various operating temperatures

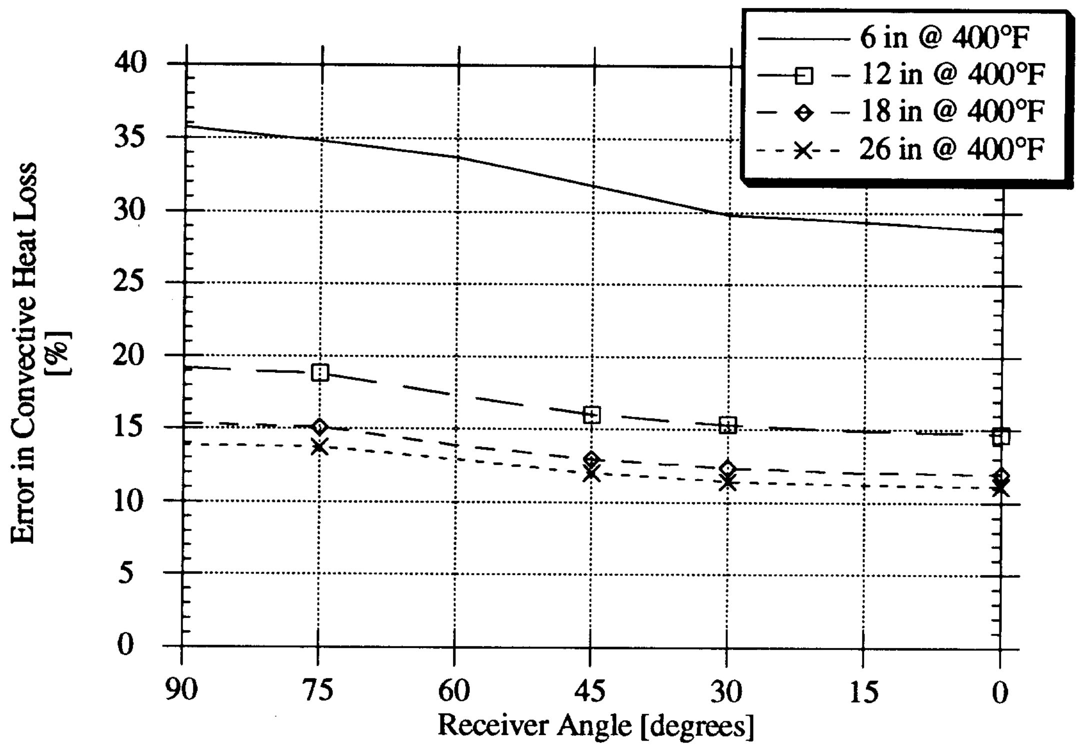

Figure 65. Error in convective heat loss for various aperture diameter operating at 400°F

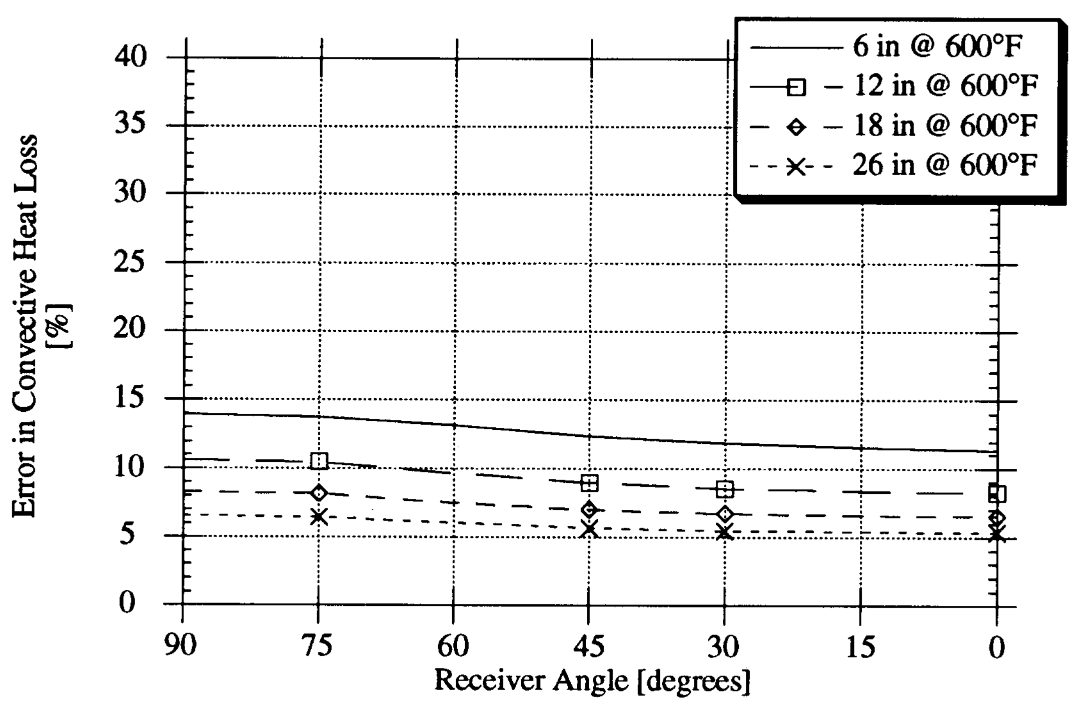

Figure 66. Error in convective heat loss for various aperture diameter operating at 600°F

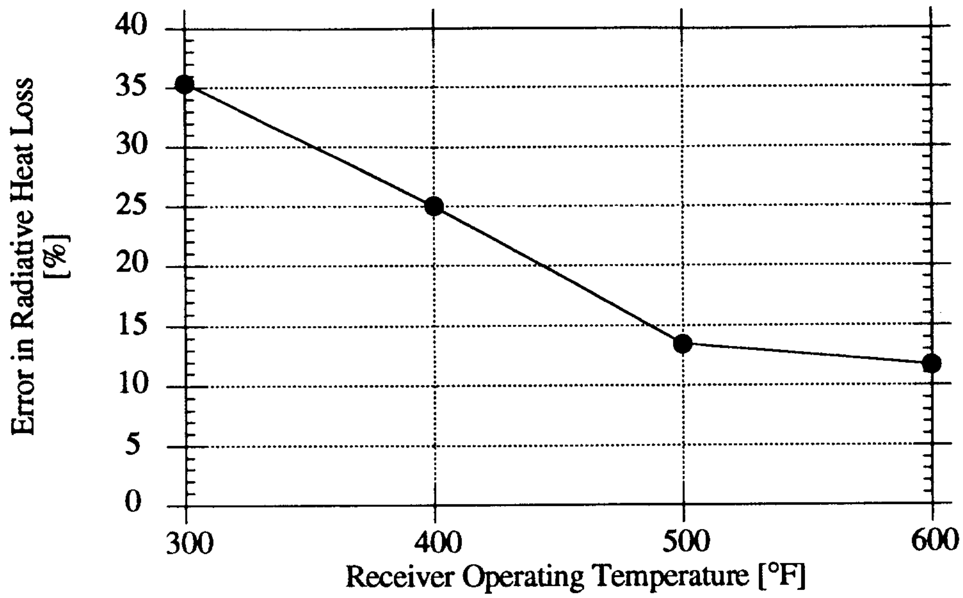

Figure 67. Error in radiative heat loss from Phase 1 test

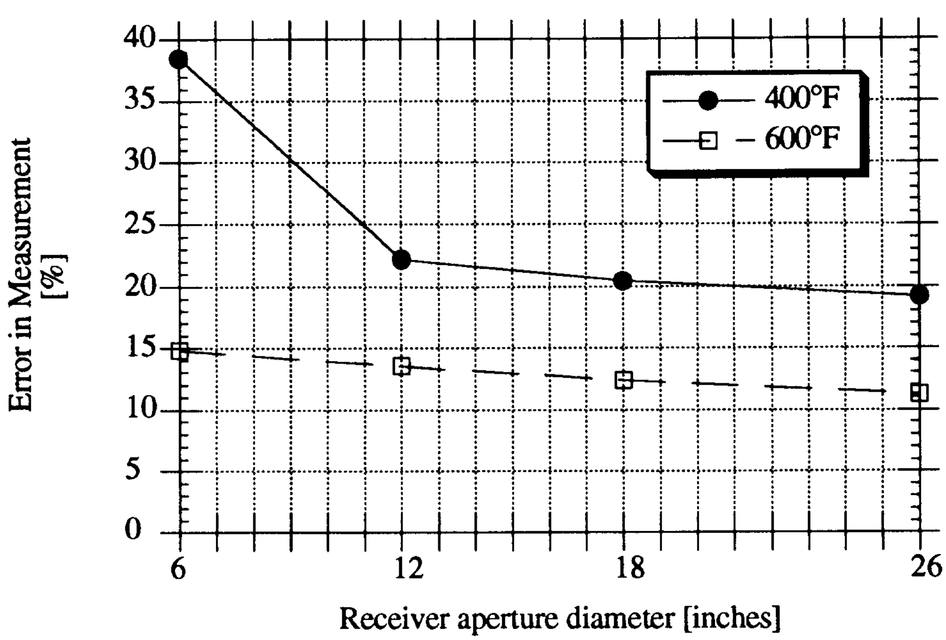

Figure 68. Error in radiative heat loss from Phase 2 test

The error in the radiative heat loss measurement increases with decrease in receiver operating temperature and receiver aperture diameter (Fig. 67 & 68). The maximum error in the radiative heat loss is 38.5% with a six inch aperture and a 400°F operating temperature.

XI. CONCLUSIONS:

The results of experimental testing of the heat loss from a solar cavity receiver for various aperture diameters and operating temperatures have been presented. With an increase in aperture size there was an increase in the convective heat loss. The effect of aperture size on the convective heat loss decreased with increases in aperture size. Decreasing the aperture diameter from 18 inches to 6 inches, reduce the convective losses by 60%. The 18 inch aperture presently used for this type of receiver has little or no effect on the free convective heat loss from the receiver.

Conduction was the primary mode of heat loss from the receiver for very small apertures (less than 12 inch diameter).

A low cost radiometer can be used to determine the radiative heat loss from a cavity within ±20% of experimentally determined radiative heat loss.

XII. RECOMMENDATIONS

Further investigation into cavity temperature distribution and internal surface emissivity and how each affects analytically determined radiative heat loss. Inquiries into convective heat loss from a cavity is necessary to consider how various wind condition will effect heat loss characteristics.

Appendix 1: Phase One; Temperature and Angle Test Results

APPENDIX 1 Temperature and Angle Test Results

Angle	Delta T	Flow SR1	Flow SR1	Flow SR1 error	Flow SR1 error	Flow 1	Flow 2	T amb.	T in	T in cal	T out	T out cal	T avg.	Delta T(mV)	Density	error Density	Cp	error Cp	Mass Flow	Heat Loss	Heat Loss	error Heat Loss
300°F	[µV]	[gpm]	[volts]	[±gpm]	[±%]	[gpm]	[gpm]	[°F]	[°F]	[°F]	[°F]	[°F]	[°F]	[°F]	[lbs/ft^3]	[±%]	[BTU/lb °F]	[±%]	[lbs/min]	[BTU/min]	[Watts]	[±%]
90P	105.99	1.42	4.7630	0.0198	1.3983	0.00	0.00	83.7	308	308.0	303.3	303.9	306.0	4.74	51.03	0.09	0.4384	0.1179	9.676	20.12	353.811	30.563
90	185.12	1.26	4.2444	0.0185	1.4622	1.10	1.03	78.5	297.8	297.7	288.5	289.0	293.4	8.26	51.35	0.09	0.4355	0.1186	8.677	31.20	548.650	17.541
75	185.12	1.27	4.2715	0.0186	1.4584	1.11	1.09	80.3	305	305.0	295.1	295.7	300.3	8.27	51.13	0.09	0.4371	0.1182	8.694	31.44	552.796	17.541
60	224.69	1.22	4.0884	0.0181	1.4857	1.05	1.05	80.2	305.1	305.1	294.6	295.1	300.1	10.04	51.12	0.09	0.4370	0.1182	8.321	36.51	642.040	14.478
45	264.26	1.17	3.9437	0.0177	1.5096	1.01	1.03	79.1	307.6	307.6	294.2	294.7	301.2	11.81	51.04	0.09	0.4373	0.1182	8.014	41.39	727.870	12.338
30	357.53	1.18	3.9467	0.0177	1.5090	1.01	1.03	79.1	308.2	308.2	291.9	292.4	300.3	15.98	51.02	0.09	0.4371	0.1182	8.017	55.99	984.466	9.177
15	397.09	1.17	3.9243	0.0177	1.5129	1.01	1.03	78.4	308.8	308.8	289.7	290.2	299.5	17.74	51.00	0.09	0.4369	0.1183	7.968	61.77	1086.103	8.289
0	477.64	1.18	3.9687	0.0178	1.5053	1.01	1.04	76.8	309	309.0	287.6	288.1	298.6	21.34	51.00	0.09	0.4367	0.1183	8.057	75.07	1320.023	6.942
-30	517.21	1.18	3.9687	0.0178	1.5053	1.00	1.05	75.8	310.2	310.3	286.5	287.0	298.6	23.10	50.96	0.09	0.4367	0.1183	8.051	81.23	1428.363	6.437
-60	517.21	1.18	3.9594	0.0178	1.5069	1.00	1.05	74.5	310.4	310.5	286.1	286.6	298.5	23.10	50.95	0.09	0.4367	0.1183	8.031	81.02	1424.721	6.437
-90	423.94	1.18	3.9594	0.0178	1.5069	1.01	1.04	73.6	311.3	311.4	291.7	292.2	301.8	18.95	50.93	0.09	0.4374	0.1181	8.027	66.55	1170.200	7.782
400°F																						
90P	145.55	1.52	5.1035	0.0208	1.3654	1.27	1.23	81.9	408.6	409.5	401.6	403.3	406.9	6.54	47.74	0.10	0.4613	0.1120	9.899	29.28	514.780	22.273
90	291.11	1.47	4.9326	0.0203	1.3812	1.27	1.31	76.5	401.5	402.4	388	389.6	396.5	13.11	47.98	0.10	0.4589	0.1126	9.421	56.66	996.372	11.202
75	278.39	1.47	4.9381	0.0203	1.3806	1.27	1.31	75.9	402.9	403.8	389.4	391.0	397.9	12.53	47.93	0.10	0.4592	0.1125	9.422	54.22	953.469	11.706
60	317.96	1.46	4.9013	0.0202	1.3842	1.27	1.31	76	402.8	403.7	387.5	389.0	396.9	14.31	47.93	0.10	0.4590	0.1126	9.353	61.45	1080.548	10.272
45	384.38	1.47	4.9402	0.0203	1.3804	1.26	1.30	76.4	402.5	403.4	384.5	386.0	395.3	17.31	47.94	0.10	0.4586	0.1127	9.429	74.84	1316.094	8.532
30	463.51	1.47	4.9326	0.0203	1.3812	1.27	1.31	77.3	402.4	403.3	380.9	382.4	393.4	20.88	47.95	0.10	0.4582	0.1128	9.415	90.06	1583.600	7.118
15	529.93	1.47	4.9474	0.0203	1.3797	1.27	1.30	78.1	405.2	406.1	380.2	381.7	394.5	23.87	47.85	0.10	0.4584	0.1127	9.425	103.11	1813.139	6.262
0	596.35	1.48	4.9855	0.0204	1.3761	1.17	1.28	79.4	404.4	405.3	377	378.4	392.4	26.86	47.88	0.10	0.4580	0.1128	9.503	116.90	2055.650	5.600
-30	662.77	1.49	4.9973	0.0205	1.3750	1.20	1.29	80.9	404.4	405.3	374	375.4	390.9	29.86	47.88	0.10	0.4576	0.1129	9.525	130.15	2288.678	5.074
-60	650.05	1.49	5.0058	0.0205	1.3742	1.21	1.30	80.9	404	404.9	373.7	375.1	390.6	29.29	47.89	0.10	0.4575	0.1129	9.544	127.89	2248.875	5.166
-90	503.08	1.50	5.0464	0.0206	1.3705	1.21	1.30	80.2	403.2	404.1	379.3	380.8	393.0	22.66	47.92	0.10	0.4581	0.1128	9.627	99.93	1757.180	6.578
Angle	Delta mV	Flow SR1	Flow SR1	Flow SR1 error	Flow SR1 error	Flow 1	Flow 2	T amb.	T in	T in cal	T out	T out cal	T avg.	Delta T(mV)	Density	error Density	Cp	error Cp	Mass Flow	Heat Loss	Heat Loss	error Heat Loss
500°F	[µV]	[gpm]	[volts]	[±gpm]	[±%]	[gpm]	[gpm]	[°F]	[°F]	[°F]	[°F]	[°F]	[°F]	[°F]	[lbs/ft^3]	[±%]	[BTU/lb °F]	[±%]	[lbs/min]	[BTU/min]	[Watts]	[±%]
90P	291.11	1.34	4.4919	0.0191	1.4293	1.19	1.09	83.8	515.4	517.2	503.5	506.3	511.8	12.78	44.00	0.12	0.4850	0.1065	7.868	48.76	857.444	11.208
90	450.79	1.35	4.5270	0.0192	1.4250	1.19	1.09	84.3	513.8	515.6	494.4	497.1	506.5	19.81	44.06	0.12	0.4838	0.1068	7.940	76.10	1338.205	7.320
75	450.79	1.37	4.5892	0.0194	1.4176	1.22	1.12	84.8	514.6	516.4	495.6	498.3	507.5	19.81	44.03	0.12	0.4840	0.1067	8.044	77.11	1356.009	7.319
60	517.21	1.32	4.4449	0.0190	1.4352	1.18	1.08	84.8	515.4	517.2	493.2	495.9	506.7	22.73	44.00	0.12	0.4839	0.1068	7.786	85.62	1505.603	6.421
45	623.20	1.32	4.4293	0.0190	1.4372	1.17	1.08	83.8	515.6	517.4	488.2	490.8	504.2	27.40	43.99	0.12	0.4833	0.1069	7.757	102.73	1806.395	5.390
30	782.88	1.32	4.4348	0.0190	1.4365	1.17	1.09	84.4	516	517.8	482.3	484.9	501.5	34.44	43.98	0.12	0.4827	0.1070	7.764	129.08	2269.826	4.379
15	901.39	1.33	4.4707	0.0191	1.4320	1.18	1.12	84.1	516.4	518.3	477.6	480.1	499.3	39.69	43.96	0.12	0.4822	0.1071	7.824	149.73	2632.958	3.868
0	982.14	1.34	4.4957	0.0191	1.4289	1.19	1.15	83.6	516.9	518.8	474.1	476.6	497.8	43.25	43.94	0.12	0.4819	0.1072	7.865	163.90	2881.977	3.595
-30	1088.12	1.34	4.4986	0.0191	1.4285	1.18	1.17	83.2	518.3	520.2	470.9	473.3	496.9	47.93	43.89	0.12	0.4816	0.1073	7.861	181.45	3190.663	3.303
-60	1127.69	1.34	4.4847	0.0191	1.4302	1.19	1.18	83.1	519.3	521.2	470.7	473.1	497.3	49.66	43.86	0.12	0.4817	0.1072	7.830	187.32	3293.966	3.211
-90	888.87	1.34	4.4847	0.0191	1.4302	1.18	1.19	82.5	521	522.9	482.8	485.4	504.2	39.08	43.79	0.12	0.4833	0.1069	7.819	147.68	2596.895	3.915
600°F																						
90P	330.68	1.49	5.0113	0.0205	1.3737	1.34	1.39	76.5	601.3	603.9	587.9	591.6	597.4	14.31	40.70	0.14	0.5044	0.1024	8.119	58.59	1030.273	9.883
90	542.65	1.50	5.0223	0.0205	1.3727	1.34	1.39	77.6	601.3	603.9	577.7	581.3	592.3	23.49	40.70	0.14	0.5033	0.1027	8.137	96.20	1691.628	6.121
75	542.65	1.51	5.0806	0.0207	1.3674	1.35	1.39	77.4	601.6	604.2	577.4	581.0	592.3	23.49	40.69	0.14	0.5033	0.1027	8.229	97.29	1710.780	6.120
60	635.92	1.48	4.9863	0.0204	1.3761	1.33	1.38	77.2	601.5	604.1	573.4	576.9	590.3	27.54	40.69	0.14	0.5028	0.1028	8.077	111.83	1966.501	5.274
45	795.60	1.49	4.9998	0.0205	1.3748	1.33	1.38	77.6	601.7	604.3	567.5	571.0	587.4	34.46	40.68	0.14	0.5022	0.1029	8.097	140.14	2464.250	4.297
30	955.29	1.48	4.9749	0.0204	1.3771	1.33	1.38	78.1	600.4	603.0	558.8	562.2	582.4	41.41	40.73	0.14	0.5010	0.1031	8.067	167.38	2943.183	3.661
15	1100.84	1.49	4.9982	0.0205	1.3749	1.34	1.36	78.2	598.4	601.0	551.3	554.6	577.6	47.75	40.81	0.14	0.4999	0.1033	8.121	193.87	3409.096	3.250
0	1181.39	1.48	4.9842	0.0204	1.3762	1.33	1.35	78.7	594.6	597.1	543.9	547.1	571.9	51.29	40.97	0.14	0.4987	0.1036	8.129	207.89	3655.536	3.070
-30	1287.38	1.49	4.9927	0.0205	1.3755	1.34	1.38	80.6	594.7	597.2	539.5	542.7	569.8	55.91	40.96	0.14	0.4982	0.1037	8.142	226.75	3987.206	2.871
-60	1300.10	1.50	5.0536	0.0206	1.3699	1.35	1.37	80.6	597.5	600.1	542.4	545.6	572.6	56.43	40.85	0.14	0.4988	0.1036	8.218	231.35	4068.151	2.847
-90	1048.56	1.51	5.0591	0.0206	1.3694	1.35	1.37	80.6	601.4	604.0	557	560.4	581.9	45.46	40.69	0.14	0.5009	0.1031	8.196	186.62	3281.530	3.381

Appendix 1: Phase One; Temperature and Angle Test Results

	normalized	normalized	normalized	normalized	normalized									
Heat Loss Conv	Heat Loss	error Heat Loss	Heat Loss Conv	error Conv	Heat Loss Cond	% Conv	% Cond	% Radiation	alpha	dalpha/dTm	error alpha	error ΔT	error ΔT	HTF viscosity
[Watts]	[Watts]	[±%]	[Watts]	[±%]	[Watts]	[%]	[%]	[%]	[μV/°F]	[±°F]	[±°F]	[±°F]	[±%]	[centistokes]
	366.084	30.635			366.084		100.0	0.0	22.3429	-0.0057	0.0131	1.4	30.5	1.7685
0.000	387.296	17.675	0.000	24.997	error Cond	0.0	62.3	37.7	22.4212	-0.0066	0.0152	1.4	17.5	1.8764
4.146	377.839	17.669	-9.457	24.992	[±%]	-1.6	63.4	38.3	22.3766	-0.0062	0.0141	1.4	17.5	1.7994
93.391	671.439	14.634	84.143	22.947	30.635	12.5	54.5	32.9	22.3778	-0.0062	0.0141	1.4	14.4	1.7984
179.220	753.799	12.517	166.503	21.659		22.1	48.6	29.3	22.3713	-0.0061	0.0139	1.4	12.2	1.7726
435.816	1023.497	9.417	436.202	20.028	Heat Loss Rad	42.6	35.8	21.6	22.3766	-0.0062	0.0141	1.4	9.1	1.7665
537.453	1129.722	8.555	542.426	19.637	[Watts]	48.0	32.4	19.6	22.3816	-0.0062	0.0142	1.4	8.1	1.7604
771.373	1369.076	7.255	781.781	19.106	221.212	57.1	26.7	16.2	22.3876	-0.0063	0.0143	1.4	6.8	1.7584
879.714	1474.466	6.770	887.170	18.928	error Rad	60.2	24.8	15.0	22.3873	-0.0063	0.0143	1.4	6.3	1.7463
876.072	1462.836	6.767	875.540	18.927	[±%]	59.9	25.0	15.1	22.3879	-0.0063	0.0144	1.4	6.3	1.7443
621.550	1179.476	8.047	592.180	19.421	35.368	50.2	31.0	18.8	22.3676	-0.0061	0.0138	1.4	7.6	1.7353
					Heat Loss Cond									
	522.653	22.320			[Watts]		100.0	0.0	22.2431	0.0035	0.0080	1.5	22.2	1.0346
0.000	1027.445	11.297	0.000	15.976	522.653	0.0	50.9	49.1	22.2106	0.0027	0.0062	1.5	11.1	1.0718
-42.903	977.075	11.796	-50.370	16.333	error Cond	-5.2	53.5	51.7	22.2145	0.0028	0.0065	1.5	11.6	1.0644
84.176	1111.118	10.374	83.673	15.338	[±%]	7.5	47.0	45.4	22.2117	0.0028	0.0063	1.5	10.2	1.0649
319.722	1362.072	8.657	334.627	14.233	22.32	24.6	38.4	37.1	22.2072	0.0026	0.0060	1.5	8.4	1.0665
587.228	1653.244	7.270	625.799	13.434	Heat Loss Rad	37.9	31.6	30.5	22.2025	0.0025	0.0057	1.5	7.0	1.0670
816.767	1891.360	6.434	863.914	13.001	[Watts]	45.7	27.6	26.7	22.2051	0.0026	0.0059	1.5	6.1	1.0522
1059.278	2167.021	5.796	1139.576	12.697	504.792	52.6	24.1	23.3	22.2001	0.0024	0.0055	1.5	5.4	1.0564
1292.306	2436.096	5.294	1408.651	12.476	error Rad	57.8	21.5	20.7	22.1966	0.0023	0.0052	1.5	4.9	1.0564
1252.503	2396.448	5.382	1369.003	12.314	[±%]	57.1	21.8	21.1	22.1958	0.0023	0.0051	1.5	5.0	1.0585
760.809	1853.833	6.746	826.387	13.158	25.016	44.6	28.2	27.2	22.2015	0.0025	0.0056	1.5	6.4	1.0628
	normalized	normalized	normalized	normalized										
Heat Loss Conv	Heat Loss	error Heat Loss	Heat Loss Conv	error Conv	Heat Loss Cond	% Conv	% Cond	% Radiation	alpha	dalpha/dTm	s alpha	error ΔT	error ΔT	HTF viscosity
[Watts]	[Watts]	[±%]	[Watts]	[±%]	[Watts]	[%]	[%]	[%]	[μV/°F]	[±°F]	[±°F]	[±°F]	[±%]	[centistokes]
	861.371	11.261			861.371		100.0	58.2	22.7828	0.0051	0.0115	1.4	11.1	0.6323
0.000	1363.068	7.403	0.000	10.470	error Cond	0.0	63.2	36.8	22.7552	0.0052	0.0119	1.4	7.2	0.6367
17.803	1379.549	7.402	16.482	10.469	[±%]	1.2	62.4	36.4	22.7604	0.0052	0.0118	1.4	7.2	0.6345
167.397	1534.667	6.516	171.600	9.862	11.26	11.2	56.1	32.7	22.7562	0.0052	0.0118	1.4	6.3	0.6323
468.190	1847.466	5.504	484.399	9.225		26.2	46.6	27.2	22.7436	0.0053	0.0120	1.4	5.2	0.6318
931.621	2340.183	4.520	977.115	8.674	Heat Loss Rad	41.8	36.8	21.4	22.7290	0.0053	0.0121	1.4	4.1	0.6307
1294.753	2726.760	4.029	1363.692	8.428	[Watts]	50.0	31.6	18.4	22.7174	0.0054	0.0122	1.4	3.6	0.6296
1543.772	2991.930	3.768	1628.863	8.307	501.697	54.4	28.8	16.8	22.7093	0.0054	0.0123	1.4	3.3	0.6283
1852.457	3316.435	3.492	1953.388	8.185	error Rad	58.9	26.0	15.1	22.7044	0.0054	0.0123	1.4	3.0	0.6245
1955.760	3419.686	3.403	2056.618	8.148	[±%]	60.1	25.2	14.7	22.7066	0.0054	0.0123	1.4	2.9	0.6218
1258.690	2647.790	4.069	1284.723	8.448	13.477	48.5	32.5	18.9	22.7436	0.0053	0.0120	1.4	3.6	0.6173
					Heat Loss Cond									
	1048.173	9.924			[Watts]		100.0	0.0	23.1152	0.0030	0.0067	1.4	9.8	0.4453
0.000	1741.860	6.189	0.000	8.752	1048.173	0.0	60.2	39.8	23.0998	0.0030	0.0069	1.4	6.0	0.4453
19.152	1760.898	6.187	19.038	8.751	error Cond	1.1	59.5	39.4	23.0998	0.0030	0.0069	1.4	6.0	0.4448
274.872	2031.461	5.352	289.600	8.182	[±%]	14.3	51.6	34.1	23.0936	0.0030	0.0069	1.4	5.1	0.4449
772.622	2561.975	4.394	820.115	7.590	9.92	32.0	40.9	27.1	23.0848	0.0031	0.0070	1.4	4.1	0.4446
1251.555	3093.465	3.776	1351.604	7.250	Heat Loss Rad	43.7	33.9	22.4	23.0690	0.0032	0.0072	1.4	3.4	0.4468
1717.468	3618.174	3.382	1876.313	7.052	[Watts]	51.9	29.0	19.2	23.0536	0.0033	0.0074	1.4	2.9	0.4503
1963.908	3927.963	3.213	2186.103	6.973	693.687	55.7	26.7	17.7	23.0349	0.0034	0.0077	1.4	2.7	0.4570
2295.578	4319.945	3.026	2578.084	6.889	error Rad	59.7	24.3	16.1	23.0276	0.0034	0.0078	1.4	2.5	0.4569
2376.523	4381.976	3.001	2640.116	6.878	[±%]	60.2	23.9	15.8	23.0373	0.0034	0.0077	1.4	2.5	0.4519
1589.902	3469.065	3.507	1727.204	7.113	11.695	49.8	30.2	20.0	23.0677	0.0032	0.0073	1.4	3.1	0.4451

Appendix 2: Phase Two; Aperture Size Test Result

Appendix 2 Aperture Size Test Results																							
Heat transfer area [m^2] =		1.0372							Saran transmittance		0.901		Radiometer radius =		0.5625		Stefan Boltzmann [W/m^2-K^4]=				5.67E-08		
Aperture=	6.00																						
Test Temperature	Receiver Angle	Flow1	Flow1	Flow1 error	Flow1 error	Flow2	Flow 3	T in	T out	T in cal	T out cal	Tmean	Delta T	alpha	dalpha/dTm	ΔT	s alpha	sDT	error ΔT	Ambient T	Ceiling T	Radio	Water
[°F]	[degrees]	[GPM]	[volts]	[±GPM]	[±%]	[GPM]	[GPM]	[°F]	[°F]	[°F]	[°F]	[°F]	[μV]	[μV/°F]	[±°F]	[°F]	[±°F]	[±°F]	[%]	[°F]	[°F]	[mV]	[°F]
	0	1.4712	4.9401	0.0203	1.3804	1.5011	1.6564	396.6	385.7	397.4	387.2	392.3	237.41	22.1998	2.399E-3	10.69	5.467E-3	1.5	13.6	67	72.7	0.0603	67.5
	15	1.4664	4.9241	0.0203	1.3820	1.4988	1.6492	395.8	385.4	396.6	386.9	391.8	217.67	22.1985	2.354E-3	9.81	5.364E-3	1.5	14.9	67.3	72.1	0.0689	67.7
400	30	1.4574	4.8940	0.0202	1.3849	1.4831	1.6219	395.4	385.8	396.2	387.3	391.8	204.91	22.1985	2.354E-3	9.23	5.365E-3	1.5	15.8	67.7	72.7	0.0718	67.3
	45	1.4630	4.9126	0.0202	1.3831	1.4854	1.6263	394.4	386.5	395.2	388.0	391.6	168.16	22.1982	2.342E-3	7.58	5.337E-3	1.5	19.2	68.2	72.6	0.0804	67.6
	60	1.4508	4.8716	0.0201	1.3871	1.4839	1.6380	397.7	390.7	398.5	392.3	395.4	145.55	22.2076	2.645E-3	6.55	6.027E-3	1.5	22.2	68	72.6	0.0574	67.2
	75	1.4592	4.9000	0.0202	1.3843	1.4865	1.6359	399.9	393.5	400.7	395.1	397.9	135.86	22.2145	2.840E-3	6.11	6.473E-3	1.5	23.9	67.2	71.9	0.0431	67.2
	90	1.4713	4.9406	0.0203	1.3804	1.4936	1.6159	394.4	388.3	395.2	389.9	392.5	128.80	22.2003	2.415E-3	5.79	5.505E-3	1.5	25.2	67.5	73.3	2.4600	67.7
	90P	1.4877	4.9955	0.0205	1.3752	1.4951	1.6195	393.1	387.8	393.9	389.3	391.6	111.64	22.1982	2.342E-3	5.03	5.337E-3	1.5	29.0	68.3	72.5	0.3932	67.4
	0	1.0690	3.5898	0.0169	1.5785	1.1168	1.3462	603.7	575.9	606.3	579.5	592.9	616.13	23.1016	3.013E-3	26.67	6.866E-3	1.4	5.3	82.1	89.1	0.0000	82
	15	1.0674	3.5843	0.0169	1.5797	1.1094	1.3514	604.8	578.9	607.4	582.5	595.0	569.50	23.1078	2.986E-3	24.65	6.805E-3	1.4	5.7	81.2	87.7	0.0057	81.2
600	30	1.0642	3.5737	0.0168	1.5820	1.1116	1.3362	605.8	582.7	608.4	586.3	597.4	510.15	23.1150	2.956E-3	22.07	6.738E-3	1.4	6.3	79.9	86.2	-0.0029	80.8
	45	1.0549	3.5424	0.0168	1.5890	1.1038	1.3218	606.6	586.6	609.2	590.3	599.8	446.55	23.1220	2.930E-3	19.31	6.677E-3	1.4	7.2	78.5	85.3	0.0057	80.1
	60	1.0494	3.5238	0.0167	1.5933	1.1045	1.3394	607.2	590	609.8	593.7	601.8	380.14	23.1279	2.908E-3	16.44	6.627E-3	1.4	8.5	77.4	83.9	-0.0057	79.1
	75	1.0545	3.5411	0.0168	1.5893	1.1068	1.3506	607.1	591.9	609.7	595.6	602.7	343.39	23.1305	2.899E-3	14.85	6.606E-3	1.4	9.4	77.4	83.1	-0.0029	78.6
	90	1.0529	3.5356	0.0167	1.5906	1.1038	1.3118	606.7	592.2	609.3	595.9	602.6	333.50	23.1304	2.899E-3	14.42	6.607E-3	1.4	9.7	74.6	81.7	5.3447	66.3
	90P	1.0516	3.5314	0.0167	1.5915	1.1023	1.3035	607.2	594	609.8	597.8	603.8	298.17	23.1357	2.887E-3	12.89	6.581E-3	1.4	10.9	73.3	79.1	1.0075	66.1
Aperture=	12.00																						
Test Temperature	Receiver Angle	Flow1	Flow1	Flow1 error	Flow1 error	Flow2	Flow 3	T in	T out	T in cal	T out cal	Tmean	Delta T	alpha	dalpha/dTm	ΔT	s alpha	sDT	sDT	Ambient T	Ceiling T	Radio	Water
[°F]	[degrees]	[GPM]	[volts]	[±GPM]	[±%]	[GPM]	[GPM]	[°F]	[°F]	[°F]	[°F]	[°F]	[μV]	[μV/°F]	[±°F]	[°F]	[±°F]	[±°F]	[%]	[°F]	[°F]	[mV]	[°F]
	0	1.0753	3.6109	0.0169	1.5739	1.1486	1.2929	401	372.7	401.8	374.1	388.0	611.89	22.1902	2.039E-3	27.57	4.647E-3	1.5	5.3	67.9	73	0.0115	65.5
	15	1.0613	3.5640	0.0168	1.5842	1.1314	1.2733	403.3	377.6	404.2	379.0	391.6	555.37	22.1981	2.341E-3	25.02	5.335E-3	1.5	5.8	68.5	73.5	0.0144	65.7
	30	1.0647	3.5754	0.0168	1.5817	1.1202	1.2849	407.9	385.9	408.8	387.4	398.1	473.40	22.2151	2.855E-3	21.31	6.506E-3	1.5	6.8	68.8	73.9	0.0144	65.8
400	45	1.0488	3.5217	0.0167	1.5938	1.1101	1.2889	413	394.9	414.0	396.5	405.2	390.03	22.2373	3.374E-3	17.54	7.689E-3	1.5	8.3	69	73.8	0.0144	65.7
	60	1.0489	3.5221	0.0167	1.5937	1.1008	1.2885	417.7	403.6	418.7	405.3	412.0	306.65	22.2616	3.822E-3	13.77	8.710E-3	1.5	10.6	69.4	74.3	0.0172	65.9
	75	1.0435	3.5039	0.0167	1.5979	1.0989	1.2845	424.5	412.8	425.6	414.6	420.1	251.54	22.2945	4.296E-3	11.28	9.790E-3	1.5	12.9	69.5	74.6	0.0144	65.6
	90	1.0416	3.4976	0.0167	1.5994	1.0997	1.2845	428.3	417.2	429.4	419.1	424.2	241.65	22.3127	4.512E-3	10.83	1.028E-2	1.5	13.4	69.9	74.9	4.8883	66.1
	90P	1.0428	3.5018	0.0167	1.5984	1.0982	1.2877	432.9	424.2	434.0	426.1	430.1	185.12	22.3400	4.786E-3	8.29	1.091E-2	1.4	17.5	70.2	75.2	0.3540	65.9
	0	1.1168	3.7300	0.0173	1.5452	1.1508	1.3342	603.6	553.1	606.2	556.4	581.3	1153.13	23.0687	3.193E-3	49.99	7.277E-3	1.4	2.8	86.2	92.3	0.0832	67.5
	15	1.1082	3.7215	0.0172	1.5509	1.1374	1.3550	603.1	557.9	605.7	561.5	583.5	1033.01	23.0720	3.135E-3	44.77	7.190E-3	1.4	3.1	85.2	91.8	0.0803	67.7
	30	1.1001	3.6942	0.0171	1.5564	1.1318	1.3430	603.4	564.4	606.0	567.8	586.9	890.28	23.0834	3.099E-3	38.57	7.062E-3	1.4	3.6	84.1	90.1	0.0775	67.6
600	45	1.0918	3.6663	0.0171	1.5622	1.1318	1.3194	603.1	571.6	605.7	575.1	590.4	717.88	23.0941	3.047E-3	31.08	6.944E-3	1.4	4.5	83	89.9	0.0689	67.6
	60	1.0933	3.6714	0.0171	1.5611	1.1262	1.3566	604.3	579.8	607.1	583.4	595.3	562.43	23.1087	2.982E-3	24.34	6.796E-3	1.4	[illegible]	80.6	87.6	0.0660	67.2
	75	1.1025	3.7022	0.0171	1.5546	1.1336	1.3514	606.1	586.1	608.7	589.8	599.3	459.27	23.1205	2.935E-3	19.80	6.689E-3	1.4	7.0	79.7	86.5	0.0803	66.9
	90	1.1045	3.7090	0.0172	1.5534	1.1363	1.3422	608.6	589.2	611.3	592.9	602.1	442.73	23.1288	2.905E-3	19.14	6.620E-3	1.4	7.3	77.7	85.4	4.7477	67
	90P	1.0993	3.6913	0.0171	1.5570	1.1374	1.3214	608.6	595.7	611.3	599.3	605.4	291.11	23.1382	2.872E-3	12.58	6.546E-3	1.4	11.1	75	81.4	0.7865	66.3

Appendix 2: Phase Two; Aperture Size Test Result

aperture=	18.00																						
Test Temperature [°F]	Receiver Angle [degrees]	Flow 1 [GPM]	Flow 1 [volts]	Flow 1 error [±gpm]	Flow 1 error [±%]	Flow 2 [GPM]	Flow 3 [GPM]	T in [°F]	T out [°F]	T in cal [°F]	T out cal [°F]	Tmean [°F]	Delta T [µV]	alpha [µV/°F]	dalpha/dTm [±°F]	ΔT [°F]	s alpha [±°F]	sDT [±°F]	sDT [%]	Ambient T [°F]	Ceiling T [°F]	Ratio [mV]	Water T [°F]
	0	1.0698	3.5924	0.0169	1.5779	1.0926	1.1819	405.3	371.7	406.2	373.1	389.6	724.94	22.1937	2.178E-3	32.66	4.964E-3	1.5	4.5	82.9	91.1	0.0373	72
	15	1.0564	3.5475	0.0168	1.5879	1.0740	1.1988	408.4	377.3	409.3	378.7	394.0	672.66	22.2040	2.536E-3	30.29	5.780E-3	1.5	4.8	81.7	90.1	0.0545	71.7
	30	1.0505	3.5276	0.0167	1.5924	1.0651	1.2152	410.7	385.5	411.8	385.0	398.5	589.28	22.2156	2.870E-3	26.53	6.541E-3	1.5	5.5	80.4	88.4	0.0373	70.3
400	45	1.0417	3.4980	0.0167	1.5993	1.0616	1.2456	412.9	390.8	413.9	392.4	403.1	483.30	22.2303	3.224E-3	21.74	7.347E-3	1.5	6.7	79	87.2	0.0316	71.7
	60	1.0353	3.4764	0.0166	1.6043	1.0496	1.2428	416	398.3	417.0	400.0	408.5	384.38	22.2485	3.593E-3	17.28	8.189E-3	1.5	8.4	78.2	86	0.0287	72
	75	1.0305	3.4605	0.0166	1.6082	1.0608	1.2332	423.3	408.8	424.3	410.6	417.5	315.72	22.2834	4.149E-3	14.06	9.456E-3	1.5	10.3	76.80	83.90	0.0402	69.70
	90	1.0345	3.4739	0.0166	1.6049	1.0593	1.2585	428.2	415.9	429.5	415.7	422.5	305.83	22.3050	4.425E-3	13.82	1.008E-2	1.5	10.7	76.1	82.6	4.7704	70.6
	90P	1.0340	3.4722	0.0166	1.6053	1.0463	1.2741	434.4	425.8	435.5	427.8	431.6	187.95	22.3475	4.853E-3	8.41	1.106E-2	1.4	17.2	75.6	82.4	0.6114	70.6
	0	1.0836	3.6388	0.0170	1.5679	1.1215	1.3136	605.1	557.2	605.7	540.4	573.0	1503.39	23.0300	3.356E-3	65.26	7.648E-3	1.4	2.2	79	85.3	-0.0029	77.7
	15	1.0663	3.5804	0.0169	1.5805	1.1215	1.3114	600.7	540.8	603.3	544.0	573.6	1367.93	23.0400	3.343E-3	59.37	7.618E-3	1.4	2.4	80.3	86.3	0.0000	71.3
	30	1.0646	3.5749	0.0168	1.5817	1.1105	1.3094	599.8	548.1	602.4	551.4	576.9	1182.80	23.0513	3.277E-3	51.31	7.468E-3	1.4	2.7	81.2	86.3	-0.0029	69.5
600	45	1.0587	3.5551	0.0168	1.5862	1.1101	1.2969	600	557.8	602.6	561.2	581.9	963.77	23.0675	3.183E-3	41.78	7.254E-3	1.4	3.4	79.6	87.2	0.0000	79
	60	1.0489	3.5221	0.0167	1.5937	1.0915	1.2877	598.9	565.7	601.5	569.2	585.3	761.69	23.0783	3.125E-3	33.00	7.121E-3	1.4	4.2	80.3	87	0.0000	77.8
	75	1.0556	3.5445	0.0168	1.5886	1.1058	1.2861	598.5	571.9	600.9	573.4	588.1	602.00	23.0871	3.080E-3	26.06	7.020E-3	1.4	5.4	81.3	87.1	0.0000	75
	90	1.0523	3.5335	0.0167	1.5911	1.1116	1.2829	597.7	572.7	600.3	576.2	588.2	582.22	23.0874	3.079E-3	25.22	7.016E-3	1.4	5.6	82.3	86.9	6.6020	73
	90P	1.0488	3.5217	0.0167	1.5938	1.1109	1.3138	598.4	585	601.0	588.7	594.8	301.00	23.1073	2.988E-3	13.03	6.809E-3	1.4	10.8	83.1	86.7	0.3468	72
aperture=	26.00																						
Test Temperature [°F]	Receiver Angle [degrees]	Flow 1 [GPM]	Flow 1 [volts]	Flow 1 error [±gpm]	Flow 1 error [±%]	Flow 2 [GPM]	Flow 3 [GPM]	T in [°F]	T out [°F]	T in cal [°F]	T out cal [°F]	Tmean [°F]	Delta T [µV]	alpha [µV/°F]	dalpha/dTm [±°F]	ΔT [°F]	s alpha [±°F]	sDT [±°F]	sDT [%]	Ambient T [°F]	Ceiling T [°F]	Ratio [mV]	Water T [°F]
	0	1.2955	4.3502	0.0188	1.4476	1.3473	1.5522	407.1	375.5	408.0	376.9	392.5	682.55	22.2002	2.410E-3	30.75	5.493E-3	1.5	4.7	84.1	89.5	0.2870	73.3
	15	1.2707	4.2668	0.0185	1.4591	1.5241	1.5478	398	368.5	398.8	369.8	384.3	642.98	22.1853	1.727E-3	28.98	3.936E-3	1.5	5.0	83.3	90.1	0.3186	73.5
	30	1.2645	4.2461	0.0185	1.4620	1.3190	1.5103	397.6	370.6	398.4	372.0	385.2	589.28	22.1846	1.802E-3	26.56	4.106E-3	1.5	5.5	83.4	90.3	0.2957	73.3
400	45	1.2577	4.2233	0.0184	1.4653	1.3132	1.5049	399	376.3	399.8	377.7	388.8	490.36	22.1918	2.107E-3	22.10	4.802E-3	1.5	6.6	82.8	89.3	1.1223	73.5
	60	1.2622	4.2385	0.0185	1.4631	1.3099	1.5606	403.2	384.9	404.1	386.4	395.2	397.05	22.2072	2.632E-3	17.88	5.999E-3	1.5	8.1	83.2	89.7	0.4679	73.7
	75	1.2632	4.2419	0.0185	1.4626	1.3129	1.5746	409	393.2	409.9	394.8	402.4	343.39	22.2279	3.170E-3	15.45	7.224E-3	1.5	9.4	82.2	89.1	0.3645	73.7
	90	1.2718	4.2707	0.0185	1.4585	1.3125	1.5598	413.3	397.8	414.3	399.5	406.9	337.74	22.2428	3.485E-3	15.18	7.942E-3	1.5	9.6	81.3	88.6	4.1851	74.1
	90P	1.2664	4.2525	0.0185	1.4611	1.3065	1.4783	403.9	394.6	404.8	396.2	400.5	197.84	22.2221	3.033E-3	8.90	6.913E-3	1.5	16.4	78.5	85.2	0.5339	72.3
	0	1.2480	4.1907	0.0183	1.4701	1.2942	1.5033	600.7	531.3	603.3	534.4	568.8	1579.90	23.0245	3.449E-3	68.62	7.859E-3	1.4	2.0	74	77.3	-0.0097	74.4
	15	1.2392	4.1611	0.0183	1.4745	1.2864	1.4809	599.7	535	602.3	536.1	569.2	1520.55	23.0256	3.440E-3	66.04	7.841E-3	1.4	2.1	74.2	77.5	0.0115	73.3
	30	1.2320	4.1370	0.0182	1.4781	1.2711	1.4640	599.4	538.5	602.0	541.7	571.8	1390.54	23.0345	3.382E-3	60.37	7.707E-3	1.4	2.3	73.9	77.7	0.0258	71.7
600	45	1.2253	4.1146	0.0182	1.4816	1.2811	1.4308	599.3	548.2	601.9	551.5	576.7	1172.91	23.0507	3.281E-3	50.88	7.477E-3	1.4	2.8	73.8	78	0.1407	69.1
	60	1.2189	4.0930	0.0181	1.4849	1.2811	1.4448	599.3	558.5	601.9	561.9	581.9	936.92	23.0675	3.183E-3	40.62	7.254E-3	1.4	3.5	74.1	78.3	0.1292	68.3
	75	1.2246	4.1121	0.0181	1.4820	1.2752	1.4324	599.6	565.3	602.2	568.8	585.5	791.36	23.0788	3.122E-3	34.29	7.115E-3	1.4	4.1	76.9	79	0.5129	67.4
	90	1.2262	4.1176	0.0182	1.4811	1.2886	1.4500	600	566.9	602.6	570.4	586.5	754.62	23.0820	3.106E-3	32.69	7.079E-3	1.4	4.3	75.4	79.2	6.2461	68.4
	90P	1.2257	4.1159	0.0182	1.4814	1.2763	1.4448	599.5	585.3	602.1	589.0	595.5	320.78	23.1095	2.979E-3	13.88	6.789E-3	1.4	10.1	74.7	79.2	0.7808	67.7

Appendix 2: Phase Two; Aperture Size Test Result

Syltherm Density	error Density	Syltherm Cp	error Cp	Syltherm viscosity	Total Heat Loss	Total Heat Loss	error Heat Loss	Convective	Normalized Total Heat Loss	Normalized error Heat Loss	Normalized Convective	normalized error Conv	Normalized k	Normalized h	Normalized Nu	normalized error Rad
[lbs/ft^3]	[±%]	[BTU/lb-°F]	[±%]	[centistokes]	[BTU/min]	[Watts]	[±%]	[Watts]	[Watts]	[±%]	[Watts]	[±%]	[W/m-K]	[W/m^2-K]		[±%]
48.32	0.10	0.4579	0.1128	1.0985	46.54	818.4	13.7	375.1	830.2	13.8	380.1	28.8	0.0072	1.9987	183.9	38.5
48.34	0.10	0.4578	0.1129	1.1029	42.54	748.0	14.9	304.7	760.8	15.0	310.7	29.4	0.0072	1.6340	150.3	heat loss Rad
48.34	0.10	0.4578	0.1129	1.1051	39.80	699.9	15.9	256.6	712.7	15.9	262.6	29.8	0.0072	1.3809	127.0	[Watts]
48.35	0.10	0.4578	0.1129	1.1107	32.79	576.6	19.3	133.3	588.3	19.3	138.2	31.8	0.0072	0.7269	66.9	52.8
48.22	0.10	0.4586	0.1127	1.0924	28.11	494.3	22.3	51.0	498.3	22.3	48.2	33.7	0.0072	0.2533	23.3	
48.14	0.10	0.4592	0.1125	1.0804	26.33	463.0	23.9	19.7	462.0	23.9	11.9	34.8	0.0072	0.0628	5.8	
48.32	0.10	0.4580	0.1128	1.1107	25.21	443.3	25.2	0.0	450.1	25.2	0.0	35.7	0.0072	0.0000	0.0	
48.35	0.10	0.4578	0.1129	1.1180	22.14	389.2	29.0		397.3	29.1						error Rad
																[±%]
41.12	0.14	0.5034	0.1026	0.4412	78.90	1387.3	5.5	852.4	1439.5	5.6	701.8	11.3	0.0072	2.2980	211.4	14.8
41.04	0.14	0.5039	0.1025	0.4393	72.71	1278.6	5.9	543.7	1319.1	6.0	581.4	11.5	0.0072	1.9037	175.1	heat loss Rad
40.94	0.14	0.5044	0.1024	0.4376	64.84	1140.2	6.5	405.3	1167.8	6.6	430.1	11.9	0.0072	1.4084	129.6	[Watts]
40.85	0.14	0.5050	0.1023	0.4363	56.18	987.8	7.4	252.9	1004.4	7.5	266.7	12.4	0.0072	0.8733	80.3	82.5
40.76	0.14	0.5054	0.1022	0.4352	47.51	835.4	8.7	100.4	844.3	8.7	106.7	13.2	0.0072	0.3492	32.1	
40.73	0.14	0.5056	0.1022	0.4354	43.10	757.9	9.6	23.0	764.7	9.6	27.0	13.8	0.0072	0.0885	8.1	
40.73	0.14	0.5056	0.1022	0.4361	41.79	734.9	9.8	0.0	737.6	9.9	0.0	14.0	0.0072	0.0000	0.0	
40.68	0.14	0.5059	0.1021	0.4352	37.29	655.8	11.0		655.2	11.0						
									Normalized	Normalized	Normalized	normalized	Normalized	Normalized	Normalized	normalized
Syltherm Density	error Density	Syltherm Cp	error Cp	Syltherm viscosity	Total Heat Loss	Total Heat Loss	error Heat Loss	Convective	Total Heat Loss	error Heat Loss	Convective	error Conv	k	h	Nu	error Rad
[lbs/ft^3]	[±%]	[BTU/lb-°F]	[±%]	[centistokes]	[BTU/min]	[Watts]	[±%]	[Watts]	[Watts]	[±%]	[Watts]	[±%]	[W/m-K]	[W/m^2-K]		[±%]
48.47	0.10	0.4570	0.1131	1.0745	87.79	1543.7	5.5	960.7	1591.6	5.7	1048.7	14.7	0.0072	5.5146	507.3	22.2
48.35	0.10	0.4578	0.1129	1.0622	78.56	1381.4	6.0	798.5	1410.9	6.2	868.0	14.9	0.0072	4.5646	419.9	heat loss Rad
48.13	0.10	0.4593	0.1125	1.0382	67.05	1179.0	7.0	596.0	1181.4	7.2	638.5	15.3	0.0072	3.3577	308.9	[Watts]
47.89	0.10	0.4609	0.1121	1.0124	54.28	954.4	8.4	371.5	936.7	8.6	393.8	16.0	0.0072	2.0710	190.5	134.0
47.67	0.10	0.4624	0.1117	0.9894	42.57	748.6	10.7	165.7	721.1	10.8	178.2	17.3	0.0072	0.9370	86.2	
47.40	0.10	0.4642	0.1113	0.9572	34.63	609.0	13.0	26.0	573.2	13.0	30.3	18.8	0.0072	0.1593	14.7	
47.26	0.10	0.4652	0.1111	0.9398	33.15	582.9	13.5	0.0	542.9	13.6	0.0	19.2	0.0072	0.0000	0.0	
47.06	0.10	0.4665	0.1108	0.9193	25.36	446.0	17.6		408.9	17.6						error Rad
																[±%]
41.57	0.14	0.5008	0.1032	0.4413	155.39	2732.4	3.2	1708.5	2924.9	3.3	1890.1	8.2	0.0072	6.1886	569.3	13.5
41.49	0.14	0.5013	0.1031	0.4422	137.94	2425.7	3.5	1401.8	2580.0	3.6	1545.2	8.4	0.0072	5.0595	465.4	heat loss Rad
41.35	0.14	0.5021	0.1029	0.4417	117.76	2070.8	4.0	1047.0	2182.7	4.1	1147.9	8.6	0.0072	3.7586	345.7	[Watts]
41.22	0.14	0.5028	0.1027	0.4422	94.03	1653.5	4.8	629.7	1727.1	4.9	692.3	9.0	0.0072	2.2668	208.5	366.7
41.02	0.14	0.5039	0.1025	0.4398	73.54	1293.2	6.0	269.4	1331.7	6.0	296.9	9.6	0.0072	0.9723	89.4	
40.87	0.14	0.5049	0.1023	0.4371	60.40	1062.1	7.2	38.3	1083.5	7.3	48.7	10.5	0.0072	0.1594	14.7	
40.75	0.14	0.5055	0.1022	0.4329	58.22	1023.8	7.5	0.0	1034.8	7.5	0.0	10.6	0.0072	0.0000	0.0	
40.62	0.14	0.5062	0.1021	0.4329	38.02	668.5	11.2		668.1	11.3						

Appendix 2: Phase Two; Aperture Size Test Result

									Normalized	Normalized	Normalized	normalized	Normalized	Normalized	Normalized	normalized
Syltherm Density	error Density	Syltherm Cp	error Cp	Syltherm viscosity	Total Heat Loss	Total Heat Loss	error Heat Loss	Convective	Total Heat Loss	error Heat Loss	Convective	error Conv	k	h	Nu	error Rad
[lbs/ft^3]	[±%]	[BTU/lb-°F]	[±%]	[centistokes]	[BTU/min]	[Watts]	[±%]	[Watts]	[Watts]	[±%]	[Watts]	[±%]	[W/m-K]	[W/m^2-K]		[±%]
48.41	0.10	0.4573	0.1130	1.0517	103.43	1818.7	4.7	1090.2	1956.6	5.0	1262.7	11.9	0.0072	6.6400	610.8	20.5
48.27	0.10	0.4583	0.1127	1.0357	94.64	1664.2	5.1	935.7	1758.4	5.3	1064.4	12.1	0.0072	5.5976	514.9	heat loss Rad
48.12	0.10	0.4593	0.1125	1.0240	82.34	1447.9	5.7	719.4	1502.9	5.9	808.9	12.4	0.0072	4.2538	391.3	[Watts]
47.97	0.10	0.4604	0.1122	1.0129	66.85	1175.6	6.9	447.1	1196.9	7.0	502.9	12.9	0.0072	2.6448	243.3	278.2
47.79	0.10	0.4616	0.1119	0.9976	52.74	927.4	8.6	198.9	926.7	8.7	232.7	13.9	0.0072	1.2237	112.6	
47.49	0.10	0.4636	0.1114	0.9628	42.70	750.8	10.4	22.4	727.4	10.5	33.4	15.1	0.0072	0.1755	16.1	
47.32	0.10	0.4648	0.1112	0.9403	41.43	728.5	10.8	0.0	694.0	10.9	0.0	15.4	0.0072	0.0000	0.0	
47.01	0.10	0.4669	0.1107	0.9127	25.51	448.6	17.3		415.8	17.3						error Rad
																[±%]
41.90	0.14	0.4989	0.1036	0.4422	197.62	3475.0	2.7	2180.7	3728.0	2.8	2372.2	6.5	0.0072	7.7673	714.5	12.4
41.87	0.14	0.4990	0.1035	0.4463	176.84	3109.6	2.9	1815.3	3340.6	3.0	1984.9	6.6	0.0072	6.4990	597.8	heat loss Rad
41.75	0.14	0.4998	0.1034	0.4479	152.37	2679.2	3.2	1385.0	2864.8	3.3	1509.0	6.7	0.0072	4.9409	454.5	[Watts]
41.55	0.14	0.5009	0.1031	0.4475	123.07	2164.2	3.7	869.9	2283.6	3.8	927.9	7.0	0.0072	3.0381	279.5	668.0
41.42	0.14	0.5017	0.1030	0.4494	96.16	1690.9	4.5	396.6	1774.5	4.6	418.7	7.5	0.0072	1.3711	126.1	
41.31	0.14	0.5023	0.1029	0.4505	76.35	1342.5	5.6	48.2	1403.8	5.7	48.0	8.2	0.0072	0.1573	14.5	
41.30	0.14	0.5024	0.1028	0.4515	73.60	1294.2	5.8	0.0	1355.8	5.9	0.0	8.3	0.0072	0.0000	0.0	
41.04	0.14	0.5038	0.1025	0.4503	37.76	664.1	10.9		687.8	10.9						
									Normalized	Normalized	Normalized	normalized	Normalized	Normalized	Normalized	normalized
Syltherm Density	error Density	Syltherm Cp	error Cp	Syltherm viscosity	Total Heat Loss	Total Heat Loss	error Heat Loss	Convective	Total Heat Loss	error Heat Loss	Convective	error Conv	k	h	Nu	error Rad
[lbs/ft^3]	[±%]	[BTU/lb-°F]	[±%]	[centistokes]	[BTU/min]	[Watts]	[±%]	[Watts]	[Watts]	[±%]	[Watts]	[±%]	[W/m-K]	[W/m^2-K]		[±%]
48.32	0.10	0.4580	0.1128	1.0424	117.82	2071.8	5.0	1070.1	2217.2	5.2	1201.8	11.1	0.0072	6.3201	581.4	19.2
48.58	0.10	0.4561	0.1133	1.0908	109.11	1918.6	5.2	916.9	2103.2	5.5	1087.9	11.2	0.0072	5.7208	526.2	heat loss Rad
48.56	0.10	0.4563	0.1132	1.0930	99.49	1749.4	5.7	747.8	1913.0	5.9	897.6	11.4	0.0072	4.7203	434.2	[Watts]
48.44	0.10	0.4571	0.1130	1.0853	82.26	1446.5	6.8	444.9	1560.1	6.9	544.8	12.0	0.0072	2.8647	263.5	415.3
48.23	0.10	0.4586	0.1127	1.0628	66.72	1173.3	8.3	171.6	1240.8	8.4	225.4	12.9	0.0072	1.1854	109.0	
47.99	0.10	0.4602	0.1123	1.0326	57.62	1013.2	9.5	11.5	1044.3	9.6	29.0	13.8	0.0072	0.1523	14.0	
47.84	0.10	0.4612	0.1120	1.0109	56.96	1001.7	9.7	0.0	1015.4	9.8	0.0	13.9	0.0072	0.0000	0.0	
48.05	0.10	0.4598	0.1124	1.0591	33.30	585.6	16.4		600.1	16.5						error Rad
																[±%]
42.06	0.14	0.4980	0.1038	0.4463	239.76	4216.0	2.5	2259.0	4515.5	2.7	2486.1	5.4	0.0072	8.1403	748.8	11.2
42.05	0.14	0.4980	0.1037	0.4481	229.07	4028.0	2.6	2071.1	4312.9	2.8	2283.5	5.4	0.0072	7.4768	687.8	heat loss Rad
41.94	0.14	0.4986	0.1036	0.4486	207.94	3656.4	2.8	1699.4	3892.0	2.9	1862.5	5.5	0.0072	6.0985	561.0	[Watts]
41.76	0.14	0.4997	0.1034	0.4487	173.92	3058.3	3.1	1101.3	3223.2	3.3	1193.8	5.7	0.0072	3.9089	359.6	1188.1
41.55	0.14	0.5009	0.1031	0.4487	137.75	2422.2	3.8	465.3	2528.3	3.9	498.8	6.0	0.0072	1.6333	150.2	
41.41	0.14	0.5017	0.1030	0.4482	116.63	2050.8	4.4	93.9	2128.9	4.4	99.5	6.4	0.0072	0.3256	30.0	
41.37	0.14	0.5020	0.1029	0.4475	111.29	1957.0	4.5	0.0	2029.4	4.6	0.0	6.5	0.0072	0.0000	0.0	
41.01	0.14	0.5040	0.1025	0.4484	47.02	826.7	10.2		841.3	10.2						

APPENDIX 3: LeQuere, Penot and Mirenayat Model Computer Program Listing

```
REM                  ************************************************************
REM
REM            P. LeQuere, F. Penot, & M. Mirenayat
REM                  ************************************************************
REM   The LeQuere, Penot, & Mirenayat model is used here to predict the convective
losses from
REM   a solar cavity receiver operating at various temperatures and receiver angles.
REM                  ************************************************************
     PRINT " P. LeQuere, F. Penot, & M. Mirenayat Model for Predicting Convective Heat
Loss"
     PRINT
     PRINT
REM                  ************************************************************
REM          ******************   Receiver   Geometry   **********************
Re=.127                    :REM   end plate radius [m]
Rc=.33                     :REM   cavity radius [m]
Ro=.45  :REM                                          receiver outside radius [m]
Lf=.292                    :REM   frustum length [m]
Lh=.254                    :REM cylinder length hot [m]
Lc=.14                     :REM cylinder length cold [m]
REM                  ************************************************************
REM          ********************     Constants     ****************************
pi=4*ATN(1)
g=9.810001                 :REM   gravitational acceleration [m/sec^2]
SB=5.6696E-08              :REM   Stefan Boltzmann const. [W/m^2 K^4]
Cp=1006.86                 :REM   specific heat capacity of air at Ta [J/kg K]
Pf=1.19406                 :REM   density of air at Ta [kg/m^3]
e=.9                       :REM   emittance of cavity
ki=.04756                  :REM   insulation conductance [W/m-K] [.33B/h/ft^2/in]
t=.0889                    :REM   thickness of insulation [m] [3.5 in]
Ta=70                      :REM   ambient temperature [F]
Ta=(Ta+459.67)/1.8         :REM   ambient temperature [K]
REM                  ************************************************************
REM     *****************        Angle   constants        ************************
DIM  a(13),b(13)
FOR I=1 TO 13
READ a(I)
DATA  .057,.047,.0545,.0465,.048,.0465,.0925,.0810,.064,.0605,.068  5,.033,0
NEXT I
FOR I=1 TO 13
READ b(I)
DATA  .353,.36,.36,.37,.369,.368,.33,.331,.332,.316,.292,.302,0
NEXT I
REM                  ************************************************************
REM   open clipboard file for transferring data to spread sheet
OPEN "CLIP:" FOR OUTPUT AS #1
100 :
REM          *****************     Print   Constants     **********************
REM
CLS
PRINT "End Plate Radius [m] = ";Re
PRINT "Cavity Radius [m] = ";Rc
PRINT "Frustum Length [m] = ";Lf
```

```
PRINT "Hot Cylindrical Section Length [m] = ";Lh
PRINT "Cold Cylindrical Section Length [m] = ";Lc
PRINT "Ambient Temperature [K] = ";
PRINT  USING"####.#";Ta
PRINT
REM        ***************          Write  to  the  clipboard      *****************
WRITE#1,"","","End Plate Radius [m] = ",Re
WRITE#1,"","", "Cavity Radius [m] = ",Rc
WRITE#1,"","", "Frustum Length [m] = ",Lf
WRITE#1, "","","Hot Cylindrical Section Length [m] = ",Lh
WRITE#1, "","","Cold Cylindrical Section Length [m] = ",Lc
WRITE#1,"","", "Ambient Temperature [K] = ",Ta
WRITE#1,
REM        *****************  Receiver  Aperture  Radius  Loop  *************
  FOR I=1 TO 4
CLS
  READ Ra
    DATA .0762,.1524,.2286,.329
   Da=2*Ra                    :REM   aperture diameter [m]
   Aa=pi*Ra^2                 :REM   aperture area [m^2]
REM                    ****************************************************
REM         *****************  Area   Constants   *************************
REM   In the following section Ah and Ar are calculated.
REM   Ah is the total interior heated cavity surface area based on the tube bundle
geometry.
REM    Ar is the total interior refractory cavity surface.
REM   At is the total cavity area.
      Ah=pi*(Re+Rc)*(Lf^2+(Rc-Re)^2)^.5+2 *pi*Rc*Lh
      Ar=pi*Re^2+pi*(Rc^2-Ra^2)+2*pi*Rc*Lc
   At=Ah+Ar
      Ao=pi*((Rc+Ro)/2)^2+2*pi*((Rc+Ro)/2)+pi*(Rc^2-Ra^2)
REM                    ****************************************************
REM        ***************      Print   Header     ***************************
REM
CLS
    PRINT "Aperture Radius [m] = ";Ra
    PRINT " Total Cavity Area [m^2] = ";
    PRINT  USING  "###.####";At
    PRINT " Total Heated Cavity Area [m^2} = ";
    PRINT  USING  "###.####";Ah
    PRINT " Total Refractory Cavity Area [m^2} = ";
    PRINT  USING  "###.####";Ar
REM       **************    write  header  to  clipboard     *****************
    WRITE#1, "","","Aperture Radius [m] = ",Ra
    WRITE#1, "",""," Total Cavity Area [m^2] = ",At
    WRITE#1, "",""," Total Heated Cavity Area [m^2} = ",Ah
    WRITE#1,"","", " Total Refractory Cavity Area [m^2} = ",Ar
REM       **************    Operating  Temperature  Loop  *****************
REM
  FOR Tmf=300 TO 600 STEP 100
  WRITE#1,
  REM      The operating temperature is converted from F to K
  Tm=(Tmf+459.67)/1.8
  Twf=Tmf-100    :REM  The refractory surfaces are assumed to be 100°F cooler
                 :REM than the heated tube surfaces.
```

```
    Tw=(Twf+459.67)/1.8
  CLS
REM          ***********************************************************
REM       ******************* Print Table Header ********************
    PRINT "T mean [K] = ";
    PRINT USING "####.#";Tm;
    PRINT "    [°F] = ";
    PRINT USING "####.";Tmf
PRINT
PRINT ;TAB(3);" Angle";TAB(12);"Q conv";TAB(24);" Nu ";TAB(35);" Gr"
PRINT ;TAB(1);" [degrees]";TAB(13);"[Watts]"
PRINT
REM          ***********************************************************
REM     ***************** write table header to clipboard *********
      WRITE#1,"", "T mean [K] = ",Tm
      WRITE#1, "","    [°F] = ",Tmf
WRITE#1,
WRITE#1," Angle","Q conv"," Nu "," Gr"
WRITE#1," [degrees]","[Watts]"
WRITE#1,
REM      ******************* Beginning of Angle Loop *****************
n=0
FOR phi=-90 TO 90 STEP 15
   z=pi*phi/180 :REM   convert angle to radian measure
REM       ********************** Angle Function ********************
n=n+1
REM          ***********************************************************
Tcav=(Tm*Ah+Tw*Ar)/At :REM  area average cavity temperature [K]
L=2*Ra
C=1.1547E+19*Ta^-4.4187  :REM  gB/v^2.
k=.0071749261015#+.000064030639041#*Ta
REM      ***************** Heat Loss Calculations ******************
Gr=C*(Tcav-Ta)*L^3      :REM   Grashof number
Pr=.7814008749#-.00037306809395#*Ta+5.2131644352D-07*Ta^2-2.
1272705278D-10*Ta^3
REM   Pr = Prandtl number
Nu=a(n)*Gr^b(n)              :REM   Nusselt number
h=Nu*k/L                         :REM   heat transfer coefficient [W/m^2 K]
REM          ***********************************************************
REM     ***************     heat loss calculations     **********************
Qc=h*At*(Tcav-Ta)   :REM                                         convective
REM      ******************   Output Loop Results ******************
PRINT ;TAB(3);phi;
PRINT TAB(12);
PRINT USING "####.#";Qc;
PRINT TAB(22);
PRINT USING "###.##";Nu;
PRINT TAB(32);
PRINT USING "##.##^^^^";Gr
REM      ****************   write to clipboard   ******************
WRITE#1,phi,Qc,Nu,Gr
REM          ***********************************************************
REM       ******************** End of Angle Loop ******************
NEXT phi
REM          ***********************************************************
```

```
REM        ********************* End of Temperature Loop ***************
  NEXT Tmf
REM        **********************************************************
REM       ********************** End of Aperture Radius Loop **********
  NEXT I
REM        **********************************************************
CLOSE#1
END
```

Appendix 4: LeQuere, Penot and Mirenayat Model Heat Loss Data

Appendix 4 LeQuere, Penot and Mirenayat Model Heat Loss Data

End Plate Radius [m] [0.127]
Cavity Radius [m] [0.133]
Frustum Length [m] [0.292]
Hot Cylindrical Section Length [m] = 0.254
Cold Cylindrical Section Length [m] = [0.1]
Ambient Temperature [K] [294.2611]

Aperture Radius [m] 0.0762 3
Total Cavity Area [m^2] [0.709]
Total Heated Cavity Area [m^2] [0.237]
Total Refractory Cavity Area [m^2] = [0.602]

T mean [K] =	422.0			477.6			533.2			588.7		
[°F] =	300			400			500			600		
Angle [degrees]	Q conv [Watts]	Nu	Gr	Q conv [Watts]	Nu	Gr	Q conv [Watts]	Nu	Gr	Q conv [Watts]	Nu	Gr
-90	939.5	30.5	5.35E+7	1661.0	35.4	8.15E+7	2477.2	39.3	1.10E+8	3371.3	42.5	1.38E+8
-75	877.4	28.5	5.35E+7	1555.8	33.1	8.15E+7	2325.2	36.8	1.10E+8	3169.5	40.0	1.38E+8
-60	1017.4	33.0	5.35E+7	1804.1	38.4	8.15E+7	2696.2	42.7	1.10E+8	3675.3	46.4	1.38E+8
-45	1037.2	33.6	5.35E+7	1846.9	39.3	8.15E+7	2768.3	43.9	1.10E+8	3782.1	47.7	1.38E+8
-30	1051.7	34.1	5.35E+7	1872.0	39.9	8.15E+7	2805.2	44.5	1.10E+8	3831.6	48.3	1.38E+8
-15	1000.9	32.5	5.35E+7	1780.8	37.9	8.15E+7	2667.7	42.3	1.10E+8	3643.0	46.0	1.38E+8
0	1012.5	32.8	5.35E+7	1772.8	37.7	8.15E+7	2626.1	41.6	1.10E+8	3555.3	44.9	1.38E+8
15	902.6	29.3	5.35E+7	1581.0	33.7	8.15E+7	2342.6	37.1	1.10E+8	3172.2	40.0	1.38E+8
30	725.9	23.6	5.35E+7	1272.1	27.1	8.15E+7	1885.5	29.9	1.10E+8	2553.8	32.2	1.38E+8
45	516.2	16.7	5.35E+7	898.5	19.1	8.15E+7	1325.5	21.0	1.10E+8	1788.7	22.6	1.38E+8
60	381.3	12.4	5.35E+7	657.0	14.0	8.15E+7	962.4	15.3	1.10E+8	1291.7	16.3	1.38E+8
75	219.5	7.1	5.35E+7	379.8	8.1	8.15E+7	557.9	8.8	1.10E+8	750.5	9.5	1.38E+8
90	0.0	0.0	5.35E+7	0.0	0.0	8.15E+7	0.0	0.0	1.10E+8	0.0	0.0	1.38E+8

Aperture Radius [ft] [0.1524] 6
Total Cavity Area [m^2] [0.747]
Total Heated Cavity Area [m^2] [0.237]
Total Refractory Cavity Area [m^2] = [0.510]

T mean [K] =	422.0			477.6			533.2			588.7		
[°F] =	300			400			500			600		
Angle [degrees]	Q conv [Watts]	Nu	Gr	Q conv [Watts]	Nu	Gr	Q conv [Watts]	Nu	Gr	Q conv [Watts]	Nu	Gr
-90	960.8	63.7	4.33E+8	1690.5	73.9	6.57E+8	2515.1	81.9	8.81E+8	3418.1	88.8	1.11E+9
-75	910.6	60.4	4.33E+8	1606.8	70.2	6.57E+8	2395.5	78.0	8.81E+8	3260.7	84.7	1.11E+9
-60	1055.9	70.0	4.33E+8	1863.1	81.4	6.57E+8	2777.8	90.5	8.81E+8	3781.0	98.2	1.11E+9
-45	1099.1	72.9	4.33E+8	1947.5	85.1	6.57E+8	2912.1	94.9	8.81E+8	3972.8	103.2	1.11E+9
-30	1112.2	73.8	4.33E+8	1969.9	86.1	6.57E+8	2944.8	95.9	8.81E+8	4016.5	104.3	1.11E+9
-15	1056.3	70.1	4.33E+8	1870.0	81.7	6.57E+8	2794.6	91.0	8.81E+8	3810.8	99.0	1.11E+9
0	986.9	65.5	4.33E+8	1719.8	75.1	6.57E+8	2541.5	82.8	8.81E+8	3436.0	89.2	1.11E+9
15	881.6	58.5	4.33E+8	1536.8	67.2	6.57E+8	2271.9	74.0	8.81E+8	3072.1	79.8	1.11E+9
30	710.6	47.1	4.33E+8	1239.2	54.1	6.57E+8	1832.4	59.7	8.81E+8	2478.4	64.4	1.11E+9
45	488.6	32.4	4.33E+8	846.5	37.0	6.57E+8	1245.9	40.6	8.81E+8	1679.0	43.6	1.11E+9
60	343.3	22.8	4.33E+8	588.8	25.7	6.57E+8	860.5	28.0	8.81E+8	1153.3	29.9	1.11E+9
75	201.8	13.4	4.33E+8	347.5	15.2	6.57E+8	509.3	16.6	8.81E+8	684.2	17.8	1.11E+9
90	0.0	0.0	4.33E+8	0.0	0.0	6.57E+8	0.0	0.0	8.81E+8	0.0	0.0	1.11E+9

Appendix 4: LeQuere, Penot and Mirenayat Model Heat Loss Data

Aperture Radius [m] = 0.2286 9
Total Cavity Area [m^2] = 1.556
Total Heated Cavity Area [m^2] = 1.037
Total Refractory Cavity Area [m^2] = 0.519

T mean [K] =	422.0			477.6			533.2			588.7		
[°F] =	300			400			500			600		
Angle [degrees]	Q conv [Watts]	Nu	Gr	Q conv [Watts]	Nu	Gr	Q conv [Watts]	Nu	Gr	Q conv [Watts]	Nu	Gr
-90	953.8	98.6	1.49E+9	1663.5	114.0	2.24E+9	2464.4	126.3	3.00E+9	3340.5	136.7	3.76E+9
-75	911.7	94.2	1.49E+9	1594.8	109.3	2.24E+9	2367.4	121.3	3.00E+9	3214.1	131.5	3.76E+9
-60	1057.2	109.3	1.49E+9	1849.2	126.7	2.24E+9	2745.2	140.7	3.00E+9	3727.0	152.5	3.76E+9
-45	1114.2	115.2	1.49E+9	1956.9	134.1	2.24E+9	2913.4	149.3	3.00E+9	3964.3	162.3	3.76E+9
-30	1126.1	116.4	1.49E+9	1977.0	135.5	2.24E+9	2942.5	150.8	3.00E+9	4003.0	163.8	3.76E+9
-15	1068.1	110.4	1.49E+9	1874.4	128.4	2.24E+9	2789.0	142.9	3.00E+9	3793.3	155.3	3.76E+9
0	952.2	98.4	1.49E+9	1645.1	112.7	2.24E+9	2421.0	124.1	3.00E+9	3264.8	133.6	3.76E+9
15	851.6	88.0	1.49E+9	1472.0	100.9	2.24E+9	2166.8	111.0	3.00E+9	2922.7	119.6	3.76E+9
30	687.3	71.0	1.49E+9	1188.3	81.4	2.24E+9	1749.8	89.7	3.00E+9	2360.7	96.6	3.76E+9
45	463.4	47.9	1.49E+9	796.0	54.5	2.24E+9	1166.6	59.8	3.00E+9	1568.3	64.2	3.76E+9
60	316.0	32.7	1.49E+9	537.5	36.8	2.24E+9	782.4	40.1	3.00E+9	1046.1	42.8	3.76E+9
75	188.0	19.4	1.49E+9	321.2	22.0	2.24E+9	468.8	24.0	3.00E+9	628.3	25.7	3.76E+9
90	0.0	0.0	1.49E+9	0.0	0.0	2.24E+9	0.0	0.0	3.00E+9	0.0	0.0	3.76E+9

Aperture Radius [m]/[in] = 0.329 13
Total Cavity Area [m^2] = 1.380
Total Heated Cavity Area [m^2] = 1.037
Total Refractory Cavity Area [m^2] = 0.343

T mean [K] =	422.0			477.6			422.0			588.7		
[°F] =	300			400			300			600		
Angle [degrees]	Q conv [Watts]	Nu	Gr	Q conv [Watts]	Nu	Gr	Q conv [Watts]	Nu	Gr	Q conv [Watts]	Nu	Gr
-90	915.2	147.1	4.63E+9	1566.2	169.3	6.88E+9	2298.3	187.1	9.14E+09	3097.6	202.3	1.14E+10
-75	881.9	141.8	4.63E+9	1513.3	163.6	6.88E+9	2225.1	181.1	9.14E+09	3003.6	196.1	1.14E+10
-60	1022.6	164.4	4.63E+9	1754.8	189.7	6.88E+9	2580.2	210.0	9.14E+09	3482.9	227.4	1.14E+10
-45	1090.0	175.2	4.63E+9	1877.9	203.0	6.88E+9	2768.9	225.4	9.14E+09	3746.0	244.6	1.14E+10
-30	1100.4	176.9	4.63E+9	1895.0	204.8	6.88E+9	2793.4	227.4	9.14E+09	3778.3	246.7	1.14E+10
-15	1042.5	167.6	4.63E+9	1794.7	194.0	6.88E+9	2644.8	215.3	9.14E+09	3576.5	233.5	1.14E+10
0	890.2	143.1	4.63E+9	1509.5	163.2	6.88E+9	2200.7	179.2	9.14E+09	2951.1	192.7	1.14E+10
15	797.1	128.1	4.63E+9	1352.1	146.1	6.88E+9	1971.8	160.5	9.14E+09	2644.8	172.7	1.14E+10
30	644.0	103.5	4.63E+9	1092.8	118.1	6.88E+9	1594.1	129.8	9.14E+09	2138.6	139.6	1.14E+10
45	426.4	68.5	4.63E+9	719.0	77.7	6.88E+9	1044.1	85.0	9.14E+09	1395.7	91.1	1.14E+10
60	283.0	45.5	4.63E+9	472.7	51.1	6.88E+9	681.7	55.5	9.14E+09	906.5	59.2	1.14E+10
75	170.3	27.4	4.63E+9	285.6	30.9	6.88E+9	413.1	33.6	9.14E+09	550.5	35.9	1.14E+10
90	0.0	0.0	4.63E+9	0.0	0.0	6.88E+9	0.0	0.0	9.14E+09	0.0	0.0	1.14E+10

APPENDIX 5: Koenig and Marvin Model Computer Program Listing

```
REM              *********************************************************
REM
REM                         Koenig and Marvin Model
REM              *********************************************************
REM   The Koenig and Marvin method is used here to predict the convective losses from
REM    a cavity solar receiver operating at various temperatures and receiver angles.
REM              *********************************************************
    PRINT " Koenig and Marvin Model for Predicting Convective Heat Loss"
    PRINT
    PRINT
REM              *********************************************************
REM          *******************  Receiver  Geometry  **********************
Re=.127                  :REM   end plate radius [m]
Rc=.33                   :REM   cavity radius [m]
Ro=.45  :REM                                    receiver outside radius [m]
Lf=.292                  :REM   frustum length [m]
Lh=.254                  :REM cylinder length hot [m]
Lc=.14                   :REM cylinder length cold [m]
REM              *********************************************************
REM          *******************     Constants      ***************************
pi=4*ATN(1)
g=9.810001               :REM   gravitational acceleration [m/sec^2]
SB=5.6696E-08            :REM   Stefan Boltzmann const. [W/m^2 K^4]
Cp=1006.86               :REM   specific heat capacity of air at Ta [J/kg K]
Pf=1.19406               :REM   density of air at Ta [kg/m^3]
e=.9                     :REM   emittance of cavity
ki=.04756                :REM    insulation conductance [W/m-K] [.33B/h/ft^2/in]
t=.0889                  :REM   thickness of insulation [m] [3.5 in]
Ta=70                    :REM   ambient temperature [F]
Ta=(Ta+459.67)/1.8       :REM   ambient temperature [K]
REM              *********************************************************
REM   open clipboard file for transferring data to spread sheet
OPEN "CLIP:" FOR OUTPUT AS #1
100 :
REM         *****************    Print  Constants     **********************
REM
CLS
PRINT "End Plate Radius [m] = ";Re
PRINT "Cavity Radius [m] = ";Rc
PRINT "Frustum Length [m] = ";Lf
PRINT "Hot Cylindrical Section Length [m] = ";Lh
PRINT "Cold Cylindrical Section Length [m] = ";Lc
PRINT "Ambient Temperature [K] = ";
PRINT  USING"####.#";Ta
PRINT
REM       ***************         Write  to  the  clipboard     *****************
WRITE#1,"","","End Plate Radius [m] = ",Re
WRITE#1,"","", "Cavity Radius [m] = ",Rc
WRITE#1,"","", "Frustum Length [m] = ",Lf
WRITE#1, "","","Hot Cylindrical Section Length [m] = ",Lh
WRITE#1, "","","Cold Cylindrical Section Length [m] = ",Lc
WRITE#1,"","", "Ambient Temperature [K] = ",Ta
WRITE#1,
```

```
REM      *****************  Receiver  Aperture  Radius  Loop  *************
  FOR I=1 TO 4
CLS
  READ Ra
  DATA  .0762,.1524,.2286,.329
  Da=2*Ra                    :REM   aperture diameter [m]
  Aa=pi*Ra^2                 :REM   aperture area [m^2]
REM                  *********************************************************
REM        *****************  Area  Constants  ************************
REM   In the following section Ah and Ar are calculated.
REM   Ah is the total interior heated cavity surface area based on the tube bundle
geometry.
REM    Ar is the total interior refractory cavity surface.
REM   At is the total cavity area.
  Ah=pi*(Re+Rc)*(Lf^2+(Rc-Re)^2)^.5+2  *pi*Rc*Lh
  Ar=pi*Re^2+pi*(Rc^2-Ra^2)+2*pi*Rc*Lc
  At=Ah+Ar
  Ao=pi*((Rc+Ro)/2)^2+2*pi*((Rc+Ro)/2)+pi*(Rc^2-Ra^2)
REM                  *********************************************************
REM        ****************     Print  Header     ***************************
REM
CLS
    PRINT "Aperture Radius [m] = ";Ra
    PRINT " Total Cavity Area [m^2] = ";
    PRINT  USING  "###.####";At
    PRINT " Total Heated Cavity Area [m^2} = ";
    PRINT  USING  "###.####";Ah
    PRINT " Total Refractory Cavity Area [m^2} = ";
    PRINT  USING  "###.####";Ar
REM        **************    write  header  to  clipboard    ******************
    WRITE#1, "","","Aperture Radius [m] = ",Ra
    WRITE#1, "",""," Total Cavity Area [m^2] = ",At
    WRITE#1, "",""," Total Heated Cavity Area [m^2} = ",Ah
    WRITE#1,"","", " Total Refractory Cavity Area [m^2} = ",Ar
REM        **************    Operating  Temperature  Loop  *****************
REM
  FOR Tmf=300 TO 600 STEP 100
  WRITE#1,
  REM      The operating temperature is converted from F to K
  Tm=(Tmf+459.67)/1.8
  Twf=Tmf-100    :REM  The refractory surfaces are assumed to be 100°F cooler
                  :REM than the heated tube surfaces.
  Tw=(Twf+459.67)/1.8
  CLS
REM                  *********************************************************
REM        *******************  Print  Table  Header  *******************
    PRINT "T mean [K] = ";
    PRINT  USING  "####.#";Tm;
    PRINT "    [°F] = ";
    PRINT  USING  "####.";Tmf
PRINT
PRINT  ;TAB(3);" Angle";TAB(12);"Q  conv";TAB(24);"Q  total";TAB(34);"% Conv";
PRINT  TAB(45);" Nu  ";TAB(56);"
Gr";TAB(66);"P(ø)";TAB(76);"k";TAB(86);"gB/v^2";TAB(96);"Pr
";TAB(106);"Tp"
```

```
PRINT  ;TAB(1);"  [degrees]";TAB(13);"[Watts]";TAB(24);"[Watts]";TAB(36);"%"
PRINT
REM                    *******************************************************
REM      *****************   write  table  header  to  clipboard     *********
      WRITE#1,"", "T mean [K] = ",Tm
      WRITE#1, "","    [°F] = ",Tmf
WRITE#1,
WRITE#1," Angle","Q conv","Q total","% Conv"," Nu "," Gr","P(ø)"
WRITE#1,"  [degrees]","[Watts]","[Watts]","%","","",""
WRITE#1,
REM       ******************  Beginning  of  Angle  Loop  *****************
FOR a=0 TO 90 STEP 15
   z=pi*a/180 :REM   convert angle to radian measure
REM        **********************   Angle   Function   *******************
IF a>45 THEN 121
P=(COS(z))^3.2
GOTO 124
121 :
IF a=90 THEN 122
P=.707*(COS(z))^2.2
GOTO 124
122 :
P=0
124 :
REM                    *******************************************************
Tcav=(Tm*Ah+Tw*Ar)/At :REM  area average cavity temperature [K]
Lcc=Ra/Rc
L=2^.5*Rc
Tp=(11*Tcav+3*Ta)/16 :REM  air properties temperature [K]
C=1.1547E+19*Tp^-4.4187  :REM  gB/v^2.
k=.0071749261015#+.000064030639041#*Tp
REM       *****************  Heat  Loss  Calculations  *******************
Gr=C*(Tcav-Ta)*L^3       :REM   Grashof number
Pr=.7814008749#-.00037306809395#*Tp+5.2131644352D-07*Tp^2-2.
1272705278D-10*Tp^3
REM   Pr = Prandtl number
C1=.52
a1=1.75
Nu=C1*P*Lcc^a1*(Gr*Pr)^.25                  :REM   Nusselt number
h=Nu*k/L                             :REM   heat transfer coefficient [W/m^2 K]
REM                    ******************************************************
REM     ***************    heat  loss  calculations     **********************
Qr=pi*Ra^2*e*SB*(Tcav^4-Ta^4)  :REM                               radiative
Qc=h*At*(Tcav-Ta)    :REM                                        convective
Qk=ki*Ao*(Tcav-Ta)/t    :REM                                     conductive
Qt=Qr+Qc+Qk
PQc=Qc/Qt*100
REM       ******************    Output  Loop  Results  ******************
PRINT ;TAB(3);a;
PRINT  TAB(12);
PRINT  USING  "####.#";Qc;
PRINT;TAB(24);
PRINT  USING  "####.#";Qt;
PRINT  TAB(34);
PRINT  USING "##.#";PQc;
```

```
PRINT TAB(44);
PRINT USING "###.##";Nu;
PRINT TAB(54);
PRINT USING "##.##^^^^";Gr;
PRINT TAB(64);
PRINT USING "#.####";P;
PRINT TAB(74);
PRINT USING "#.####";k;
PRINT TAB(84);
PRINT USING "###.##^^^^";C;
PRINT TAB(94);
PRINT USING "#.####";Pr;
PRINT TAB(104);
PRINT USING "####.#";Tp
REM        ****************   write to clipboard   ********************
WRITE#1,a,Qc,Qt,PQc,Nu,Gr,P
REM                  **************************************************
REM        ********************  End of Angle Loop  ********************
NEXT a
REM                  **************************************************
REM        ******************** Output Radiation & Conduction **********
PRINT"Radiation (Watts) = ";Qr
PRINT"Conduction (Watts) = ";Qk
REM        ****************** Write radiation & conduction to clipboard **
WRITE#1,"","","Radiation (Watts) = ",Qr
WRITE#1,"","","Conduction (Watts) = ",Qk
REM                  **************************************************
REM        ******************** End of Temperature Loop **************
  NEXT Tmf
REM                  **************************************************
REM        ******************** End of Aperture Radius Loop **********
  NEXT I
REM                  **************************************************
CLOSE#1
END
```

Appendix 6: Koenig and Marvin Model Heat Loss

Appendix 6 Koenig and Marvin Heat Loss Data						
		End Plate Radius [m] =	0.127			
		Cavity Radius [m] =	0.33			
		Frustum Length [m] =	0.292			
		Hot Cylindrical Section Length [m] =	0.254			
		Cold Cylindrical Section Length [m] =	0.14			
		Ambient Temperature [K] =	294.3			
		Aperture Radius [m] =	0.0762			
		Total Cavity Area [m^2] =	1.7021			
		Total Heated Cavity Area [m^2] =	1.0372			
		Total Refractory Cavity Area [m^2] =	0.6648			
	T mean [K] =	422.0				
	[°F] =	300				
Angle	Q conv	Q total	% Conv	Nu	Gr	P(ø)
[degrees]	[Watts]	[Watts]	%			
0	70.0	271.3	25.8	6.39	9.21E+8	1
15	62.7	264.2	23.7	5.72	9.21E+8	0.8949939
30	44.2	245.7	18.0	4.03	9.21E+8	0.6310997
45	23.1	224.6	10.3	2.11	9.21E+8	0.3298769
60	10.8	212.3	5.1	0.98	9.21E+8	0.1538698
75	2.5	204.0	1.2	0.23	9.21E+8	3.61E-02
90	0.0	201.5	0.0	0.00	9.21E+8	0
		Radiation (Watts) =	16.9			
		Conduction (Watts) =	184.6			
	T mean [K] =	477.6				
	[°F] =	400				
Angle	Q conv	Q total	% Conv	Nu	Gr	P(ø)
[degrees]	[Watts]	[Watts]	%			
0	114.0	428.5	26.6	6.28	8.65E+8	1
15	102.0	416.5	24.5	5.62	8.65E+8	0.8949939
30	72.0	386.4	18.6	3.97	8.65E+8	0.6310997
45	37.6	352.1	10.7	2.07	8.65E+8	0.3298769
60	17.5	332.0	5.3	0.97	8.65E+8	0.1538698
75	4.1	318.6	1.3	0.23	8.65E+8	3.61E-02
90	0.0	314.4	0.0	0.00	8.65E+8	0
		Radiation (Watts) =	33.2			
		Conduction (Watts) =	281.2			
	T mean [K] =	533.2				
	[°F] =	500				
Angle	Q conv	Q total	% Conv	Nu	Gr	P(ø)
[degrees]	[Watts]	[Watts]	%			
0	159.5	594.1	26.9	6.06	7.52E+8	1
15	142.8	577.4	24.7	5.43	7.52E+8	0.8949939
30	100.7	535.3	18.8	3.83	7.52E+8	0.6310997
45	52.6	487.2	10.8	2.00	7.52E+8	0.3298769
60	24.5	459.1	5.3	0.93	7.52E+8	0.1538698
75	5.8	440.4	1.3	0.22	7.52E+8	3.61E-02
90	0.0	434.6	0.0	0.00	7.52E+8	0
		Radiation (Watts) =	56.7			
		Conduction (Watts) =	377.9			
	T mean [K] =	588.7				
	[°F] =	600				
Angle	Q conv	Q total	% Conv	Nu	Gr	P(ø)
[degrees]	[Watts]	[Watts]	%			
0	206.1	769.8	26.8	5.81	6.35E+8	1
15	184.4	748.2	24.7	5.20	6.35E+8	0.8949939
30	130.1	693.8	18.7	3.67	6.35E+8	0.6310997
45	68.0	631.7	10.8	1.92	6.35E+8	0.3298769
60	31.7	595.5	5.3	0.89	6.35E+8	0.1538698
75	7.4	571.2	1.3	0.21	6.35E+8	3.61E-02
90	0.0	563.8	0.0	0.00	6.35E+8	0
		Radiation (Watts) =	89.2			
		Conduction (Watts) =	474.5			

Appendix 6: Koenig and Marvin Model Heat Loss

	Aperture Radius [m] = 0.1524					
	Total Cavity Area [m^2] = 1.6473					
	Total Heated Cavity Area [m^2] = 1.0372					
	Total Refractory Cavity Area [m^2] = 0.6101					
	T mean [K] = 422.0					
	[°F] = 300					
Angle	Q conv	Q total	% Conv	Nu	Gr	P(ɸ)
[degrees]	[Watts]	[Watts]	%			
0	230.8	483.0	47.8	21.49	9.21E+8	1
15	206.6	458.8	45.0	19.24	9.21E+8	0.8949939
30	145.7	397.9	36.6	13.56	9.21E+8	0.6310997
45	76.1	328.3	23.2	7.09	9.21E+8	0.3298769
60	35.5	287.7	12.3	3.31	9.21E+8	0.1538698
75	8.3	260.6	3.2	0.78	9.21E+8	3.61E-02
90	0.0	252.2	0.0	0.00	9.21E+8	0
	Radiation (Watts) = 68.8					
	Conduction (Watts) = 183.4					
	T mean [K] = 477.6					
	[°F] = 400					
Angle	Q conv	Q total	% Conv	Nu	Gr	P(ɸ)
[degrees]	[Watts]	[Watts]	%			
0	374.1	787.0	47.5	21.12	8.63E+8	1
15	334.8	747.7	44.8	18.91	8.63E+8	0.8949939
30	236.1	649.0	36.4	13.33	8.63E+8	0.6310997
45	123.4	536.3	23.0	6.97	8.63E+8	0.3298769
60	57.6	470.5	12.2	3.25	8.63E+8	0.1538698
75	13.5	426.4	3.2	0.76	8.63E+8	3.61E-02
90	0.0	412.9	0.0	0.00	8.63E+8	0
	Radiation (Watts) = 134.5					
	Conduction (Watts) = 278.4					
	T mean [K] = 533.2					
	[°F] = 500					
Angle	Q conv	Q total	% Conv	Nu	Gr	P(ɸ)
[degrees]	[Watts]	[Watts]	%			
0	522.4	1124.9	46.4	20.37	7.50E+8	1
15	467.5	1070.1	43.7	18.23	7.50E+8	0.8949939
30	329.7	932.2	35.4	12.86	7.50E+8	0.6310997
45	172.3	774.9	22.2	6.72	7.50E+8	0.3298769
60	80.4	682.9	11.8	3.13	7.50E+8	0.1538698
75	18.9	621.4	3.0	0.74	7.50E+8	3.61E-02
90	0.0	602.6	0.0	0.00	7.50E+8	0
	Radiation (Watts) = 229.1					
	Conduction (Watts) = 373.4					
	T mean [K] = 588.7					
	[°F] = 600					
Angle	Q conv	Q total	% Conv	Nu	Gr	P(ɸ)
[degrees]	[Watts]	[Watts]	%			
0	674.0	1502.4	44.9	19.52	6.33E+8	1
15	603.2	1431.6	42.1	17.47	6.33E+8	0.8949939
30	425.3	1253.8	33.9	12.32	6.33E+8	0.6310997
45	222.3	1050.8	21.2	6.44	6.33E+8	0.3298769
60	103.7	932.1	11.1	3.00	6.33E+8	0.1538698
75	24.4	852.8	2.9	0.71	6.33E+8	3.61E-02
90	0.0	828.4	0.0	0.00	6.33E+8	0
	Radiation (Watts) = 360.0					
	Conduction (Watts) = 468.5					

Appendix 6: Koenig and Marvin Model Heat Loss

	Aperture Radius [m] =		0.2286			
	Total Cavity Area [m^2] =		1.5561			
	Total Heated Cavity Area [m^2] =		1.0372			
	Total Refractory Cavity Area [m^2] =		0.5189			
	T mean [K] =	422.0				
	[°F] =	300				
Angle [degrees]	Q conv [Watts]	Q total [Watts]	% Conv %	Nu	Gr	P(φ)
0	453.2	794.1	57.1	43.70	9.21E+8	1
15	405.6	746.5	54.3	39.11	9.21E+8	0.8949939
30	286.0	626.9	45.6	27.58	9.21E+8	0.6310997
45	149.5	490.3	30.5	14.42	9.21E+8	0.3298769
60	69.7	410.6	17.0	6.72	9.21E+8	0.1538698
75	16.4	357.2	4.6	1.58	9.21E+8	3.61E-02
90	0.0	340.8	0.0	0.00	9.21E+8	0
	Radiation (Watts) =		159.3			
	Conduction (Watts) =		181.6			
	T mean [K] =	477.6				
	[°F] =	400				
Angle [degrees]	Q conv [Watts]	Q total [Watts]	% Conv %	Nu	Gr	P(φ)
0	728.9	1312.0	55.6	42.90	8.60E+8	1
15	652.3	1235.4	52.8	38.40	8.60E+8	0.8949939
30	460.0	1043.1	44.1	27.07	8.60E+8	0.6310997
45	240.4	823.6	29.2	14.15	8.60E+8	0.3298769
60	112.1	695.3	16.1	6.60	8.60E+8	0.1538698
75	26.3	609.5	4.3	1.55	8.60E+8	3.61E-02
90	0.0	583.1	0.0	0.00	8.60E+8	0
	Radiation (Watts) =		309.2			
	Conduction (Watts) =		273.9			
	T mean [K] =	533.2				
	[°F] =	500				
Angle [degrees]	Q conv [Watts]	Q total [Watts]	% Conv %	Nu	Gr	P(φ)
0	1013.9	1904.9	53.2	41.36	7.45E+8	1
15	907.4	1798.4	50.5	37.02	7.45E+8	0.8949939
30	639.9	1530.8	41.8	26.10	7.45E+8	0.6310997
45	334.5	1225.4	27.3	13.64	7.45E+8	0.3298769
60	156.0	1047.0	14.9	6.36	7.45E+8	0.1538698
75	36.6	927.6	4.0	1.49	7.45E+8	3.61E-02
90	0.0	891.0	0.0	0.00	7.45E+8	0
	Radiation (Watts) =		524.8			
	Conduction (Watts) =		366.2			
	T mean [K] =	588.7				
	[°F] =	600				
Angle [degrees]	Q conv [Watts]	Q total [Watts]	% Conv %	Nu	Gr	P(φ)
0	1305.2	2586.3	50.5	39.62	6.29E+8	1
15	1168.2	2449.3	47.7	35.46	6.29E+8	0.8949939
30	823.7	2104.8	39.1	25.00	6.29E+8	0.6310997
45	430.6	1711.7	25.2	13.07	6.29E+8	0.3298769
60	200.8	1482.0	13.6	6.10	6.29E+8	0.1538698
75	47.2	1328.3	3.6	1.43	6.29E+8	3.61E-02
90	0.0	1281.1	0.0	0.00	6.29E+8	0
	Radiation (Watts) =		822.6			
	Conduction (Watts) =		458.5			

Appendix 6: Koenig and Marvin Model Heat Loss

		Aperture Radius [m] =	0.329			
		Total Cavity Area [m^2] =	1.3803			
		Total Heated Cavity Area [m^2] =	1.0372			
		Total Refractory Cavity Area [m^2] =	0.3430			
	T meap [K] =	422.0				
	[°F] =	300				
Angle	Q conv	Q total	% Conv	Nu	Gr	P(ø)
[degrees]	[Watts]	[Watts]	%			
0	798.6	1329.1	60.1	82.62	9.21E+8	1
15	714.8	1245.3	57.4	73.94	9.21E+8	0.8949939
30	504.0	1034.5	48.7	52.14	9.21E+8	0.6310997
45	263.5	793.9	33.2	27.25	9.21E+8	0.3298769
60	122.9	653.4	18.8	12.71	9.21E+8	0.1538698
75	28.9	559.3	5.2	2.99	9.21E+8	3.61E-02
90	0.0	530.5	0.0	0.00	9.21E+8	0
		Radiation (Watts) =	351.8			
		Conduction (Watts) =	178.7			
	T mean [K] =	477.6				
	[°F] =	400				
Angle	Q conv	Q total	% Conv	Nu	Gr	P(ø)
[degrees]	[Watts]	[Watts]	%			
0	1262.6	2201.1	57.4	80.91	8.51E+8	1
15	1130.1	2068.5	54.6	72.42	8.51E+8	0.8949939
30	796.9	1735.3	45.9	51.06	8.51E+8	0.6310997
45	416.5	1355.0	30.7	26.69	8.51E+8	0.3298769
60	194.3	1132.8	17.2	12.45	8.51E+8	0.1538698
75	45.6	984.1	4.6	2.92	8.51E+8	3.61E-02
90	0.0	938.5	0.0	0.00	8.51E+8	0
		Radiation (Watts) =	672.7			
		Conduction (Watts) =	265.8			
	T mean [K] =	533.2				
	[°F] =	500				
Angle	Q conv	Q total	% Conv	Nu	Gr	P(ø)
[degrees]	[Watts]	[Watts]	%			
0	1741.8	3226.8	54.0	77.94	7.35E+8	1
15	1558.9	3043.9	51.2	69.76	7.35E+8	0.8949939
30	1099.3	2584.3	42.5	49.19	7.35E+8	0.6310997
45	574.6	2059.6	27.9	25.71	7.35E+8	0.3298769
60	268.0	1753.0	15.3	11.99	7.35E+8	0.1538698
75	63.0	1548.0	4.1	2.82	7.35E+8	3.61E-02
90	0.0	1485.0	0.0	0.00	7.35E+8	0
		Radiation (Watts) =	1132.2			
		Conduction (Watts) =	352.9			
	T mean [K] =	588.7				
	[°F] =	600				
Angle	Q conv	Q total	% Conv	Nu	Gr	P(ø)
[degrees]	[Watts]	[Watts]	%			
0	2231.2	4436.4	50.3	74.64	6.20E+8	1
15	1996.9	4202.1	47.5	66.80	6.20E+8	0.8949939
30	1408.1	3613.4	39.0	47.10	6.20E+8	0.6310997
45	736.0	2941.3	25.0	24.62	6.20E+8	0.3298769
60	343.3	2548.6	13.5	11.48	6.20E+8	0.1538698
75	80.6	2285.9	3.5	2.70	6.20E+8	3.61E-02
90	0.0	2205.3	0.0	0.00	6.20E+8	0
		Radiation (Watts) =	1765.3			
		Conduction (Watts) =	440.0			

Appendix 7: Zone and Shear Plane Area Formulas

1. Zone Area Formulas

The receiver cavity is divided into two zones (Fig. 23). The boundary between the zones is formed by a horizontal plane cutting through the cavity at the upper lip of the aperture. The upper zone is assumed stagnate while the lower zone has active convective currents. Zone 1 area represents the internal surface area of the receiver above the horizontal plane. The zone 2 area represents the internal surface area of the receiver below the horizontal plane. The zone 1 and zone 2 areas vary with receiver angle for a given receiver geometry. The following formulas describe the zone 1 and zone 2 surface areas of the receiver cavity

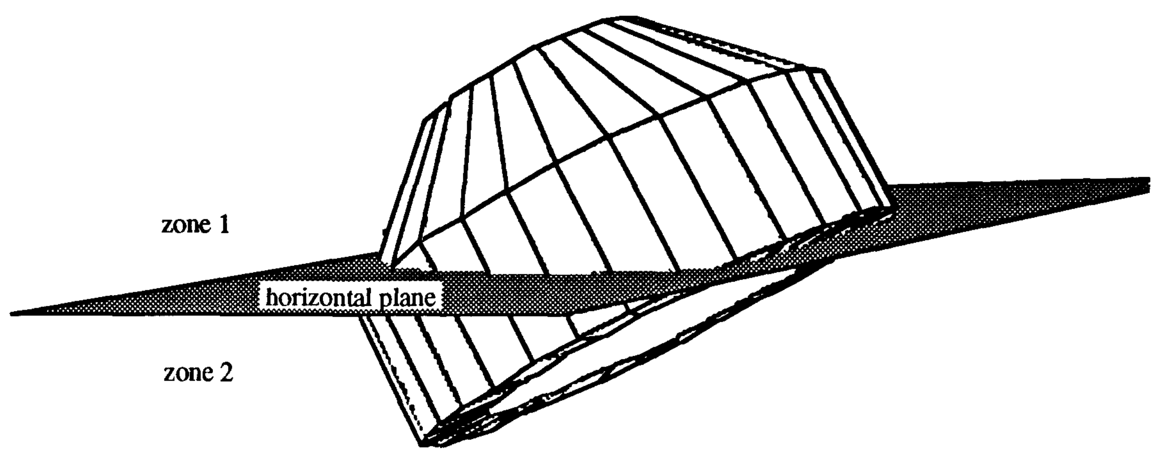

Figure 23. Cavity zones areas.

The receiver internal geometry is divided into five sections representing the hot and cold surfaces in the receiver (Fig. 24). The hot surfaces are actively heated. The cold surfaces represent the refractory surfaces . Section 1 is the circular plate at the end of the frustum. Section 2 is the frustum portion of the tube bundle. Section 3 is the cylindrical portion of the tube bundle. Section 4 is the short refractory portion of the cylindrical section. Section 5 is the refractory ring that forms the aperture.

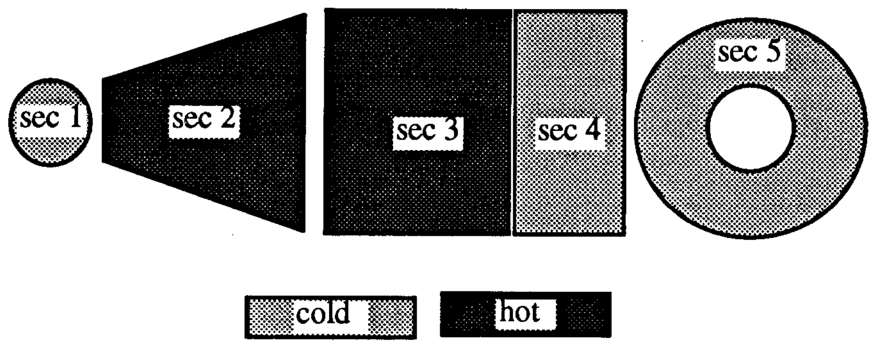

Figure 24. Cavity sections.

As the receiver is rotated through various angles, each section of the internal receiver geometry may be divided by the horizontal plane that cuts through the upper inside edge of section 5. The critical angles represent limits for the various algebraic expression of the zone areas (Fig. 69). The following formulas define the portion of the area of each section that is in zone 1 for a given receiver angle range. The remaining surface area of each section in zone 2 is determined by subtracting the zone 1 area from the total surface area for that section.

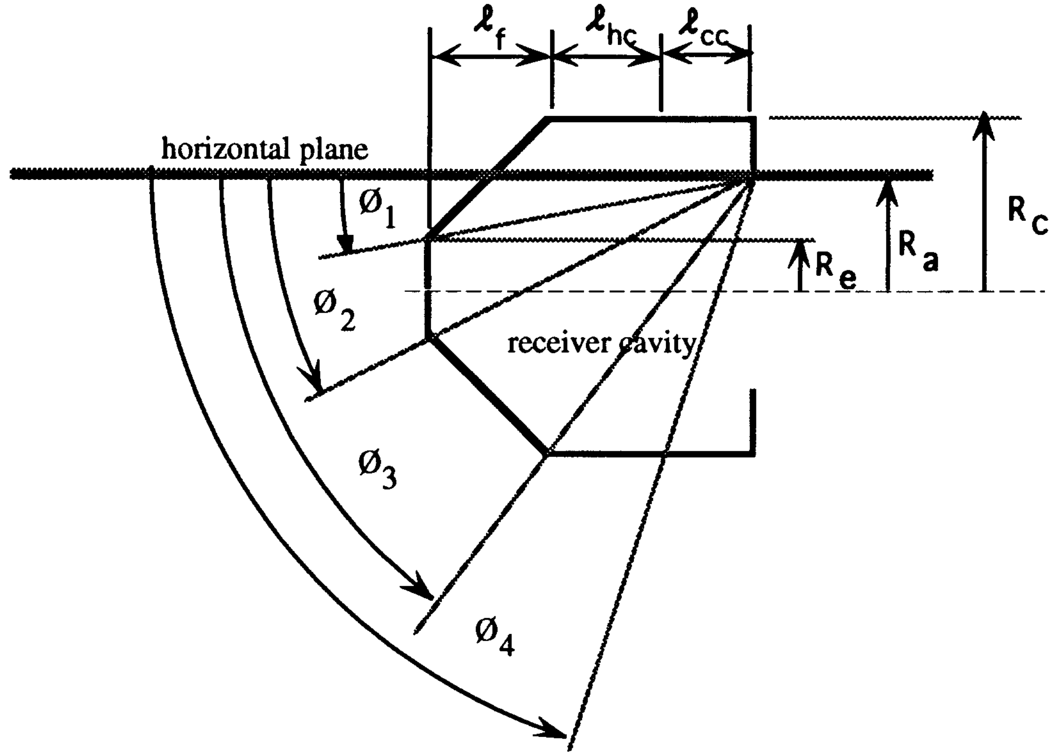

Figure 69. Critical angles.

where:

$$Ø_1 = \tan^{-1} \left[\frac{R_a - R_e}{\ell_{cc} + \ell_{hc} + \ell_f}\right] \tag{115}$$

$$Ø_2 = \tan^{-1} \left[\frac{R_a + R_e}{\ell_{cc} + \ell_{hc} + \ell_f}\right] \tag{116}$$

$$Ø_3 = \tan^{-1} \left[\frac{R_a + R_c}{\ell_{cc} + \ell_{hc}}\right] \tag{117}$$

$$Ø_4 = \tan^{-1} \left[\frac{R_a + R_c}{\ell_{cc}}\right] \tag{118}$$

where:

R_e = radius of the end plate

(a) section 1

Range $0 \le \varnothing \le \varnothing_1$

$$\text{Area} = 0$$

Range $\varnothing_1 \le \varnothing \le \varnothing_2$

$$\text{Area} = R_e^2 \cos^{-1}\left[\frac{R_a - (\ell_{cc} + \ell_{hc} + \ell_f)\tan\varnothing}{R_e}\right] + \left[(\ell_{cc} + \ell_{hc} + \ell_f)\tan\varnothing - R_a\right]$$

$$\left\{2R_e\left[(\ell_{cc} + \ell_{hc} + \ell_f)\tan\varnothing - R_a + R_e\right] - \left[(\ell_{cc} + \ell_{hc} + \ell_f)\tan\varnothing - R_a + R_e\right]^2\right\}^{1/2} \quad (119)$$

Range $\varnothing_2 \le \varnothing \le \frac{\pi}{2}$

$$\text{Area} = \pi R_e^2 \quad (120)$$

(b) section 2

Range $0 \le \varnothing\ \varnothing_1$

$$\text{Area} = \left\{\frac{\left[\left(\frac{R_c - R_e}{\ell_f}\right)(R_c - R_a) + (\ell_{cc} + \ell_{hc})\right]\sin\varnothing}{\sin\left[\frac{\pi}{2} - \varnothing - \tan^{-1}\left(\frac{R_c - R_e}{\ell_f}\right)\right]} + \frac{(R_c - R_a)}{\sin\left[\tan^{-1}\left(\frac{R_c - R_e}{\ell_f}\right)\right]}\right\}$$

$$R_c \cos^{-1}\left[\frac{R_a - (\ell_{cc} + \ell_{hc}) \tan \varnothing}{R_c}\right] \tag{121}$$

Range $\varnothing_1 \leq \varnothing \leq \varnothing_2$

$$\text{Area} = \sqrt{\ell_f^2 + (R_c - R_e)^2}\left\{R_e \cos^{-1}\left[\frac{R_a - (\ell_{cc} + \ell_{hc} + \ell_f) \tan \varnothing}{R_e}\right]\right.$$

$$\left. + R_c \cos^{-1}\left[\frac{R_a - (\ell_{cc} + \ell_{hc}) \tan \varnothing}{R_c}\right]\right\} \tag{122}$$

Range $\varnothing_2 \leq \varnothing \leq \varnothing_3$

$$\text{Area} = \left\{\pi R_e + \pi\left\{R_e + a \sin\left[\tan^{-1}\left(\frac{R_c - R_e}{\ell_f}\right)\right]\right\}\right\} a$$

$$+ \left\{R_c \cos^{-1}\left[\frac{R_a - (\ell_{cc} + \ell_{hc}) \tan \varnothing}{R_c}\right] + \pi\left\{R_e + a \sin\left[\tan^{-1}\left(\frac{R_c - R_e}{\ell_f}\right)\right]\right\}\right\}$$

$$\left[\sqrt{(R_c - R_e)^2 + \ell_f^2} - a\right] \tag{123}$$

where:

$$a = \left\{\frac{\sqrt{(R_e + R_a)^2 + (\ell_{cc} + \ell_{hc} + \ell_f)^2}\ \sin\left[\varnothing - \tan^{-1}\left(\frac{R_a + R_e}{\ell_{cc} + \ell_{hc} + \ell_f}\right)\right]}{\sin\left[\pi - \varnothing - \tan^{-1}\left(\frac{R_c - R_e}{\ell_f}\right)\right]}\right. \tag{124}$$

Range $\varnothing_3 \leq \varnothing \leq \frac{\pi}{2}$

$$\text{Area} = \pi (R_c + R_e)\sqrt{(R_c - R_e)^2 + \ell_f^2} \tag{125}$$

(c) section 3

Range $0 \leq \varnothing \leq \varnothing_3$

$$\text{Area} = R_c\ \ell_{hc} \left\{ \cos^{-1} \left[\frac{R_a - \ell_{cc} \tan \emptyset}{R_c} \right] + \cos^{-1} \left[\frac{R_a - (\ell_{cc} + \ell_{hc}) \tan \emptyset}{R_c} \right] \right\} \tag{126}$$

Range $\emptyset_3 \le \emptyset \le \emptyset_4$

$$\text{Area} = 2\pi R_c \left[\ell_{cc} + \ell_{hc} - \frac{(R_a + R_c)}{\tan \emptyset} \right]$$

$$+ R_c \left[\frac{(R_a + R_c)}{\tan \emptyset} - \ell_{cc} \right] \left\{ \pi + \cos^{-1} \left[\frac{R_a - \ell_{cc} \tan \emptyset}{R_c} \right] \right\} \tag{127}$$

Range $\emptyset_4 \le \emptyset \le \frac{\pi}{2}$

$$\text{Area} = 2\pi R_c\ \ell_{hc} \tag{128}$$

(d) section 4

Range $0 \le \emptyset \le \emptyset_4$

$$\text{Area} = R_c\ \ell_{cc} \left\{ \cos^{-1} \left[\frac{R_a}{R_c} \right] + \cos^{-1} \left[\frac{R_a - \ell_{cc} \tan \emptyset}{R_c} \right] \right\} \tag{129}$$

Range $\emptyset_4 \le \emptyset \le \frac{\pi}{2}$

$$\text{Area} = 2\pi R_c \left[\ell_{cc} - \frac{(R_a + R_c)}{\tan \emptyset} \right] + R_c \left\{ \pi + \cos^{-1} \left[\frac{R_a}{R_c} \right] \right\} \frac{(R_a + R_c)}{\tan \emptyset} \tag{130}$$

(e) section 5

Range $0 \le \emptyset \le \frac{\pi}{2}$

$$\text{Area} = R_c^2 \cos^{-1} \left[\frac{R_a}{R_c} \right] - R_a \sqrt{R_c^2 - R_a^2} \tag{131}$$

Range $\emptyset = \frac{\pi}{2}$

$$\text{Area} = \pi \left(R_c^2 - R_a^2 \right) \tag{132}$$

2. Shear Plane Area

The shear plane area is the area of the horizontal plane within the cavity (Fig. 25). The shear plane area is divided into two sections. The first section is formed by the horizontal plane cutting through the cylindrical portion of the receiver cavity. Not all of the horizontal plane in the cylindrical portion participates in the convective heat loss. The sides of the aperture reduce the effective shear plane area by restricting flow along the horizontal plane at the sides of the cavity near the aperture. The shear plane expands parabolically from the upper lip of the aperture in the horizontal plane. The second section is formed where the horizontal plane cuts the frustum portion of the receiver cavity. The following formulas describe the shear plane area in the specified portion of the cavity for a given receiver angle

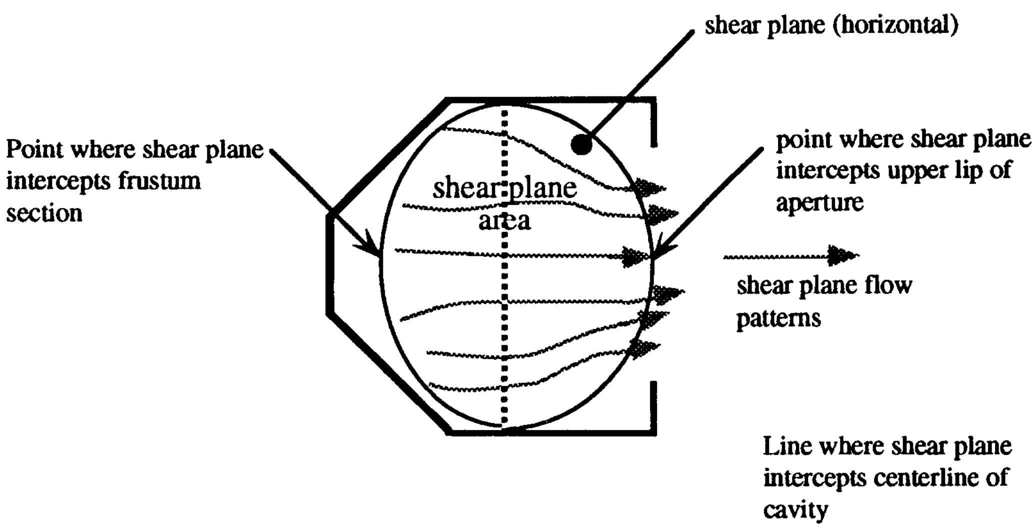

Figure 25. View looking down showing the effective shear plane area.

(a) Shear Plane Area -cylindrical section

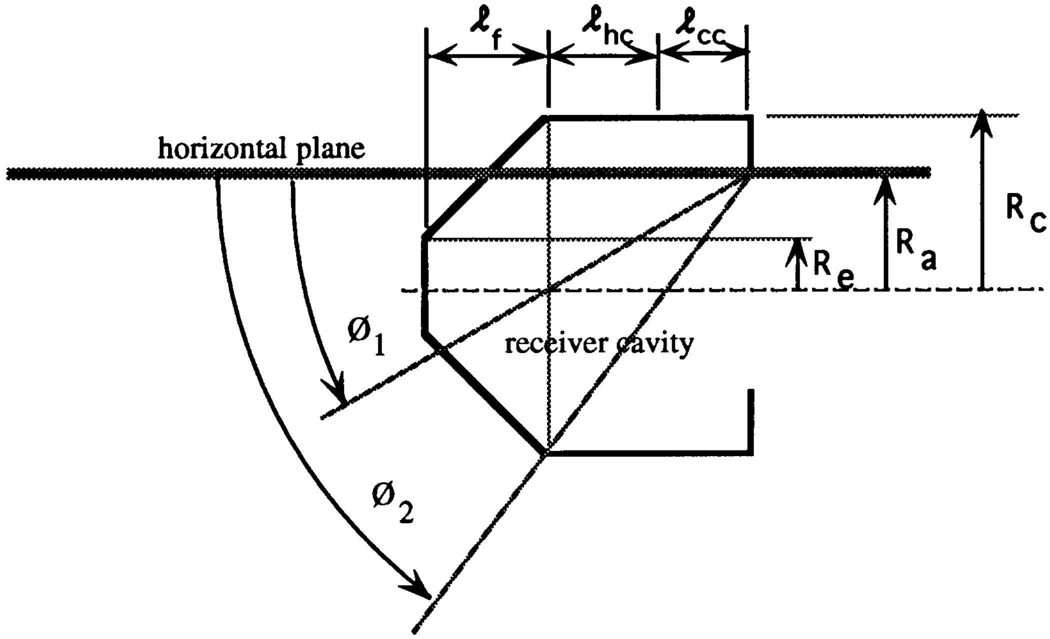

Figure 70. Cylindrical section shear plane angles.

The angles in figure 70 are defined as follows:

$$Ø_1 = \tan^{-1} \left[\frac{R_a}{\ell_{cc} + \ell_{hc}}\right] \tag{133}$$

$$Ø_2 = \tan^{-1} \left[\frac{R_a + R_c}{\ell_{cc} + \ell_{hc}}\right] \tag{134}$$

Range $0 \le Ø \le Ø_1$

$$D = \frac{(\ell_{cc} + \ell_{hc})}{\cos Ø} \tag{135}$$

$$L = 2\sqrt{R_c^2 - R_a^2} \tag{136}$$

$$L_e = 2\sqrt{R_c^2 - [\, R_a - (\,\ell_{cc} + \ell_{hc})\tan Ø]^2} \tag{137}$$

$$\text{Area}_{shear} = \frac{2D}{3}\left[\frac{L^2 + LL_e + L_e^2}{L + L_e}\right] \tag{138}$$

Range $\quad \varnothing_1 \le \varnothing \le \varnothing_2$

$$L = 2\sqrt{R_c^2 - R_a^2} \tag{139}$$

$$L_e = 2R_c \tag{140}$$

$$D = \frac{R_a}{\sin \varnothing} \tag{141}$$

$$L^* = 2R_c$$

$$L_e^* = 2\sqrt{R_c^2 - [\, R_a - (\, \ell_{cc} + \ell_{hc}) \tan\varnothing]^2} \tag{142}$$

$$D^* = \frac{(\, \ell_{cc} + \ell_{hc}) \tan\varnothing - R_a}{\sin \varnothing} \tag{143}$$

$$\text{Area}_{shear} = \frac{2D}{3}\left[\frac{L^2 + LL_e + L_e^2}{L + L_e}\right] + \frac{2D^*}{3}\left[\frac{L^{*2} + L^*L_e^* + L_e^{*2}}{L^* + L_e^*}\right] \tag{144}$$

Range $\quad \varnothing_2 \le \varnothing \le \frac{\pi}{2}$

$$L = 2\sqrt{R_c^2 - R_a^2} \tag{145}$$

$$L_e = 2R_c \tag{146}$$

$$D = \frac{R_a}{\sin \varnothing} \tag{147}$$

$$L^* = 2R_c \tag{148}$$

$$L_e^* = 0 \tag{149}$$

$$D^* = \frac{R_c}{\sin \varnothing} \tag{150}$$

$$\text{Area}_{shear} = \frac{2D}{3}\left[\frac{L^2 + LL_e + L_e^2}{L + L_e}\right] + \frac{2D^*}{3}\left[\frac{L^{*2} + L^*L_e^* + L_e^{*2}}{L^* + L_e^*}\right] \tag{151}$$

Shear Plane Area -frustum section

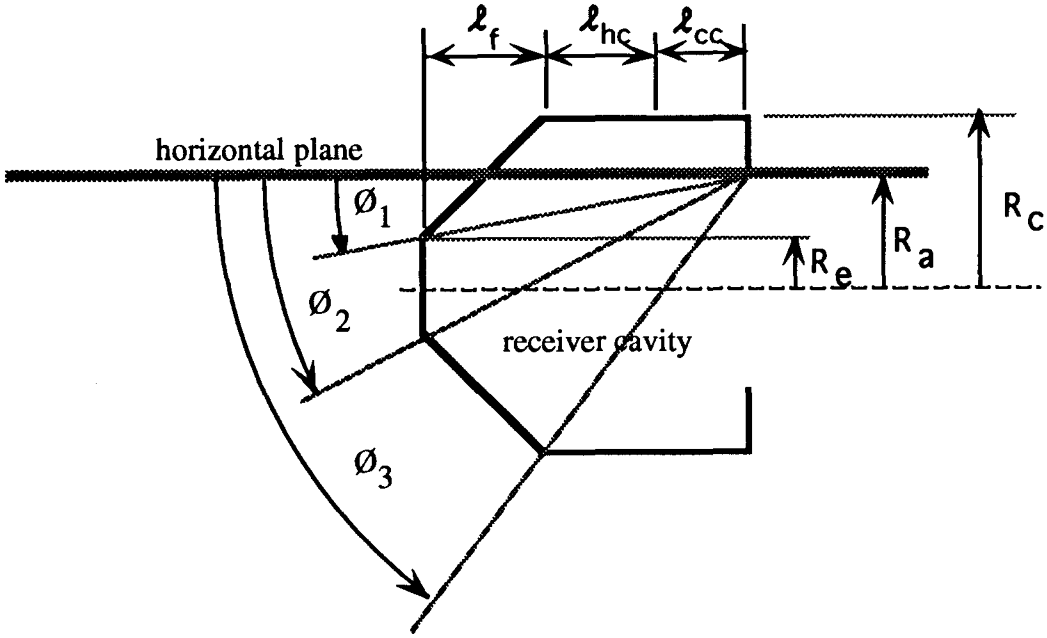

Figure 71. Frustum section shear plane angles.

The angles in figure 71 are defined as follows:

$$\varnothing_1 = \tan^{-1}\left[\frac{R_a - R_e}{\ell_{cc} + \ell_{hc} + \ell_f}\right] \quad (152)$$

$$\varnothing_2 = \tan^{-1}\left[\frac{R_a + R_e}{\ell_{cc} + \ell_{hc} + \ell_f}\right] \quad (153)$$

$$\varnothing_3 = \tan^{-1}\left[\frac{R_a + R_c}{\ell_{cc} + \ell_{hc}}\right] \quad (154)$$

Range $\quad 0 \leq \varnothing \leq \varnothing_1$

$$L = 2\sqrt{R_c^2 - [\, R_a - (\, \ell_{cc} + \ell_{hc})\tan\varnothing]^2} \quad (155)$$

$L_e = 0$

$$D = \frac{\ell_f\,[\, R_c + (\, \ell_{cc} + \ell_{hc})\tan\varnothing - R_a]}{(R_c - R_e)\cos\varnothing - \ell_f \sin\varnothing} \quad (156)$$

$$Area_{shear} = \frac{2D}{3}\left[\frac{L^2 + LL_e + L_e^2}{L + L_e}\right] \quad (157)$$

Range $\quad \varnothing_1 \le \varnothing \le \varnothing_2$

$$L = 2\sqrt{R_c^2 - [R_a - (\ell_{cc} + \ell_{hc})\tan\varnothing]^2} \quad (158)$$

$$L_e = 2\sqrt{R_e^2 - [R_a - (\ell_{cc} + \ell_{hc} + \ell_f)\tan\varnothing]^2} \quad (159)$$

$$D = \frac{\ell_f}{\cos\varnothing} \quad (160)$$

$$Area_{shear} = \frac{2D}{3}\left[\frac{L^2 + LL_e + L_e^2}{L + L_e}\right] \quad (161)$$

Range $\quad \varnothing_2 \le \varnothing \le \varnothing_3$

$$L = 2\sqrt{R_c^2 - [R_a - (\ell_{cc} + \ell_{hc})\tan\varnothing]^2} \quad (162)$$

$L_e = 0$

$$D = \frac{\ell_f [R_c - (\ell_{cc} + \ell_{hc})\tan\varnothing + R_a]}{(R_c - R_e)\cos\varnothing + \ell_f \sin\varnothing} \quad (163)$$

$$Area_{shear} = \frac{2D}{3}\left[\frac{L^2 + LL_e + L_e^2}{L + L_e}\right] \quad (164)$$

Range $\quad \varnothing_3 \le \varnothing \le \frac{\pi}{2}$

$$Area_{shear} = 0 \quad (165)$$

The total shear area in the cavity at any one angle is the sum of the shear areas of the cylindrical section and the frustum section.

Appendix 8: Clausing's Model Computer Program Listing

```
REM             ********************************************************
REM
REM                        Clausing's Method
REM      5 sections program w/ shear plane area
REM             ********************************************************
REM    The Clausing method is used here to predict the convective, radiative,
REM    and conductive losses from a cavity solar receiver operating at various
REM    temperatures and receiver angles.
REM             ********************************************************
    PRINT " Clausing's Method of Predicting Heat Losses"
    PRINT
    PRINT
REM             ********************************************************
REM    The program allows some variations in receiver geometry. These
REM    variables are inputted in this section of the program.
REM             ********************************************************
REM        ******************* Receiver  Geometry  ********************
Re=.127                 :REM   end plate radius [m]
Rc=.33                  :REM   cavity radius [m]
Lf=.292                 :REM   frustum length [m]
Lh=.254                 :REM cylinder length hot [m]
Lc=.14                  :REM cylinder length cold [m]
REM             ********************************************************
REM        ********************     Constants     ************************
pi=4*ATN(1)
g=9.810001              :REM   gravitational acceleration [m/sec^2]
SB=5.6696E-08           :REM   Stefan Boltzmann const. [W/m^2 K^4]
Cp=1006.86              :REM   specific heat capacity of air at Ta [J/kg K]
Pf=1.19406              :REM   density of air at Ta [kg/m^3]
e=1                     :REM   emittance of cavity
ki=.04756               :REM   insulation conductance [W/m-K] [.33B/h/ft^2/in]
t=.0889                 :REM   thickness of insulation [m] [3.5 in]
Ta=70                   :REM   ambient temperature [F]
Ta=(Ta+459.67)/1.8      :REM   ambient temperature [K]
REM             ********************************************************
Pflag=0
INPUT "Do you want a hard copy ";Q$
IF LEFT$(Q$,1)="y" THEN 50
IF LEFT$(Q$,1)="Y" THEN 50
Pflag=1
50 :
REM    open clipboard file for transferring data to spread sheet
OPEN "CLIP:" FOR OUTPUT AS #1
100 :
IF Pflag=1 THEN 55
REM        *****************    Print  Constants     **********************
REM
CLS
LPRINT "End Plate Radius [m] = ";Re
LPRINT "Cavity Radius [m] = ";Rc
LPRINT "Frustum Length [m] = ";Lf
LPRINT "Hot Cylindrical Section Length [m] = ";Lh
LPRINT "Cold Cylindrical Section Length [m] = ";Lc
```

```
LPRINT "Ambient Temperature [K] = ";
LPRINT  USING"####.#";Ta
LPRINT
55 :
REM       ***************          Write  to  the  clipboard     *****************
WRITE#1,"","","End Plate Radius [m] = ",Re
WRITE#1,"","", "Cavity Radius [m] = ",Rc
WRITE#1,"","", "Frustum Length [m] = ",Lf
WRITE#1, "","","Hot Cylindrical Section Length [m] = ",Lh
WRITE#1, "","","Cold Cylindrical Section Length [m] = ",Lc
WRITE#1,"","", "Ambient Temperature [K] = ",Ta
WRITE#1,
REM       *****************  Receiver  Aperture  Radius  Loop  *************
  FOR I=1 TO 4
  IF Pflag=1 THEN 58
LPRINT CHR$(12)
58 :
  READ Ra
  DATA  .0762,.1524,.2286,.329
  Da=2*Ra                :REM   aperture diameter [m]
  Aa=pi*Ra^2             :REM   aperture area [m^2]
REM              *******************************************************
REM         *********************   Angle   Limits   ***********************
REM   In this section the 3 angle limits, z1, z2, z3,  and z4 are calculated.
  z1=ATN((Ra-Re)/(Lf+Lc+Lh))       :p1=z1*180/pi
  z2=ATN((Ra+Re)/(Lf+Lc+Lh))        :p2=z2*180/pi
  z3=ATN((Ra+Rc)/(Lc+Lh))             :p3=z3*180/pi
  z4=ATN((Ra+Rc)/Lc)           :p4=z4*180/pi
  z5=ATN(Ra/(Lc+Lh))     :p5=z5*180/pi
REM      *****************************************************
REM         *****************   Area   Constants   ************************
REM   In the following section Ah and Ac are calculated.
REM   Ah is the total interior heated cavity surface area based on the tube bundle
geometry.
REM    Ar is the total interior refractory cavity surface.
REM   Aha is the interior heated cavity surface area is zone 2, the convective zone.
REM    Ara is the interior refractory cavity surface area is zone 2, the convective zone.
REM   AT is the total cavity area.
  Ah=pi*(Re+Rc)*(Lf^2+(Rc-Re)^2)^.5+2   *pi*Rc*Lh
  Ar=pi*Re^2+pi*(Rc^2-Ra^2)+2*pi*Rc*Lc
  AT=Ah+Ar
REM   Aha and Aca are functions of the receiver angle and are determined by
REM   calculating the heated and refractory areas in zone 1, above the
REM    horizontal plane, and then subtracting these values from their
REM   respective total areas.
REM              *******************************************************
IF Pflag=1 THEN 60
REM         ****************      Print   Header      ***************************
REM
CLS
   LPRINT "Aperture Radius [m] = ";Ra
   LPRINT " Total Cavity Area [m^2] = ";
   LPRINT  USING  "###.####";AT
   LPRINT " Total Heated Cavity Area [m^2} = ";
   LPRINT  USING  "###.####";Ah
```

```
    LPRINT " Total Refractory Cavity Area [m^2} = ";
    LPRINT USING "###.####";Ar
60 :
REM      **************    write header to clipboard    *****************
    WRITE#1, "","","Aperture Radius [m] = ",Ra
    WRITE#1, "",""," Total Cavity Area [m^2] = ",AT
    WRITE#1, "",""," Total Heated Cavity Area [m^2} = ",Ah
    WRITE#1,"","", " Total Refractory Cavity Area [m^2} = ",Ar
REM      **************    Operating Temperature Loop ****************
REM
   FOR Tmf=300 TO 600 STEP 100
   WRITE#1,
   REM      The operating temperature is converted from F to K
   Tm=(Tmf+459.67)/1.8
   Twf=Tmf-100    :REM The refractory surfaces are assumed to be 100°F cooler
                  :REM than the heated tube surfaces.
   Tw=(Twf+459.67)/1.8
   CLS
REM                 ******************************************************
IF Pflag=1 THEN 62
REM         *******************  Print Table Header  *******************
    LPRINT "T mean [K] = ";
    LPRINT USING "####.#";Tm;
    LPRINT "    [°F] = ";
    LPRINT USING "####.";Tmf
LPRINT
LPRINT ;TAB(3);" Angle";TAB(12);"Tube Area";TAB(22);"Refrac. Area";TAB(34);"Q
conv";
LPRINT;TAB(44);"Q total";TAB(54);"% Conv";TAB(65);" Nu ";TAB(76);"
Gr";TAB(87);" Ashear"
LPRINT ;TAB(1);"
[degrees]";TAB(13);"[m^2]";TAB(23);"[m^2]";TAB(34);"[Watts]"   ;
LPRINT;TAB(44);"[Watts]";TAB(56);"%";TAB(88);"[m^2]"
LPRINT
REM                 ******************************************************
62 :
REM      ****************   write table header to clipboard    *********
      WRITE#1,"", "T mean [K] = ",Tm
      WRITE#1, "","    [°F] = ",Tmf
WRITE#1,
WRITE#1," Angle","Tube Area","Refrac. Area","Q conv","Q total","% Conv"," Nu ","
Gr","Ashear"
WRITE#1,"  [degrees]","[m^2]","[m^2]","[Watts]","[Watts]","%","","","[m  ^2]"
WRITE#1,
REM       ******************  Beginning of Angle Loop  ****************
FOR A=0 TO 90 STEP 15
    z=pi*A/180
REM         **********************    Zone   Areas   ***********************
REM   The receiver cavity is divided into 5 sections to accommodate the
REM   zone area calculations. The sections are defined as follows;
REM      section 1 = end plate
REM      section 2 = frustum
REM      section 3 = hot cylinder
REM      section 4 = cold cylinder
REM      section 5 = ring
```

```
REM      AZ1 = area of section 1 in zone 1
REM      AZ2 = area of section 2 in zone 1
REM      AZ3 = area of section 3 in zone 1
REM      AZ4 = area of section 4 in zone 1
REM      AZ5 = area of section 5 in zone 1
REM            ******************SECTION   1****************************
  IF z>z1 THEN 101
    AZ1=0
  GOTO 201
101 :
   IF z>z2 THEN 102
    x=(Ra-(Lf+Lc+Lh)*TAN(z))/Rc
    cx=-ATN(x/SQR(-x*x+1))+1.5708
    m=(Lf+Lc+Lh)*TAN(z)-Ra+Re
    AZ1=Re^2*cx+((Lf+Lc+Lh)*TAN(z)-Ra)*SQR(2*Re*m-m^2)
  GOTO 201
102 :
    AZ1=pi*Re^2
201 :
REM            ******************SECTION   2****************************
  IF z>z1 THEN 202
    x=(Ra-(Lc+Lh)*TAN(z))/Rc
    cx=-ATN(x/SQR(-x*x+1))+1.5708
    m=ATN((Rc-Re)/Lf)
    AZ2=(((Rc-Re)/Lf)*(Rc-Ra)+Lc+Lh)*SIN(z)/SIN(pi/2-z-m)
    AZ2=(AZ2+(Rc-Ra)/SIN(m))*Rc*cx
  GOTO 251
202 :
  IF z>z2 THEN 203
    x1=(Ra-(Lc+Lf+Lh)*TAN(z))/Re
    cx1=-ATN(x1/SQR(-x1*x1+1))+1.5708
    x2=(Ra-(Lc+Lh)*TAN(z))/Rc
    cx2=-ATN(x2/SQR(-x2*x2+1))+1.5708
    AZ2=SQR(Lf^2+(Rc-Re)^2)*(Re*cx1+Rc*cx2)
  GOTO 251
203 :
  IF z>z3 THEN 204
    m=ATN((Rc-Re)/Lf)
    n=ATN((Ra+Re)/(Lc+Lf+Lh))
    l=SQR((Lc+Lf+Lh)^2+(Ra+Re)^2)*SIN(z-n)/SIN(pi-z-m)
    x=(Ra-(Lc+Lh)*TAN(z))/Rc
    cx=-ATN(x/SQR(-x*x+1))+1.5708
    AZ2=(pi*Re+pi*(Re+l*SIN(m)))*l
    AZ2=AZ2+(Rc*cx+pi*(Re+l*SIN(m)))*(SQR(Lf^2+(Rc-Re)^2)-l)
  GOTO 251
204 :
   AZ2=pi*(Re+Rc)*SQR(Lf^2+(Rc-Re)^2)
251 :
REM            ******************SECTION   3****************************
  IF z>z4 THEN 253
  IF z>z3 THEN 252
  x1=(Ra-Lc*TAN(z))/Rc
  x2=(Ra-(Lc+Lh)*TAN(z))/Rc
  cx1=-ATN(x1/SQR(-x1*x1+1))+1.5708
  cx2=-ATN(x2/SQR(-x2*x2+1))+1.5708
```

```
  AZ3=Rc*(cx1+cx2)*Lh
 GOTO 301
252 :
    m=(Ra+Rc)/TAN(z)
    x=(Ra-Lc*TAN(z))/Rc
    cx=-ATN(x/SQR(-x*x+1))+1.5708
    AZ3=2*pi*Rc*(Lh+Lc-m)+Rc*(m-Lc)*(pi+cx)
    GOTO 301
253 :
    AZ3=2*pi*Rc*Lh
301 :
REM          *****************   SECTION   4   *****************************
  IF z>z4 THEN 302
    x1=Ra/Rc
    x2=(Ra-Lc*TAN(z))/Rc
    cx1=-ATN(x1/SQR(-x1*x1+1))+1.5708
    cx2=-ATN(x2/SQR(-x2*x2+1))+1.5708
    AZ4=Rc*(cx1+cx2)*Lc
  GOTO 401
302 :
    x=Ra/Rc
    cx=-ATN(x/SQR(-x*x+1))+1..5708
    m=(Ra+Rc)/TAN(z)
    AZ4=2*pi*Rc*(Lc-m)+Rc*m*(pi+cx)
401 :
REM          *****************   SECTION   5   *****************************
  zm=pi/2
  IF z<zm THEN 402
    AZ5=pi*(Rc^2-Ra^2)
  GOTO 500
402 :
    x=Ra/Rc
    cx=-ATN(x/SQR(-x*x+1))+1.5708
    AZ5=Rc^2*cx-Ra*SQR(Rc^2-Ra^2)
500 :
REM  Aha and Aca are calculated here.
    Aha=Ah-AZ2-AZ3
    Ara=Ar-AZ1-AZ4-AZ5
REM          *****************   Shear  Area  Calculations    *************
REM       ***********  Cylindrical  Shear  Area  Section  ******************
800 :
  IF z>z5 THEN 810
 L1=0
  Le=2*(Rc^2-(Ra-(Lc+Lh)*TAN(z))^2)^.5
  D=(Lc+Lh)/COS(pi*A/180)
  Acshear=2*D*(L1^2  +L1*Le+Le^2)/(3*(L1+Le))
  GOTO 850
810 :
  IF z>z3 THEN 820
 L1=0
 Le=2*Rc
 D=Ra/SIN(z)
 L2=2*Rc
  Le2=2*(Rc^2-(Ra-(Lc+Lh)*TAN(z))^2)^.5
  D2=((Lc+Lh)*TAN(z)-Ra)/SIN(z)
```

```
Acshear=2*D*(L1^2   +L1*Le+Le^2)/(3*(L1+Le))+2*D2*(L2^2
+L2*Le2+Le2^2)/(3*(L2+Le2))
  GOTO 850
820 :
 L1=0
 Le=2*Rc
 D=Ra/SIN(z)
 L2=2*Rc
 Le2=0
 D2=Rc/SIN(z)
Acshear=2*D*(L1^2   +L1*Le+Le^2)/(3*(L1+Le))+2*D*(L2^2
+L2*Le2+Le2^2)/(3*(L2+Le2))
850 :
REM                    ********  Frustum  Shear  Area  Section  ***************
  IF z>z1 THEN 860
  L1=2*(Rc^2-(Ra-(Lc+Lh)*TAN(z))^2)^.5
 Le=0
  D=Lf*(Rc+(Lc+Lh)*TAN(z)-Ra)/((Rc-Re)*COS(z)-Lf*SIN(z))
Afshear=2*D*(L1^2   +L1*Le+Le^2)/(3*(L1+Le))
  GOTO 890
860 :
  IF z>z2 THEN 870
  L1=2*(Rc^2-(Ra-(Lc+Lh)*TAN(z))^2)^.5
  Le=2*(Re^2-(Ra-(Lc+Lh+Lf)*TAN(z))^2)^.5
 D=Lf/COS(z)
Afshear=2*D*(L1^2   +L1*Le+Le^2)/(3*(L1+Le))
  GOTO 890
870 :
  IF z>z3 THEN 880
  L1=2*(Rc^2-(Ra-(Lc+Lh)*TAN(z))^2)^.5
 Le=0
  D=Lf*(Rc-(Lc+Lh)*TAN(z)+Ra)/(COS(z)*(Rc-Re)+Lf*SIN(z))
Afshear=2*D*(L1^2   +L1*Le+Le^2)/(3*(L1+Le))
  GOTO 890
880 :
 Afshear=0
890 :Ashear=Acshear+Afshear
REM              *******************************************************
REM          *****************  Heat  Loss  Calculations  *******************
La=Da*COS(z)      :REM   projected length of aperture [m]
IF La<0 THEN La=0
T1=.08*(Tm-Ta)+273       :REM    first guess temp of air leaving the aperture
XP=200  :REM
350 :
Tc=T1
GOTO Temp
370 :
Q1=DQ
380 :
Tc=XP
GOTO Temp
400 :
Q2=DQ
Tx=(T1*Q2-XP*Q1)/(Q2-Q1)
Tc=Tx
```

```
Temp:
Tb=(Tc+Ta)/2                          :REM   bulk temp inside cavity [K]
B1=1/Tb                                 :REM   coefficient of volume expansion [1/K]
Tf=(Tm+Tb)/2                           :REM   film temp [K]
B2=1/Tf                                 :REM   coefficient of volume expansion [1/K]
U=1.462E-06*Tf^.5/(1+112/Tf)  :REM     absolute viscosity [kg/m-sec]
Pa=352.95/Tf                          :REM   density of air [kg/m^3]
V=U/Pa                                   :REM   kinematic viscosity [m^2/sec]
Tff=Tf*1.8                              :REM   film temp from [K] to [°R]
k=.00679+3.5353E-05*Tff           :REM     thermal conductivity [W/m-K]
Tv=ABS(Tc-Ta)
Vb=SQR(g*B1*Tv*La)                :REM   characteristic velocity due to buoyancy [m/sec]
Va=.5*Vb                               :REM   average velocity [m/sec]
Qc=(Pf*.5*Aa*Va)*Cp*(Tc-Ta)      :REM     heat transfer through aperture [W]
Gr=g*B2*(Tm-Tb)*La^3/V^2        :REM   Grashof number
Pr=.7                                    :REM   Prandtl number
Nu=.1*(Gr*Pr)^.333                  :REM   Nusselt number
h=Nu*k/Da                               :REM   heat transfer coefficient [W/m^2 K]
Qi=h*Aha*(Tm-Tb)+h*Ara*(Tw-Tb)+h*Ashear*(Tm-Tb) :REM heat transfer within
the aperture [W]
DQ=Qi-Qc
IF Tc=T1 THEN 370
IF Tc=XP THEN 400
IF ABS(DQ)<.1 THEN 740
IF DQ<0 THEN GOTO 720
XP=Tx
GOTO 380
720 :
T1=Tx
GOTO 350
740 :
Qr=Aa*e*SB*((Ac/(Ah+Ac))*(Tw^4-Ta^4)+(Ah/(Ah+Ac))*(Tm^4-Ta^4 )) :REM
radiative loss [W]
Qk=(ki/t)*(Ah*(Tm-Ta)+Ar*(Tw-Ta))
QT=Qc+Qr+Qk                               :REM   total heat loss from receiver
PQc=100*Qc/QT                            :REM   %convective
REM          ***********************************************************
IF Pflag=1 THEN 66
REM        ******************    Output  Loop  Results   ******************
LPRINT ;TAB(3);A;
LPRINT TAB(12);
LPRINT USING "##.###";Aha;
LPRINT TAB(22);
LPRINT USING "##.###";Ara;
LPRINT TAB(32);
LPRINT USING "####.##";Qc;
LPRINT;TAB(42);
LPRINT USING "####.##";QT;
LPRINT TAB(54);
LPRINT USING "##.##";PQc;
LPRINT TAB(64);
LPRINT USING "###.##";Nu;
LPRINT TAB(74);
LPRINT USING "##.##^^^^";Gr;
LPRINT TAB(88);
```

```
LPRINT USING "##.##";Ashear
66 :
REM       ****************   write to clipboard   *******************
WRITE#1,A,Aha,Ara,Qc,QT,PQc,Nu,Gr,Ashear
REM              ******************************************************
REM       ******************** End of Angle Loop *******************
NEXT A
REM              ******************************************************
IF Pflag=1 THEN 68
REM       ****************** Output Radiation & Conduction **********
LPRINT"Radiation (Watts) = ";Qr
LPRINT"Conduction (Watts) = ";Qk
68 :
REM       ****************** Write radiative & conduction to clipboard **
WRITE#1,"","","Radiation (Watts) = ",Qr
WRITE#1,"","","Conduction (Watts) = ",Qk
REM              ******************************************************
REM       ******************** End of Temperature Loop **************
  NEXT Tmf
REM              ******************************************************
REM       ********************* End of Aperture Radius Loop **********
  NEXT I
REM              ******************************************************
CLOSE#1
END
```

Appendix 9: Clausing Model Heat Loss Data

Appendix 9 Claussing Model Heat Loss Data								
			End Plate Radius [m] =	0.127				
			Cavity Radius [m] =	0.330				
			Frustum Length [m] =	0.292				
			Hot Cylindrical Section Length [m] =	0.254				
			Cold Cylindrical Section Length [m] =	0.140				
			Ambient Temperature [K] =	294.261				
			Aperture Radius [m] =	0.076				
			Total Cavity Area [m^2] =	1.702				
			Total Heated Cavity Area [m^2} =	1.037				
			Total Refractory Cavity Area [m^2} =	0.665				
T mean [K] =	422.0							
[°F] =	300.0							
Angle [degrees]	Tube Area [m^2]	Refrac. Area [m^2]	Q conv [Watts]	Q total [Watts]	% Conv %	Nu	Gr	Ashear [m^2]
0	0.614	0.406	345.5	467.1	74.0	20.5	1.26E+07	0.30
15	0.465	0.377	312.5	434.2	72.0	20.2	1.19E+07	0.34
30	0.284	0.358	244.1	365.7	66.7	18.7	9.48E+06	0.32
45	0.139	0.350	164.7	286.4	57.5	15.9	5.84E+06	0.26
60	0.033	0.334	69.4	191.1	36.3,	12.0	2.51E+06	0.08
75	0.000	0.267	29.5	151.2	19.5	6.4	3.82E+05	0.07
90	0.000	0.000	0.0	121.6	0.0	0.0	0.00E+00	0.07
	Radiation (Watts) =		25.1					
	Conduction (Watts) =		96.6					
T mean [K] =	477.6							
[°F] =	400.0							
Angle [degrees]	Tube Area [m^2]	Refrac. Area [m^2]	Q conv [Watts]	Q total [Watts]	% Conv %	Nu	Gr	Ashear [m^2]
0	0.614	0.406	570.7	763.9	74.7	20.1	1.19E+07	0.30
15	0.465	0.377	516.7	709.9	72.8	19.8	1.13E+07	0.34
30	0.284	0.358	406.5	599.8	67.8	18.4	9.07E+06	0.32
45	0.139	0.350	278.6	471.8	59.0	15.7	5.63E+06	0.26
60	0.033	0.334	124.6	317.8	39.2	11.9	2.45E+06	0.08
75	0.000	0.267	53.4	246.6	21.6	6.4	3.78E+05	0.07
90	0.000	0.000	0.0	193.2	0.0	0.0	0.00E+00	0.07
	Radiation (Watts) =		46.1					
	Conduction (Watts) =		147.2					
T mean [K] =	533.2							
[°F] =	500.0							
Angle [degrees]	Tube Area [m^2]	Refrac. Area [m^2]	Q conv [Watts]	Q total [Watts]	% Conv %	Nu	Gr	Ashear [m^2]
0	0.614	0.406	808.9	1082.4	74.7	19.5	1.07E+07	0.30
15	0.465	0.377	732.4	1006.0	72.8	19.2	1.02E+07	0.34
30	0.284	0.358	578.0	851.6	67.9	17.8	8.25E+06	0.32
45	0.139	0.350	398.8	672.3	59.3	15.3	5.15E+06	0.26
60	0.033	0.334	182.9	456.5	40.1	11.6	2.26E+06	0.08
75	0.000	0.267	78.4	352.0	22.3	6.2	3.53E+05	0.07
90	0.000	0.000	0.0	273.6	0.0	0.0	0.00E+00	0.07
	Radiation (Watts) =		75.8					
	Conduction (Watts) =		197.8					
T mean [K] =	588.7							
[°F] =	600.0							
Angle [degrees]	Tube Area [m^2]	Refrac. Area [m^2]	Q conv [Watts]	Q total [Watts]	% Conv %	Nu	Gr	Ashear [m^2]
0	0.614	0.406	1055.1	1419.9	74.3	18.7	9.45E+06	0.30
15	0.465	0.377	955.3	1320.1	72.4	18.4	9.05E+06	0.34
30	0.284	0.358	755.0	1119.8	67.4	17.2	7.34E+06	0.32
45	0.139	0.350	522.6	887.5	58.9	14.7	4.61E+06	0.26
60	0.033	0.334	243.0	607.9	40.0	11.2	2.04E+06	0.08
75	0.000	0.267	104.2	469.1	22.2	6.1	3.21E+05	0.07
90	0.000	0.000	0.0	364.8	0.0	0.0	0.00E+00	0.07
	Radiation (Watts) =		116.5					
	Conduction (Watts) =		248.4					

Appendix 9 Clausing Model Heat Loss Data

			Aperture Radius [m] =	0.132				
			Total Cavity Area [m^2] =	1.647				
			Total Heated Cavity Area [m^2] =	1.037				
			Total Refractory Cavity Area [m^2] =	0.610				
	T mean [K] =	422.0						
	[°F] =	300.0						
Angle [degrees]	Tube Area [m^2]	Refrac. Area [m^2]	Q conv [Watts]	Q total [Watts]	% Conv %	Nu	Gr	Ashear [m^2]
0	0.742	0.435	605.0	799.7	75.7	47.7	1.58E+08	0.25
15	0.566	0.399	535.8	730.5	73.3	46.4	1.45E+08	0.32
30	0.370	0.372	408.4	603.1	67.7	42.2	1.09E+08	0.33
45	0.213	0.364	277.0	471.7	58.7	35.0	6.23E+07	0.31
60	0.059	0.350	118.2	312.9	37.8	25.4	2.38E+07	0.15
75	0.000	0.282	46.4	241.1	19.2	13.3	3.45E+06	0.14
90	0.000	0.000	0.0	194.7	0.0	0.0	0.00E+00	0.13
		Radiation (Watts) =	100.2					
		Conduction (Watts) =	94.5					
	T mean [K] =	477.6						
	[°F] =	400.0						
Angle [degrees]	Tube Area [m^2]	Refrac. Area [m^2]	Q conv [Watts]	Q total [Watts]	% Conv %	Nu	Gr	Ashear [m^2]
0	0.742	0.435	984.4	1312.0	75.0	47.6	1.57E+08	0.25
15	0.566	0.399	871.9	1199.6	72.7	46.4	1.45E+08	0.32
30	0.370	0.372	667.8	995.5	67.1	42.2	1.09E+08	0.33
45	0.213	0.364	457.6	785.3	58.3	35.0	6.26E+07	0.31
60	0.059	0.350	203.2	530.8	38.3	25.5	2.40E+07	0.15
75	0.000	0.282	80.5	408.2	19.7	13.4	3.50E+06	0.14
90	0.000	0.000	0.0	327.7	0.0	0.0	0.00E+00	0.13
		Radiation (Watts) =	184.2					
		Conduction (Watts) =	143.4					
	T mean [K] =	533.2						
	[°F] =	500.0						
Angle [degrees]	Tube Area [m^2]	Refrac. Area [m^2]	Q conv [Watts]	Q total [Watts]	% Conv %	Nu	Gr	Ashear [m^2]
0	0.742	0.435	1380.6	1876.2	73.6	46.6	1.47E+08	0.25
15	0.566	0.399	1222.7	1718.3	71.2	45.4	1.36E+08	0.32
30	0.370	0.372	938.5	1434.1	65.4	41.3	1.03E+08	0.33
45	0.213	0.364	645.9	1141.6	56.6	34.4	5.89E+07	0.31
60	0.059	0.350	292.1	787.7	37.1	25.0	2.27E+07	0.15
75	0.000	0.282	116.2	611.8	19.0	13.2	3.32E+06	0.14
90	0.000	0.000	0.0	495.6	0.0	0.0	0.00E+00	0.13
		Radiation (Watts) =	303.2					
		Conduction (Watts) =	192.4					
	T mean [K] =	588.7						
	[°F] =	600.0						
Angle [degrees]	Tube Area [m^2]	Refrac. Area [m^2]	Q conv [Watts]	Q total [Watts]	% Conv %	Nu	Gr	Ashear [m^2]
0	0.742	0.435	1786.1	2493.3	71.6	45.1	1.34E+08	0.25
15	0.566	0.399	1581.5	2288.8	69.1	44.0	1.24E+08	0.32
30	0.370	0.372	1215.1	1922.4	63.2	40.1	9.38E+07	0.33
45	0.213	0.364	838.3	1545.5	54.2	33.3	5.39E+07	0.31
60	0.059	0.350	382.9	1090.1	35.1	24.3	2.08E+07	0.15
75	0.000	0.282	152.5	859.8	17.7	12.8	3.05E+06	0.14
90	0.000	0.000	0.0	707.2	0.0	0.0	0.00E+00	0.13
		Radiation (Watts) =	465.9					
		Conduction (Watts) =	241.4					

Appendix 9 Clausing Model Heat Loss Data

	Aperture Radius [m] =			0.229				
	Total Cavity Area [m^2] =			1.556				
	Total Heated Cavity Area [m^2] =			1.037				
	Total Refractory Cavity Area [m^2] =			0.519				
T mean [K] =		422.0						
	[°F] =	300.0						
Angle [degrees]	Tube Area [m^2]	Refrac. Area [m^2]	Q conv [Watts]	Q total [Watts]	% Conv %	Nu	Gr	Ashear [m^2]
0	0.855	0.411	706.4	1021.9	69.0	75.0	6.15E+08	0.17
15	0.664	0.387	646.6	963.1	67.1	72.6	5.59E+08	0.30
30	0.467	0.347	496.7	813.2	61.1	65.6	4.12E+08	0.33
45	0.283	0.338	338.3	654.8	51.7	54.0	2.30E+08	0.34
60	0.092	0.323	154.4	470.9	32.8	38.7	8.46E+07	0.23
75	0.002	0.274	59.0	375.5	15.7	20.2	1.21E+07	0.21
90	0.000	0.000	0.0	316.5	0.0	0.0	0.00E+00	0.20
	Radiation (Watts) =		225.5					
	Conduction (Watts) =		91.0					
T mean [K] =		477.6						
	[°F] =	400.0						
Angle [degrees]	Tube Area [m^2]	Refrac. Area [m^2]	Q conv [Watts]	Q total [Watts]	% Conv %	Nu	Gr	Ashear [m^2]
0	0.855	0.411	1137.7	1689.4	67.3	75.3	6.22E+08	0.17
15	0.664	0.387	1042.5	1594.2	65.4	72.9	5.65E+08	0.30
30	0.467	0.347	802.4	1354.1	59.3	65.9	4.17E+08	0.33
45	0.283	0.338	550.6	1102.3	50.0	54.3	2.33E+08	0.34
60	0.092	0.323	257.8	809.5	31.9	39.0	8.61E+07	0.23
75	0.002	0.274	99.8	651.5	15.3	20.4	1.23E+07	0.21
90	0.000	0.000	0.0	551.7	0.0	0.0	0.00E+00	0.20
	Radiation (Watts) =		414.5					
	Conduction (Watts) =		137.2					
T mean [K] =		533.2						
	[°F] =	500.0						
Angle [degrees]	Tube Area [m^2]	Refrac. Area [m^2]	Q conv [Watts]	Q total [Watts]	% Conv %	Nu	Gr	Ashear [m^2]
0	0.855	0.411	1586.6	2452.3	64.7	73.9	5.88E+08	0.17
15	0.664	0.387	1453.4	2319.1	62.7	71.6	5.35E+08	0.30
30	0.467	0.347	1119.4	1985.1	56.4	64.8	3.96E+08	0.33
45	0.283	0.338	770.9	1636.6	47.1	53.4	2.22E+08	0.34
60	0.092	0.323	365.5	1231.2	29.7	38.3	8.19E+07	0.23
75	0.002	0.274	142.2	1007.9	14.1	20.1	1.17E+07	0.21
90	0.000	0.000	0.0	865.7	0.0	0.0	0.00E+00	0.20
	Radiation (Watts) =		682.3					
	Conduction (Watts) =		183.5					
T mean [K] =		588.7						
	[°F] =	600.0						
Angle [degrees]	Tube Area [m^2]	Refrac. Area [m^2]	Q conv [Watts]	Q total [Watts]	% Conv %	Nu	Gr	Ashear [m^2]
0	0.855	0.411	2043.8	3321.7	61.5	71.8	5.40E+08	0.17
15	0.664	0.387	1871.8	3149.7	59.4	69.6	4.91E+08	0.30
30	0.467	0.347	1442.1	2720.0	53.0	63.0	3.64E+08	0.33
45	0.283	0.338	995.0	2273.0	43.8	51.9	2.04E+08	0.34
60	0.092	0.323	475.0	1752.9	27.1	37.3	7.54E+07	0.23
75	0.002	0.274	185.4	1463.4	12.7	19.5	1.08E+07	0.21
90	0.000	0.000	0.0	1277.9	0.0	0.0	0.00E+00	0.20
	Radiation (Watts) =		1048.2					
	Conduction (Watts) =		229.7					

Appendix 9 Clausing Model Heat Loss Data

	Aperture Radius [m] =		0.329						
	Total Cavity Area [m^2] =		1.380						
	Total Heated Cavity Area [m^2] =		1.037						
	Total Refractory Cavity Area [m^2] =		0.343						
T mean [K] =		422.0							
[°F] =		300.0							
Angle	Tube Area	Refrac. Area	Q conv	Q total	% Conv	Nu	Gr	Ashear	
[degrees]	[m^2]	[m^2]	[Watts]	[Watts]	%			[m^2]	
0	1.024	0.336	740.0	1291.2	57.3	110.7	1.98E+09	0.01	
15	0.883	0.317	743.7	1295.0	57.4	106.9	1.78E+09	0.22	
30	0.628	0.270	592.6	1143.8	51.8	96.2	1.30E+09	0.34	
45	0.384	0.244	385.3	936.6	41.1	79.0	7.19E+08	0.36	
60	0.146	0.228	191.5	742.7	25.8	56.3	2.60E+08	0.33	
75	0.011	0.187	69.0	620.2	11.1	29.3	3.67E+07	0.30	
90	0.000	0.000	0.0	551.3	0.0	0.0	0.00E+00	0.29	
	Radiation (Watts) =		467.1						
	Conduction (Watts) =		84.2						
T mean [K] =		477.6							
[°F] =		400.0							
Angle	Tube Area	Refrac. Area	Q conv	Q total	% Conv	Nu	Gr	Ashear	
[degrees]	[m^2]	[m^2]	[Watts]	[Watts]	%			[m^2]	
0	1.024	0.336	1181.3	2165.0	54.6	111.4	2.02E+09	0.01	
15	0.883	0.317	1183.5	2167.2	54.6	107.6	1.82E+09	0.22	
30	0.628	0.270	941.6	1925.3	48.9	96.8	1.32E+09	0.34	
45	0.384	0.244	614.8	1598.5	38.5	79.6	7.35E+08	0.36	
60	0.146	0.228	309.0	1292.7	23.9	56.7	2.66E+08	0.33	
75	0.011	0.187	112.3	1096.0	10.2	29.6	3.76E+07	0.30	
90	0.000	0.000	0.0	983.7	0.0	0.0	0.00E+00	0.29	
	Radiation (Watts) =		858.5						
	Conduction (Watts) =		125.2						
T mean [K] =		533.2							
[°F] =		500.0							
Angle	Tube Area	Refrac. Area	Q conv	Q total	% Conv	Nu	Gr	Ashear	
[degrees]	[m^2]	[m^2]	[Watts]	[Watts]	%			[m^2]	
0	1.024	0.336	1637.7	3217.1	50.9	109.6	1.92E+09	0.01	
15	0.883	0.317	1638.0	3217.4	50.9	105.8	1.73E+09	0.22	
30	0.628	0.270	1302.1	2881.4	45.2	95.3	1.26E+09	0.34	
45	0.384	0.244	851.7	2431.1	35.0	78.3	7.00E+08	0.36	
60	0.146	0.228	430.5	2009.9	21.4	55.8	2.53E+08	0.33	
75	0.011	0.187	157.0	1736.4	9.0	29.1	3.59E+07	0.30	
90	0.000	0.000	0.0	1579.4	0.0	0.0	0.00E+00	0.29	
	Radiation (Watts) =		1413.2						
	Conduction (Watts) =		166.2						
T mean [K] =		588.7							
[°F] =		600.0							
Angle	Tube Area	Refrac. Area	Q conv	Q total	% Conv	Nu	Gr	Ashear	
[degrees]	[m^2]	[m^2]	[Watts]	[Watts]	%			[m^2]	
0	1.024	0.336	2101.1	4479.5	46.9	106.6	1.77E+09	0.01	
15	0.883	0.317	2099.4	4477.8	46.9	103.0	1.59E+09	0.22	
30	0.628	0.270	1667.9	4046.3	41.2	92.7	1.16E+09	0.34	
45	0.384	0.244	1092.1	3470.4	31.5	76.2	6.46E+08	0.36	
60	0.146	0.228	553.7	2932.1	18.9	54.4	2.34E+08	0.33	
75	0.011	0.187	202.5	2580.9	7.8	28.4	3.31E+07	0.30	
90	0.000	0.000	0.0	2378.4	0.0	0.0	0.00E+00	0.29	
	Radiation (Watts) =		2171.2						
	Conduction (Watts) =		207.2						

Appendix 10 Siebers and Kraabel Computer Program Listing

```
REM     *************************************************************
REM
REM                          Siebers & Kraabel Method
REM
REM     *************************************************************
REM   The Siebers & Kraabel method is used here to predict the convective
REM    from a solar cavity receiver operating at various temperatures and
REM   receiver angles.
REM     *************************************************************
    PRINT " Siebers & Kraabel Method of Predicting Convective Losses"
    PRINT
    PRINT
REM     *************************************************************
REM   The program allows some variations in receiver geometry. These
REM    variables are inputted in this section of the program. The characteristic
REM    length, as called for in the reference, is simply the cavity diameter
REM   given here as 'Cl'.
REM     *************************************************************
REM        ******************* Receiver  Geometry  *********************
Re=.127                    :REM   end plate radius [m]
Rc=.33                     :REM   cavity radius [m]
Lf=.292                    :REM   frustum length [m]
Lh=.254                    :REM cylinder length hot [m]
Lc=.14                     :REM cylinder length cold [m]
Cl=2*Rc                    :REM characteristic length [m]
REM     *************************************************************
REM         ******************** Constants  **************************
  pi=4*ATN(1)
  Ta=70                    :REM  ambient temperature [°F]
REM     *************************************************************
OPEN "CLIP:" FOR OUTPUT AS #1
REM        *************  write  header  to  clipboard    ********************
WRITE#1, " Siebers & Kraabel Method"
WRITE#1,
     WRITE#1,"","","End Plate Radius [m] = ",Re
    WRITE#1,"","","Cavity Radius [m] = ",Rc
    WRITE#1,"","","Frustum Length [m] = ",Lf
    WRITE#1,"","","Hot Cylindrical Section Length [m] = ",Lh
    WRITE#1,"","","Cold Cylindrical Section Length [m] = ",Lc
    WRITE#1,"","","T amb [°F] = ",Ta
WRITE#1,
REM        ***************** Receiver  Aperture  Radius  Loop  *************
  FOR rad=1 TO 4
  READ Ra
  DATA .0762, .1524, .2286, .329
  Da=2*Ra
REM     *************************************************************
REM         ********************* Angle  Limits  **********************
REM   In this section the 4 angle limits, z1, z2, z3, and z4 are calculated.
  z1=ATN((Ra-Re)/(Lf+Lc+Lh))        :p1=z1*180/pi
  z2=ATN((Ra+Re)/(Lf+Lc+Lh))        :p2=z2*180/pi
  z3=ATN((Ra+Rc)/(Lc+Lh))           :p3=z3*180/pi
  z4=ATN((Ra+Rc)/Lc)                :p4=z4*180/pi
```

```
REM     **************************************************************
REM             ****************  Area  Constants  ************************
REM   In the following section area 1, area 2, and area 3 are calculated.
REM   A1 is the total interior cavity surface area.
REM   A2 is the total interior cavity surface area minus the lower lip.
REM   A3 is the interior cavity surface area below the horizontal plane
REM   cutting through the receiver at the top of the aperture.
REM
  Ah=pi*(Re+Rc)*(Lf^2+(Rc-Re)^2)^.5+2*pi*Rc*Lh
  Ar=pi*Re^2+pi*(Rc^2-Ra^2)+2*pi*Rc*Lc
  A1=Ah+Ar
  A2=A1-Rc^2*(-ATN((Ra/Rc)/SQR(-(Ra/Rc)*(Ra/Rc)+1))+1.5708)+Ra
*SQR(Rc^2-Ra^2)
REM   Area 3 is a function of the receiver angle and is determined by
REM   calculating the total area in zone 1, above the horizontal
REM   plane, and then subtracting this value from the total area.
REM     **************************************************************
REM             ****************  Print  Header  ***************************
PRINT " Siebers & Kraabel Method"
PRINT
    PRINT "End Plate Radius [m] = ";Re
    PRINT "Cavity Radius [m] = ";Rc
    PRINT "Aperture Radius [m] = ";Ra
    PRINT "Frustum Length [m] = ";Lf
    PRINT "Hot Cylindrical Section Length [m] = ";Lh
    PRINT "Cold Cylindrical Section Length [m] = ";Lc
    PRINT "T amb = ";Ta
    PRINT " Total Area [m^2] = ";A1
PRINT
REM     **************************************************************
REM       *************   write  header  to  clipboard   ********************
WRITE#1,
    WRITE#1,"","","Aperture Radius [m] = ",Ra
    WRITE#1,"",""," Total Area [m^2] = ",A1
REM       **************   Operating  Temperature  Loop   *****************
REM
  FOR Th=300 TO 600 STEP 100
  REM mean system operating temperature of receiver [°F]
  Tr=Th-100
  Tw=(Th*Ah+Tr*Ar)/A1
  CLS
REM     **************************************************************
REM           **********************  Air  Properties  *********************
REM   The value of 'k' calculated here is the product of the gravitational
REM   constant times the coefficient of volumetric expansion divided by
REM    the kinematic viscosity squared. (i.e.. g ß/v^2 [1/K-m^3]) The
REM   equation for 'k' is based on data from Table A-1, p. 388, Kays & Crawford,
REM   " Convective Heat and Mass Transfer ", second edition, McGraw-Hill.
PRINT
  k=2.651E+08-2186000!*Ta+7935.4726#*Ta^2-13.3076*Ta^3+.0082*T   a^4
   Gr=k*(Tw-Ta)/1.8*Cl^3     :REM Grashoff number
  Nu=.088*Gr^(1/3)*((Tw+459.67)/(Ta+459.67))^.18      :REM  Nusselt  number
  hc=.81*((Tw-Ta)/1.8)^.426
   REM  hc=natural convection no lip heat transfer coefficient
REM     **************************************************************
```

```
REM          ********************  Print  Table  Header  ******************
    PRINT "Nusselt Number =";Nu
    PRINT "Grashoff Number =";Gr
    PRINT "T mean [°F] = ";Th
PRINT ;TAB(3);" Angle";TAB(11);"Sec 1";TAB(19);"Sec 2";TAB(27);"Sec 3";
PRINT;TAB(35);"Sec 4";TAB(43);"Sec 5";TAB(50);"Heat Loss";TAB(61);"   h   ";
PRINT;TAB(72);"Total Zone 1"
PRINT  ;TAB(1);"  [degrees]";TAB(11);"[m^2]";TAB(19);"[m^2]";TAB(27);"[m^2]";
PRINT;TAB(35);"[m^2]";TAB(43);"[m^2]";TAB(51);"[Watts]";TAB(
60);"[Watts/K-m^2]";
PRINT;TAB(73);"[m^2]"
PRINT
REM      ***********************************************************
REM      ************  WRITE  HEADER  TO  CLIPBOARD  ******************
WRITE#1,"","Nusselt Number =",Nu
WRITE#1,"","Grashoff Number =",Gr
WRITE#1,"T mean = ",Th
WRITE#1,
WRITE#1,"Angle","Sec 1","Sec 2","Sec 3","Sec 4","Sec 5","Heat Loss","h","Total Zone
1"
WRITE#1,"[degrees]","[m^2]","[m^2]","[m^2]","[m^2]","[m^2]",
"[Watts]","[Watts/K-m^2]","[m^2]"
WRITE#1,
REM          ******************  Beginning  of  Angle  Loop  ****************
FOR A=0 TO 90 STEP 15
   z=pi*A/180
REM      ***********************************************************
REM          **********************  Zone  Areas  ***********************
REM   The receiver cavity is divided into 5 section to accommodate the
REM   zone area calculations. The sections are defined as follows;
REM      section 1 = end plate
REM       section 2 = frustum
REM       section 3 = hot cylinder
REM       section 4 = cold cylinder
REM       section 5 = ring
REM      AZ1 = area of section 1 in zone 1
REM      AZ2 = area of section 2 in zone 1
REM      AZ3 = area of section 3 in zone 1
REM      AZ4 = area of section 4 in zone 1
REM      AZ5 = area of section 5 in zone 1
REM            *******************SECTION  1****************************
  IF z>z1 THEN 101
    AZ1=0
  GOTO 201
101 :
  IF z>z2 THEN 102
    x=(Ra-(Lf+Lc+Lh)*TAN(z))/Rc
    cx=-ATN(x/SQR(-x*x+1))+1.5708
    m=(Lf+Lc+Lh)*TAN(z)-Ra+Re
    AZ1=Re^2*cx+((Lf+Lc+Lh)*TAN(z)-Ra)*SQR(2*Re*m-m^2)
  GOTO 201
102 :
    AZ1=pi*Re^2
201 :
```

```
REM            ******************SECTION   2****************************
  IF z>z1 THEN 202
    x=(Ra-(Lc+Lh)*TAN(z))/Rc
    cx=-ATN(x/SQR(-x*x+1))+1.5708
    m=ATN((Rc-Re)/Lf)
    AZ2=(((Rc-Re)/Lf)*(Rc-Ra)+Lc+Lh)*SIN(z)/SIN(pi/2-z-m)
  AZ2=(AZ2+(Rc-Ra)/SIN(m))*Rc*cx
  GOTO 301
202 :
  IF z>z2 THEN 203
    x1=(Ra-(Lc+Lf+Lh)*TAN(z))/Re
    cx1=-ATN(x1/SQR(-x1*x1+1))+1.5708
    x2=(Ra-(Lc+Lh)*TAN(z))/Rc
    cx2=-ATN(x2/SQR(-x2*x2+1))+1.5708
    AZ2=SQR(Lf^2+(Rc-Re)^2)*(Re*cx1+Rc*cx2)
  GOTO 301
203 :
  IF z>z3 THEN 204
    m=ATN((Rc-Re)/Lf)
    n=ATN((Ra+Re)/(Lc+Lf+Lh))
    l=SQR((Lc+Lf+Lh)^2+(Ra+Re)^2)*SIN(z-n)/SIN(pi-z-m)
    x=(Ra-(Lc+Lh)*TAN(z))/Rc
    cx=-ATN(x/SQR(-x*x+1))+1.5708
    AZ2=(pi*Re+pi*(Re+l*SIN(m)))*l
    AZ2=AZ2+(Rc*cx+pi*(Re+l*SIN(m)))*(SQR(Lf^2+(Rc-Re)^2)-l)
  GOTO 301
204 :
    AZ2=pi*(Re+Rc)*SQR(Lf^2+(Rc-Re)^2)
301 :
REM          ****************   SECTION   3   ****************************
  IF z>z3 THEN 302
    x1=(Ra-Lc*TAN(z))/Rc
      x2=(Ra-(Lc+Lh)*TAN(z))/Rc
    cx1=-ATN(x1/SQR(-x1*x1+1))+1.5708
    cx2=-ATN(x2/SQR(-x2*x2+1))+1.5708
    AZ3=Rc*(cx1+cx2)*Lh
  GOTO 401
302 :
  IF z>z4 THEN 303
    m=(Ra+Rc)/TAN(z)
    x=(Ra-Lc*TAN(z))/Rc
    cx=-ATN(x/SQR(-x*x+1))+1.5708
    AZ3=2*pi*Rc*(Lh+Lc-m)+Rc*(m-Lc)*(pi+cx)
  GOTO 401
303 :
    AZ3=2*pi*Rc*Lh
401 :
REM          ****************   SECTION   4   ****************************
  IF z>z4 THEN 402
    x1=Ra/Rc
    x2=(Ra-Lc*TAN(z))/Rc
      cx1=-ATN(x1/SQR(-x1*x1+1))+1.5708
    cx2=-ATN(x2/SQR(-x2*x2+1))+1.5708
    AZ4=Rc*(cx1+cx2)*Lc
  GOTO 501
```

```
402 :
    x=Ra/Rc
    cx=-ATN(x/SQR(-x*x+1))+1.5708
    m=(Ra+Rc)/TAN(z)
    AZ4=2*pi*Rc*(Lc-m)+Rc*m*(pi+cx)
501 :
REM         ****************   SECTION   5   *****************************
  zm=pi/2
  IF z<zm THEN 502
    AZ5=pi*(Rc^2-Ra^2)
  GOTO 600
502 :
    x=Ra/Rc
    cx=-ATN(x/SQR(-x*x+1))+1.5708
    AZ5=Rc^2*cx-Ra*SQR(Rc^2-Ra^2)
600 :
REM         *************   Calculate   Area   3   ***************************
    AZT=AZ1+AZ2+AZ3+AZ4+AZ5
    A3=A1-AZT
REM     **********************************************************
REM         ****************   Heat   Loss   Calculation   *******************
    zz=pi*30/180
    IF z>zz THEN 601
    n=.63
    GOTO 700
601 :
    n=.8
700 :
    h=hc*(A1/A2)*(A3/A1)^n
    q=h*A1*(Tw-Ta)/1.8
REM         ******************   PRINTER   Output   ***********************
REM
PRINT;TAB(4);
PRINT  USING"###.";A;
PRINT;TAB(9);
PRINT  USING  "###.####";AZ1;
PRINT;TAB(17);
PRINT  USING  "###.####";AZ2;
PRINT;TAB(25);
PRINT  USING  "###.####";AZ3;
PRINT;TAB(33);
PRINT  USING  "###.####";AZ4;
PRINT;TAB(41);
PRINT  USING  "###.####";AZ5;
PRINT;TAB(50);
PRINT  USING  "#####.#";q;
PRINT;TAB(60);
PRINT  USING  "###.####";h;
PRINT;TAB(70);
PRINT  USING  "###.####";AZT
REM  **************     OUTPUT   TO   CLIPBOARD      **********************
WRITE #1,A,AZ1,AZ2,AZ3,AZ4,AZ5,q,h,AZT
NEXT A
NEXT Th
NEXT rad
```

```
PRINT "bye!"
CLOSE #1
END
```

Appendix 11 Siebers and Kraabel Model Heat Loss

Appendix 11 Siebers & Kraabel Heat Loss Data								
End Plate Radius [m] =	0.127							
Cavity Radius [m] =	0.33							
Frustum Length [m] =	0.292							
Hot Cylindrical Section Length [m] =	0.254							
Cold Cylindrical Section Length [m] =	0.14							
T amb [°F] =	70							
Aperture Radius [m] =	0.076							
Total Area [m^2] =	1.702							
Nusselt Number =	153.23							
Grashoff Number =	4.47E+9							
T mean =	300							
Angle	Sec 1	Sec 2	Sec 3	Sec 4	Sec 5	Heat Loss	h	Total Zone 1
[degrees]	[m^2]	[m^2]	[m^2]	[m^2]	[m^2]	[Watts]	[Watts/K-m^2]	[m^2]
0	0.014	0.199	0.224	0.124	0.121	831.9	4.607	0.682
15	0.038	0.311	0.261	0.129	0.121	736.9	4.081	0.860
30	0.051	0.449	0.304	0.135	0.121	621.3	3.441	1.060
45	0.051	0.510	0.388	0.143	0.121	423.1	2.343	1.213
60	0.051	0.511	0.494	0.159	0.121	336.3	1.863	1.335
75	0.051	0.311	0.327	0.225	0.121	261.3	1.447	1.435
90	0.051	0.511	0.327	0.290	0.324	0.0	0.000	1.702
Nusselt Number =	180.50							
Grashoff Number =	6.81E+9							
T mean =	400							
Angle	Sec 1	Sec 2	Sec 3	Sec 4	Sec 5	Heat Loss	h	Total Zone 1
[degrees]	[m^2]	[m^2]	[m^2]	[m^2]	[m^2]	[Watts]	[Watts/K-m^2]	[m^2]
0	0.014	0.199	0.224	0.124	0.121	1516.6	5.313	0.682
15	0.038	0.311	0.261	0.129	0.121	1343.4	4.883	0.860
30	0.051	0.449	0.304	0.135	0.121	1132.7	4.117	1.060
45	0.051	0.510	0.388	0.143	0.121	771.4	2.804	1.213
60	0.051	0.511	0.494	0.159	0.121	613.2	2.229	1.335
75	0.051	0.311	0.327	0.225	0.121	476.3	1.731	1.435
90	0.051	0.311	0.327	0.290	0.324	0.0	0.000	1.702
Nusselt Number =	203.34							
Grashoff Number =	9.15E+9							
T mean =	500							
Angle	Sec 1	Sec 2	Sec 3	Sec 4	Sec 5	Heat Loss	h	Total Zone 1
[degrees]	[m^2]	[m^2]	[m^2]	[m^2]	[m^2]	[Watts]	[Watts/K-m^2]	[m^2]
0	0.014	0.199	0.224	0.124	0.121	2311.3	6.252	0.682
15	0.038	0.311	0.261	0.129	0.121	2047.3	5.538	0.860
30	0.051	0.449	0.304	0.135	0.121	1726.2	4.669	1.060
45	0.051	0.510	0.388	0.143	0.121	1175.6	3.180	1.213
60	0.051	0.511	0.494	0.159	0.121	934.4	2.528	1.335
75	0.051	0.311	0.327	0.225	0.121	725.9	1.964	1.435
90	0.051	0.511	0.327	0.290	0.324	0.0	0.000	1.702
Nusselt Number =	223.49							
Grashoff Number =	1.15E+10							
T mean =	600							
Angle	Sec 1	Sec 2	Sec 3	Sec 4	Sec 5	Heat Loss	h	Total Zone 1
[degrees]	[m^2]	[m^2]	[m^2]	[m^2]	[m^2]	[Watts]	[Watts/K-m^2]	[m^2]
0	0.014	0.199	0.224	0.124	0.121	3198.2	6.889	0.682
15	0.038	0.311	0.261	0.129	0.121	2832.9	6.102	0.860
30	0.051	0.449	0.304	0.135	0.121	2388.6	5.145	1.060
45	0.051	0.510	0.388	0.143	0.121	1626.7	3.504	1.213
60	0.051	0.511	0.494	0.159	0.121	1293.0	2.785	1.335
75	0.051	0.511	0.327	0.225	0.121	1004.5	2.164	1.435
90	0.051	0.311	0.327	0.290	0.324	0.0	0.000	1.702

Appendix 11 Siebers and Kraabel Model Heat Loss

	Aperture Radius [m] =		0.152						
	Total Area [m^2] =		1.647						
Nusselt Number =		153.85							
Grashoff Number =		4.52E+09							
T mean =	300								
Angle [degrees]	Sec 1 [m^2]	Sec 2 [m^2]	Sec 3 [m^2]	Sec 4 [m^2]	Sec 5 [m^2]	Heat Loss [Watts]	h [Watts/K-m^2]	Total Zone 1 [m^2]	
0	0.000	0.112	0.183	0.101	0.074	888.2	5.029	0.470	
15	0.031	0.250	0.222	0.107	0.074	783.2	4.435	0.683	
30	0.051	0.403	0.264	0.113	0.074	664.4	3.762	0.905	
45	0.051	0.495	0.329	0.121	0.074	474.3	2.686	1.070	
60	0.051	0.511	0.467	0.136	0.074	359.8	2.037	1.239	
75	0.051	0.511	0.527	0.203	0.074	267.7	1.516	1.365	
90	0.051	0.511	0.527	0.290	0.269	0.0	0.000	1.647	
Nusselt Number =		180.99							
Grashoff Number =		6.86E+09							
T mean =	400								
Angle [degrees]	Sec 1 [m^2]	Sec 2 [m^2]	Sec 3 [m^2]	Sec 4 [m^2]	Sec 5 [m^2]	Heat Loss [Watts]	h [Watts/K-m^2]	Total Zone 1 [m^2]	
0	0.000	0.112	0.183	0.101	0.074	1610.9	6.008	0.470	
15	0.031	0.250	0.222	0.107	0.074	1420.5	5.298	0.683	
30	0.051	0.403	0.264	0.113	0.074	1205.1	4.495	0.905	
45	0.051	0.495	0.329	0.121	0.074	860.3	3.209	1.070	
60	0.051	0.511	0.467	0.136	0.074	652.6	2.434	1.239	
75	0.051	0.511	0.527	0.203	0.074	485.6	1.811	1.365	
90	0.051	0.511	0.527	0.290	0.269	0.0	0.000	1.647	
Nusselt Number =		203.77							
Grashoff Number =		9.20E+09							
T mean =	500								
Angle [degrees]	Sec 1 [m^2]	Sec 2 [m^2]	Sec 3 [m^2]	Sec 4 [m^2]	Sec 5 [m^2]	Heat Loss [Watts]	h [Watts/K-m^2]	Total Zone 1 [m^2]	
0	0.000	0.112	0.183	0.101	0.074	2448.8	6.809	0.470	
15	0.031	0.250	0.222	0.107	0.074	2159.4	6.004	0.683	
30	0.051	0.403	0.264	0.113	0.074	1831.8	5.094	0.905	
45	0.051	0.495	0.329	0.121	0.074	1307.8	3.636	1.070	
60	0.051	0.511	0.467	0.136	0.074	992.0	2.758	1.239	
75	0.051	0.511	0.527	0.203	0.074	738.1	2.052	1.365	
90	0.051	0.511	0.527	0.290	0.269	0.0	0.000	1.647	
Nusselt Number =		223.88							
Grashoff Number =		1.15E+10							
T mean =	600								
Angle [degrees]	Sec 1 [m^2]	Sec 2 [m^2]	Sec 3 [m^2]	Sec 4 [m^2]	Sec 5 [m^2]	Heat Loss [Watts]	h [Watts/K-m^2]	Total Zone 1 [m^2]	
0	0.000	0.112	0.183	0.101	0.074	3383.4	7.499	0.470	
15	0.031	0.250	0.222	0.107	0.074	2983.5	6.613	0.683	
30	0.051	0.403	0.264	0.113	0.074	2531.0	5.610	0.905	
45	0.051	0.495	0.329	0.121	0.074	1807.0	4.005	1.070	
60	0.051	0.511	0.467	0.136	0.074	1370.6	3.038	1.239	
75	0.051	0.511	0.527	0.203	0.074	1019.9	2.261	1.365	
90	0.051	0.511	0.527	0.290	0.269	0.0	0.000	1.647	

Appendix 11 Siebers and Kraabel Model Heat Loss

	Aperture Radius [m] =		0.229						
	Total Area [m^2] =		1.556						
	Nusselt Number =	154.96							
	Grashoff Number =	4.80E+09							
T mean =	300								
Angle	Sec 1	Sec 2	Sec 3	Sec 4	Sec 5	Heat Loss	h	Total Zone 1	
[degrees]	[m^2]	[m^2]	[m^2]	[m^2]	[m^2]	[Watts]	[Watts/K-m^2]	[m^2]	
0	0.000	0.047	0.135	0.074	0.033	912.7	5.368	0.290	
15	0.018	0.194	0.180	0.081	0.033	811.2	4.771	0.506	
30	0.051	0.346	0.224	0.088	0.033	690.8	4.063	0.742	
45	0.051	0.470	0.285	0.097	0.033	498.1	2.930	0.936	
60	0.051	0.511	0.435	0.112	0.033	361.2	2.125	1.141	
75	0.051	0.511	0.525	0.161	0.033	260.4	1.532	1.280	
90	0.051	0.511	0.327	0.290	0.178	0.0	0.000	1.556	
	Nusselt Number =	181.90							
	Grashoff Number =	6.95E+09							
T mean =	400								
Angle	Sec 1	Sec 2	Sec 3	Sec 4	Sec 5	Heat Loss	h	Total Zone 1	
[degrees]	[m^2]	[m^2]	[m^2]	[m^2]	[m^2]	[Watts]	[Watts/K-m^2]	[m^2]	
0	0.000	0.047	0.135	0.074	0.033	1640.3	6.396	0.290	
15	0.018	0.194	0.180	0.081	0.033	1457.8	5.684	0.506	
30	0.051	0.346	0.224	0.088	0.033	1241.5	4.841	0.742	
45	0.051	0.470	0.285	0.097	0.033	895.3	3.491	0.936	
60	0.051	0.511	0.435	0.112	0.033	649.2	2.531	1.141	
75	0.051	0.511	0.525	0.161	0.033	468.0	1.825	1.280	
90	0.051	0.511	0.327	0.290	0.178	0.0	0.000	1.556	
	Nusselt Number =	204.56							
	Grashoff Number =	9.29E+09							
T mean =	500								
Angle	Sec 1	Sec 2	Sec 3	Sec 4	Sec 5	Heat Loss	h	Total Zone 1	
[degrees]	[m^2]	[m^2]	[m^2]	[m^2]	[m^2]	[Watts]	[Watts/K-m^2]	[m^2]	
0	0.000	0.047	0.135	0.074	0.033	2482.1	7.238	0.290	
15	0.018	0.194	0.180	0.081	0.033	2206.1	6.433	0.506	
30	0.051	0.346	0.224	0.088	0.033	1878.7	5.479	0.742	
45	0.051	0.470	0.285	0.097	0.033	1354.8	3.951	0.936	
60	0.051	0.511	0.435	0.112	0.033	982.3	2.865	1.141	
75	0.051	0.511	0.525	0.161	0.033	708.2	2.065	1.280	
90	0.051	0.511	0.327	0.290	0.178	0.0	0.000	1.556	
	Nusselt Number =	224.58							
	Grashoff Number =	1.16E+10							
T mean =	600								
Angle	Sec 1	Sec 2	Sec 3	Sec 4	Sec 5	Heat Loss	h	Total Zone 1	
[degrees]	[m^2]	[m^2]	[m^2]	[m^2]	[m^2]	[Watts]	[Watts/K-m^2]	[m^2]	
0	0.000	0.047	0.135	0.074	0.033	3420.3	7.966	0.290	
15	0.018	0.194	0.180	0.081	0.033	3039.9	7.080	0.506	
30	0.051	0.346	0.224	0.088	0.033	2588.8	6.029	0.742	
45	0.051	0.470	0.285	0.097	0.033	1866.8	4.348	0.936	
60	0.051	0.511	0.435	0.112	0.033	1353.6	3.153	1.141	
75	0.051	0.511	0.525	0.161	0.033	975.9	2.273	1.280	
90	0.051	0.511	0.327	0.290	0.178	0.0	0.000	1.556	

Appendix 11 Siebers and Kraabel Model Heat Loss

	Aperture Radius [m] =		0.329					
	Total Area [m^2] =		1.380					
Nusselt Number =	157.49							
Grashoff Number =	4.80E+09							
T mean =	300							
Angle	Sec 1	Sec 2	Sec 3	Sec 4	Sec 5	Heat Loss	h	Total Zone 1
[degrees]	[m^2]	[m^2]	[m^2]	[m^2]	[m^2]	[Watts]	[Watts/K-m^2]	[m^2]
0	0.000	0.000	0.013	0.007	0.000	949.3	6.034	0.020
15	0.000	0.044	0.110	0.026	0.000	877.4	5.578	0.180
30	0.036	0.244	0.166	0.037	0.000	730.9	4.646	0.482
45	0.051	0.424	0.229	0.048	0.000	510.6	3.246	0.752
60	0.051	0.511	0.381	0.064	0.000	337.2	2.143	1.006
75	0.051	0.511	0.515	0.105	0.000	203.2	1.292	1.182
90	0.051	0.511	0.327	0.290	0.002	0.0	0.000	1.380
Nusselt Number =	183.96							
Grashoff Number =	7.14E+09							
T mean =	400							
Angle	Sec 1	Sec 2	Sec 3	Sec 4	Sec 5	Heat Loss	h	Total Zone 1
[degrees]	[m^2]	[m^2]	[m^2]	[m^2]	[m^2]	[Watts]	[Watts/K-m^2]	[m^2]
0	0.000	0.000	0.013	0.007	0.000	1672.2	7.146	0.020
15	0.000	0.044	0.110	0.026	0.000	1545.6	6.605	0.180
30	0.036	0.244	0.166	0.037	0.000	1287.5	5.502	0.482
45	0.051	0.424	0.229	0.048	0.000	899.4	3.844	0.752
60	0.051	0.511	0.381	0.064	0.000	594.0	2.539	1.006
75	0.051	0.511	0.515	0.105	0.000	357.9	1.530	1.182
90	0.051	0.511	0.327	0.290	0.002	0.0	0.000	1.380
Nusselt Number =	206.34							
Grashoff Number =	9.49E+09							
T mean =	500							
Angle	Sec 1	Sec 2	Sec 3	Sec 4	Sec 5	Heat Loss	h	Total Zone 1
[degrees]	[m^2]	[m^2]	[m^2]	[m^2]	[m^2]	[Watts]	[Watts/K-m^2]	[m^2]
0	0.000	0.000	0.013	0.007	0.000	2505.2	8.064	0.020
15	0.000	0.044	0.110	0.026	0.000	2315.3	7.453	0.180
30	0.036	0.244	0.166	0.037	0.000	1928.8	6.209	0.482
45	0.051	0.424	0.229	0.048	0.000	1347.4	4.337	0.752
60	0.051	0.511	0.381	0.064	0.000	889.9	2.864	1.006
75	0.051	0.511	0.515	0.105	0.000	536.2	1.726	1.182
90	0.051	0.511	0.327	0.290	0.002	0.0	0.000	1.380
Nusselt Number =	226.19							
Grashoff Number =	1.18E+10							
T mean =	600							
Angle	Sec 1	Sec 2	Sec 3	Sec 4	Sec 5	Heat Loss	h	Total Zone 1
[degrees]	[m^2]	[m^2]	[m^2]	[m^2]	[m^2]	[Watts]	[Watts/K-m^2]	[m^2]
0	0.000	0.000	0.013	0.007	0.000	3431.3	8.858	0.020
15	0.000	0.044	0.110	0.026	0.000	3171.5	8.188	0.180
30	0.036	0.244	0.166	0.037	0.000	2641.9	6.820	0.482
45	0.051	0.424	0.229	0.048	0.000	1845.5	4.764	0.752
60	0.051	0.511	0.381	0.064	0.000	1218.8	3.147	1.006
75	0.051	0.511	0.515	0.105	0.000	734.4	1.896	1.182
90	0.051	0.511	0.327	0.290	0.002	0.0	0.000	1.380

APPENDIX 12: Stine and McDonald Model Computer Program Listing

```
REM     **********************************************************
REM
REM                     Stine & McDonald Method
REM
REM     **********************************************************
REM     **********************************************************
    PRINT " Stine & McDonald Method of Predicting Convective Losses"
    PRINT
    PRINT
REM     **********************************************************
REM     **********************************************************
REM        ******************  Receiver  Geometry  ********************
Re=.127                 :REM  end plate radius [m]
Rc=.33                  :REM  cavity radius [m]
Lf=.292                 :REM  frustum length [m]
Lh=.254                 :REM cylinder length hot [m]
Lc=.14                  :REM cylinder length cold [m]
L=2*Rc                  :REM characteristic length [m]
REM     **********************************************************
REM        *******************  Constants  ************************
  pi=4*ATN(1)
  Ta=70 :Tak=(Ta+459.67)/1.8                 :REM  ambient temperature [°F]
REM     **********************************************************
OPEN "CLIP:" FOR OUTPUT AS #1
REM       *************  write  header  to  clipboard  *******************
WRITE#1, " Stine & McDonald Method"
WRITE#1,
    WRITE#1,"","","End Plate Radius [m] = ",Re
    WRITE#1,"","","Cavity Radius [m] = ",Rc
    WRITE#1,"","","Frustum Length [m] = ",Lf
    WRITE#1,"","","Hot Cylindrical Section Length [m] = ",Lh
    WRITE#1,"","","Cold Cylindrical Section Length [m] = ",Lc
    WRITE#1,"","","T amb [°F] = ",Ta
WRITE#1,
REM       ****************  Receiver  Aperture  Radius  Loop  *************
  FOR rad=1 TO 4
  READ Ra
  DATA .0762, .1524, .2286, .329
  Da=2*Ra
REM     **********************************************************
REM        ****************  Area  Constants  ************************
REM   In the following section area 1, area 2, and area 3 are calculated.
REM   At is the total interior cavity surface area.
REM   Ah is the simplified cavity tube surface area
REM   Ar  is the simplified refractory cavity surface area
  Ah=pi*(Re+Rc)*(Lf^2+(Rc-Re)^2)^.5+2*pi*Rc*Lh
  Ar=pi*Re^2+pi*(Rc^2-Ra^2)+2*pi*Rc*Lc
  At=Ah+Ar
REM     **********************************************************
REM        ****************  Print  Header  ***************************
PRINT " Stine & McDonald Method"
PRINT
    PRINT "End Plate Radius [m] = ";Re
```

```
    PRINT "Cavity Radius [m] = ";Rc
    PRINT "Aperture Radius [m] = ";Ra
    PRINT "Frustum Length [m] = ";Lf
    PRINT "Hot Cylindrical Section Length [m] = ";Lh
    PRINT "Cold Cylindrical Section Length [m] = ";Lc
    PRINT "T amb [°F] = ";Ta; "  [k] = ";Tak
    PRINT " Total Area [m^2] = ";At
PRINT
REM       ************************************************************
REM       *************   write header to clipboard   ********************
WRITE#1,
    WRITE#1,"","","Aperture Radius [m] = ",Ra
    WRITE#1,"",""," Total Area [m^2] = ",At
REM       **************   Operating Temperature Loop   *****************
REM
   FOR Th=300 TO 600 STEP 100
   REM mean system operating temperature of receiver [°F]
   Tr=Th-100
   Tw=(Th*Ah+Tr*Ar)/At
   CLS
REM       ************************************************************
REM            **********************   Air  Properties   *********************
REM   The value of 'k' calculated here is the product of the gravitational
REM   constant times the coefficient of volumetric expansion divided by
REM    the kinematic viscosity squared. (i.e.. g B/v^2 [1/K-m^3]) The
REM   equation for 'k' is based on data from Table A-1, p. 388, Kays & Crawford,
REM   " Convective Heat and Mass Transfer ", second edition, McGraw-Hill.
PRINT
   gBv=1.1547E+19*Tak^-4.4187
   Gr=gBv*(Th-Ta)/1.8*L^3     :REM Grashoff number
k=.0071749261015#+.000064030639041#*Tak :REM thermal conductivity of air
REM       ************************************************************
REM          ********************   Print  Table  Header   ******************
    PRINT "Grashoff Number =";Gr
    PRINT "T mean [°F] = ";Th
PRINT ;TAB(3);" Angle";TAB(11);"Nu";TAB(19);"Heat Loss";TAB(27);"   h   "
PRINT  ;TAB(1);"  [degrees]";TAB(11);"";TAB(19);"[Watts]";TAB(27);"[Watts/K-m^
2]"
PRINT
REM       ************************************************************
REM       ************   WRITE  HEADER  TO  CLIPBOARD   ******************
WRITE#1,"","Grashoff Number =",Gr
WRITE#1,"T mean = ",Th
WRITE#1,
WRITE#1,"Angle","Nu","Heat Loss","h"
WRITE#1,"[degrees]","","[Watts]","[Watts/K-m^2]"
REM         *******************   Beginning  of  Angle  Loop  *****************
FOR a=-90 TO 90 STEP 15
    z=pi*a/180
REM       ************************************************************
REM         *****************   Heat  Loss  Calculation   ********************
s=-.982*(Da/L)+1.12
IF a=90 THEN 200
Nu=.088*Gr^(1/3)*((Tw+459.67)/(Ta+459.67))^.18*(COS(z))^2.47   *(Da/L)^s
GOTO 300
```

```
200 :
Nu=0
300 :
:REM Nusselt number
h=Nu*k/L
q=h*At*(Tw-Ta)/1.8
REM          *******************   PRINTER   Output   *************************
REM
PRINT;TAB(4);
PRINT  USING"###.";a;
PRINT;TAB(9);
PRINT  USING  "###.##";Nu;
PRINT;TAB(17);
PRINT  USING  "#####.#";q;
PRINT;TAB(25);
PRINT  USING  "###.####";h
REM  ***************    OUTPUT   TO   CLIPBOARD     ************************
WRITE  #1,a,Nu,q,h
NEXT a
NEXT Th
NEXT rad
PRINT  "bye!"
CLOSE #1
END
```

Appendix 13: Stein and McDonald Model Heat Loss

Stine & McDonald Method			
	End Plate Radius [m] =		0.127
	Cavity Radius [m] =		0.33
	Frustum Length [m] =		0.292
	Hot Cylindrical Section Length [m] =		0.254
	Cold Cylindrical Section Length [m] =		0.14
		T amb [°F] =	70
	Aperture Radius [m] =		0.0762
	Total Area [m^2] =		1.70207
Grashoff Number =		5.24E+9	
T mean =	300		
Angle	Nu	Heat Loss	h
[degrees]		[Watts]	[Watts/K-m^2]
0	44.0	230.0	1.736
15	40.4	211.1	1.593
30	30.9	161.2	1.217
45	18.7	97.7	0.737
60	7.9	41.5	0.313
75	1.6	8.2	0.062
90	0.0	0.0	0.000
Grashoff Number =		7.51E+9	
T mean =	400		
Angle	Nu	Heat Loss	h
[degrees]		[Watts]	[Watts/K-m^2]
0	50.8	380.6	2.002
15	46.6	349.4	1.837
30	35.6	266.8	1.403
45	21.6	161.7	0.850
60	9.2	68.7	0.361
75	1.8	13.5	0.071
90	0.0	0.0	0.000
Grashoff Number =		9.79E+9	
T mean =	500		
Angle	Nu	Heat Loss	h
[degrees]		[Watts]	[Watts/K-m^2]
0	56.6	552.5	2.230
15	51.9	507.2	2.047
30	39.7	387.3	1.563
45	24.0	234.7	0.947
60	10.2	99.7	0.402
75	2.0	19.6	0.079
90	0.0	0.0	0.000
Grashoff Number =		1.21E+10	
T mean =	600		
Angle	Nu	Heat Loss	h
[degrees]		[Watts]	[Watts/K-m^2]
0	61.7	743.3	2.434
15	56.7	682.3	2.234
30	43.3	521.1	1.706
45	26.2	315.8	1.034
60	11.1	134.2	0.439
75	2.2	26.4	0.086
90	0.0	0.0	0.000

Appendix 13: Stein and McDonald Model Heat Loss

	Aperture Radius [m] =		0.1524
	Total Area [m^2] =		1.647346
	Grashoff Number =	5.24E+9	
T mean =	300		
Angle	Nu	Heat Loss	h
[degrees]		[Watts]	[Watts/K-m^2]
0	97.4	509.0	3.841
15	89.4	467.3	3.525
30	68.3	356.8	2.692
45	41.4	216.3	1.632
60	17.6	91.9	0.693
75	3.5	18.1	0.136
90	0.0	0.0	0.000
	Grashoff Number =	7.51E+9	
T mean =	400		
Angle	Nu	Heat Loss	h
[degrees]		[Watts]	[Watts/K-m^2]
0	112.4	842.3	4.429
15	103.1	773.2	4.066
30	78.8	590.4	3.105
45	47.7	357.8	1.882
60	20.3	152.0	0.799
75	4.0	29.9	0.157
90	0.0	0.0	0.000
	Grashoff Number =	9.79E+9	
T mean =	500		
Angle	Nu	Heat Loss	h
[degrees]		[Watts]	[Watts/K-m^2]
0	125.2	1222.7	4.935
15	114.9	1122.4	4.530
30	87.8	857.1	3.459
45	53.2	519.5	2.096
60	22.6	220.7	0.891
75	4.4	43.4	0.175
90	0.0	0.0	0.000
	Grashoff Number =	1.21E+10	
T mean =	600		
Angle	Nu	Heat Loss	h
[degrees]		[Watts]	[Watts/K-m^2]
0	136.6	1645.0	5.386
15	125.4	1510.0	4.944
30	95.8	1153.1	3.776
45	58.0	698.9	2.288
60	24.7	296.9	0.972
75	4.8	58.4	0.191
90	0.0	0.0	0.000

Appendix 13: Stein and McDonald Model Heat Loss

	Aperture Radius [m] =	0.2286	
	Total Area [m^2] =	1.556138	
	Grashoff Number =	5.24E+9	
T mean =	300		
Angle	Nu	Heat Loss	h
[degrees]		[Watts]	[Watts/K-m^2]
0	138.7	724.9	5.469
15	127.4	665.4	5.020
30	97.3	508.1	3.834
45	58.9	308.0	2.324
60	25.0	130.8	0.987
75	4.9	25.7	0.194
90	0.0	0.0	0.000
	Grashoff Number =	7.51E+9	
T mean =	400		
Angle	Nu	Heat Loss	h
[degrees]		[Watts]	[Watts/K-m^2]
0	160.0	1199.4	6.307
15	146.9	1101.0	5.790
30	112.2	840.8	4.421
45	68.0	509.6	2.680
60	28.9	216.5	1.138
75	5.7	42.6	0.224
90	0.0	0.0	0.000
	Grashoff Number =	9.79E+9	
T mean =	500		
Angle	Nu	Heat Loss	h
[degrees]		[Watts]	[Watts/K-m^2]
0	178.3	1741.2	7.027
15	163.6	1598.3	6.450
30	125.0	1220.5	4.926
45	75.7	739.7	2.985
60	32.2	314.3	1.268
75	6.3	61.8	0.249
90	0.0	0.0	0.000
	Grashoff Number =	1.21E+10	
T mean =	600		
Angle	Nu	Heat Loss	h
[degrees]		[Watts]	[Watts/K-m^2]
0	194.6	2342.5	7.670
15	178.6	2150.2	7.041
30	136.4	1642.0	5.376
45	82.7	995.2	3.259
60	35.1	422.8	1.384
75	6.9	83.1	0.272
90	0.0	0.0	0.000

Appendix 13: Stein and McDonald Model Heat Loss

	Aperture Radius [m] =		0.329
	Total Area [m^2] =		1.380262
	Grashoff Number =	5.24E+9	
T mean =	300		
Angle	Nu	Heat Loss	h
[degrees]		[Watts]	[Watts/K-m^2]
0	163.0	851.5	6.425
15	149.6	781.6	5.897
30	114.2	596.9	4.504
45	69.2	361.8	2.729
60	29.4	153.7	1.160
75	5.8	30.2	0.228
90	0.0	0.0	0.000
	Grashoff Number =	7.51E+9	
T mean =	400		
Angle	Nu	Heat Loss	h
[degrees]		[Watts]	[Watts/K-m^2]
0	188.0	1409.0	7.409
15	172.5	1293.3	6.801
30	131.8	987.6	5.194
45	79.9	598.6	3.148
60	33.9	254.3	1.337
75	6.7	50.0	0.263
90	0.0	0.0	0.000
	Grashoff Number =	9.79E+9	
T mean =	500		
Angle	Nu	Heat Loss	h
[degrees]		[Watts]	[Watts/K-m^2]
0	209.4	2045.4	8.255
15	192.2	1877.5	7.577
30	146.8	1433.8	5.786
45	89.0	869.0	3.507
60	37.8	369.2	1.490
75	7.4	72.6	0.293
90	0.0	0.0	0.000
	Grashoff Number =	1.21E+10	
T mean =	600		
Angle	Nu	Heat Loss	h
[degrees]		[Watts]	[Watts/K-m^2]
0	228.6	2751.7	9.010
15	209.8	2525.9	8.270
30	160.2	1928.9	6.316
45	97.1	1169.0	3.828
60	41.3	496.7	1.626
75	8.1	97.7	0.320
90	0.0	0.0	0.000

Appendix 14: Shape Factors Formulas

All formulas are developed from the basic disc-to-disc shape factor formula [20]. The N by N coefficient matrix of the heat loss equation requires N^2 shape factor equations (Eqn. 1). The shape factor equations are solved using a digital computer. The following section shows the development of the shape factor formulas used in the coefficient matrix.

<u>(a) End Plate (section 1 ↔ aperture):</u>

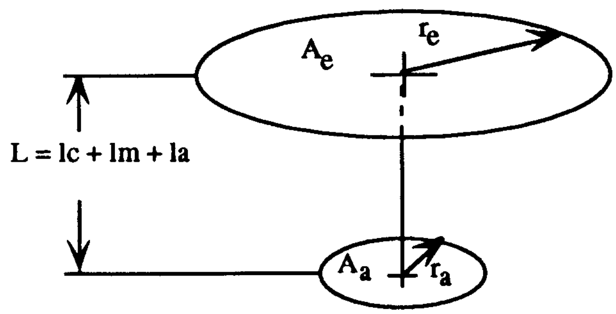

let $R_e = \frac{r_e}{L}$, $R_a = \frac{r_a}{L}$, and $X = 1 + \frac{1 + R_e^2}{R_a^2}$

$$F_{A_e - A_a} = \frac{A_a}{A_e} F_{A_a - A_e}$$

$$F_{A_e - A_a} = \frac{A_a}{2A_e} \left[X - \sqrt{X^2 - 4 \left(R_e / R_a\right)^2} \right]$$

$$F_{A_e - A_a} = \frac{r_a^2}{2r_e^2} \left[1 + \frac{L^2 + r_e^2}{r_a^2} - \sqrt{\left(1 + \frac{L^2 + r_e^2}{r_a^2}\right)^2 - 4 \left(\frac{r_e}{r_a}\right)^2} \right]$$

$$F_{A_e - A_a} = \frac{1}{2r_e^2} \left\{ (l_c + l_m + l_a)^2 + r_a^2 + r_e^2 - \sqrt{\left[(l_c + l_m + l_a)^2 + r_a^2 + r_e^2\right]^2 - 4 (r_e r_a)^2} \right\}$$

<u>(b) Center Cylinder (section 3 ↔ aperture):</u>

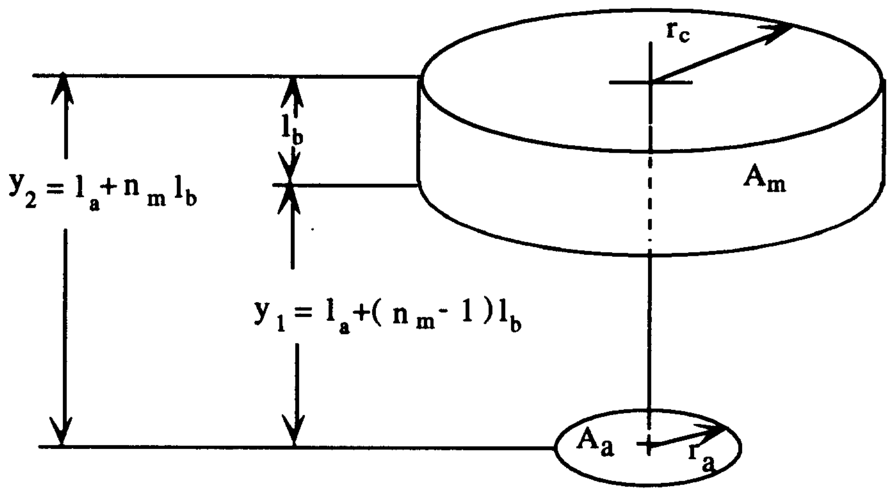

$$F_{A_a - A_{section}} = F_{A_a - x\text{-}section_1} - F_{A_a - x\text{-}section_2}$$

$$A_a F_{A_a - A_{section}} = A_{section} F_{A_{section} - A_a}$$

$$F_{A_{section} - A_a} = \frac{A_a}{A_{section}} F_{A_a - A_{section}}$$

$$F_{A_{section} - A_a} = \frac{A_a}{A_{section}} [F_{A_a - x\text{-}section_1} - F_{A_a - x\text{-}section_2}]$$

$$F_{A_{section} - A_a} = \frac{A_a}{A_{section}} [\frac{A_c}{A_a} F_{x\text{-}section_1 - A_a} - \frac{A_c}{A_a} F_{x\text{-}section_2 - A_a}]$$

$$F_{A_{section} - A_a} = \frac{A_c}{A_{section}} [F_{x\text{-}section_1 - A_a} - F_{x\text{-}section_2 - A_a}]$$

$$F_{A_{section} - A_a} = \frac{r_c}{2l_b} [F_{x\text{-}section_1 - A_a} - F_{x\text{-}section_2 - A_a}]$$

let $R_1 = \frac{r_c}{y}$, $\quad R_2 = \frac{r_a}{y}$, $\quad X = 1 + \frac{1 + R_2^2}{R_1^2}$

then $F_{A_{x\text{-}section} - A_a} = \frac{1}{2} [X - \sqrt{X^2 - 4\left(\frac{R_2}{R_1}\right)^2}]$

$$F_{A_{x\text{-}section} - A_a} = \frac{1}{2} [1 + \frac{1 + R_2^2}{R_1^2} - \sqrt{\left(1 + \frac{1 + R_2^2}{R_1^2}\right)^2 - 4\left(\frac{R_2}{R_1}\right)^2}]$$

$$F_{A_{x\text{-section}_2}-A_a} = \frac{1}{2}\left[1 + \frac{1 + r_a^2/y_2^2}{r_c^2/y_2^2} - \sqrt{\left(1 + \frac{1 + r_a^2/y_2^2}{r_c^2/y_2^2}\right)^2 - 4\left(\frac{r_a}{r_c}\right)^2} \right]$$

$$F_{A_{x\text{-section}_2}-A_a} = \frac{1}{2}\left[1 + \frac{y_2^2 + r_a^2}{r_c^2} - \sqrt{\left(1 + \frac{y_2^2 + r_a^2}{r_c^2}\right)^2 - 4\left(\frac{r_a}{r_c}\right)^2} \right]$$

and similarly:

$$F_{A_{x\text{-section}_1}-A_a} = \frac{1}{2}\left[1 + \frac{y_1^2 + r_a^2}{r_c^2} - \sqrt{\left(1 + \frac{y_1^2 + r_a^2}{r_c^2}\right)^2 - 4\left(\frac{r_a}{r_c}\right)^2} \right]$$

$$F_{A_{section}-A_a} = \frac{r_c}{4l_b}\left[\frac{y_1^2 + r_a^2}{r_c^2} - \sqrt{\left(1 + \frac{y_1^2 + r_a^2}{r_c^2}\right)^2 - 4\left(\frac{r_a}{r_c}\right)^2} - \frac{y_2^2 + r_a^2}{r_c^2} + \sqrt{\left(1 + \frac{y_2^2 + r_a^2}{r_c^2}\right)^2 - 4\left(\frac{r_a}{r_c}\right)^2} \right]$$

$$F_{A_{section}-A_a} = \frac{1}{4r_c l_b}\left[y_1^2 - y_2^2 - \sqrt{(r_a^2 + y_1^2 + r_c^2)^2 - 4(r_c r_a)^2} + \sqrt{(r_a^2 + y_2^2 + r_c^2)^2 - 4(r_c r_a)^2} \right]$$

$$F_{A_{section}-A_a} = \frac{1}{4r_c l_b}\left[(l_a + (n_m - 1)l_b)^2 - (l_a + n_m l_b)^2 - \sqrt{[(l_a + (n_m - 1)l_b)^2 + r_a^2 + r_c^2]^2 - 4(r_c r_a)^2} + \sqrt{[(l_a + n_m l_b)^2 + r_a^2 + r_c^2]^2 - 4(r_c r_a)^2} \right]$$

(c) Frustum (section 2 ↔ aperture):

The view factor for a section of the frustum from A_a is equal to the view factor from A_a to the circular cross-sectional area on the bottom of the frustum section minus the view factor from A_a to the circular cross-section on the top of the frustum section.

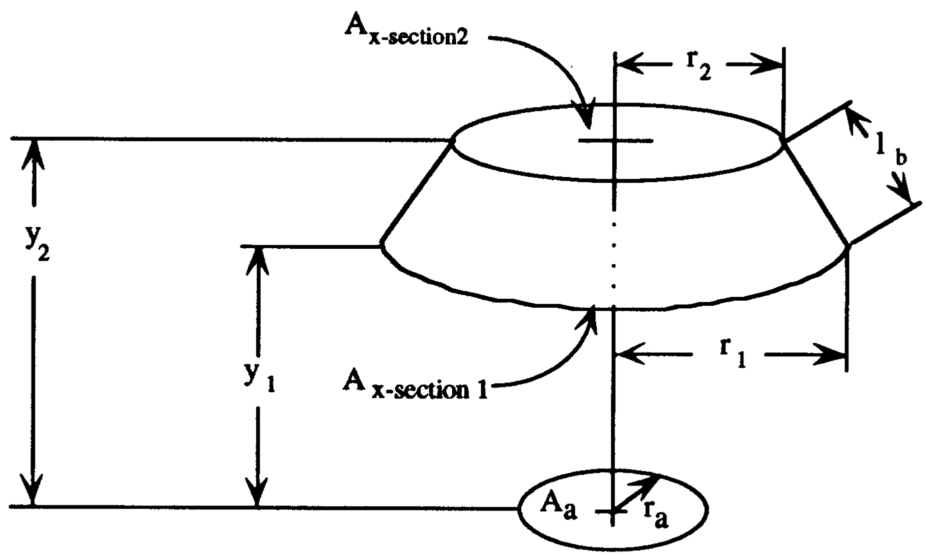

$$F_{A_a - A_{section}} = F_{A_a - x\text{-}section_1} - F_{A_a - x\text{-}section_2}$$

$$A_a F_{A_a - A_{section}} = A_{section} F_{A_{section} - A_a}$$

$$F_{A_{section} - A_a} = \frac{A_a}{A_{section}} F_{A_a - A_{section}}$$

$$F_{A_{section} - A_a} = \frac{A_a}{A_c} [F_{A_a - x\text{-}section_1} - F_{A_a - x\text{-}section_2}]$$

$$F_{A_{section} - A_a} = \frac{A_a}{A_{section}} [\frac{A_{x\text{-}section_1}}{A_a} F_{x\text{-}section_1 - A_a} - \frac{A_{x\text{-}section_2}}{A_a} F_{x\text{-}section_2 - A_a}]$$

$$F_{A_{section} - A_a} = \frac{1}{A_{section}} [A_{x\text{-}section_1} F_{x\text{-}section_1 - A_a} - A_{x\text{-}section_2} F_{x\text{-}section_2 - A_a}]$$

$$F_{A_{section} - A_a} = \frac{1}{(r_1 + r_2) l_b} [r_1^2 F_{x\text{-}section_1 - A_a} - r_2^2 F_{x\text{-}section_2 - A_a}]$$

let $R_1 = \frac{r_{x\text{-}section}}{y}$, $R_2 = \frac{r_a}{y}$, $X = 1 + \frac{1 + R_2^2}{R_1^2}$

$$\text{then } F_{A_{x\text{-section}} - A_a} = \frac{1}{2}\left[X - \sqrt{X^2 - 4\left(\frac{R_2}{R_1}\right)^2}\right]$$

$$F_{A_{x\text{-section}} - A_a} = \frac{1}{2}\left[1 + \frac{1 + R_2^2}{R_1^2} - \sqrt{\left(1 + \frac{1 + R_2^2}{R_1^2}\right)^2 - 4\left(\frac{R_2}{R_1}\right)^2}\right]$$

$$F_{A_{x\text{-section}_2} - A_a} = \frac{1}{2}\left[1 + \frac{1 + r_a^2/h_2^2}{r_2^2/h_2^2} - \sqrt{\left(1 + \frac{1 + r_a^2/h_2^2}{r_2^2/h_2^2}\right)^2 - 4\left(\frac{r_a}{r_2}\right)^2}\right]$$

$$F_{A_{x\text{-section}_2} - A_a} = \frac{1}{2}\left[1 + \frac{h_2^2 + r_a^2}{r_2^2} - \sqrt{\left(1 + \frac{h_2^2 + r_a^2}{r_2^2}\right)^2 - 4\left(\frac{r_a}{r_2}\right)^2}\right]$$

and similarly:

$$F_{A_{x\text{-section}_1} - A_a} = \frac{1}{2}\left[1 + \frac{h_1^2 + r_a^2}{r_1^2} - \sqrt{\left(1 + \frac{h_1^2 + r_a^2}{r_1^2}\right)^2 - 4\left(\frac{r_a}{r_1}\right)^2}\right]$$

$$F_{A_{section} - A_a} = \frac{1}{2l_b(r_1 + r_2)}\left[r_1^2 - r_2^2 + h_1^2 - h_2^2 - \sqrt{(r_1^2 + h_1^2 + r_a^2)^2 - 4(r_1 r_a)^2} + \sqrt{(r_2^2 + h_2^2 + r_a^2)^2 - 4(r_2 r_a)^2}\right]$$

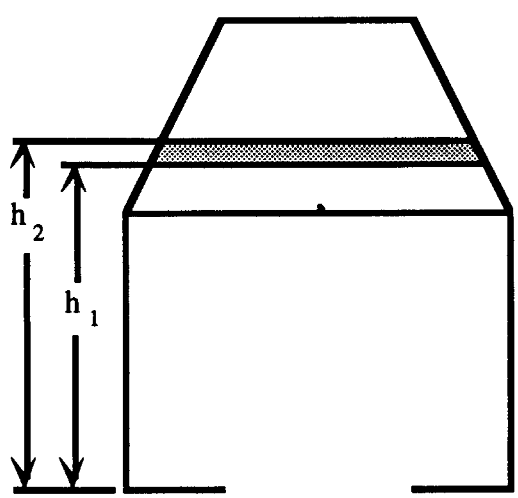

$$h_1 = l_a + l_m + (n_m - 1)\frac{l_c}{N_c} \qquad h_2 = l_a + l_m + n_m \frac{l_c}{N_c}$$

$$r_2 = r_c - n_m \frac{r_c - r_e}{N_c} \qquad r_1 = r_c - (n_m - 1)\frac{r_c - r_e}{N_c}$$

$$F_{n_m - A_a} = \frac{1}{2l_b\left[2r_c - (2n_m - 1)\frac{(r_c - r_e)}{N_c}\right]} \left\{\left[r_c - (n_m - 1)\left(\frac{r_c - r_e}{N_c}\right)\right]^2 - \left[r_c - n_m\left(\frac{r_c - r_e}{N_c}\right)\right]^2\right.$$

$$+\left[l_a + l_m + (n_m - 1)\frac{l_c}{N_c}\right]^2 - \left[l_a + l_m + n_m \frac{l_c}{N_c}\right]^2$$

$$-\sqrt{\left\{\left[r_c - (n_m - 1)\left(\frac{r_c - r_e}{N_c}\right)\right]^2 + \left(l_a + l_m + (n_m - 1)\frac{l_c}{N_c}\right)^2 + r_a^2\right\}^2 - 4\left\{\left[r_c - (n_m - 1)\left(\frac{r_c - r_e}{N_c}\right)\right]r_a\right\}^2}$$

$$+\sqrt{\left\{\left[r_c - n_m\left(\frac{r_c - r_e}{N_c}\right)\right]^2 + \left(l_a + l_m + n_m \frac{l_c}{N_c}\right)^2 + r_a^2\right\}^2 - 4\left\{\left[r_c - n_m\left(\frac{r_c - r_e}{N_c}\right)\right]r_a\right\}^2}$$

(d) Spacer Ring (section 4 ↔ aperture):

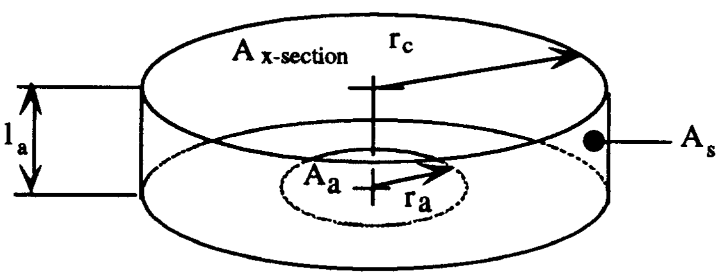

$$F_{A_a - A_s} = 1 - F_{A_a - A_{x\text{-section}}}$$

$$F_{A_s - A_a} = \frac{A_a}{A_s} F_{A_a - A_s}$$

$$F_{A_a - A_{x\text{-section}}} = \frac{A_{x\text{-section}}}{A_a} F_{A_{x\text{-section}} - A_a}$$

$$F_{A_s - A_a} = \frac{A_a}{A_s}\left[1 - \frac{A_{x\text{-section}}}{A_a} F_{A_{x\text{-section}} - A_a}\right]$$

$$F_{A_{x\text{-section}} - A_a} = \frac{1}{2}\left[X - \sqrt{X^2 - 4\left(\frac{R_a}{R_c}\right)^2}\right]$$

$$F_{A_s - A_a} = \frac{r_a^2}{2r_c l_a}\left\{1 - \frac{r_c^2}{2r_a^2}\left[X - \sqrt{X^2 - 4\left(\frac{R_a}{R_c}\right)^2}\right]\right\}$$

where $R_a = \frac{r_a}{l_a}$, $R_c = \frac{r_c}{l_a}$

$$X = 1 + \frac{1 + (r_a/l_a)^2}{(r_c/l_a)^2}$$

$$X = 1 + \frac{l_a^2 + r_a^2}{r_c^2}$$

therefore:

$$F_{A_{x\text{-section}} - A_a} = \frac{1}{2}\left[1 + \frac{l_a^2 + r_a^2}{r_c^2} - \sqrt{\left(1 + \frac{l_a^2 + r_a^2}{r_c^2}\right)^2 - 4\left(\frac{r_a}{r_c}\right)^2}\right]$$

$$F_{A_s - A_a} = \frac{r_a^2}{2r_c l_a}\left\{1 - \frac{r_c^2}{2r_a^2}\left[1 + \frac{l_a^2 + r_a^2}{r_c^2} - \sqrt{\left(1 + \frac{l_a^2 + r_a^2}{r_c^2}\right)^2 - 4\left(\frac{r_a}{r_c}\right)^2}\right]\right\}$$

$$F_{A_s - A_a} = \frac{r_a^2}{2r_c l_a}\{1 - \frac{1}{2r_a^2}[(r_c^2 + l_a^2 + r_a^2) - \sqrt{(r_c^2 + l_a^2 + r_a^2)^2 - 4(r_a r_c)^2}\ ]\}$$

<u>(e)(section i_{band} $j \leftrightarrow$ section i_{band} j): Shape Factors from a Surface Onto Itself</u>

For the flat surfaces (aperture, annulus, and end plate) $F_{i-i} = 0$

For the cylindrical and frustum sections:

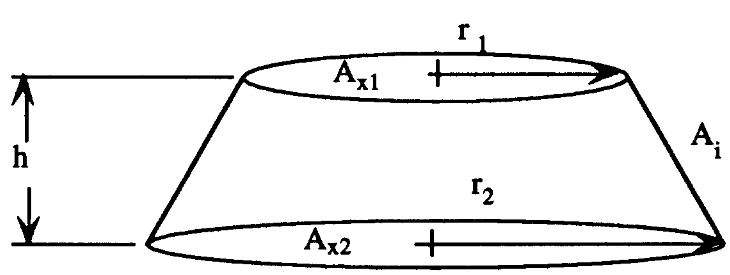

$$F_{i-i} = 1 - F_{i-x1} - F_{i-x2}$$

$$F_{i-x1} = \frac{A_{x1}}{A_i}F_{x1-i} \quad \text{and} \quad F_{i-x2} = \frac{A_{x2}}{A_i}F_{x2-i}$$

therefore

$$F_{i-x1} = \frac{A_{x1}}{A_i}F_{x1-i} \quad \text{and} \quad F_{i-x2} = \frac{A_{x2}}{A_i}F_{x2-i}$$

and

$$F_{x1-i} = 1 - F_{x1-x2} \quad \text{and} \quad F_{x2-i} = 1 - F_{x2-x1}$$

$$F_{x2-x1} = \frac{A_{x1}}{A_{x2}} F_{x1-x2}$$

$$F_{i-i} = 1 - \frac{A_{x1}}{A_i}\left[1 - F_{x1-x2}\right] - \frac{A_{x2}}{A_i}\left[1 - \frac{A_{x1}}{A_{x2}} F_{x1-x2}\right]$$

$$F_{i-i} = 1 - \frac{A_{x1}}{A_i} - \frac{A_{x2}}{A_i} + 2\frac{A_{x1}}{A_i} F_{x1-x2}$$

$$F_{x1-x2} = \frac{1}{2}\left[X - \sqrt{X^2 - 4\left[\frac{R_2}{R_2}\right]^2}\,\right]$$

$$\text{where} \quad R_1 = \frac{r_1}{h}, \quad R_2 = \frac{r_2}{h}, \quad \text{and } X = 1 + \frac{h^2 + r_2^2}{r_1^2}$$

$$F_{x1-x2} = \frac{1}{2}\left[1 + \frac{h^2 + r_2^2}{r_1^2} - \sqrt{\left[1 + \frac{h^2 + r_2^2}{r_1^2}\right]^2 - 4\left[\frac{r_2}{r_1}\right]^2}\,\right]$$

$$F_{i-i} = 1 - \frac{A_{x1}}{A_i} - \frac{A_{x2}}{A_i} + \frac{A_{x1}}{A_i}\left[1 + \frac{h^2 + r_2^2}{r_1^2} - \sqrt{\left[1 + \frac{h^2 + r_2^2}{r_1^2}\right]^2 - 4\left[\frac{r_2}{r_1}\right]^2}\,\right]$$

$$F_{i-i} = 1 - \frac{r_2^2}{(r_1 + r_2)l_b} + \frac{r_1^2}{(r_1 + r_2)l_b}\left[\frac{h^2 + r_2^2}{r_1^2} - \sqrt{\left[1 + \frac{h^2 + r_2^2}{r_1^2}\right]^2 - 4\left[\frac{r_2}{r_1}\right]^2}\,\right]$$

For the spacer ring (section 4 $\leftrightarrow$ section 4):

$$r_1 = r_2 = r_c \quad \text{and} \quad h = l_a$$

For the hot cylinder (section $3_{\text{band } i}$ $\leftrightarrow$ section $3_{\text{band } i}$):

$$r_1 = r_2 = r_c \quad \text{and} \quad h = l_b$$

For the frustum (section $2_{band\ i} \leftrightarrow$ section $2_{band\ i}$):

$$r_1 = r_c - (r_c - r_e)\frac{(n_c - 1)}{N_c}\ ,\ r_2 = r_c - (r_c - r_e)\frac{n_c}{N_c},\quad \text{and } h = \frac{l_c l_b}{\sqrt{l_c^2 + (r_c - r_e)^2}}$$

<u>Shape Factors from Bands of the Cylindrical and Frustum Sections to other Bands of the Cylindrical and Frustum Sections (section $i_{band\ j} \leftrightarrow$ section $i_{band\ k}$):</u>

The following shape factor formulas are used between different bands of the frustum section, between different bands of the hot cylindrical section, between bands of the hot cylindrical section and bands of the frustum section, between the spacer ring and bands of the hot cylindrical section, and between the spacer ring and bands of the frustum section.

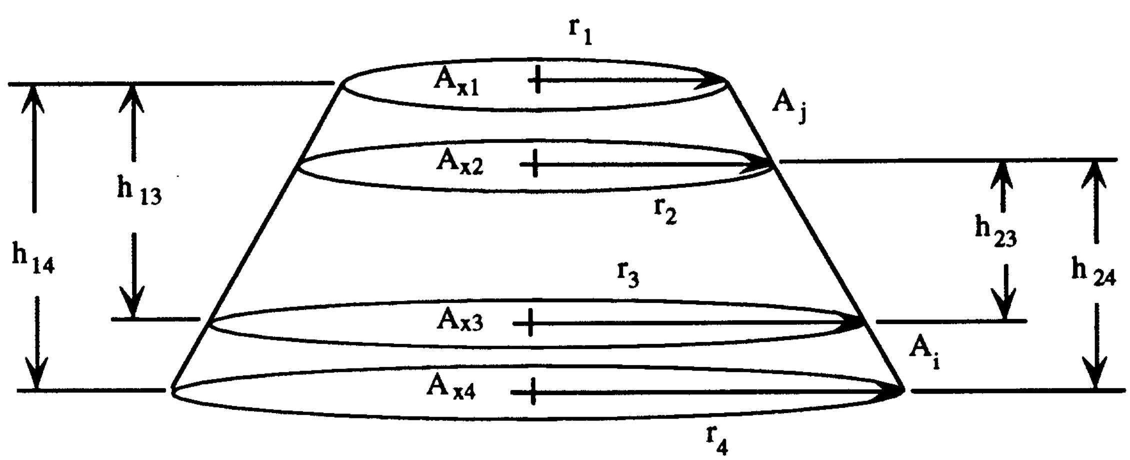

$$F_{i-j}=F_{i-x2}-F_{i-x1}$$

$$F_{x1-i}= F_{xi-x3} - F_{x1-x4}$$

$$F_{x2-i}= F_{x2-x3} - F_{x2-x4}$$

$$F_{i-x1}=\frac{A_{x1}}{A_i}F_{x1-i} \quad \text{and} \quad F_{i-x2}=\frac{A_{x2}}{A_i}F_{x2-i}$$

$$F_{i-j} = \frac{A_{x2}}{A_i}\left[F_{x2-x3} - F_{x2-x4}\right] - \frac{A_{x1}}{A_i}\left[F_{x1-x3} - F_{x1-x4}\right]$$

$$F_{i-j} = \frac{r_2^2}{(r_3 + r_4)l_b}\left[F_{x2-x3} - F_{x2-x4}\right] - \frac{r_1^2}{(r_3 + r_4)l_b}\left[F_{x1-x3} - F_{x1-x4}\right]$$

$$F_{xn-xm} = \frac{1}{2}\left[1 + \frac{h_{nm}^2 + r_m^2}{r_n^2} - \sqrt{\left[1 + \frac{h_{nm}^2 + r_m^2}{r_n^2}\right]^2 - 4\left[\frac{r_m}{r_n}\right]^2}\right]$$

between different bands of the frustum section (section $2_{\text{band } i} \leftrightarrow$ section $2_{\text{band } j}$):

$$r_1 = r_c - (r_c - r_e)\frac{n_j}{N_c}$$

$$r_2 = r_c - (r_c - r_e)\frac{(n_j - 1)}{N_c}$$

$$r_3 = r_c - (r_c - r_e)\frac{n_i}{N_c}$$

$$r_4 = r_c - (r_c - r_e)\frac{(n_i - 1)}{N_c}$$

$$h = \frac{l_c l_b}{\sqrt{l_c^2 + (r_c - r_e)^2}}$$

$$h_{13} = h_{24} = (n_j - n_i)h$$

$$h_{14} = (n_j - n_i + 1)h$$

$$h_{23} = (n_j - n_i - 1)h$$

between different bands of the hot cylindrical section (section $3_{\text{band } i} \leftrightarrow$ section $3_{\text{band } j}$) :

$$r_1 = r_2 = r_3 = r_4 = r_c$$

$$h_{13} = h_{24} = (n_j - n_i)l_b$$

$$h_{14} = (n_j - n_i + 1)l_b$$

$$h_{23} = (n_j - n_i - 1)l_b$$

between bands of the hot cylindrical section and bands of the frustum section (section $2_{\text{band i}} \leftrightarrow$ section $3_{\text{band j}}$):

$$r_1 = r_c - (r_c - r_e)\frac{n_j}{N_c}$$

$$r_2 = r_c - (r_c - r_e)\frac{(n_j - 1)}{N_c}$$

$$r_3 = r_4 = r_c$$

$$h = \frac{l_c l_b}{\sqrt{l_c^2 + (r_c - r_e)^2}}$$

$$h_{13} = h_{24} = l_m - n_i l_b + n_j h$$

$$h_{14} = l_m - (n_i - 1)l_b + n_j h$$

$$h_{23} = l_m - n_i l_b + (n_j - 1)\, h$$

between the spacer ring and bands of the hot cylindrical section (section $4 \leftrightarrow$ section $3_{\text{band i}}$):

$$F_{\text{spacer - j}} = \frac{r_2^2}{(r_3 + r_4)l_a}\left[F_{x2 - x3} - F_{x21 - x4}\right] - \frac{r_1^2}{(r_3 + r_4)l_a}\left[F_{x1 - x3} - F_{x1 - x4}\right]$$

$$F_{xn - xm} = \frac{1}{2}\left[1 + \frac{h_{nm}^2 + r_m^2}{r_n^2} - \sqrt{\left[1 + \frac{h_{nm}^2 + r_m^2}{r_n^2}\right]^2 - 4\left[\frac{r_m}{r_n}\right]^2}\right]$$

$$r_1 = r_2 = r_3 = r_4 = r_c$$

$$h_{13} = n_j\; l_b$$

$$h_{14} = n_j\; l_b + l_a$$

$$h_{23} = (n_j - 1)\; l_b$$

$$h_{24} = (n_j - 1)\; l_b + l_a$$

between the spacer ring and bands of the frustum section (section $4 \leftrightarrow$ section $2_{\text{band i}}$):

$$r_1 = r_c - (r_c - r_e)\frac{n_j}{N_c}$$

$$r_2 = r_c - (r_c - r_e)\frac{(n_j - 1)}{N_c}$$

$$r_3 = r_4 = r_c$$

$$h = \frac{l_c l_b}{\sqrt{l_c^2 + (r_c - r_e)^2}}$$

$$h_{13} = l_m + n_j\ h$$

$$h_{14} = l_m + n_j\ h + l_a$$

$$h_{23} = l_m + (n_j - 1)\ h$$

$$h_{24} = l_m + (n_j - 1)\ h + l_a$$

Shape Factors from Circular Sections to Bands of the Cylindrical and Frustum Sections:

The following shape factor formulas are used between the end plate and bands of the hot cylindrical section, bands of the frustum section, and the spacer section, between the aperture and the bands of the hot cylindrical section, bands of the frustum section, and the spacer section, and between the annulus and aperture combined and bands of the hot cylindrical section, bands of the frustum section, and the spacer section.

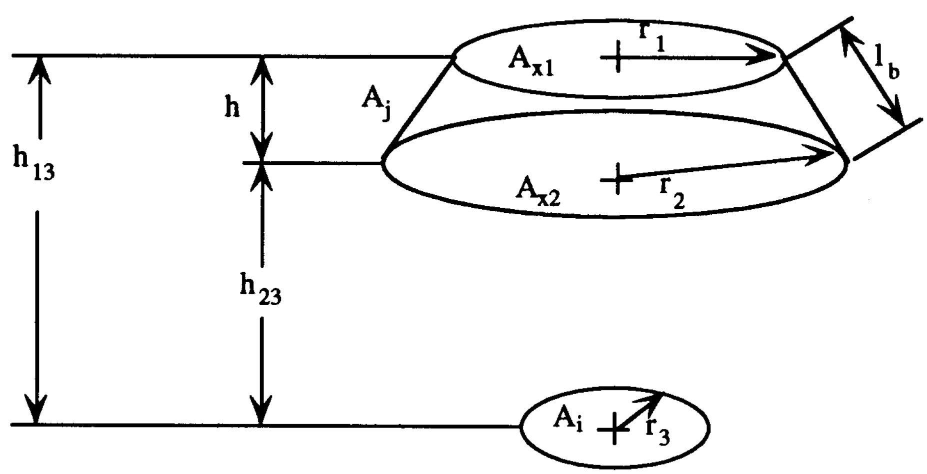

$$F_{i\text{-}j} = F_{i\,\text{-}\,x2} - F_{i\,\text{-}\,x1}$$

$$F_{i\,\text{-}\,x1} = \frac{1}{2}\left[1 + \frac{h_{13}^2 + r_1^2}{r_3^2} - \sqrt{\left[1 + \frac{h_{13}^2 + r_1^2}{r_3^2}\right]^2 - 4\left[\frac{r_1}{r_3}\right]^2}\,\right]$$

$$F_{i\,\text{-}\,x2} = \frac{1}{2}\left[1 + \frac{h_{23}^2 + r_2^2}{r_3^2} - \sqrt{\left[1 + \frac{h_{23}^2 + r_2^2}{r_3^2}\right]^2 - 4\left[\frac{r_2}{r_3}\right]^2}\,\right]$$

$$F_{i\,\text{-}\,j} = \frac{1}{2}\left[\frac{h_{23}^2 + r_2^2}{r_3^2} - \sqrt{\left[1 + \frac{h_{23}^2 + r_2^2}{r_3^2}\right]^2 - 4\left[\frac{r_2}{r_3}\right]^2}\,\right] - \frac{1}{2}\left[\frac{h_{13}^2 + r_1^2}{r_3^2} - \sqrt{\left[1 + \frac{h_{13}^2 + r_1^2}{r_3^2}\right]^2 -$$

between the end plate and bands of the hot cylindrical section (section 1 $\leftrightarrow$ section $3_{\text{band i}}$):

$$r_1 = r_2 = r_c$$

$$r_3 = r_e$$

$$h_{23} = l_c + (N_m - n_j)\, l_b$$

$$h_{13} = l_c + (N_m - n_j + 1)\, l_b$$

between the end plate and bands of the frustum section (section 1 $\leftrightarrow$ section $2_{\text{band i}}$):

$$r_1 = r_e + (r_c - r_e)\left[1 - \frac{n_j - 1}{N_c}\right]$$

$$r_2 = r_e + (r_c - r_e)\left[1 - \frac{n_j}{N_c}\right]$$

$$r_3 = r_e$$

$$h = \frac{l_c l_b}{\sqrt{l_c^2 + (r_c - r_e)^2}}$$

$$h_{23} = (N_c - n_j)\, h$$

$$h_{13} = (N_c - n_j + 1)\, h$$

between the end plate and the spacer section
(section 1 ↔ section 4):

$$r_1 = r_2 = r_c$$

$$r_3 = r_e$$

$$h_{23} = l_c + l_m$$

$$h_{13} = l_c + l_m + l_a$$

between the annulus and aperture combined and bands of the hot cylindrical section
(section 5+ aperture ↔ section $3_{\text{band } i}$):

$$r_1 = r_2 = r_3 = r_c$$

$$h_{23} = l_a + (n_j - 1)\, l_b$$

$$h_{13} = l_a + n_j\, l_b$$

between the annulus and aperture combined and bands of the frustum section
(section 5+ aperture ↔ section $2_{\text{band } i}$):

$$r_1 = r_c - n_j \frac{(r_c - r_e)}{N_c}$$

$$r_2 = r_c - (n_j - 1) \frac{(r_c - r_e)}{N_c}$$

$$r_3 = r_c$$

$$h = \frac{l_c l_b}{\sqrt{l_c^2 + (r_c - r_e)^2}}$$

$$h_{23} = l_a + l_m + (n_j - 1)\, h$$

$$h_{13} = l_a + l_m + n_j\, h$$

between the annulus and aperture combined and the spacer section
(section 5+ aperture ↔ section 4):

$$r_1 = r_2 = r_3 = r_c$$

$$h_{23} = 0$$

$$h_{13} = l_s$$

between the aperture and bands of the hot cylindrical section (aperture ↔ section $3_{\text{bands i}}$):

$$r_1 = r_2 = r_c$$

$$r_3 = r_a$$

$$h_{23} = l_a + (n_j - 1)\, l_b$$

$$h_{13} = l_a + n_j\, l_b$$

between the aperture and bands of the frustum section

(aperture ↔ section $2_{\text{bands i}}$):

$$r_1 = r_c - n_j \frac{(r_c - r_e)}{N_c}$$

$$r_2 = r_c - (n_j - 1) \frac{(r_c - r_e)}{N_c}$$

$$r_3 = r_a$$

$$h = \frac{l_c l_b}{\sqrt{l_c^2 + (r_c - r_e)^2}}$$

$$h_{23} = l_a + l_m + (n_j - 1)\, h$$

$$h_{13} = l_a + l_m + n_j\, h$$

between the aperture and the spacer section (aperture ↔ section 4):

$$r_1 = r_2 = r_c$$

$$r_3 = r_a$$

$$h_{23} = 0$$

$$h_{13} = l_a$$

Shape Factors from Circular Sections to Other Circular Sections:

The following shape factor formulas are used between the end plate and the aperture: and between the end plate and the aperture and annulus combined.

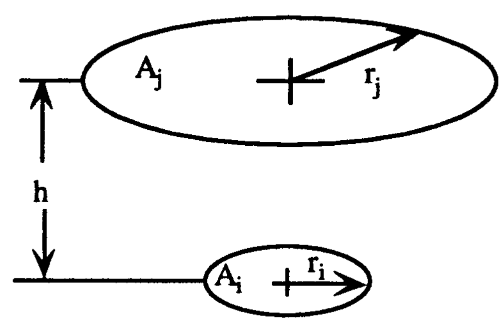

$$F_{i-j} = \frac{1}{2}\left[1 + \frac{h^2 + r_j^2}{r_i^2} - \sqrt{\left[1 + \frac{h^2 + r_j^2}{r_i^2}\right]^2 - 4\left[\frac{r_j}{r_i}\right]^2}\,\right]$$

between the end plate and the aperture
(section 1 ↔ aperture):

$$r_i = r_e$$

$$r_j = r_a$$

$$h = l_a + l_m + l_c$$

between the end plate and the aperture and annulus combined
(section 1 ↔ aperture + section 5):

$$r_i = r_e$$

$$r_j = r_c$$

$$h = l_a + l_m + l_c$$

For shape factors from the spacer section, bands of the hot cylindrical section, and bands of the frustum section to the annulus section the following relationship is used:

$$F_{i\text{ - annulus}} = F_{i\text{ - (annulus + aperture)}} - F_{i\text{ - aperture}}$$

Appendix 15: Analytical Thermal Radiation Heat Loss Program Listing

```
REM
REM
REM              **********************************************
REM  THEORETICAL THERMAL RADIATION HEAT LOSS PROGRAM
REM              **********************************************
REM    This program predicts the thermal radiative heat loss from
REM    the cavity solar receiver using the net radiation method.
REM
REM  DIFFUSE GRAY BODY VERSION
REM      This section of the program is used to verify the thermal radiation
REM     shape factor formulas of the solar cavity receiver.
REM
REM                **************************************************
REM
OPEN "Ther Rad Program Output" FOR OUTPUT AS #1
WRITE#1,"aperture","operating","radiative"
WRITE#1,"diameter","temperature","heat  loss"
WRITE#1,"[in]","[°F]","[Watts]"
REM     ***********
REM   nomenclature
REM     ***********
REM   re = end plate radius
REM    rc = cavity radius
REM    ra = aperture radius
REM    lc = length of frustum section
REM    lm = length of hot cylindrical section
REM    la = length of cold cylindrical section
REM    lbc = width of hot isothermal bands in frustum section
REM    lbm = width of hot isothermal bands in hot cylindrical section
REM    Nc = number of bands in frustum section
REM    Nm = number of bands in hot cylindrical section
REM
REM  constants
REM      ********
S=5.729*10^-8        :REM    Stephan-Boltzmann constant W/(m^2 K^4)
pi=3.14
REM             ***************************************************
REM  CAVITY GEOMETRY
REM             ***************************************************
re=.254/2
rc=.33
lc=.292
la=.14
lm=.686-lc-la
Nm=15!
lbm=lm/Nm
Nc=23!
lbc=SQR((rc-re)^2+lc^2)/Nc
hc=lc*lbc/SQR((rc-re)^2+lc^2)
DIM  rad(12),Top(12)
FOR n=1 TO 12
READ rad(n)
DATA     0.2286,0.2286,0.2286,0.2286,.0762,.0762,.1524,.1524,.2286,.2
```

```
286,.3302,.3302
NEXT n
FOR n=1 TO 12
READ Top(n)
DATA     300,400,500,600,400,600,400,600,400,600,400,600
NEXT n
Tdiff=20  :REM  assumed temperature difference between inlet and outlet
REM                    ***************************************************
REM   This section determines the total number of elements that make
REM    up the internal surface of the cavity receiver.
REM                    ***************************************************
NT=Nc+Nm+4
DIM  F(NT,NT),sum(NT),A(NT,NT),E(NT),T(NT),C(NT),q(NT),G(NT,NT+1)
,M(NT+1)
REM   F(I,J)      is the shape factor matrix
REM   sum(NT)  is a shape factor verification array
REM   A(NT,NT)  is the coefficient matrix
REM   E(NT)   is the emissivity array
REM   T(NT)    is the temperature array
REM   C(NT)   is the constant array
REM   G(NT,NT+1)      is the augmented Gaussian matrix
REM   q(NT)   is the outgoing radiant energy flux ( radiosity )
REM                    ***************************************************
REM   This section defines the numbering of elements that make
REM    up the internal surface of the cavity receiver.
REM                    ***************************************************
REM   aperture = 1
REM   annulus = 2
REM   spacer ring = 3
REM   end plate = 4
REM    hot cylindrical section is numbered 5 thru Nm+4
REM    frustum section is numbered Nm+5 thru Nc + 6
REM                    ***************************************************
REM          EMISSIVITY ARRAY INPUT SECTION
REM                    ***************************************************
E(1)=0        :REM   emissivity of the aperture
E(2)=.7        :REM   emissivity of the annulus
E(3)=.7        :REM   emissivity of the spacer section
E(4)=.7        :REM   emissivity of the end plate
FOR n=5 TO NT
E(n)=.85
NEXT n
REM                    ***************************************************
REM          BEGINNING OF APERTURE RADIUS VARIATION LOOP
REM                    ***************************************************
numT=4
FOR samp=1 TO 12
ra=rad(samp)
REM                    ***************************************************
REM          SHAPE FACTORS CALCULATION SECTION
REM                    ***************************************************
REM
REM     *********  Shape factors for each element onto itself  ******
REM                    ****************************************************
REM       ********   For flat surfaces Fi-i = 0   ******************
```

```
F(1,1)=0
F(2,2)=0
F(4,4)=0    :REM aperture, annulus , and end plate
REM         ************    spacer  section        ******************
ri=rc
rj=rc
h=la
GOSUB shape
F(3,3)=1-ri^2/((ri+rj)*la)*(1-FF)-rj^2/((ri+rj)*la)*(1-rj^2/    ri^2*FF)
REM         ************    hot  cylindrical    section    ******************
ri=rc
rj=rc
h=lbm
GOSUB shape
FOR n=1 TO Nm
k=n+4
F(k,k)=1-ri^2/((ri+rj)*lbm)*(1-FF)-rj^2/((ri+rj)*lbm)*(1-rj^    2/ri^2*FF)
NEXT n
REM         ************    frustum     section     ******************
h=hc
FOR n=1 TO Nc
ri=rc-(rc-re)*n/Nc
rj=rc-(rc-re)*(n-1)/Nc
GOSUB shape
k=Nm+4+n
F(k,k)=1-ri^2/((ri+rj)*lbc)*(1-FF)-rj^2/((ri+rj)*lbc)*(1-ri^    2/rj^2*FF)
NEXT n
REM                   **************************************************
REM    Shape factor from elements of the cylindrical and frustum sections
REM    to other elements of the cylindrical and frustum sections
REM                   **************************************************
REM     *****  between different elements of the frustum section ******
FOR M=1 TO Nc-1
FOR n=M+1 TO Nc
r1=rc-(rc-re)*n/Nc
r2=rc-(rc-re)*(n-1)/Nc
r3=rc-(rc-re)*M/Nc
r4=rc-(rc-re)*(M-1)/Nc
h13=(n-M)*hc
h24=h13
h14=(n-M+1)*hc
h23=(n-M-1)*hc
h=h13
ri=r1
rj=r3
GOSUB shape
F13=FF
h=h23
ri=r2
rj=r3
GOSUB shape
F23=FF
h=h14
ri=r1
rj=r4
```

```
GOSUB shape
F14=FF
h=h24
ri=r2
rj=r4
GOSUB shape
F24=FF
i=Nm+4+M
j=Nm+4+n
F(i,j)=r2^2/((r3+r4)*lbc)*(F23-F24)-r1^2/((r3+r4)*lbc)*(F13-F14)
F(j,i)=(r3+r4)/(r1+r2)*F(i,j)
NEXT n
NEXT M
REM    *** between different elements of the hot cylindrical section ****
FOR M=1 TO Nm-1
FOR n=M+1 TO Nm
r1=rc
r2=rc
r3=rc
r4=rc
h13=(n-M)*lbm
h24=h13
h14=(n-M+1)*lbm
h23=(n-M-1)*lbm
h=h13
ri=r1
rj=r3
GOSUB shape
F13=FF
h=h23
ri=r2
rj=r3
GOSUB shape
F23=FF
h=h14
ri=r1
rj=r4
GOSUB shape
F14=FF
h=h24
ri=r2
rj=r4
GOSUB shape
F24=FF
i=4+M
j=4+n
F(i,j)=r2^2/((r3+r4)*lbm)*(F23-F24)-r1^2/((r3+r4)*lbm)*(F13-F14)
F(j,i)=(r3+r4)/(r1+r2)*F(i,j)
NEXT n
NEXT M
REM                    **************************************************
REM    *** Shape factors between elements of the hot cylindrical  ***
REM    ***  section and elements of the frustum section  ****
REM                    **************************************************
FOR M=1 TO Nm
```

```
FOR n=1 TO Nc
r1=rc-(rc-re)*n/Nc
r2=rc-(rc-re)*(n-1)/Nc
r3=rc
r4=rc
h13=lm-M*lbm+n*hc
h24=lm-(M-1)*lbm+(n-1)*hc
h14=lm-(M-1)*lbm+n*hc
h23=lm-M*lbm+(n-1)*hc
h=h13
ri=r1
rj=r3
GOSUB shape
F13=FF
h=h23
ri=r2
rj=r3
GOSUB shape
F23=FF
h=h14
ri=r1
rj=r4
GOSUB shape
F14=FF
h=h24
ri=r2
rj=r4
GOSUB shape
F24=FF
i=M+4
j=n+4+Nm
F(i,j)=r2^2/((r3+r4)*lbm)*(F23-F24)-r1^2/((r3+r4)*lbm)*(F13-F14)
F(j,i)=(r3+r4)*lbm/((r1+r2)*lbc)*F(i,j)
NEXT n
NEXT M
REM           **************************************************
REM   ***  Shape factors between  the spacer section and  elements  ****
REM   ***     of the hot cylindrical section*******
REM           **************************************************
FOR n=1 TO Nm
r1=rc
r2=rc
r3=rc
r4=rc
h13=n*lbm
h24=(n-1)*lbm+la
h14=n*lbm+la
h23=(n-1)*lbm
h=h13
ri=r1
rj=r3
GOSUB shape
F13=FF
h=h23
ri=r2
```

```
rj=r3
GOSUB shape
F23=FF
h=h14
ri=r1
rj=r4
GOSUB shape
F14=FF
h=h24
ri=r2
rj=r4
GOSUB shape
F24=FF
i=3
j=n+4
F(i,j)=r2^2/((r3+r4)*la)*(F23-F24)-r1^2/((r3+r4)*la)*(F13-F1     4)
F(j,i)=(r3+r4)*la/((r1+r2)*lbm)*F(i,j)
NEXT n
REM          ****************************************************
REM    ***  Shape factors between  the spacer section and  elements  ***
REM    ***  of the frustum section                                    ***
REM          ****************************************************
FOR n=1 TO Nc
r1=rc-(rc-re)*n/Nc
r2=rc-(rc-re)*(n-1)/Nc
r3=rc
r4=rc
h13=lm+n*hc
h24=lm+la+(n-1)*hc
h14=lm+la+n*hc
h23=lm+(n-1)*hc
h=h13
ri=r1
rj=r3
GOSUB shape
F13=FF
h=h23
ri=r2
rj=r3
GOSUB shape
F23=FF
h=h14
ri=r1
rj=r4
GOSUB shape
F14=FF
h=h24
ri=r2
rj=r4
GOSUB shape
F24=FF
i=3
j=n+4+Nm
F(i,j)=r2^2/((r3+r4)*la)*(F23-F24)-r1^2/((r3+r4)*la)*(F13-F1     4)
F(j,i)=(r3+r4)*la/((r1+r2)*lbc)*F(i,j)
```

```
NEXT n
REM              ***************************************************
REM   Shape factors between circular sections and the spacer section,
REM   elements of the hot cylindrical section, and elements of the
REM   frustum section.
REM              ***************************************************
REM   **between the end plate and elements of the hot cylindrical section *
r3=re
r1=rc
r2=rc
FOR n=1 TO Nm
h23=lc+lm-n*lbm
h13=lc+lm-(n-1)*lbm
ri=r3
rj=r1
h=h13
GOSUB shape
F31=FF
ri=r3
rj=r2
h=h23
GOSUB shape
F32=FF
i=4
j=4+n
F(i,j)=F32-F31
F(j,i)=r3^2/((r1+r2)*lbm)*F(i,j)
NEXT n
REM   **between the end plate and elements of the frustum section **
r3=re
FOR n=1 TO Nc
r1=re+(rc-re)*(1-(n-1)/Nc)
r2=re+(rc-re)*(1-n/Nc)
h23=lc-n*hc
h13=lc-(n-1)*hc
ri=r3
rj=r1
h=h13
GOSUB shape
F31=FF
ri=r3
rj=r2
h=h23
GOSUB shape
F32=FF
i=4
j=4+Nm+n
F(i,j)=F32-F31
F(j,i)=r3^2/((r1+r2)*lbc)*F(i,j)
NEXT n
REM   **between the end plate and the spacer section **
r3=re
r1=rc
r2=rc
h23=lc+lm
```

```
h13=lc+lm+la
ri=r3
rj=r1
h=h13
GOSUB shape
F31=FF
ri=r3
rj=r2
h=h23
GOSUB shape
F32=FF
i=4
j=3
F(i,j)=F32-F31
F(j,i)=r3^2/((r1+r2)*la)*F(i,j)
REM    **between the aperture and elements of the hot cylindrical section **
r3=ra
r1=rc
r2=rc
FOR n=1 TO Nm
h23=la+(n-1)*lbm
h13=la+n*lbm
ri=r3
rj=r1
h=h13
GOSUB shape
F31=FF
ri=r3
rj=r2
h=h23
GOSUB shape
F32=FF
i=1
j=4+n
F(i,j)=F32-F31
F(j,i)=r3^2/((r1+r2)*lbm)*F(i,j)
NEXT n
REM    **between the aperture and elements of the frustum section **
r3=ra
FOR n=1 TO Nc
r1=rc-n*(rc-re)/Nc
r2=rc-(n-1)*(rc-re)/Nc
h23=la+lm+(n-1)*hc
h13=la+lm+n*hc
ri=r3
rj=r1
h=h13
GOSUB shape
F31=FF
ri=r3
rj=r2
h=h23
GOSUB shape
F32=FF
i=1
```

```
j=4+n+Nm
F(i,j)=F32-F31
F(j,i)=r3^2/((r1+r2)*lbc)*F(i,j)
NEXT n
REM    **between the aperture and the spacer section **
ri=ra
rj=rc
h=la
GOSUB shape
i=1
j=3
F(i,j)=1-FF
F(j,i)=ri^2/(2*rj*la)*F(i,j)
REM               ******************************************************
REM    Shape factors for the annulus section are determined by the differences
REM    between shape factors of the annulus and aperture combined with
REM    an element and the aperture with an element.
REM               ******************************************************
REM    **between the annulus and elements of the hot cylindrical section **
r3=rc
r1=rc
r2=rc
FOR n=1 TO Nm
h23=la+(n-1)*lbm
h13=la+n*lbm
ri=r3
rj=r1
h=h13
GOSUB shape
F31=FF
ri=r3
rj=r2
h=h23
GOSUB shape
F32=FF
i=2
j=4+n
F(i,j)=(rc^2*(F32-F31)-ra^2*F(1,j))/(rc^2-ra^2)
F(j,i)=(rc^2-ra^2)/((r1+r2)*lbm)*F(i,j)
NEXT n
REM    **between the annulus and elements of the frustum section **
r3=rc
FOR n=1 TO Nc
r1=rc-n*(rc-re)/Nc
r2=rc-(n-1)*(rc-re)/Nc
h23=la+lm+(n-1)*hc
h13=la+lm+n*hc
ri=r3
rj=r1
h=h13
GOSUB shape
F31=FF
ri=r3
rj=r2
h=h23
```

```
GOSUB shape
F32=FF
i=2
j=4+n+Nm
F(i,j)=(rc^2*(F32-F31)-ra^2*F(1,j))/(rc^2-ra^2)
F(j,i)=(rc^2-ra^2)/((r1+r2)*lbc)*F(i,j)
NEXT n
REM    **between the annulus and the spacer section **
r1=rc
r2=rc
r3=ra
ri=r1
rj=r2
h=la
GOSUB shape
F12=FF
ri=r1
rj=r3
GOSUB shape
F13=FF
i=2
j=3
F(i,j)=1-rc^2/(rc^2-ra^2)*(F12-F13)
F(j,i)=(rc^2-ra^2)/((r1+r2)*la)*F(i,j)
REM              ****************************************************
REM    Shape factors from circular section to other circular sections
REM              ****************************************************
REM     **********  between the end plate and the aperture ******
ri=re
rj=ra
h=la+lm+lc
GOSUB shape
i=4
j=1
F(i,j)=FF
F(j,i)=re^2/ra^2*F(i,j)
REM     **********  between the end plate and the annulus ******
ri=re
rj=rc
h=la+lm+lc
GOSUB shape
i=4
j=2
F(i,j)=FF-F(i,1)
F(j,i)=re^2/(rc^2-ra^2)*F(i,j)
REM              ***************************************************
REM                    Shape factors matrix output
REM              ***************************************************
FOR i=1 TO NT
FOR j=1 TO NT-1
PRINT  USING  "#.###";F(i,j);
PRINT SPC(1);
NEXT j
PRINT  USING  "#.###";F(i,NT)
PRINT
```

```
NEXT i
111 :
REM                 *************************************************
REM   The sum of the shape factors for one element to all the elements
REM   of the enclosure is equal to one. This property is used to verify
REM   the shape factors previously calculated. For an enclosure of N
REM   elements the sum of all the shape factors should equal N.
REM                 *************************************************
FOR i=1 TO NT
FOR j=1 TO NT
sum(i)=0
NEXT j
NEXT i
SUMT=0
FOR i=1 TO NT
FOR j=1 TO NT
sum(i)=sum(i)+F(i,j)
SUMT=SUMT+sum(i)
NEXT j
NEXT i
PRINT     "*********************************"
FOR i=1 TO NT-1
PRINT "     SUM ";i;" = ";
PRINT  USING  "##.####";sum(i)
NEXT i
i=NT
PRINT "SUM ";i;" = ";
PRINT  USING  "##.####";sum(i)
PRINT     "*********************************"
222 :
REM                 *******************************************************
REM          END OF SHAPE FACTOR SECTION
REM                    ****************************************************
REM                    ****************************************************
REM                    ****************************************************
REM         COEFFICIENTS MATRIX CALCULATIONS SECTION
REM                 ******************************************************
FOR i=1 TO NT
FOR j=1 TO NT
KD=1
IF i=j THEN 400
KD=0
400 :
A(i,j)=KD-(1-E(i))*F(i,j)
NEXT j
NEXT i
REM                 *************************************************
REM                    coefficient matrix output
REM                 *************************************************
FOR i=1 TO NT
FOR j=1 TO NT-1
PRINT  USING  "#.###";A(i,j);
PRINT  SPC(1);
NEXT j
PRINT  USING  "#.###";A(i,NT)
```

```
PRINT
NEXT i
333 :
REM                    **************************************************
REM                  BEGINNING OF TEMPERATURE
REM                    **************************************************
REM                    **************************************************
REM               TEMPERATURE ARRAY INPUT SECTION
REM                    **************************************************
Tmean=Top(samp)
Tin=Top(samp)+Tdiff/2:Tout=Top(samp)-Tdiff/2
PRINT Tin,Tout,Tmean
REM
REM   Each element is assumed to be isothermal. Angular temperature
REM    measurements for the hot cylindrical section and the frustum
REM   section are averaged to give one temperature for each band. The
REM    axial temperature values are determined from linear extrapolation
REM    from band with temperature measurements. Temperature values
REM    are in Kelvin.
T(1)=0    :REM  temperature of the aperture opening
FOR n=2 TO 4   :REM  temperature of the refractory surfaces
T(n)=((Tmean-40)-32)*5/9+273.15
NEXT n
FOR n=5 TO NT
T(n)=((Tout+(Tin-Tout)*(n-5)/(NT-5))-32)*5/9+273.15
NEXT n
REM    *********  OUTPUT THE TEMPERATURE DISTRIBUTION ********
FOR n=1 TO NT
PRINT  "T(";n;")=  ";T(n)
NEXT n
REM                    **************************************************
REM       CONSTANT ARRAY CALCULATION SECTION
REM                    **************************************************
FOR n=1 TO NT
C(n)=E(n)*S*T(n)^4
NEXT n
REM                    **************************************************
REM          HEAT FLUX SOLUTIONS
REM                    **************************************************
REM
REM   Gaussian Elimination method is used to solve for the heat output
REM    of each surface, including the total heat lost from the receiver
REM    through the aperture.
REM
REM         ***********    augmented  matrix        ***********************
FOR i=1 TO NT
FOR j=1 TO NT
G(i,j)=A(i,j)
NEXT j
G(i,NT+1)=C(i)
NEXT i
GOSUB Gauss
REM                    ***************************************************
REM       OUTPUT OF HEAT LOSS THROUGH APERTURE AND HEAT
REM    RADIATED FROM ALL OTHER ELEMENTS
```

```
REM                *************************************************
FOR i=1 TO 4
READ Nm$
PRINT  Nm$;SPC(5);q(i)
NEXT i
FOR i=5 TO Nm+4
PRINT  "hot cylindrical  element";SPC(5);q(i)
NEXT i
FOR i=Nm+5 TO NT
PRINT  "frustum  element";SPC(5);q(i)
NEXT i
DATA  "aperture","annulus","spacer  ring","end  plate"
RESTORE
REM                *************************************************
REM       SUMMARY OUTPUT
REM                *************************************************
PRINT       ****************************************************
PRINT "                    SUMMARY OUTPUT"
PRINT       ****************************************************
PRINT  SPC(2);"aperture";TAB(10);"operating";TAB(20);"radiative"
PRINT  SPC(2);"diameter";TAB(10);"temperature";TAB(20);"heat  loss"
PRINT  SPC(4);"[in]";TAB(13);"[°F]";TAB(23);"[Watts]"
PRINT SPC(4);
PRINT  USING  "###.#";ra*200/2.54;
PRINT TAB(13);Tmean;
PRINT  TAB(23);q(1)*pi*ra^2
WRITE#1,ra*200/2.54,Tmean,q(1)*pi*ra^2
BEEP
NEXT samp
FOR k=1 TO 5
BEEP
NEXT k
CLOSE#1
END
shape:
FF=.5*(1+(h*h+rj*rj)/(ri*ri)-SQR((1+(h*h+rj*rj)/(ri*ri))^2-4
*(rj/ri)^2))
RETURN
Gauss:
REM
$$$$$$$$$$$$$$$$$$$$$$$$$$$$$$$$$$$$$$$$$$$$$$$$$$$$$$$$$$$$$$$$$
REM          GAUSSIAN ELIMINATION METHOD
REM
$$$$$$$$$$$$$$$$$$$$$$$$$$$$$$$$$$$$$$$$$$$$$$$$$$$$$$$$$$$$$$$$$
REM
REM      ************** Check  Augmented  Matrix  Form     **************
REM
REM   For the Gaussian elimination method to work the A(1,1) element
REM   of the augmented matrix can not have a value of one. If A(1,1) is
REM   equal to one then rows of the matrix will be shifted until a non-
REM   zero value is in element A(1,1).
Flag=0
IF G(1,1)<>0 THEN Elimination
Flag=Flag+1
FOR j=1 TO NT+1
```

```
M(j)=G(1,j)
NEXT j
FOR i=1 TO NT-1
FOR j=1 TO NT+1
G(i,j)=G(i+1,j)
NEXT j
NEXT i
FOR j=1 TO NT+1
G(NT,j)=M(j)
NEXT j
GOTO 444
REM        ************       PRINT   CYCLE       ****************
CLS
FOR M=1 TO NT
FOR n=1 TO NT
PRINT  G(M,n);SPC(5);
NEXT n
PRINT  G(M,NT+1)
NEXT M
REM               ****************************************************
444 :
GOTO Gauss
Elimination:
REM        **************     Gaussian   Elimination     ********************
FOR k=1 TO NT
ss=G(k,k)
FOR j=1 TO NT+1
G(k,j)=G(k,j)/ss
NEXT j
FOR i=k+1 TO NT
ss=G(i,k)
FOR j=1 TO NT+1
G(i,j)=G(i,j)-ss*G(k,j)
NEXT j
NEXT i
NEXT k
REM
FOR k=1 TO NT-1
FOR i=1 TO NT-k
ss=G(i,NT-k+1)
FOR j=1 TO NT+1
G(i,j)=G(i,j)-ss*G(NT-k+1,j)
NEXT j
NEXT i
NEXT k
GOTO 555
REM        ************       PRINT   CYCLE       ****************
CLS
FOR M=1 TO NT
FOR n=1 TO NT
PRINT  G(M,n);SPC(5);
NEXT n
PRINT  G(M,NT+1)
NEXT M
REM               ******************************************
```

```
555 :
FOR i=1 TO NT
q(i)=G(i,NT+1)
NEXT i
IF Flag=0 GOTO 600
FOR k=1 TO Flag
qq=q(NT)
FOR i=2 TO NT
q(i)=q(i-1)
NEXT i
q(1)=qq
NEXT k
600 :
RETURN
```

Appendix 16: Flow Meter Factory Calibration Specifications

FLOW TECHNOLOGY, INC.
MECHANICAL DATASHEET
7412

Customer: CAL POLY KELLOG UNIT
Meter Model #: FT4-8AEXB-LAD-G
Meter Serial #: 8407412
End Fitting: MS-32656-8
Bearing Type: CARBIDE
Pickoff Type: HI-TEMP MAG
Pickoff P/N: 80666-104

Job #: 25194
Tag #:
Size: 1/2"
Cal. Media: FREON TE
Viscosity: 0.83 CTS
Temperature: 75.00 ° F
Density: 12.18 #/

Meter Freq (Hz)	Meter Flow Rate (GAL/Min)	Meter K Factor (P/GAL)	Freq / Viscosity (Hz/CTS)
2052.7	3.0718	40094.49	2464.262
1472.5	2.1931	40285.28	1767.664
1066.1	1.5824	40424.25	1279.887
777.27	1.1515	40501.43	933.099
559.29	0.8308	40391.61	671.420
408.40	0.6096	40198.27	490.281
286.39	0.4313	39845.83	343.811
205.55	0.3158	39056.52	246.761
151.03	0.2351	38542.37	181.309
113.86	0.1797	38012.29	136.690

Calibrated by: R. GAYAGAN
Certified by: [signature]
Signal Output: 7 Mv @ 11.3 Hz

Calib Inv #: 5109?
Calib Recal Date: 10/1/87
Date: 4/10/87

Appendix 17: Flow Meters Voltage Output

Factory Flow (volts)	Flow 1 (volts)	Flow 2 (volts)	cor Flow (volts)	cor Flow 2 (volts)	ΔFlow 1 (volts)	ΔFlow 2 (volts)
-0.0017	0.9092	1.0031	-0.214859	-0.09714	-0.2131588	-0.0954395
-0.0017	0.9088	1.0022	-0.216043	-0.100002	-0.2143432	-0.0983022
-0.0017	0.9122	1.0022	-0.205976	-0.100002	-0.2042758	-0.0983022
-0.0017	0.9147	1.0022	-0.198573	-0.100002	-0.1968733	-0.0983022
-0.0017	0.9164	1.0022	-0.19354	-0.100002	-0.1918596	-0.0983022
1.7420	1.6329	1.6224	1.9280169	1.8727299	0.1860169	0.13072992
1.8092	1.6321	1.6240	1.9256481	1.8778192	0.1164481	0.0686192
1.8396	1.6329	1.6262	1.9280169	1.884817	0.0884169	0.04521696
1.8527	1.6359	1.6274	1.9368999	1.8886339	0.0841999	0.03598392
2.5587	1.8756	1.8519	2.6466516	2.6027235	0.0879516	0.04402352
2.5667	1.8751	1.8472	2.6451711	2.5877738	0.0784711	0.02107376
2.5768	1.8785	1.8536	2.6552385	2.6081309	0.0784385	0.03133088
2.5844	1.8764	1.8493	2.6490204	2.5944534	0.0646204	0.01005344
2.7933	1.9715	[illegible]	2.9306115	[illegible]	0.1373115	[illegible]
2.8626	1.9846	1.9478	2.9694006	2.9077622	0.1068006	0.04516224
2.8841	1.9939	1.9529	2.9969879	2.9239845	0.1128879	0.03988432
3.3314	2.1343	2.0831	3.4126623	3.3381245	0.0812623	0.00672448
3.3360	2.1419	2.0852	3.4351659	3.3448042	0.0991659	0.00880416
3.3369	2.1490	2.0886	3.456189	3.3556189	0.119289	0.01871888
3.3411	2.1469	2.0886	3.4499709	3.3556189	0.1088709	0.01451888
3.3478	2.1440	2.0852	3.441384	3.3448042	0.093584	-0.0029958
3.3508	2.1465	2.0916	3.4487865	3.3651613	0.0979865	0.01436128
3.7837	2.3059	2.2382	3.9207699	3.8314666	0.1370699	0.04776656
3.8225	2.2805	2.2458	3.8455605	3.8556406	0.0230605	0.03314064
3.8310	2.2805	2.2458	3.8455605	3.8556406	0.0145605	0.02464064
3.8310	2.2805	2.2442	3.8455605	3.8505514	0.0145605	0.01955136
4.1404	2.3722	2.3333	4.1170842	4.1339606	-0.0233158	-0.0064394
4.1472	2.3786	2.3363	4.1360346	4.143503	-0.0111654	-0.003697
4.6016	2.5413	2.4855	4.6177893	4.6180784	0.0161893	0.0164784
4.6181	2.5422	[illegible]	4.6204542	4.612671	0.0023542	-0.005429
4.6223	2.5434	2.4859	4.6240074	4.6193507	0.0017074	-0.0029493
4.6270	2.5434	2.4881	4.6240074	4.6263485	-0.0029926	-0.0006515
4.9816	2.6508	2.6018	4.9420188	4.9880054	-0.0395812	0.00640544
4.9829	2.6673	2.6018	4.9908753	4.9880054	0.0079753	0.00510544
4.9884	2.6491	2.6030	4.9369851	4.9918224	-0.0514149	0.0034224
4.9888	2.6504	2.6030	4.9408344	4.9918224	-0.0479656	0.0030224
4.9888	2.6538	2.6018	4.9509018	4.9880054	-0.0378982	-0.0007946
5.0484	2.6893	2.6195	5.0560173	5.0443056	0.0076173	-0.0040944
5.3942	2.7992	2.7332	5.3814312	5.4059626	-0.0127688	0.01176256
5.4022	2.7945	2.7320	5.3675145	5.4021456	-0.0346855	-5.44E-05
5.4098	2.7992	2.7345	5.3814312	5.4100976	-0.0283688	0.0002976
5.7831	2.9302	2.8541	5.7693222	5.7905213	-0.0137778	0.00742128
5.7987	2.9378	2.8579	5.7918258	5.8026083	-0.0068742	0.00390832
5.8004	2.9357	2.8579	5.7856077	5.8026083	-0.0147923	0.00220832
5.8025	2.9370	2.8609	5.789457	5.8121507	-0.013043	0.00965072
6.0485	3.0211	2.9549	6.0384771	6.0475299	-0.0100229	-0.0009701
6.1305	3.0431	2.9645	6.1036191	6.1416816	-0.0268809	0.0111816
6.1305	3.0456	2.9653	6.1110216	6.1442262	-0.0194784	0.01372624
6.1365	3.0465	2.9670	6.1136865	6.1496336	-0.0228135	0.0131336
6.1398	3.0473	2.9683	6.1160553	6.1537686	-0.0237447	0.01396864
6.1462	3.0503	2.9683	6.1249383	6.1537686	-0.0212617	0.00756864
6.1470	3.0494	2.9670	6.1222734	6.1496336	-0.0247266	0.0026336
6.1504	3.0494	2.9691	6.1222734	6.1563133	-0.0281266	0.00591328
6.1517	3.0515	2.9670	6.1284915	6.1496336	-0.0232085	-0.0020664
6.1580	3.0536	2.9716	6.1347096	6.1642653	-0.0232904	0.00626528
6.1635	3.0570	2.9733	6.144777	6.1696726	-0.018723	0.00617264
6.1643	3.0536	2.9683	6.1347096	6.1537686	-0.0295904	-0.0105314
6.1656	3.0604	2.9725	6.1548444	6.167128	-0.0107556	0.001528
6.5718	3.1952	3.1018	6.5539872	6.5784054	-0.0178128	0.00660544
6.5718	3.1919	3.0984	6.5442159	6.5675907	-0.0275841	-0.0042093
6.5773	3.1978	3.1023	6.5616858	6.5799958	-0.0156142	0.00269584
6.5773	3.1957	3.1027	6.5554677	6.5812682	-0.0218323	0.00396816
6.5921	3.1969	3.1031	6.5590209	6.5825405	-0.0330791	-0.0095595
7.0178	3.3610	3.2510	7.044821	7.0529808	0.027121	0.0351808
7.0224	3.3483	3.2422	7.0073163	7.0249898	-0.0150837	0.00258976
7.0351	3.3529	3.2430	7.0209869	7.0275344	-0.0141681	-0.0075656
7.0364	3.3529	3.2481	7.0209869	7.0437565	-0.0154831	0.00735648
7.0410	3.3517	3.2608	7.0173837	7.0841526	-0.0236163	0.04315264
7.0487	3.3719	3.2468	7.0771959	7.0396214	0.0284959	-0.0090786
7.3386	3.4556	3.3449	7.3250816	7.3516579	-0.0135684	0.01305792
7.3496	3.4535	3.3440	7.3188135	7.3487952	-0.0307865	-0.0008048
7.3627	3.4632	3.3462	7.3475352	7.355793	-0.0151648	-0.006907
7.3636	3.4556	3.3428	7.3250816	7.3449782	-0.0385684	-0.0186218
7.3830	3.4641	3.3432	7.3502001	7.3462506	-0.0327999	-0.0367494
7.3856	3.4586	3.3432	7.3339146	7.3462506	-0.0516854	-0.0393494
7.4320	3.4869	3.3491	7.4177109	7.3650173	-0.0142891	-0.0669827
7.4456	3.4709	3.3554	7.3703349	7.3850563	-0.0752651	-0.0605437
7.7782	3.6116	3.4788	7.7868476	7.7791574	0.0086476	0.0009574
7.7766	3.6027	3.4911	7.7605947	7.8166909	-0.0160053	0.04009088
7.7968	3.6091	3.4772	7.7795451	7.7724778	-0.0172549	-0.0243222
7.7998	3.6125	3.4780	7.7896125	7.7750224	-0.0101875	-0.0247776
7.8911	3.6463	3.4869	7.8896943	7.8033515	-0.0014057	-0.0877485
7.8924	3.6442	3.5106	7.8834762	7.8787165	-0.0089238	-0.0136835
7.8945	3.6442	3.4878	7.8834762	7.8061942	-0.0110238	-0.0883058

Appendix 18 Calibrated Thermocouple Probe Specification

the OMEGA Group

CALIBRATION REPORT

CUSTOMER: CALIFORNIA POLYTECH STATE UNIVERSITY FOUNDATION MECH ENGR DEPT 3801 W TEMPLE AVENUE PIMONA CA 91768

REPORT NO: OM-70609592

TEST ITEM: KQSS-18G

TEST DATE: JUNE 9, 1987

PURCHASE ORDER NO: CPF66026ADD2

OMEGA ENGINEERING certifies that the above item has been calibrated and that its calibration is certified as traceable to the U.S. National Bureau of Standards. Traceability of these measurements is derived from the included NBS test numbers.

Probe No.	Nominal Temperature	Actual Test Temperature	Indicated Temperature	Deviation
1	300 DEG F	300.06	300.56	.50
1	500	499.77	499.39	.38
1	700	701.0	699.09	1.91

Reference: NATIONAL BUREAU OF STANDARDS TEST NO(s): 236495-37778

Tony D'Inverno
Supervisor, Instrumentation

CAL-4

OMEGA ENGINEERING, INC.
OMEGA PRESS   OMEGA INTERNATIONAL CORP.   BIOMEGA
One Omega Drive, Box 4047, Stamford, CT 06907-0047 (203) 359-1660 Telex 996404 Cable OMEGA FAX (203) 359-7700

CERTIFICATE OF CALIBRATION

HY-CAL Engineering
9650 Telstar Avenue · El Monte, CA 91731-3098

DATE 05-29-87

CUSTOMER CAL-POLY POM.

P.O. NO. CPEG6088

INST. TYPE PYRHELIOMETER

MODEL P-8400-B-1-120-XC

ABSORPTIVITY —

CERTIFIED RECORD OF CALIBRATION DATA ON THE INSTRUMENT DESCRIBED ABOVE. THE DATA WAS OBTAINED IN HY-CAL ENGINEERING'S THERMAL FLUX FACILITY

REFERENCE STANDARD 19955

TESTED BY HC 13

Q.C. APPROVAL HC 8

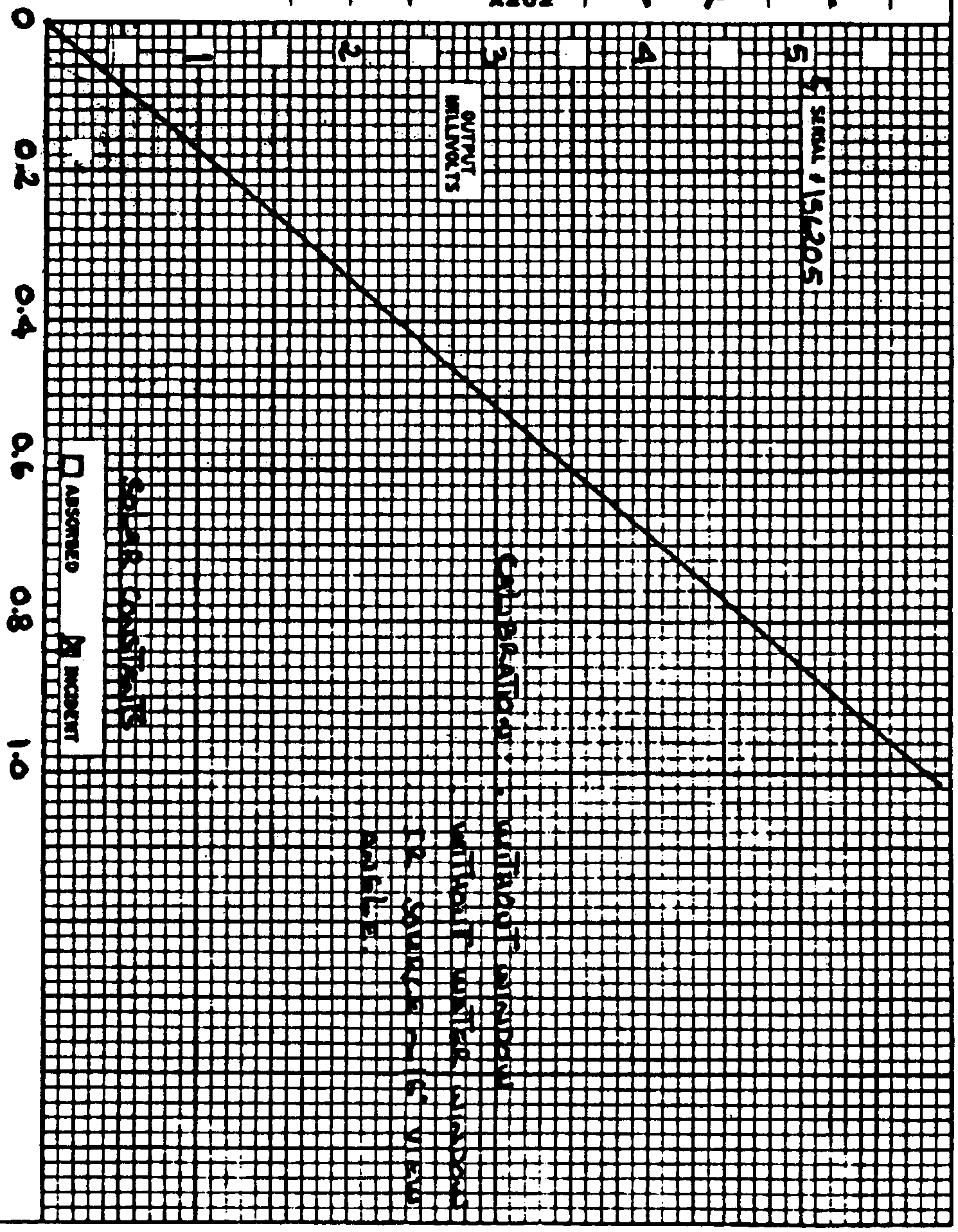

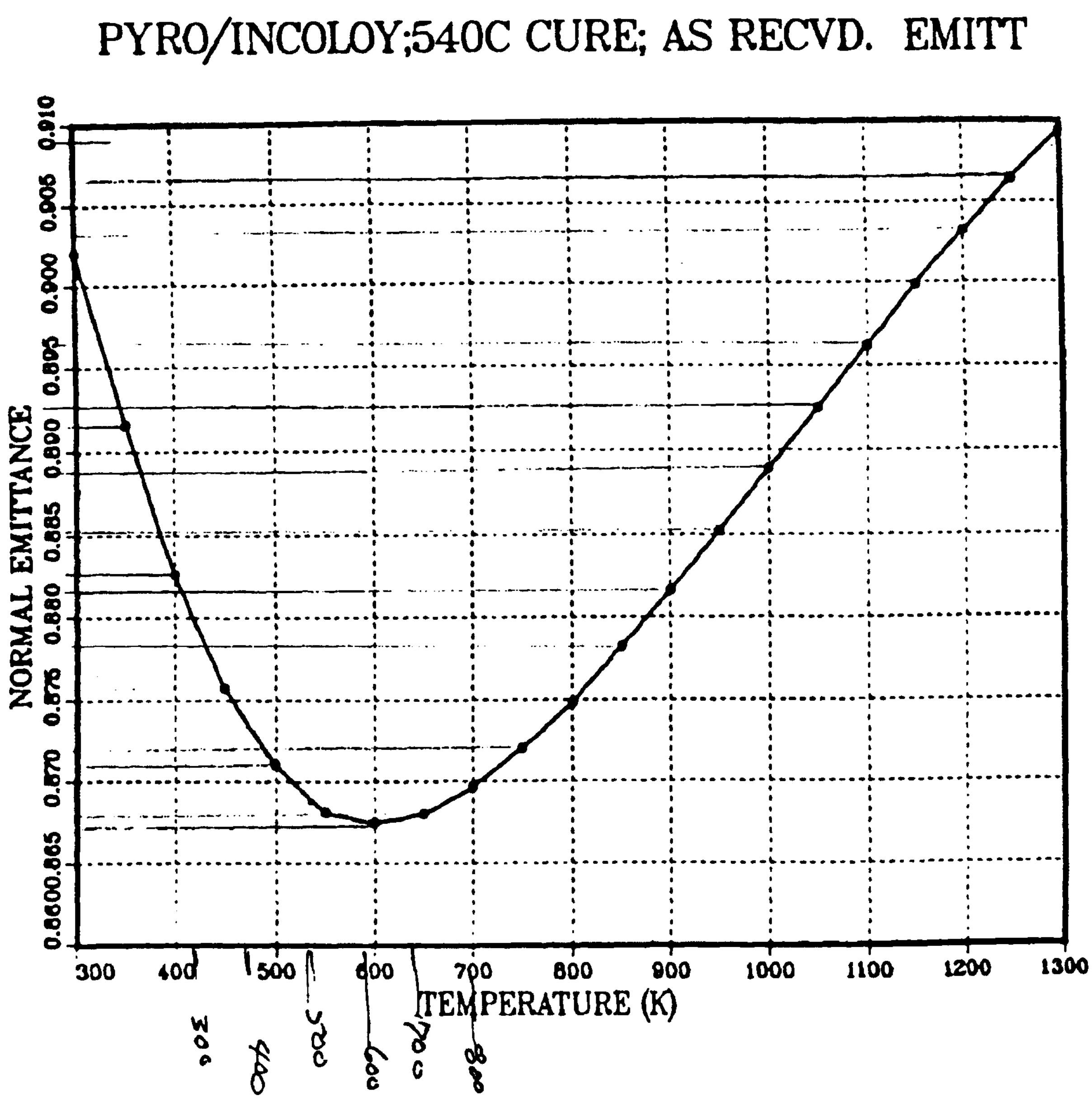
PYRO/INCOLOY;540C CURE; AS RECVD. EMITT
NORMAL EMITTANCE
0.8600.865
0.865
0.870
0.875
0.880
0.885
0.890
0.895
0.900
0.905
0.910
300
400
500
600
700
800
900
1000
1100
1200
1300
TEMPERATURE (K)

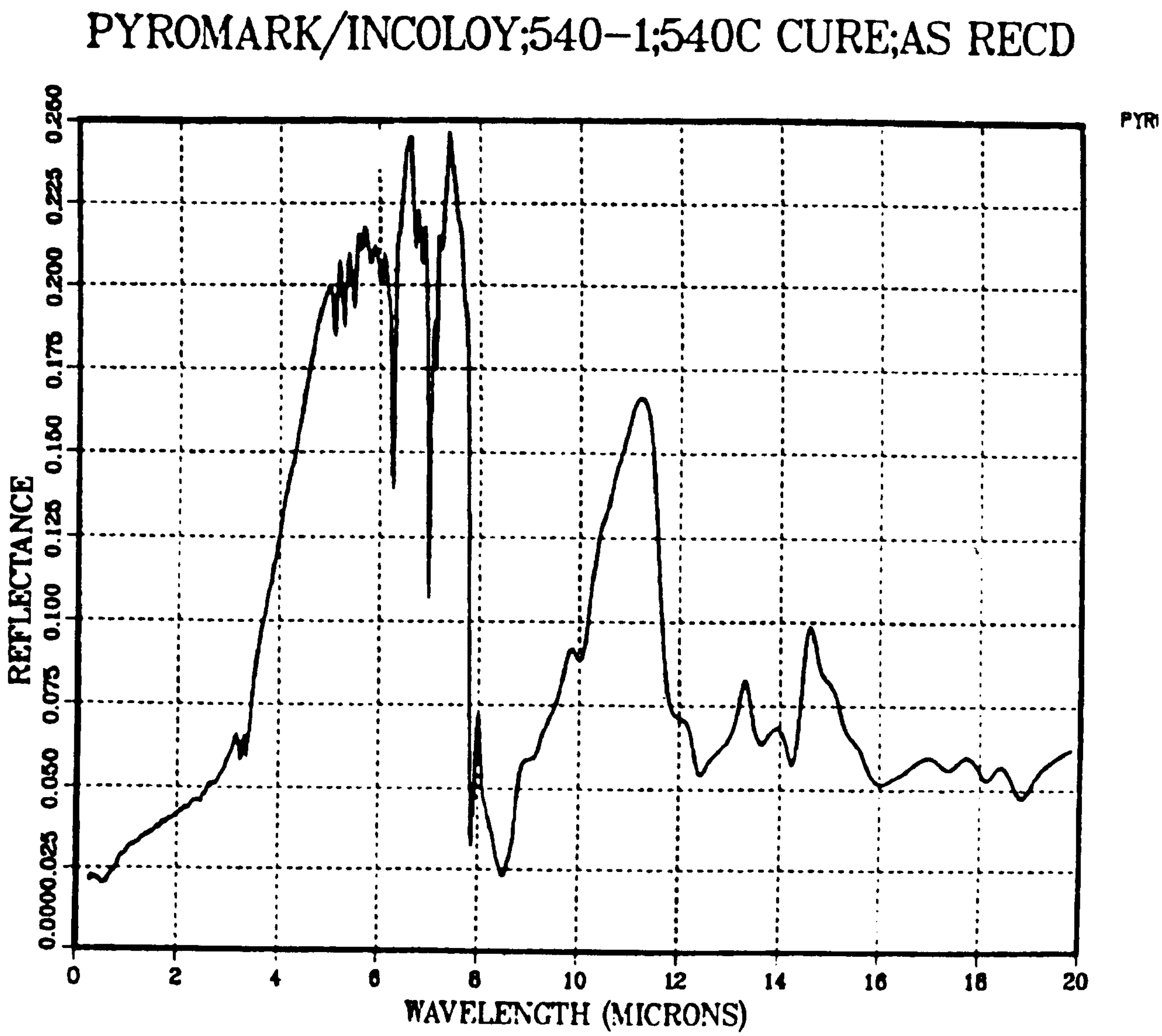
PYROMARK/INCOLOY;540-1;540C CURE;AS RECD
REFLECTANCE
0.000
0.025
0.050
0.075
0.100
0.125
0.150
0.175
0.200
0.225
0.250
0
2
4
6
8
10
12
14
16
18
20
WAVELENGTH (MICRONS)
PYRI

Appendix 21: Radiometer Window Test Data

Constants r (hot plate) [in] = 3.5 radiometer response [S.C./mV] = 0.171 r (radiometer) [in] = 0.5625 Stefan-Boltzmann [W/(m^2-K^4)] = 57.30E-9

Paint emittance poly. coeff.

m0	m1	m2	m3	m4	m5
1.033983	-6E-04	6.88E-07	-1.48E-11	-2.89E-13	1.07E-16

window	vertical *r(plate)		0.32			0.32			0.75			1.23			1.8			2.5			9.88	restricted
	Shape Factor		0.0234			0.0234			0.0165			0.0103			0.00609			0.0036			0.0003	
	T mean		amb			300°F			400°F			500°F			600°F			700°F			700°F	
	position	background	plate	background	background	plate	background	background	plate	background	background	plate	background	background	plate	background	background	plate	background	background	plate	background
	T1 [°F]	74.1	74.2	74.3	298.1	299.2	301.5	392.5	394.9	396.8	464.9	466.9	468.5	570.5	572.5	572.5	674.8	675.7	676	673.5	673.5	674.5
	T2 [°F]	74	74	74.2	312	313.6	316	414.4	418.2	419.4	493.5	496.3	496.7	607.1	610.8	611	716.8	715.9	716.2	720.2	722	723.6
	T3 [°F]	73.8	73.9	74.1	305.1	307.2	309.3	404.3	408.6	409.9	482.2	483.7	484.7	595	595	595.6	701.8	701.1	701.5	698	699.5	700.9
	T4 [°F]	74.2	74.4	74.4	313.2	315.3	317	415.5	418.9	420.2	496.2	496.9	497.5	612.5	613.5	613.7	728.2	728.5	728.6	724.8	725.7	727.3
	T5 [°F]	74	74	74.1	313.6	315.8	317.9	417	421	422.5	497.1	499	500.3	614.6	615.3	615.7	725.8	725.9	725.9	723	723.8	725.1
	T6 [°F]	74	74	74.2	317.2	319.3	321.4	424.4	427.7	429	508.1	509.6	510	632.3	632.9	633.1	756.3	755.4	756.3	753.8	754.3	756.2
saran	T7 [°F]	73.8	73.9	73.8	316.4	318.3	320.6	423	427.1	428.5	506.5	508.2	509.1	630.7	630.7	631.1	750.8	750.2	750.4	747	748.3	750
	T8 [°F]	74.2	74.4	74.6	319.4	321.4	324	426.9	431	432.3	511.4	513.2	513.8	637.5	637.3	637.2	759.8	759.6	759.8	756.2	757.4	759.2
	T9 [°F]	75.1	75.2	75.3	313.4	315.1	317	417.2	420.5	422.2	498.3	500.8	501.2	617.5	619.7	619.4	737.7	738.3	738.5	735.6	736.3	737.7
	T amb [°F]	74.8	75.2	74.8	72.3	72.3	72.3	69	68.9	69.2	71.5	71.7	71.7	73.2	73.2	73.1	70.1	70.2	70.5	71.2	71.5	71.3
	T water [°F]	83.8	84.5	85.1	76.2	76.5	76	68.1	68.5	68.5	69.3	69.6	68.5	70	70.4	69.8	73.3	73.5	73.6	74	74.2	74.1
	T avg [°F]	74.22	74.3	74.4	316	317.98	320.18	421.7	425.46	426.9	504.28	506.16	506.88	626.52	627.18	627.3	746.08	745.88	746.18	743.12	744.02	745.64
	Radiometer [mV]	-0.1177	-0.181	-0.1349	0.0029	4.3487	-0.0029	0.0632	6.1284	0.0431	0.089	5.6806	0.1148	0.1177	5.7179	0.132	0.0086	5.2098	-0.0144	-0.0144	0.3617	0.0057
	Radiometer [Watts]		-0.0081			0.6452			0.9014			0.8277			0.8299			0.7734			0.0543	
	HP emittance		0.9034			0.8779			0.8720			0.8693			0.8676			0.8684			0.8684	
	Hot Plate [Watts]		-0.0011			0.7962			1.0465			0.9572			0.9417			0.8526			0.0713	
	window transmittance		7.3636			0.8103			0.8613			0.8647			0.8813			0.9071			0.7616	

	T1 [°F]	73.7	74	74.1	288.5	292.4	295.5	379.5	385.4	389.8	470.4	470.5	471	575.2	575.2	575.2	676.6	675.5	674
	T2 [°F]	73.6	74	74	302.9	306.8	309.3	403.1	408.3	411.8	499.8	499.2	497.9	612.8	613.3	612.1	716.5	715.7	715.9
	T3 [°F]	73.4	73.9	73.9	296	299.7	302.4	392	397.8	401.4	487.8	487	487.3	597.3	596.8	596.9	701.6	702.2	702.3
	T4 [°F]	73.8	74.1	74.3	303.9	307.8	311.1	403.2	408.6	412.7	501.5	500.7	500.4	615.2	615.2	614.8	729.2	727.3	726.8
	T5 [°F]	73.4	73.9	73.9	303.7	307.7	311.1	402.7	409.5	413.6	503.7	503.2	502.7	617.2	617.1	616.4	726.4	725.2	725.7
	T6 [°F]	73.6	73.9	74	308	312	315.2	412.2	417.4	421.3	513	512.9	511.9	635.2	635.1	635.1	757	755.3	755.4
quartz	T7 [°F]	73.4	73.7	73.9	307.1	310.9	313.5	411	416.5	419.9	512.2	511.4	511.4	632.5	632.5	631.9	750.8	750.8	750.5
	T8 [°F]	73.8	74.2	74.3	310.4	313.9	316.8	415.1	420	424	517.4	516.7	515.6	639.1	639.1	638.3	760.3	760.4	759.9
	T9 [°F]	74.8	75.1	75.1	303.6	307.7	310.9	404.9	410.3	414.7	503.4	503.7	504.4	621.8	622.2	622.1	739.7	737.9	736.7
	T amb [°F]	76	75.7	75.7	72.7	72.5	72.5	68.3	68.5	68.8	72.1	72.3	72.5	73.6	73.5	73.4	70.6	70.9	71
	T water [°F]	81	82.1	83.1	77	76.8	76.4	67.3	67.8	67.9	69.2	69.5	69.7	70.2	70.4	70.4	73.5	73.9	73.9
	T avg [°F]	73.8	74.16	74.24	306.56	310.44	313.5	409.18	414.74	418.7	509.94	509.58	509.2	629.16	629.2	628.76	746.84	745.92	745.64
	Radiometer [mV]	-0.0459	-0.066	-0.0574	0	1.197	-0.0086	0.0144	1.8715	0.0144	0.0316	2.0897	0.0373	0.0545	2.348	0.0345	0	2.3624	0.0057
	Radiometer [Watts]		-0.0021			0.1782			0.2755			0.3049			0.3418			0.3501	
	HP emittance		0.9034			0.8784			0.8724			0.8692			0.8676			0.8684	
	Hot Plate [Watts]		-0.0029			0.7572			0.9904			0.9716			0.9490			0.8525	
	window transmittance		0.7241			0.2353			0.2782			0.3138			0.3602			0.4107	

Appendix 21 Radiometer Window Test Data

glad	T1 [°F]	74.3	74.3	74.4	303.3	305.8	306.6	398	397.7	399.3	468.3	468.8	469.2	572.3	573.8	573.4	669.5	673.2	674
	T2 [°F]	74.2	74	74.1	317.4	319.5	321.2	421.2	421	421.3	497.6	498.9	500.3	611.2	610	612.6	712.9	715.7	716
	T3 [°F]	74	73.9	74	310.7	312.5	313.8	411.6	412.2	412.4	485.6	486.4	487.6	597	595	596	698.4	700.3	701.4
	T4 [°F]	74.6	74.6	74.6	318.8	321.4	322.5	421.5	422.7	424.1	498.5	499.5	501	613	614.5	615	723.1	726.5	727.4
	T5 [°F]	74.2	74	74.1	319.5	321.8	323.7	424	425	425.9	500.9	502.3	503.2	615.6	615.8	616.2	721.3	723.9	725.3
	T6 [°F]	74.2	74	74.1	323.1	325.6	327	430.3	430.9	432.1	511	512.6	513.1	632.7	634.1	634.4	751.7	754.4	755.3
	T7 [°F]	74	73.9	74	322.1	324	325.4	429.9	430.5	430.8	509.8	510.9	512.3	632	630.5	631.6	747	749.9	750.2
	T8 [°F]	74.6	74.6	74.6	325.3	327.2	329.1	434.2	434.9	435.5	514.3	516	517.2	638.6	637.1	638.5	755.8	758.3	759.3
	T9 [°F]	75.3	75.4	75.4	319.2	321.6	322.7	423.3	423.8	425.1	501.9	502.6	503.1	619	620.9	620	732.8	736	737
	T amb [°F]	74.6	74.7	74.4	72.1	71.9	71.7	69.5	69.6	69.7	72	72	72.1	73.2	73.3	73.2	69.6	69.6	69.7
	T water [°F]	86.2	88	77.5	76	76.2	75.8	68.7	70.1	70.4	68.5	68.8	69.1	69.6	69.9	69.9	73.1	73.2	73.2
	T avg [°F]	74.46	74.38	74.44	321.84	324.04	325.58	428.34	429.02	429.88	507.58	508.88	509.78	627.58	627.68	628.14	741.72	744.5	745.42
	Radiometer [mV]	-0.1607	-0.287	0	0.0086	4.5439	-0.0201	0.0402	6.2575	0.0258	0.1349	5.7581	0.0947	0.155	5.7724	0.1292	0	5.2156	0.0144
	Radiometer [Watts]		-0.0307			0.6751			0.9236			0.8373			0.8354			0.7728	
	HP emittance		0.9034			0.8775			0.8718			0.8692			0.8676			0.8684	
	Hot Plate [Watts]		-0.0003			0.8287			1.0650			0.9687			0.9435			0.8487	
	window transmittance		######			0.8146			0.8672			0.8644			0.8854			0.9106	

no window	T1 [°F]	74.2	74.2	74.2	274.4	278.8	281.1	399.6	399.8	400.4	458.4	456.5	460.8	573.8	575.4	575.1	668.2	666.9	668.5	677.2	676.5	674.9
	T2 [°F]	74.2	74.2	74.2	287.9	292.3	294.7	422.7	422.5	423.3	482.4	488.6	492.6	612.9	613.8	612.6	709.4	708.7	709.1	725.8	726.4	725.1
	T3 [°F]	74	74.1	74	281.5	286.2	288.2	413.5	413.4	414.2	475.2	477.8	480.6	597.1	597.3	597.2	695.7	694.4	694.7	702.6	703.7	702.7
	T4 [°F]	74.6	74.6	74.6	289.1	293.1	295.2	423.9	424	424.2	479.4	488.2	493	614.4	615	615.9	720.3	720	721.2	729.3	729.6	727.6
	T5 [°F]	74.1	74.1	74.1	289.1	293.8	296.2	426.3	426.3	427.2	491.9	491.5	495	616.4	616.8	617.4	719.6	718.2	718.3	727.2	728	726.7
	T6 [°F]	74.1	74.1	74.1	292.5	296.8	299.2	432.1	432.6	433.2	493.7	501.1	505.2	634.3	634.9	635.2	748.3	747.1	748.6	758.7	759.3	757.2
	T7 [°F]	74	74.1	74	291.7	296.3	298.4	432	431.8	432.7	501.9	502.4	505.1	632.2	633.1	632.5	743.4	742.5	743.4	752	752.8	751.7
	T8 [°F]	74.6	74.7	74.7	295	299.2	301.7	436.3	436	437	502.7	506.6	510	638.8	639.2	639.1	751.9	751.2	752.2	761.2	761.8	760.2
	T9 [°F]	75.3	75.3	75.2	288.6	293.1	295.3	425.3	425.9	426	476.7	489.8	494.4	620.7	620.8	622	729.7	729.1	730.8	740.3	740.1	738.1
	T amb [°F]	74.5	73.9	73.8	72.8	72.6	72.5	70	69.9	70.1	71.8	71.7	71.8	73.5	73.4	73.4	69.1	69.2	69.4	71.4	71.1	71.1
	T water [°F]	75.3	76.2	76.9	77	77.1	77	70.4	70.4	70.4	68.4	68.9	69.1	70.1	70.4	70.4	72.9	73.3	73.1	74.3	74.2	74.3
	T avg [°F]	74.42	74.46	74.42	291.38	295.84	298.16	430.4	430.52	431.22	493.38	498.28	501.94	628.48	628.96	629.24	738.58	737.62	738.66	747.88	748.4	746.78
	Radiometer [mV]	-0.0373	-0.066	-0.0316	-0.0373	4.2569	-0.0345	0.0144	7.1101	0.0201	0.1177	6.1485	0.1062	0.1722	6.4384	0.178	-0.0431	5.6892	-0.0115	-0.0115	0.4593	0.0086
	Radiometer [Watts]		-0.0047			0.6369			1.0524			0.8957			0.9293			0.8482			0.0684	
	HP emittance		0.9034			0.8795			0.8717			0.8695			0.8676			0.8683			0.8684	
	Hot Plate [Watts]		0.0007			0.6857			1.0726			0.9234			0.9482			0.8287			0.0724	
	window transmittance		-6.7143			0.9288			0.9812			0.9700			0.9801			1.0235			0.9448	

Appendix 22: Saran Wrap® Specifications

Table 2 — Properties of Various SARAN WRAP Films

Property	Test Method	Remarks	Units	3	8	18	18L	19	560
General									
Specific Gravity	ASTM D 1505 68 (79)			1 60	1 71	1 71	1 71	1 71	1 65
Coefficient of Friction	ASTM D 1894 78	Static — film to film		-	—	0 60	0 60	0 29	-
		Static — film to metal		—	-	0 38	0 38	0 38	..
		Kinetic — film to film		..	—	0 33	0 33	0 24	.
		Kinetic — film to metal		—	—	0 38	0 38	0 32	..
Barrier									
Water Absorption	ASTM D 570 77			all types negligible					
Water Vapor Transmission Rate (24 hr — 90% RH 37 8°C (100°F))	PermaTran W		g mil 100 in² (g mil/m²)	all types 0 20 (3 1)					
Gas Transmission Rate (24 hr — atm — 23 C (73 F))	ASTM D 3985 81 and ASTM D1434 75		cc mil 100 in² (cc mil/m²)						
			oxygen	all types 0 8-1 1 (12 4-17 1)					
			carbon dioxide	all types 3 8-6 0 (58 9-93 0)					
			nitrogen	all types 0 12-0 16 (1 9-2 5)					
			air	all types 0 21-0 44 (3 3-6 8)					
Optical									
White Light Transmission		See Figure 21 page 16	%	these types 90					-
Ultraviolet Cut Off			Angstroms	these types 3000					—
Infrared Light Transmission			%	88	88	85	85	85	..
Resistance to Sunlight				exposure to direct sunlight is not recommended					
Clarity	ASTM D 1746-70 (78)		%	85	88	86	72	28	70
Gloss	ASTM D 2457 70 (77)	45° Specular Gloss		113	121	90	108	88	101
Haze	ASTM D 1003-61 (77)		%	1 12	0 43	4 2	4 5	9 4	2 3
Mechanical									
Ultimate Tensile Strength	ASTM D 882 81	Values determined on 100 ga film except 560 600 ga	lb in² (kg cm²)	7000 13 800 (492 914)		8000 16 000 (562 1125)			14 500 16 500 (1019 1160)
Ultimate Elongation	ASTM D 882 81		%	30	-	60 for these types			-
Thermal									
Heat Seal Temperature			F (C)	250 300 (121 149)	-	275 300 (135 149)			- -
Shrink				see Figures 3 and 4 page 17					
Electrical									
Dielectric Strength	ASTM D 149 81		volts 50 ga		-	6000 7000		-	
			100 ga		-	3000 5000		-	
			200 ga		-	1000 4500		-	
Surface Resistivity	ASTM D 257 78		ohms		-	10^{12} 10^{15}		-	
Volume Resistivity	ASTM D 257 78		ohm cm		-	10^{12} 10^{15}		-	

10 11

Light Transmission Characteristics

SARAN WRAP films offer good resistance to sunlight under glass. Such properties as tensile strength, elongation, flexibility, and impermeability to water vapor and gases decrease only slightly. Outdoor exposure to direct sunlight, however, is not recommended. Figure 2 below shows typical light transmission values for SARAN WRAP films.

Figure 2 — Light Transmission vs Wave Length for 100 Gauge SARAN WRAP 3, 8, 18, 18L, and 19 Films

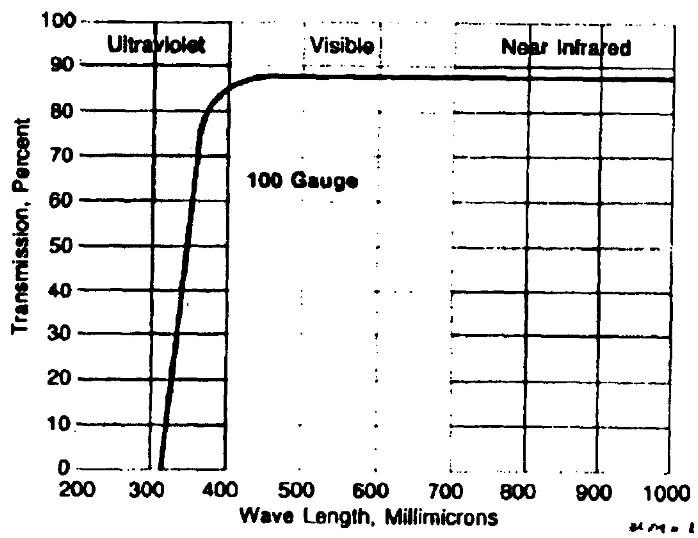

FDA and USDA Status

SARAN WRAP films, when used unmodified and according to good manufacturing practices — when used for food contact applications — can comply with the U.S. Food, Drug and Cosmetic Act as amended.

Many of these films also have been accepted by the U.S. Department of Agriculture for packaging of meat and meat food products, and poultry and poultry products, prepared in Federally inspected plants.

Government regulations are subject to change. While it is the responsibility of users of SARAN WRAP to check the suitability of their intended use with regulatory agencies, resources of The Dow Chemical Company are available to assist customers with pertinent data and other information.

Shrink Characteristics

SARAN WRAP plastic films become highly oriented during manufacture. This orientation makes the film susceptible to shrinkage on exposure to elevated temperatures — a property very desirable in applications such as overwraps. Further, by control of the shrink-inducing temperature, the film user can control the degree of shrinkage obtained.

For use in laminates where shrink is undesirable, preshrunk SARAN WRAP 18L film is available. Differences in the shrinkage rates of 18L and other films are shown in Figures 3 and 4.

$Å = 1 \mu m \times E-3$

$1 Å = .0001 \mu m$

$\sigma = 0.1712 E-8 \frac{BTU}{(h \cdot ft^2 \cdot R^4)}$

$\sigma = 5.6696 E-8 \frac{W}{(m^2 \cdot K^4)}$

Appendix 23 Radiometer Displacement Sensitivity Test Data

Constants: r (hot plate)[in]= 3.5; seran window trans= 0.87; radiometer response [S.C./mV] = 0.171

Stefan-Boltzmann [W/m^2-K^4]= 57.29E-9; r (radiometer)[in]= 0.5425

Paint emittance poly. coeff.: m0 = 1.039368231; m1 = -0.00068278; m2 = 6.88E-07; m3 = -1.49E-11; m4 = -2.89E-13; m5 = 1.07E-16

Mean Temp.	Vertical Disp. *r(plate)	1		2		2.96		4		5.02		5.95	
	position	Plate	Ambient	Plate	Ambient	Plate	Ambient	Plate	Ambient	Plate	Ambient	Plate	Ambient
400 °F	T1 [°F]	410.5	409.8	409.2	409.2	407.4	408	408.2	406.7	406.7	406.7	408.1	409.1
	T2 [°F]	433.8	433.4	433.1	434	432.4	431.6	432.1	431.1	431.5	430.5	431.9	433.5
	T3 [°F]	422.9	423	422.5	423.2	422	421.4	421.2	420.6	420.1	419.6	420.8	422.5
	T4 [°F]	436.2	435.8	435.4	435	434.1	434.5	434.4	433.2	432.9	433.1	434.4	435
	T5 [°F]	437.4	438.2	437.3	437.6	436.4	436.2	436.1	435.2	435.3	435	436	437.3
	T6 [°F]	445.8	445.7	444.9	445.5	444.3	443.5	444.1	442.9	443	442.7	444.1	445.2
	T7 [°F]	443.5	443.3	442.6	443.5	442.6	441.7	441.7	440.8	441	440.2	441.3	442.9
	T8 [°F]	448.3	448.9	448.1	448.5	447.2	447.3	447.2	446.2	446.1	446	447.1	448
	T9 [°F]	438.3	438	437	436.7	435.5	435.8	436	434.7	434.4	434.3	435.8	436.2
	T Amb. [°F]	66.5	66.9	66.7	66.7	66.4	65.8	65.8	65.8	65.6	65.3	65.6	65.7
	T Water [°F]	67.4	67.4	67.3	67.4	67.3	67.4	67.3	67.6	67.5	67.4	67.6	67.8
	T Ceiling [°F]	74.1	74.1	73.6	73.2	72	71.9	71.1	71	70.8	70.1	70.6	70.8
	T avg [°F]	442.66	442.82	441.98	442.36	441.2	440.9	441.02	439.96	439.96	439.64	440.86	441.92
	Radiometer [mV]	5.1926	0.0517	2.0237	0.0804	1.1281	0.0086	0.6631	-0.0057	0.3846	-0.0373	0.2784	-0.0689
	Radiometer [Watts]	0.8790		0.3322		0.1914		0.1143		0.0721		0.0594	
	Shape Factor	0.0129		0.0052		0.0026		0.0015		0.0010		0.0007	
	HP emittance	0.8712		0.8713		0.8713		0.8713		0.8714		0.8713	
	Q calc [Watts]	0.8938		0.3563		0.1818		0.1044		0.0674		0.0487	
	Q read by radio [%/100]	0.9833		0.9326		1.0526		1.0955		1.0707		1.2190	

Mean Temp.	Vertical Disp. *r(plate)	2.04		4		5.95		8.04		9.88		11.96	
	position	Plate	Ambient	Plate	Ambient	Plate	Ambient	Plate	Ambient	Plate	Ambient	Plate	Ambient
700°F	T1 [°F]	673.3		672.3		673		672.6		673.3		672.3	669.9
	T2 [°F]	723.4		720.3		721.9		721.4		721.9		721.6	717.9
	T3 [°F]	699.9		697.9		699.2		699.3		698.9		698.7	696.8
	T4 [°F]	724		724.3		725.2		725.6		725.7		724.8	720.2
	T5 [°F]	723.8		722.3		722.7		723		723.6		722.3	719.3
	T6 [°F]	755.1		753.1		754.2		754		754.4		753.7	747.6
	T7 [°F]	749.1		746.7		748.1		747.9		748.1		747.6	744.8
	T8 [°F]	757.3		755.9		757		757.5		757		756.6	752.5
	T9 [°F]	735		734.5		735.1		735.5		735.7		734.8	730.6
	T Amb. [°F]	72.7		72.7		72.6		72.6		72.6		72.4	72.4
	T Water [°F]	76.2		76		76		76.6		76.6		75.2	76
	T Ceiling [°F]	75		75.4		75.3		75.7		75.5		75	74.3
	T avg [°F]	744.06		742.5		743.42		743.58		743.76		743	738.96
	Radiometer [mV]	7.2622		2.2963		1.1453		0.6918		0.4708		0.3215	0.0258
	Radiometer [Watts]	1.2416		0.3926		0.1958		0.1183		0.0805		0.0505	
	Shape Factor	0.0050		0.0015		0.0007		0.0004		0.0003		0.0002	
	HP emittance	0.8684		0.8684		0.8684		0.8684		0.8684		0.8684	
	Q calc [Watts]	1.1889		0.3590		0.1682		0.0933		0.0622		0.0425	
	Q read by radio [%/100]	1.0443		1.0935		1.1641		1.2672		1.2947		1.1908	

Mean Temp.	Horizontal Disp. *r(hot plate)	0		0.5		1		1.5		2	
	radiometer position	Plate	Ambient	Plate	Ambient	Plate	Ambient	Plate	Ambient	Plate	Ambient
400 °F	T1 [°F]	405	405.8	407.2	408.2	408.5	408.6	409.2	410.7	410.9	410.4
	T2 [°F]	429.2	430.5	431.1	431.8	433	433.9	434	434	433.6	434
	T3 [°F]	418.2	419.3	420.1	421.4	421.5	422.2	422.2	423.2	423.8	423.7
	T4 [°F]	430.7	431.4	433.2	432.6	433.9	434.2	435.9	435.1	437.1	436.7
	T5 [°F]	431.9	433.6	434.6	434.7	436	436.4	436.7	437.1	438.2	438.2
	T6 [°F]	439.7	440.7	442.6	442	444.1	444.4	445.2	445.2	445.9	445.9
	T7 [°F]	438.7	439.8	440.3	441.7	442.2	443.1	442.5	443.6	443	443.6
vertical disp 0.75	T8 [°F]	443.5	445	445.7	446.7	447.1	447.8	448.5	448.4	449.6	449.4
	T9 [°F]	432.4	432.9	435.2	435.5	435.8	436.1	437.3	438.1	438.9	438.8
	T amb [°F]	66.1	66.5	66.4	66.6	66.9	66.9	67.1	67.3	66.8	67
	T water [°F]	69.6	69.4	69	68.5	68.6	68.3	68.2	67.9	67.8	67.7
	T ceiling [°F]	73.5	73.5	73.9	74.1	74.5	74.7	74.6	74.4	74.2	74.1
	T avg [°F]	437.24	438.4	439.68	440.12	441.04	441.56	442.04	442.48	443.12	443.18
	Radiometer [mV]	6.3408	0.0373	5.3361	0.0344	2.8848	0.0603	1.0994	0.0603	0.4736	0.0574
	Radiometer [Watts]	1.0777		0.9064		0.4829		0.1777		0.0712	
	Shape Factor	0.0165		0.0160		0.0151		0.0144		0.0139	
	HP emittance	0.8715		0.8714		0.8713		0.8713		0.8712	
	Q calc [Watts]	1.1140		1.0934		1.0376		0.9928		0.9661	
	Q read by radio [%/100]	0.9674		0.8290		0.4654		0.1790		0.0737	

Mean Temp.	Horizontal Disp. *r(hot plate)	0		1		2		3		4		5		6	
	radiometer position	Plate	Ambient	Plate	Ambient	Plate	Ambient	Plate	Ambient	Plate	Ambient	Plate	Ambient	Plate	Ambient
700°F	T1 [°F]	673.5	675.5	672.4		673.5		672.8		671.4		671.9		671.6	
	T2 [°F]	723.5	725.7	721.6		722		722		721.7		722.2		722.2	
	T3 [°F]	701.1	703.1	699.8		699.1		697.6		697.8		697.1		697.1	
	T4 [°F]	726.9	728.8	725.4		724.7		723.9		723.8		722.9		724	
	T5 [°F]	725.5	727.5	723.7		723.9		722.6		722.2		722		722	
	T6 [°F]	754.9	757.5	754.2		754.3		753.8		753.7		754.2		754.2	
	T7 [°F]	750	752.1	748		748.2		747.8		747.5		747		747.5	
	T8 [°F]	759.2	761.3	757.6		757.2		755.8		755.6		755.1		755.6	
vertical disp 2.5	T9 [°F]	753.9	737.6	735		734.9		734.1		733.1		733.2		733.6	
	T Amb. [°F]	72.2	72.1	72.4		72.2		72.2		72.3		72.2		72.1	
	T Water [°F]	75.3	75.1	75.3		75.3		75.2		75.5		75.4		75.6	
	T Ceiling [°F]	74.6	74.3	75		75.1		74.7		74.7		74.4		74.6	
	T avg [°F]	748.7	747.2	743.7		743.7		742.82		742.42		742.3		742.58	
	Radiometer [mV]	5.1725	0.0115	3.9067		2.1241		1.0219		0.4908		0.2210		0.1062	
	Radiometer [Watts]	0.8824		0.6679		0.3632		0.1747		0.0839		0.0378		0.0182	
	Shape Factor	0.0036		0.0047		0.0069		0.0087		0.0100		0.0108		0.0113	
	HP emittance	0.8684		0.8684		0.8684		0.8684		0.8683		0.8683		0.8684	
	Q calc [Watts]	0.8603		1.1145		1.6346		2.0684		2.3623		2.5536		2.6825	
	Q read by radio [%/100]	1.0257		0.5993		0.2222		0.0845		0.0355		0.0148		0.0068	

REFERENCE LIST

1. FINAL REPORT ON TEST OF STEP SHENANDOAH PARABOLIC DISH SOLAR COLLECTOR QUADRANT FACILITY; A. R. Saydah, A. A. Koenig, R. H. Lambert, D. A. Kugath; *Contractor Report SAND82-7153, UC - 62a, April 1983.*

2. EXPERIMENTAL STUDY OF HEAT LOSS THROUGH NATURAL CONVECTION FROM AN ISOTHERMAL CUBIC OPEN CAVITY; P. LeQuere, F. Penot, and M. Mirenayat; *Laboratoire d'Energétique Solaire, 40 avenue du Recteur Pineau, 86022 Poitiers Cédex, France.*

3. THERMAL PERFORMANCE OF SOLAR CONCENTRATOR/CAVITY RECEIVER SYSTEMS; James A. Harris and Terry G. Lenze; *Solar Energy, vol. 34. # 2, pp 135-142, 1985.*

4. CONVECTIVE LOSSES FROM CAVITY SOLAR RECEIVERS- COMPARISONS BETWEEN ANALYTICAL PREDICTIONS AND EXPERIMENTAL RESULTS; A. M. Clausing; *Journal of Solar Energy Engineering, Vol. 105, p 29-33, Feb. 1983.*

5. ESTIMATING CONVECTIVE ENERGY LOSSES FROM SOLAR CENTRAL RECEIVERS; D. L. Siebers & J. S. Kraabel, *Sandia National Laboratories Report, SAND84-8717, Unlimited Release, UC-62c, Printed April 1984.*

6. CAVITY RECEIVER HEAT LOSS MEASUREMENTS; Wm. B. Sine & C. G. McDonald, *presented at the ASME Solar Energy Division Conference, Denver, Colorado, April 10-14, 1988.*

7. ENERGY AND AVAILABILITY TRANSPORT LOSSES IN A POINT-FOCUS SOLAR CONCENTRATOR FIELD ; Wm. B. Sine & A. A. Heckes, *Sandia National Laboratories Report, SAND 86-0004A*

8. CAVITY RECEIVER HEAT LOSS MEASUREMENTS (revised 10/20/89); Wm. B. Sine & C. G. McDonald, *presented at the International Solar Energy Society Solar World Congress 1989 Kobe, September 4-8, 1989, Kobe, Japan*

9. EXPERIMENTAL STUDY OF HEAT LOSS THROUGH NATURAL CONVECTION FROM AN ISOTHERMAL CUBIC OPEN CAVITY; P. LeQuere, F. Penot, and M. Mirenayat; *Laboratoire d'Energétique Solaire, 40 avenue du Recteur Pineau, 86022 Poitiers Cédex, France.*

10. THERMAL PERFORMANCE OF SOLAR CONCENTRATOR/CAVITY RECEIVER SYSTEMS: James A. Harris and Terry G. Lenze; *Solar Energy, vol. 34. # 2, pp 135-142, 1985.*

11. CONVECTIVE LOSSES FROM CAVITY SOLAR RECEIVERS- COMPARISONS BETWEEN ANALYTICAL PREDICTIONS AND EXPERIMENTAL RESULTS; A. M. Clausing; *Journal of Solar Energy Engineering, Vol. 105, p 29-33, Feb. 1983.*

12. ESTIMATING CONVECTIVE ENERGY LOSSES FROM SOLAR CENTRAL RECEIVERS; D. L. Siebers & J. S. Kraabel, *Sandia Report, SAND84-8717, Unlimited Release, UC-62c, Printed April 1984.*

13. INSTALLATION & OPERATION MANUAL, PRC-408 SERIES PULSE RATE CONVERTER; *Flow Technology, Inc., 4250 E. Broadway Road, Phoenix, Arizona 85040 1986.*

14. Bryan Wilson, *Technical Support, Flow Technology, Inc., 4250 E. Broadway Road, Phoenix, Arizona 85040 1986.*

15. OMEGA TEMPERATURE MEASUREMENT HANDBOOK AND ENCYCLOPEDIA; *Omega Engineering, Inc., One Omega Drive, Stamford, CT 06907-0047, 1986.*

16. DATA AND ERROR ANALYSIS IN THE INTRODUCTORY PHYSICS LABORATORY; William Lichten, *Allyn and Bacon, Inc., Newton, Massachusetts, 02159, © 1988.*

17. INFORMATION ABOUT SYLTHERM® 800 HEAT TRANSFER LIQUID; *Dow Corning Corporation, Midland, Michigan 48684-0994, Form #22-761G-86, 1986.*

18. "personal communication"; Bryan Wilson, *Technical Support, Flow Technology, Inc., 4250 E. Broadway Road, Phoenix, Arizona 85040 , October 1990..*

19. ANALOG CONNECTION II MANUAL; *Strawberry Tree Computers, 1010 W. Fremont Ave., Sunnyvale, CA 94087, 1986.*

20. THERMAL RADIATION HEAT TRANSFER, Second Edition; Robert Siegal and John R. Howell; *Hemishere Publishing Corporation, New York, © 1981.*

U.S. Department of Energy (2)
Attn: R. (Bud) Annan
Code EE-13
Forrestal Building
1000 Independence Ave. SW
Washington, DC 20585

U.S. Department of Energy (5)
Attn: G. Burch
S. Gronich
EE-132
Forrestal Building
1000 Independence Ave. SW
Washington, DC 20585

U.S. Department of Energy
Attn: R. Hughey
San Francisco Operations Office
1333 Broadway
Oakland, CA 94612

U.S. Department of Energy (2)
Attn: N. Lackey
G. Tennyson
Albuquerque Operations Office
P.O. Box 5400
Albuquerque, NM 87115

Arizona Public Service Co.
Attn: Scott McLellan
P.O. Box 53999
MS 1424
Phoenix, AZ 85072-3999

Arizona Solar Energy Office
Attn: Frank P. Mancini, Ph.D.
Department of Commerce
3800 N. Central
Suite 1200
Phoenix, AZ 85012

Austrialian National University
Attn: Stephen Kaneff
Information Technology
0200 Canberra ACT, AUSTRALIA

Battelle Pacific Northwest Lab (2)
Attn: D. Brown
P.O. Box 999
Richland, WA 99352

California State Polytechnic University (10)
Attn: William B. Stine
Department of Mechanical Engineering
3801 West Temple Avenue
Pomona, CA 91768-4062

Clever Fellows
Attn: John A. Corey, P.E.
Innovation Consortium, Inc.
R.D. 1, Box 410, River Road
Melrose, NY 12121

Cummins Power Generation Inc. (2)
Attn: Isoroku (Rocky) Kubo
Mail Code 60125
P.O. Box 3005
500 Jackson Street
Columbus, IN 47202-3005

Cummins Power Generation South
Attn: Monte McGlaun
150 Tannehill Drive
Abilene, TX 79602

DLR
Attn: R. Buck
Pfaffenwaldring 38-40
7000 Stuttgart 80 GERMANY

Electric Power Research Institute
Attn: J. Schaeffer
P.O. Box 10412
3412 Hillview Avenue
Palo Alto, CA 94303

Energy Research Centre (2)
Attn: K. Inall
R. S. Phy. Sc.
Australian National University
Canberra ACT 2601 AUSTRALIA

Energy Technology Engr. Center (2)
Attn: W. Bigelow
R. LeChevalier
Rockwell International Corp.
P.O. Box 1449
Canoga Park, CA 91304

Florida Solar Energy Center
Attn: Library
300 State Road, Suite 401
Cape Canaveral, FL 32920-4099

Georgia Power
Attn: W. King
7 Solar Circle
Shenandoah, GA 30265

Lawrence Berkeley Laboratory
Attn: Arlon Hunt
University of California
MS 90-2024
One Cyclotron Road
Berkeley, CA 94720

McDonnell-Douglas Astronautics Co. (3)
Attn: R.L. Gervais
J. Rogan
D. Steinmeyer
5301 Bolsa Avenue
Huntington Beach, CA 92647-2048

Mechanical Technology, Inc.
Attn: D. Dochat
968 Albany Shaker Road
Latham, NY 12110

National Renewable Energy Laboratory
Attn: Mark Bohn
G. Jorgensen
A. Lewandowski
L. M. Murphy
T. Wendelin
T. Williams
1617 Cole Blvd.
Branch 4710/132
Golden, CO 80401-3393

Northern Research and Eng. Corp.
Attn: J. Kesseli
39 Olympia Avenue
Woburn, MA 01801-2073

Pacific Gas and Electric Co.
Attn: G. Braun
3400 Crow Canyon Road
San Ramon, CA 94583

Pacific Power
Attn: P. Lynch
Park and Elizabeth Streets
GPO Box 5257, Sydney
New South Wales 2001
AUSTRALIA

Power Kinetics, Inc.
Attn: W.E. Rogers
415 River Street
Troy, NY 12180-2822

SBP - Schlaich, Bergermann und. Partner
Attn: Wolfgang Schiel
Hohenzollernstr. 1
D-70178 Stuttgart, GERMANY

Science Applications International Corp.
Attn: Kelly Beninga
15000 W. 6th Avenue
Suite 202
Golden, CO 80401

Science Applications International Corp.
Attn: Barry L. Butler
Room 2043, M/S C2J
10260 Campus Point Dr.
San Diego, CA 92121

Solar Energy Industries Association (2)
Attn: Ken Sheinkopf
S. Sklar
122 C Street, NW
4th Floor
Washington, DC 20001-2109

Solar Kinetics, Inc. (2)
Attn: Gus Hutchison
D. White
10635 King William Drive
P.O. Box 540636
Dallas, TX 75354-0636

Stirling Machine World
Attn: B. Ross
1823 Hummingbird Court
West Richland, WA 99352-9542

Stirling Technology Co.(2)
Attn: Maurice A. White
2952 George Washington Way
Richland, WA 99352

Stirling Thermal Motors (2)
Attn: Lennart Johansson
275 Metty Drive
Ann Arbor, MI 48103

Thermacore, Inc. (2)
Attn: Donald Ernst
780 Eden Road
Lancaster, PA 17601

University of Minnesota
Attn: E.A. Fletcher
1111 Church Street, SE
Dept. of Mech. Engr.
Minneapolis, MN 55455

Internal Distribution:

MS 0702	D.E. Arvizu, 6200
MS 0703	C.E. Andraka, 6216
MS 0703	R.B. Diver, 6216 (5)
MS 0703	D.R. Gallup, 6216
MS 0703	T.R. Mancini, 6216
MS 0703	D.F. Menicucci, 6216
MS 0703	J.B. Moreno, 6216
MS 0703	T.A. Moss, 6216
MS 0703	C.E. Tyner, 6216
MS 0704	P.C. Klimas, 6201
MS 0835	R.E. Hogan, Jr., 1513
MS 0835	R.D. Skocypec, 1513
MS 1127	J.M. Chavez, 6215
MS 1127	Cordeiro, 6215
MS 1127	V.E. Dudley, 6215
MS 1127	Library, 6215 (5)
MS 1127	A.R. Mahoney, 6215
MS 1127	K.S. Rawlinson, 6215
MS 0100	Document Proc. for DOE/OSTI, 7613-2 (2)
MS 0619	Print Media, 12615
MS 0899	Technical Library, 4414 (5)
MS 9018	Central Technical Files, 8523-2

* U.S. GOVERNMENT PRINTING OFFICE 1996- 774 030-20013